

# Mechanisms of Cyclic-di-GMP Signaling

Insight into the  
Biochemistry, Signal Transduction and Regulation  
of the Bacterial Second Messenger Cyclic-di-GMP

**Inauguraldissertation**

zur

Erlangung der Würde eines Doktors der Philosophie

vorgelegt der

Philosophisch-Naturwissenschaftlichen Fakultät

Der Universität Basel

Von

Matthias Christen aus Basel, Schweiz

Basel 2007

Genehmigt von der Philosophisch-Naturwissenschaftlichen Fakultät auf

Antrag von

Prof. Dr. Urs Jenal

Prof. Dr. Tilman Schirmer

Prof. Dr. Helma Wennemers

Basel, den 14.2.2007

Prof. Dr. Hans-Peter Hauri

This work was carried out in the Laboratory of Prof. Dr. Urs Jenal in the division of Molecular Microbiology at the Biozentrum of the University of Basel and was supported by Swiss Science Foundation Fellowship 3100A0-108186 to U.J..

## Abstract

Bacteria are able to switch between two mutually exclusive lifestyles, motile single cells and sedentary multicellular communities that colonize surfaces. These behavioral changes contribute to an increased fitness in structured environments and are controlled by the ubiquitous bacterial second messenger c-di-GMP. In response to changing environments, fluctuating levels of c-di-GMP antagonistically affect motility and virulence of single, planktonic cells as well as cell surface adhesins and persistence of sedentary, multicellular communities. The cellular levels of c-di-GMP are controlled by opposing enzymatic activities of diguanylate cyclases (DGCs) and phosphodiesterases (PDEs), which represent two large families of output domains found in bacterial one- and two-component systems. The present work investigates structural, functional and regulatory aspects of diguanylate cyclases and phosphodiesterases, and explores their role in signal transduction processes transmitting environmental stimuli into a range of different cellular functions. Furthermore we report the isolation and characterization of novel components of the c-di-GMP signaling network mediating its output functions.

In (Christen et al. 2005, JBC 280:30829-30837), we report the finding that the c-di-GMP specific phosphodiesterase activity resides in the widespread EAL domain. By analyzing the enzymatic reaction products and investigating the substrate specificity of wild type and various mutant enzymes, we demonstrate that a single EAL domain itself catalyzes, in a  $Mg^{2+}$  dependent manner, the cleavage of the second messenger c-di-GMP into the linear dinucleotide pGpG. Furthermore, we report the discovery that in a GGDEF-EAL protein a catalytic inactive GGDEF domain can bind GTP and in response allosterically activates the EAL domain. Thus we conclude that GGDEF domains can have either catalytic or regulatory function and suggest, that the cellular GTP pool may serve as an input signal into c-di-GMP-mediated signal transduction.

In (Christen & Christen et al. 2006, JBC 281:32015-32024), we describe an important novel feature of GGDEF proteins, which produce the ubiquitous bacterial signaling molecule c-di-GMP. This paper reports the results of in depth structure-function analysis of an allosteric feedback inhibition mechanism that generally acts to regulate diguanylate cyclase activities in bacteria. The mechanism involves binding of the second messenger product, c-di-GMP at an inhibition site (I-site) that is coupled via a conserved beta-strand to the active site (A-site) of the enzyme. The study involves an array of biochemical and genetic techniques applied on various diguanylate cyclases to establish the sequence determinants of the I-site as well as the in vivo physiological relevance of I-site function. Allosteric product inhibition of diguanylate cyclases turns out to have fundamental functional and physiological implications, including threshold setting for c-di-GMP production by

particular GGDEF proteins, which can contribute to precision, robustness, noise reduction and accelerated kinetics of c-di-GMP signaling. The definition of the I-site binding pocket provides an entry point into unraveling the molecular mechanisms of ligand-protein interactions involved in c-di-GMP signaling, and makes DGCs a valuable target for drug design to develop new strategies against biofilm-related diseases.

In (Christen & Christen et al. 2007, PNAS), we enlighten the signal transduction mechanism of the bacterial second messenger c-di-GMP and demonstrate the existence of diguanylate receptor proteins mediating its output functions. We report the biochemical purification of c-di-GMP receptor proteins from *C. crescentus* crude extract and describe their physiological role in c-di-GMP dependent repression of cell motility. A multitude of biochemical, genetic and NMR experiments was used to characterize these effector proteins and homologs from *S. enterica* and *P. aeruginosa* down to molecular level. In particular we used [<sup>33</sup>P] c-di-GMP UV cross linking studies to demonstrate that these receptors specifically bind c-di-GMP in the sub micromolar range and, in combination with NMR spectrometry, to elicit determinants for c-di-GMP binding. Furthermore, we performed genetic suppressor analysis and epistasis experiments with receptor deletion and pointmutants, to corroborate that the identified diguanylate receptors from *C. crescentus* act in vivo downstream of the second messenger c-di-GMP.

We further report the isolation and characterization of a *C. crescentus* adenylosuccinate synthetase (PurA, CC3103), an enzyme of the purine biosynthesis pathway that has high affinity for c-di-GMP. Using recombinant purified PurA for kinetic and ligand binding studies, we show that c-di-GMP is a potent inhibitor of PurA activity. Initial rate kinetics revealed that c-di-GMP inhibition is competitive with respect to GTP and noncompetitive with respect to IMP. These findings suggest a role for c-di-GMP as regulator of the cellular nucleotide pool. We propose that c-di-GMP inhibits the first step of the *de novo* biosynthesis of AMP and by that directs IMP toward guanine biosynthesis, thereby preventing the drainage of the guanine pool.

## Index

1	Introduction.....	1
2	Aim of the thesis.....	8
3	Results.....	9
	3.1 Identification and Characterization of a Cyclic di-GMP-specific Phospho-diesterase and Its Allosteric Control by GTP.....	10
	3.2 Allosteric Control of Cyclic di-GMP Signaling.....	19
	3.3 DgrA is a member of a new family of cyclic di-GMP receptors and controls flagellar motor functions in <i>Caulobacter crescentus</i> .....	39
	3.4 The structure-function relationship of WspR; a <i>Pseudomonas fluorescens</i> response regulator with a GGDEF output domain.....	80
	3.5 Unpublished results.....	115
	3.5.1 Cyclic di-GMP regulates adenylosuccinate synthetase - a key enzyme in purine biosynthesis pathway.....	116
	3.5.2 The substrate specificity of diguanylate cyclases.....	127
	3.5.3 Diguanylate cyclase Inhibition studies.....	130
	3.5.4 The enzymatic synthesis of c-di-GMP.....	135
	3.5.5 In vivo c-di-GMP levels.....	141
4	Discussion.....	145
5	Outlooks.....	154
	Appendix.....	155
	References.....	156
	GGDEF and EAL proteins from <i>C. crescentus</i> .....	160
	List of constructs.....	161
	List of figures.....	169
	Acknowledgments.....	170
	Curriculum vitae.....	171

## Abbreviations

AC	adenylate cyclase
c-di-GMP	cyclic diguanylic acid
CR	Congo Red
DGC	diguanylate cyclase
DgcA	diguanylate cyclase A (CC3285)
DgrA	diguanylate receptor protein A (CC1599)
DgrB	diguanylate receptor protein B (CC3165)
EAL	glutamate-alanine-leucine domain harboring c-di-GMP specific PDE activity
EDTA	ethylenediaminetetraacetic acid
EGTA	ethylene glycol-bis( $\beta$ -aminoethyl ether)-N,N,N',N'-tetra acetic acid
ESI-MS	electrospray ionization-mass spectrometry
EXSY	exchange spectroscopy
GC	guanylate cyclase
GGDEF	glycine-glycine-aspartate-glutamate-glutamate A-site motif of DGC's
H6	hexa-histidine tag
Hepes	N-2-Hydroxyethylpiperazin-N-2-ethansulfonic acid
HPLC	high performance liquid chromatography
HSQC	heteronuclear single quantum coherence
IPTG	isopropyl 1-thio- $\beta$ -D-galactopyranoside
LB	luria broth
MeOH	methanol
NMR	nuclear magnetic resonance
NOESY	nuclear overhauser effect spectroscopy
PAGE	polyacrylamide gel electrophoresis
PDE	phosphodiesterase
PYE	peptone yeast extract medium
PdeA	phosphodiesterase A (CC3396)
pGpG	linear diguanylic acid
rdar	red, dry, and rough phenotype

## 1 Introduction

### Signal transduction mechanisms

The simultaneous coordination of metabolic processes within a multicomponent system is characteristic for the chemical machinery of life. Cellular homeostasis is the result of tight coordination and regulation of different interconnected metabolic pathways. The required information transfer within different components of the network is accomplished through highly selective molecular recognition between signaling molecules and their respective regulatory receptor molecules.

Bacteria regulate their cellular metabolic state in response to a wide variety of external environmental signals including change in temperature, light, pH-shift, availability of oxygen and nutrients. These environmental stimuli are sensed and converted into internal signals leading to a reprogramming of the cellular metabolic state by a process termed signal transduction. During signal transduction processes an increasing number of enzymes and other molecules become engaged in the events that proceed from the initial external stimulus. In a widely used signal transduction mechanism, stimulus sensing is initiated upon binding of the signaling molecule to its corresponding membrane-bound receptor, which, in turn, transfers the information upon structural changes across the cell membrane to its cytosolic output domain and thereby activates the synthesis of small diffusible signaling molecules called second messengers, which are then fed into cytoplasmatic second messenger cascades. Regulatory networks based on the controlled synthesis and degradation of second messengers are able to integrate a wide variety of signaling inputs and offer flexibility of recognition combined with signal amplification, autoregulation and signal adaptation.

Two widely used bacterial second messengers are adenosine 3',5'-monophosphate (cAMP) and guanosine-3',5'-bis(pyrophosphate) (ppGpp) (Figure 1). Upon carbon source starvation, adenylate cyclases (AC) synthesize the second messenger cAMP, which allosterically activates a transcription factor called catabolite regulatory protein (CRP), in order to regulate transcriptionally catabolic operons for the use of alternative carbon sources and other cellular processes (1).

The stringent response ppGpp is produced from GTP by the ribosome-associated protein RelA in response to low levels of charged tRNAs. The second messenger ppGpp binds to RNA polymerase and alters its activity to repress genes encoding ribosomal RNA and tRNA (2), whereas genes involved in amino acid synthesis and transport are activated (3). While guanosine



3',5'-monophosphate (cGMP), is an important second messenger in eukaryotes, it appears to be rarely used in bacteria. Rather, new evidence suggests that the cyclic dinucleotide 3',5'-cyclic diguanylic acid (c-di-GMP) is widely used by bacteria as a second messenger.

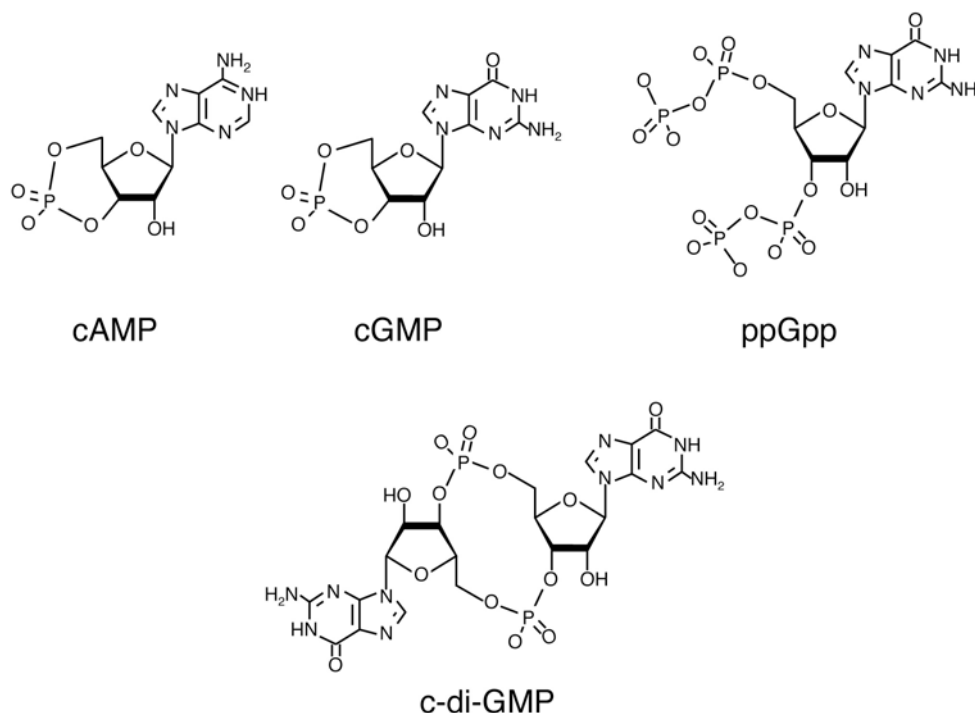


Figure 1 Ubiquitous ribonucleotide second messengers

### **C-di-GMP is an allosteric activator of cellulose synthase**

The bacterial second messenger (3'-5')-cyclic-di-guanosine monophosphate (c-di-GMP) has been discovered 20 years ago by Ross et al. (4) as an allosteric activator of the cellulose synthetase in the fruitdegrading bacterium *Gluconacetobacter xylinus*. Further biochemical isolation and characterization of enzymes involved in the synthesis and degradation of this unusual cyclic nucleotide provided the basis for the molecular analysis of the c-di-GMP signaling network (5). Biochemical studies revealed that c-di-GMP is synthesized from two molecules of GTP by enzymes called diguanylate cyclases (DGCs) and degraded by c-di-GMP-specific phosphodiesterases (PDEs) into the linear dinucleotide pGpG. Using GTP-agarose affinity chromatography Tal et al. isolated a soluble diguanylate cyclase and identified 3 operons involved in c-di-GMP turnover (5). Each of these operons consists of a pair of isoenzymes harboring opposing enzymatic DGC and PDE activity. Multiple alignments of the DGC and PDE protein sequences revealed that all six isoenzymes share significant structural conservation over a stretch of 390 amino acid residues and contain GGDEF and EAL domains. Both the GGDEF and the EAL

domains are ubiquitous in bacteria and are often linked to regulatory domains, such as phosphorylation receiver or oxygen sensing domains, however, their physiological function was to that time unknown. Their occurrence in transmembrane or membrane-associated proteins, that contain N-terminal sensory domains, led to the assumption, that GGDEF and EAL domains are important in relaying external sensory information into the cytoplasm. Environmental stimuli such as oxygen, amino acids, light etc. are believed to regulate the assumed enzymatic activity of GGDEF and EAL domain proteins. GGDEF and EAL domain proteins consist of the largest known family of orthologs with up to 60 paralogs existing in some species. Whereas GGDEF domain proteins are found in most bacterial species, they are absent in archae and eucaryotes.

The discovery that the DGC and PDE isoenzymes from *Gluconacetobacter xylinus* contain GGDEF and EAL domains, strongly suggested that GGDEF and the EAL domain might be involved in c-di-GMP metabolism (5). This key discovery raised the possibility, that c-di-GMP plays a more general role as a bacterial signaling molecule and might have a broader scientific significance than acting as an allosteric regulator of cellulose biosynthesis in *G. xylinus*.

#### **c-di-GMP regulates bacterial cell adhesion and extracellular matrix production.**

Bacterial genetics provided a number of functional analyses of GGDEF proteins supporting the idea that DGCs might have evolved to control bacterial growth on surfaces through the regulation of cellular adhesion components that enable cells for cell–cell and cell–surface interactions.

The production and secretion of cellulose by *G. xylinus* leads to a dramatic change in colony morphology resulting in aggregation of cells into a thick pellicle in liquid culture and colonies with a rough surface on agar plates (7, 8). Both, pellicle formation and colony morphology represent visible phenotypes, associated with the production of extra-cellular matrix components. These phenotypes were used in genetic screens in diverse bacterial species to identify components required for the synthesis of extra cellular matrix components. These studies provided strong evidences for a role of GGDEF proteins in the regulation of cell surface adhesives and extra cellular matrix components: In *P. aeruginosa*, the wrinkled colony morphology phenotype was linked to the activity of the GGDEF-type response regulator WspR (9). *Salmonella enterica* serovar Typhimurium and other related *Enterobacteria* including *E. coli* K-12 typically form after prolonged incubation below 37°C colonies with a distinctive morphology named rdar (congo-red binding, dry and rough) (10-13). In the absence of the GGDEF-type regulator AdrA, colonies are unable to develop the rdar phenotype (14). Similarly, it has been reported that the GGDEF-type regulator *hmsT* is required for auto-aggregation and plaque formation in *Yersinia pestis* (15). Deletions in *mbaA*, a GGDEF-type regulator from *Vibrio cholera*, result in altered biofilm structure caused by a

decrease in the amount of extra-cellular matrix material (16). From *Myxococcus xanthus* whose development of fruiting bodies resembles biofilm formation, it has been reported that expression of CsgA, a cell surface associated protein required for fruitingbody formation, is dependent on ActA, a PleD ortholog. Mutant *M. xanthus* cells lacking functional *actA* are able to aggregate but fail fruiting body formation and do not form spores (17, 18). In all these bacterial species, regulation of cellular adhesion components and synthesis of extra-cellular matrix components has been linked genetically to the activity of GGDEF-type regulators, suggesting an important role for c-di-GMP signaling in the coordination of these cellular processes.

### **C-di-GMP is involved in polar organell morphogenesis and cell differentiation**

Several lines of evidence have suggested that c-di-GMP-dependent signaling is used by the  $\alpha$ -proteobacterium *Caulobacter crescentus* to control cell differentiation. In *C. crescentus*, obligate asymmetric cell division at each replicative cycle generates two genetically identical but morphologically different daughter cells, which undergo different developmental programs (Figure 2A): The sessile stalked cell, equipped with an adhesive holdfast and stalk, initiates a new replication cycle immediately after cell division has completed, whereas the motile, polar flagellated swarmer cell undergoes an obligate, planktonic stage, during which cell division programs and DNA replication are inhibited (19, 20). In order to become replication competent and progress cell cycle, the swarmer cell has to differentiate and undergoes subsequent remodeling of its polar organelles, which involves ejection of the flagellum, retraction of the pili, and generation of a stalk and adhesive holdfast at the pole previously occupied by the flagellum. Precise timing of assembly and loss of polar organelles is critical for optimal surface colonization. Both acquisition of flagellar motility in the predivisional cell and its replacement by an adhesive holdfast later in development are dependent on the polar localized diguanylate cyclase PleD (21-26), which originally has been identified in a genetic screen for regulators of bacterial development by Hecht et al. (22). PleD contains two N-terminal receiver domains and an unusual novel output domain, which has been termed GGDEF according to a highly conserved amino acid motif. *C. crescentus* cells lacking a functional PleD protein, retained motility throughout the cell cycle, fail to shed the flagellum during swarmer-to-stalk cell transition and do not form stalks. The presence of a constitutive active mutant protein PleD\* results the opposite way around in non motile cells, which harbor elongated stalks (23, 27).

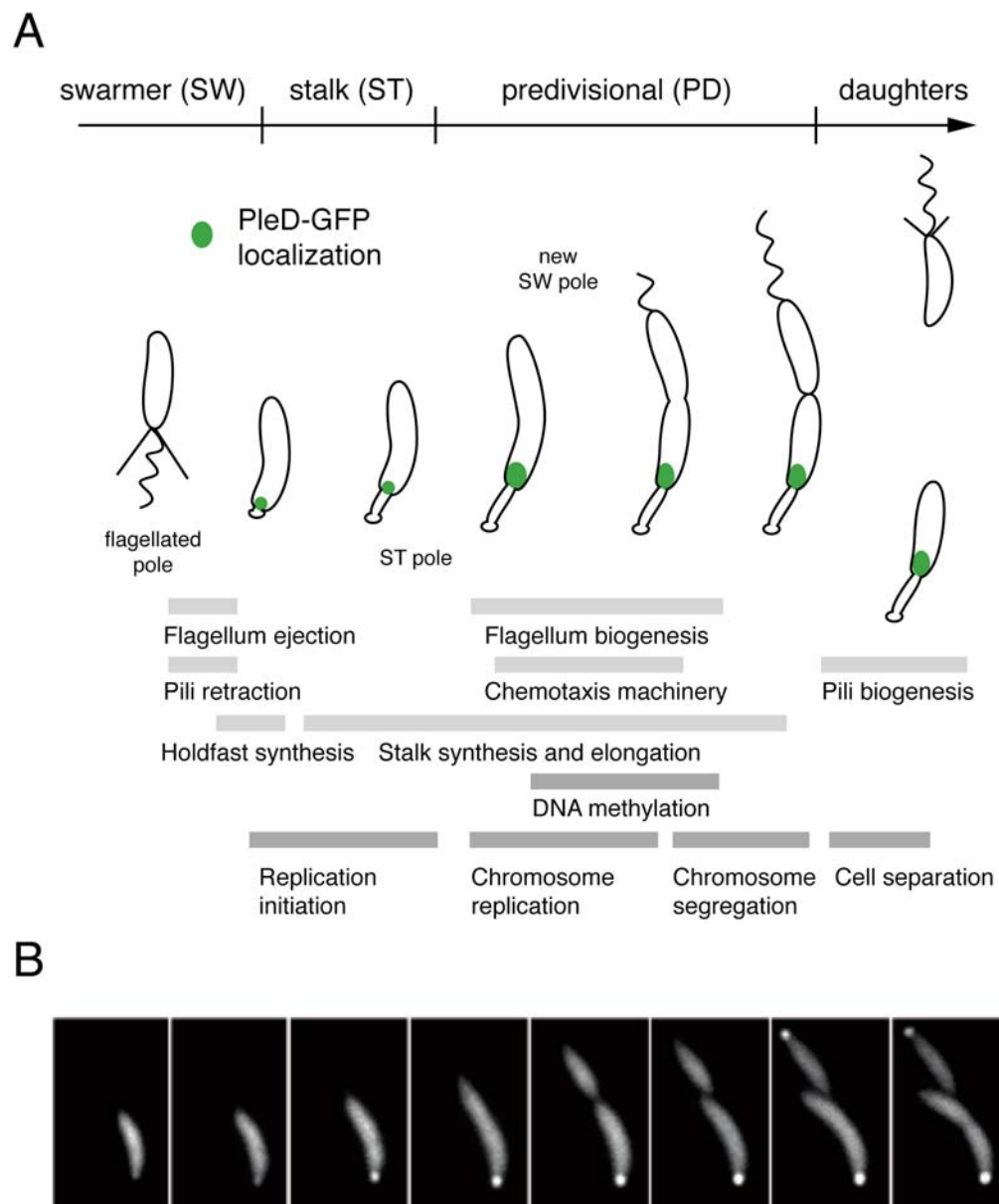


Figure 2 The cell cycle of *Caulobacter crescentus* and polar localization of PleD

**A)** *Caulobacter crescentus* divides asymmetrically to produce two daughter cells with different function and morphology. The PleD-GFP localization pattern is shown in green (the figure was drawn according to Jacobs-Wagner 2004 (28) and adapted according to Paul 2004 (25)). **B)** Polar localization of the diguanylate cyclase PleD according to Paul 2004 (25).

Subsequent biochemical characterization revealed that PleD is a diguanylate cyclase, catalyzing the conversion of GTP into the second messenger c-di-GMP (25). The diguanylate cyclase activity of PleD resides in the C-terminal GGDEF domain and is activated upon phosphorylation by DivJ and PleC (23), two sensor histidine kinases involved in *C. crescentus* cell differentiation, that

dynamically localise to opposing cell poles. *In vivo* studies with PleD-GFP fusions revealed that PleD is sequestered to the differentiating cell pole in dependence of its phosphorylation state (25) (Figure 2B) this suggesting that only activated PleD reaches the stalk pole and therefore providing a possible mechanism that restricts PleD activity and consequently the synthesis of the second messenger c-di-GMP to the locus where it coordinates polar morphogenesis. The finding that pole morphogenesis in *C. crescentus* is controlled by the diguanylate cyclase PleD implicated that the role of the second messenger c-di-GMP goes beyond a function as an allosteric regulator of cellulose synthetase and regulator of exopolysaccharide synthesis.

### **Biochemistry of the GGDEF domain**

Although known to be involved in c-di-GMP turnover for some time, the enzymatic role of the GGDEF and EAL domain in c-di-GMP turnover remained obscure. Since the previously characterized diguanylate cyclases and c-di-GMP specific phosphodiesterases isoenzymes from *G. xylinus* are composed of highly homologous GGDEF-EAL composite proteins it was, based on these data, not possible to assign neither the enzymatic diguanylate cyclase nor its opposing phosphodiesterase activity to one of these signaling domains. But exactly this knowledge is extremely important to link the second messenger c-di-GMP with its genetically defined output functions and to unravel mechanisms controlling its synthesis and degradation.

Therefore, the biochemical finding that the GGDEF domain itself has diguanylate cyclase activity (25) represented a key discovery, challenging the c-di-GMP field (25). Using purified *C. crescentus* PleD protein, Paul et al. demonstrated for the first time, that a GGDEF protein synthesizes c-di-GMP, and further that the conserved GGDEF residues are required for enzymatic diguanylate cyclase activity. An additional major effort, opening the field for structure function analyses on DGC enzymes, was provided by the first X-ray structure of the diguanylate cyclase PleD by Chan et al. (24). The resolution of the three-dimensional structure of the full-length PleD response regulator in complex with c-di-GMP not only revealed that the overall fold of the GGDEF domain is virtually identical to the adenylate cyclase, but has also proposed a catalytic mechanism for the condensation of two GTP molecules into c-di-GMP (24).

The demonstrated activation of PleD DGC activity upon phosphorylation of the N-terminal receiver domain represents a model system for the tightly controlled synthesis of the second messenger c-di-GMP upon signal-induced activation. This concept seems to represent a general signal transduction mechanism, since many GGDEF domain proteins are associated in a modular fashion to a wide variety of N-terminal fused signal-sensing domains of known or predicted signal input.

Thus, the DGC activity of the GGDEF domain appears to be part of a novel complex bacterial signaling system dedicated to convert environmental stimuli of various cellular compartments into the synthesis of the second messenger c-di-GMP.

In contrast to the molecular nature of the DGC, the c-di-GMP-specific PDE activity had not been determined so far. Initial genetic and biochemical studies have linked PDE activity to proteins that contain both GGDEF and EAL domains (5, 29-31). Like GGDEF, the EAL domain, named after its signature amino acid motif Glu- Ala-Leu, is found only in bacteria and its distribution more or less mirrors that of the GGDEF domains (32, 33). Together, this has led to the proposal that the c-di-GMP-specific PDE activity might reside in the EAL domain (32). But biochemical data validating this hypothesis were still missing.

## 2 Aim of the thesis

The aim of this PhD project was to identify and characterize novel components of the c-di-GMP signaling network. In a first part, mechanisms involved in the regulation of c-di-GMP turnover should be identified and analyzed with respect to their biochemical function, enzymatic activity, role in c-di-GMP metabolism and their effect on c-di-GMP related phenotypes. In particular, the nature of the c-di-GMP specific PDE activity responsible for the degradation of the second messenger has to be determined and the protein domain in which this activity is confined has to be identified. Furthermore, the molecular mode of action and the regulatory mechanisms controlling PDE activity and DGC activities inside the cell should be addressed. And finally, beside these questions focusing on the turnover of the second messenger c-di-GMP, the remaining key question concerns the yet unknown downstream effectors of the second messenger c-di-GMP mediating its output function. The wide variety of cellular functions that are affected by the second messenger c-di-GMP calls for multiple receptors and signaling mechanisms. However, little information was available on specific targets of c-di-GMP action. In particular, how are increased levels of c-di-GMP sensed and how is this information transmitted to the flagellar motor? With the exception of a component of the cellulose synthetase complex from *G. xylinum*, which is absent in the *C. crescentus* genome, no c-di-GMP binding proteins had been reported. Therefore, a biochemical purification strategy had to be developed in order to purify and characterize c-di-GMP binding proteins from *C. crescentus* crude cell extracts. For this, an array of biochemical methods had to be designed, including a method for the synthesis of radio-labeled second messenger, an appropriate c-di-GMP binding assay to monitor and characterize ligand-receptor interactions, a procedure for labeling specifically c-di-GMP binding proteins within a protein crude extract, the development and optimization of enzymatic assays to monitor c-di-GMP turnover and finally an analytic method allowing the detection and quantification of the intracellular second messenger concentration in various mutant strains.

### **3 Results**



### **3.1 Identification and Characterization of a Cyclic di-GMP-specific Phosphodiesterase and Its Allosteric Control by GTP**

M. Christen, B. Christen, M. Folcher, A. Schauerte, and U. Jenal  
**JBC** 280:30829-30837 (2005)

## Summary

This paper adds a new twist to the story of the signaling molecule c-di-GMP (c-di-GMP), which controls motility and biofilm formation in bacteria and is produced by GGDEF domain proteins. We report the finding that the c-di-GMP specific phosphodiesterase activity resides in the widespread EAL domain. By analyzing the enzymatic reaction products and investigating the substrate specificity of wild type and various mutant enzymes, we demonstrate that a single EAL domain itself catalyzes in  $Mg^{2+}$  dependent manner the cleavage of the second messenger c-di-GMP into the linear dinucleotide pGpG. Furthermore we report the discovery that in a GGDEF-EAL protein a catalytic inactive GGDEF domain can bind GTP and in response allosterically activates the EAL domain. Thus we conclude that the GGDEF domain can have either catalytic or regulatory function and suggest, that the cellular GTP pool may serve as an input signal into c-di-GMP-mediated signal transduction.

# Identification and Characterization of a Cyclic di-GMP-specific Phosphodiesterase and Its Allosteric Control by GTP\*

Received for publication, April 22, 2005, and in revised form, June 23, 2005  
Published, JBC Papers in Press, July 1, 2005, DOI 10.1074/jbc.M504429200

Matthias Christen, Beat Christen, Marc Folcher, Alexandra Schauerte, and Urs Jenal‡

From the Division of Molecular Microbiology, Biozentrum, University of Basel, Klingelbergstrasse 70,  
4056 Basel, Switzerland

Cyclic diguanylic acid (c-di-GMP) is a global second messenger controlling motility and adhesion in bacterial cells. Synthesis and degradation of c-di-GMP is catalyzed by diguanylate cyclases (DGC) and c-di-GMP-specific phosphodiesterases (PDE), respectively. Whereas the DGC activity has recently been assigned to the widespread GGDEF domain, the enzymatic activity responsible for c-di-GMP cleavage has been associated with proteins containing an EAL domain. Here we show biochemically that CC3396, a GGDEF-EAL composite protein from *Caulobacter crescentus* is a soluble PDE. The PDE activity, which rapidly converts c-di-GMP into the linear dinucleotide pGpG, is confined to the C-terminal EAL domain of CC3396, depends on the presence of Mg<sup>2+</sup> ions, and is strongly inhibited by Ca<sup>2+</sup> ions. Remarkably, the associated GGDEF domain, which contains an altered active site motif (GEDEF), lacks detectable DGC activity. Instead, this domain is able to bind GTP and in response activates the PDE activity in the neighboring EAL domain. PDE activation is specific for GTP ( $K_D$  4  $\mu$ M) and operates by lowering the  $K_m$  for c-di-GMP of the EAL domain to a physiologically significant level (420 nM). Mutational analysis suggested that the substrate-binding site (A-site) of the GGDEF domain is involved in the GTP-dependent regulatory function, arguing that a catalytically inactive GGDEF domain has retained the ability to bind GTP and in response can activate the neighboring EAL domain. Based on this we propose that the c-di-GMP-specific PDE activity is confined to the EAL domain, that GGDEF domains can either catalyze the formation of c-di-GMP or can serve as regulatory domains, and that c-di-GMP-specific phosphodiesterase activity is coupled to the cellular GTP level in bacteria.

The cyclic nucleotides cAMP and cGMP are universally used as second messengers in intracellular signal transduction pathways. They mediate cellular processes such as vision, electrolyte homeostasis, or smooth muscle relaxation by modulating the activity of protein kinases, GTPases, or ion channels (1, 2). The intracellular levels of cAMP and cGMP are tightly controlled by their rate of synthesis (catalyzed by adenylyl or guanylyl cyclases) and hydrolysis (catalyzed by phosphodies-

terases). Phosphodiesterases (PDE)<sup>1</sup> play a mayor role in the cellular response mediated by cyclic nucleotides and are used as primary therapeutic targets for several diseases (3). They act as effectors of signal transduction, function as homeostatic regulators of cyclic nucleotide levels, have been implicated in desensitization and termination of stimulation, and may also play an important role in controlling the diffusion of cyclic nucleotides and in channeling cyclic nucleotide signals (4, 5) (e.g. photoreception in human rod cells is mediated by rhodopsin and light signal transduction results from a dramatic reduction in cGMP concentrations, catalyzed by cGMP-specific PDE (1)).

Whereas cAMP signaling is common to both prokaryotes and eukaryotes, cGMP does not seem to be used by bacterial cells. However, there is accumulating evidence that the cyclic dimer of GMP, c-di-GMP, plays a critical role in bacterial signaling (6, 7). c-di-GMP is synthesized from two GTP molecules by diguanylate cyclases (DGCs), and hydrolyzed by PDEs via the linear intermediate pGpG to GMP (Fig. 1A). Even though c-di-GMP was discovered almost two decades ago (8), its global role in bacterial signaling has become apparent only recently in the view of the growing bacterial genome sequence information available. In recent years, a rapidly increasing number of genetic studies has linked proteins involved in c-di-GMP synthesis or turnover to the ability of different bacteria to switch between a motile, single-cell state and a multicellular behavior associated with the production of extracellular matrix components and surface adhesion (9–21). Biochemical studies have associated the DGC activity with the readout domain of the *Caulobacter crescentus* PleD response regulator protein (22). This domain, termed GGDEF (after its signature amino acid motif Gly-Gly-Asp-Glu-Phe), is widespread in bacteria but is not found outside the bacterial kingdom (23). The observation that GGDEF domains are often associated with domains involved in signal perception or signal transduction, argued for the existence of a dedicated regulatory network that converts a variety of different signals into the production of the second messenger c-di-GMP (6, 23). The resolution of the three-dimensional structure of the PleD response regulator in complex with c-di-GMP has not only revealed that the overall fold of the GGDEF domain is virtually identical to the adenylyl cyclase, but has also proposed a catalytic mechanism for the condensation of two GTP molecules into c-di-GMP (24). In contrast to the molecular nature of the DGC, the c-di-GMP-specific PDE activity has remained somewhat of a mystery. Initial genetic and biochemical studies have linked PDE activity to proteins that contain both GGDEF and EAL domains (18, 19, 25, 26). Like

\* This work was supported by Swiss National Science Foundation Fellowships 31–59050.99 and 3100A0–108186/1 (to U. J.). The costs of publication of this article were defrayed in part by the payment of page charges. This article must therefore be hereby marked “advertisement” in accordance with 18 U.S.C. Section 1734 solely to indicate this fact.

‡ To whom correspondence should be addressed: Division of Molecular Microbiology, Biozentrum, University of Basel, Klingelbergstrasse 70, 4056 Basel, Switzerland. Tel.: 41-61-267-2135; Fax: 41-61-267-2118; E-mail: urs.jenal@unibas.ch.

<sup>1</sup> The abbreviations used are: PDE, phosphodiesterase; c-di-GMP, cyclic diguanylic acid; pGpG, linear diguanylic acid; MeOH, methanol; DGC, diguanylate cyclase; H6, hexahistidine tag; HPLC, high performance liquid chromatography; ESI-MS, electrospray ionization-mass spectrometry.

GGDEF, the EAL (after its signature amino acid motif Glu-Ala-Leu) domain is found only in bacteria and its distribution more or less mirrors that of the GGDEF domains (23, 27). Together, this has led to the proposal that the c-di-GMP-specific PDE activity might reside in the EAL domain (23).

The PleD response regulator is required for pole development during the *C. crescentus* cell cycle (11). During *Caulobacter* cell differentiation PleD specifically sequesters to one pole of the cell, where the morphological changes take place (22). Polar sequestration of PleD is coupled to the activation of the C-terminal GGDEF output domain via phosphorylation of the N-terminal receiver domain (22). This observation was lending support for the idea that synthesis of c-di-GMP by PleD might be limited to one cell pole may be to locally activate downstream targets or to restrict c-di-GMP production to one compartment during *Caulobacter* asymmetric cell division (22). One would imagine that in both cases, a potent cellular PDE activity is required to rapidly counteract the DGC activity over time and to maintain spatial gradients established by PleD. To monitor and characterize the c-di-GMP-specific PDE activity in *C. crescentus*, we first developed an assay based on the hydrolysis of <sup>33</sup>P-radiolabeled c-di-GMP. We then showed that the soluble fraction of *C. crescentus* cell extracts indeed contains a strong PDE activity. To characterize this activity more closely, we concentrated on EAL proteins encoded in the *C. crescentus* chromosome. A mutant lacking gene CC3396, which codes for a GGDEF-EAL composite protein, showed a more than 80% reduction of the soluble PDE activity (Table I). Enzymatic assays and UV cross-link experiments with purified full-length protein and single domain fragments confirmed that the PDE activity is contained within the EAL domain of CC3396. Remarkably, EAL-based PDE activity of CC3396 is allosterically controlled by GTP. Consistent with this, the GGDEF domain of CC3396, which contains an unorthodox active site motif (GEDEF), lacks DGC activity, but has retained the ability to bind GTP at the active site. Based on this and on the finding that the GGDEF domain is strictly required for the GTP-specific activation of the EAL phosphodiesterase, we postulate that in CC3396 and possibly in other GGDEF-EAL protein homologues, the GGDEF domain acts as an allosteric regulatory domain for the EAL-borne PDE activity (Fig. 1B).

#### MATERIALS AND METHODS

**Strains, Plasmids, and Media**—*C. crescentus* strains were grown in complex peptone yeast extract or in minimal glucose media (28). *Escherichia coli* strains were grown in Luria broth (LB) supplemented with antibiotics for selection, where necessary. The exact procedure of strain and plasmid construction is available on request.

**Purification of CC3396 and Preparation of *C. crescentus* Cell Extracts**—*E. coli* BL21 cells carrying the respective expression plasmid were grown in LB medium with ampicillin (100 µg/ml), and expression was induced by adding isopropyl 1-thio-β-D-galactopyranoside at A<sub>600</sub> 0.4 to a final concentration of 0.4 mM. After harvesting by centrifugation, cells were resuspended in buffer containing 50 mM Tris-HCl, pH 8.0, 250 mM NaCl, 5 mM β-mercaptoethanol, lysed by passage through a French pressure cell, and the suspension was clarified by centrifugation for 10 min at 5,000 × g. Soluble and insoluble protein fractions were separated by a high-spin centrifugation step (100,000 × g, 1 h). The supernatant was loaded onto nickel-nitrilotriacetic acid affinity resin (Qiagen), washed with buffer, and eluted with an imidazole gradient. Protein preparations were examined for purity by SDS-PAGE, and fractions containing pure protein were pooled and dialyzed for 12 h at 4 °C.

*C. crescentus* CB15 cells were grown in peptone yeast extract and harvested by centrifugation at an A<sub>660</sub> of 0.4. Cells were resuspended in buffer containing 50 mM Tris-HCl, pH 8.0, 250 mM NaCl, 5 mM mercaptoethanol, and 5 mM EDTA. Soluble and insoluble protein fractions were separated by a high-spin centrifugation step (100,000 × g, 1 h). The supernatant was dialyzed for 4 h in buffer containing EDTA and then for 8 h in the same buffer without EDTA. Protein concentrations were measured by UV absorption.

**Synthesis and Purification of [<sup>33</sup>P]c-di-GMP**—<sup>33</sup>P-Labeled c-di-GMP was produced enzymatically using α-labeled [<sup>33</sup>P]GTP (3000 Ci/mmol, Amersham Bioscience) and purified hexahistidine-tagged PleD\*, a phosphorylation independent constitutive active form of the PleD diguanylate cyclase (22). To a mixture of 87.5 µl of reaction buffer (250 mM NaCl, 25 mM Tris-HCl, pH 8.0, 10 mM MgCl<sub>2</sub>, 5 mM β-mercaptoethanol, and 10.5 µM PleD\*-H6), 12.5 µl of α-labeled [<sup>33</sup>P]GTP (125 µCi, 41.66 pmol, 3000 Ci/mmol) was added. After 5 min at 25 °C, the reaction was stopped by adding an equal volume of 0.5 M EDTA, pH 8.0. The protein was precipitated by heating for 5 min at 95 °C followed by centrifugation for 2 min at 10,000 × g. The supernatant was loaded on a batch RP-18 column, salt was removed by washing 5 times with 200 µl of 25 mM triethylenammonium carbonate buffer, pH 7.0, containing 1% (v/v) MeOH. c-di-GMP was eluted with 2 × 200 µl of triethylenammonium carbonate containing 5% (v/v) MeOH. The buffer was subsequently removed in the SpeedVac and the purity of the compound was tested by separation on polyethyleneimine-cellulose plates (1:1.5 (v/v) saturated NH<sub>4</sub>SO<sub>4</sub> and 1.5 M KH<sub>2</sub>PO<sub>4</sub>, pH 3.6).

**Phosphodiesterase Assay**—c-di-GMP-specific phosphodiesterase activity was measured by monitoring the decrease of [<sup>33</sup>P]c-di-GMP and the increase of [<sup>33</sup>P]pGpG by thin-layer chromatography. The PDE reaction buffer for the 100,000 × g supernatant of *C. crescentus* cell extracts or purified preparations of hexahistidine-tagged protein contained 250 mM NaCl, 25 mM Tris, pH 8.0, 10 mM MgCl<sub>2</sub>, and 5 mM β-mercaptoethanol. The GTP/protein mixtures were preincubated for 2 min prior to the addition of c-di-GMP. The reactions were carried out at 30 °C, aliquots were removed at different time points, and the reaction was stopped by adding an equal volume of 0.5 M EDTA, pH 8.0.

**Diguanylate Cyclase Assay**—The reaction mixtures with purified hexahistidine-tagged protein contained 25 mM Tris-HCl, pH 8.0, 250 mM NaCl, 10 mM MgCl<sub>2</sub> and were started by the addition of 100 µM [<sup>33</sup>P]GTP (Amersham Biosciences; 3000 Ci/mmol). At regular time intervals the reaction was stopped with an equal volume of 0.5 M EDTA, pH 8.0.

**Polyethyleneimine-cellulose Chromatography**—Samples were dissolved in 5 µl of running buffer containing 1:1.5 (v/v) saturated NH<sub>4</sub>SO<sub>4</sub> and 1.5 M KH<sub>2</sub>PO<sub>4</sub>, pH 3.60, and blotted on Polygram® CEL 300 polyethyleneimine-cellulose thin-layer chromatography plates (Macherey-Nagel). Plates were developed in 1:1.5 (v/v) saturated NH<sub>4</sub>SO<sub>4</sub> and 1.5 M KH<sub>2</sub>PO<sub>4</sub>, pH 3.60 (R<sub>f</sub>(c-di-GMP) 0.2, R<sub>f</sub>(pGpG) 0.4), dried, and exposed on a Storage PhosphorScreen (Amersham Biosciences). The intensity of the various radioactive species was calculated by quantifying the intensities of the relevant spots using ImageJ software, version 1.33.

**Limited Tryptic Proteolysis**—To 90 µl of purified hexahistidine-tagged protein samples (0.5–11 mg/ml) dissolved in PDE Reaction Buffer (see above), 10 µl of trypsin solution (2 µg/ml trypsin in 1 mM HCl and 250 mM NaCl) was added. After incubation for 5 min at 37 °C, 2 µl of freshly prepared phenylmethylsulfonyl fluoride (AppliChem) solution (0.1% in ethanol) was added, and the reaction was filtered through a 0.45-µm syringe filter (Whatman) before the digest products were separated by gel filtration. Gel filtration experiments were performed on a SMART System using a Superdex 75 column (Amersham Biosciences) at a flow rate of 80 µl/min. The buffer contained 250 mM NaCl, 25 mM Tris, pH 8.0, 10 mM MgCl<sub>2</sub>, and 5 mM β-mercaptoethanol. Fractions of 80 µl were collected for the phosphodiesterase activity assay and for UV cross-linking experiments.

**UV Cross-linking with [<sup>33</sup>P]GTP and [<sup>33</sup>P]c-di-GMP**—Protein samples were incubated for 10 min on ice in PDE reaction buffer containing 10 µM c-di-GMP, 100 µM GTP, and [<sup>33</sup>P]c-di-GMP (0.75 µCi, 6000 Ci/mmol) or [<sup>33</sup>P]GTP (0.75 µCi, 3000 Ci/mmol). Samples were irradiated at 254 nm for 20 min on an ice-cooled, parafilm-wrapped 96-well aluminum block in an RPR-100 photochemical reactor with a RPR-3500 UV lamp (The Southern New England Ultraviolet Co.). After irradiation, samples were mixed with 2× SDS-PAGE sample buffer (250 mM Tris-HCl, pH 6.8, 40% glycerol, 8% SDS, 2.4 M β-mercaptoethanol, 0.06% bromophenol blue, 40 mM EDTA) and heated for 5 min at 95 °C. Labeled proteins were separated by SDS-PAGE and quantified by autoradiography.

**HPLC Analysis and ESI-MS Mass Spectrometry**—Reaction products were analyzed on an Agilent 1100 analytical reverse phase high performance liquid chromatography system with a diode array detector at 254 nm. Macherey-Nagel CC125/3 LiChrospher 100 RP-18, 5-µm particle size, was used at 30 °C with 25 mM triethylammonium carbonate buffer, pH 7.0, containing 5% (v/v) methanol as mobile phase and a flow rate of 0.3 ml/min. ESI-MS mass spectra were measured on an Esquire 3000plus (Bruker Daltonics) and on a TSQ7000 (Finnigan) mass spectrometer. Matrix-assisted laser desorption ionization spectra were measured on a Reflex III spectrometer (Bruker Daltonics).

TABLE I  
Comparison of specific PDE activities in *C. crescentus* crude extracts and purified CC3396

Strain/protein	PDE activity		DGC activity <sup>a</sup>
	c-di-GMP-specific	pGpG-specific	
<i>C. crescentus</i> CB15 <sup>b</sup>	0.12 ± 0.02 μmol/(mg min)	0.054 ± 0.004 μmol/(mg min)	ND <sup>c</sup>
UJ2812 (ΔCC3396) <sup>b</sup>	0.02 ± 0.01 μmol/(mg min)	ND	ND
CC3396-His <sub>6</sub> <sup>d</sup>	2.42 ± 0.28 μmol/(μmol min)	0.12 ± 0.06 μmol/(μmol min)	10 ± 5 pmol/(μmol min)

<sup>a</sup> Diguanylate cyclase activity of purified CC3396-His<sub>6</sub> was determined as indicated in Ref. 22.

<sup>b</sup> c-di-GMP and pGpG-specific activity of 100,000 × g supernatant as measured by TLC.

<sup>c</sup> ND, not determined.

<sup>d</sup> c-di-GMP and pGpG-specific activity of purified CC3396-His<sub>6</sub> as measured by thin layer chromatography.

## RESULTS

**PDE Activity in the Soluble Fraction of *C. crescentus* Cell Extracts**—To analyze the *C. crescentus* protein fractions for c-di-GMP-specific PDE activity, we developed an enzymatic assay, which is based on the hydrolysis of radiolabeled c-di-GMP and separation of the products on thin layer chromatography plates (see “Materials and Methods”). The constitutive active PleD mutant form, PleD\*-H6 (22), was purified to homogeneity and used to enzymatically convert [<sup>33</sup>P]GTP to [<sup>33</sup>P]-c-di-GMP. When purified [<sup>33</sup>P]-c-di-GMP was added to aliquots of the dialyzed 100,000 × g supernatant of cell extracts of *C. crescentus* wild-type strain CB15, the dicyclic nucleotide was rapidly hydrolyzed (Table I), arguing for the presence of a potent PDE activity in the soluble fraction of these cells.

A total of five genes encoding soluble EAL proteins were found on the *C. crescentus* chromosome. To identify a candidate PDE protein and to verify that it contributes to the enzymatic activity found in cell extracts, we selected CC3396 for further analysis. This decision was mainly based on the relatively small size and simple domain architecture of CC3396 (Fig. 1B). An in-frame deletion mutation of gene CC3396 was generated, and extracts of the resulting mutant strain UJ2812 were assayed for PDE activity *in vitro*. As shown in Table I, PDE activity of strain UJ2812 was reduced by about 80% as compared with wild-type, arguing that under the conditions tested, CC3396 is responsible for a major fraction of the PDE activity of the cell.

**Purified CC3396 Is a c-di-GMP-specific PDE, Which Converts c-di-GMP into the Linear Form pGpG**—The above experiments suggested that CC3396 is a prime candidate for a soluble PDE in *C. crescentus*. A hexahistidine-tagged version of the CC3396 protein was expressed in *E. coli* and purified to homogeneity on a nickel affinity column. When used in the PDE assay described above, purified fractions of the CC3396 protein could readily hydrolyze radiolabeled c-di-GMP (Table I). Separation of the reaction mixture on TLC plates revealed that the labeled c-di-GMP was rapidly converted into a new nucleotide species (Fig. 2B). HPLC analysis (Fig. 2A) and mass spectrometry identified this compound as the linearized diguanylate derivative pGpG (Fig. 2C, *m/z* = 689.0, for c-di-GMP and *m/z* = 707.0 for pGpG). Although the conversion of c-di-GMP into pGpG was relatively rapid (turnover rate: 2.42 ± 0.28 min<sup>-1</sup>), GMP appeared as a secondary product of the reaction at an about 10-fold slower rate (Table I). Thus, CC3396 specifically and rapidly cleaves c-di-GMP into its linear form, whereas the formation of GMP might be a nonspecific byproduct of the enzymatic reaction. The PDE activity of CC3396 is highly specific for the cyclic dimer of GMP and showed no significant affinity for monocyclic nucleotides cGMP and cAMP (data not shown). Also, whereas Mg<sup>2+</sup> ions were critical for PDE activity, Ca<sup>2+</sup> showed a strong inhibitory effect on the hydrolysis of c-di-GMP (Table II). Under no conditions were we able to detect DGC activity of the purified protein, arguing that the GGDEF domain of CC3396 is not a DGC (Table I).

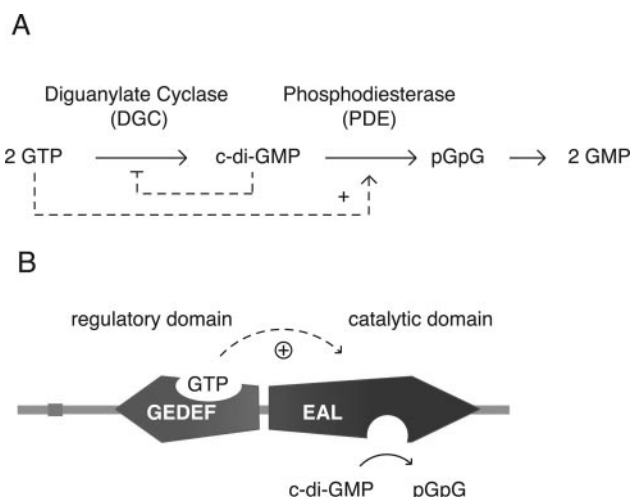


FIG. 1. Schematic of c-di-GMP synthesis and degradation (A) and model for GTP controlled PDE activity of CC3396 (B). A, the conversion of GTP into c-di-GMP is catalyzed by diguanylate cyclases that reside in the GGDEF domain (22, 41). Synthesis of c-di-GMP can be subject to negative allosteric feedback regulation (24) (indicated by the dashed line). Degradation of c-di-GMP into the linear form 5'-pGpG is catalyzed by the EAL domain and positively regulated by GTP (dashed line). The protein(s) responsible for the hydrolysis of pGpG into GMP have not been identified so far. B, the PDE activity of CC3396 is fully comprised within the EAL domain. The associated GGDEF domain with its altered active site motif (GEDEF) mediates activation of the C-terminal PDE by GTP. This domain lacks DGC activity but presumably binds GTP in a similar way, like the catalytic active GGDEF domains (22). We postulate that this novel role for GGDEF is either caused by the selective loss of DGC catalytic activity because of a slightly altered active site pocket formed by the GDEEF motif or is the result of an altered interaction surface of the DGC that prevents dimerization.

**Stimulation of the c-di-GMP-specific PDE Activity of CC3396 by GTP**—The activity of monocyclic PDEs is controlled by binding small effector molecules (including cAMP or cGMP) to N-terminal regulatory domains (5). To test the possibility that CC3396 could also be allosterically regulated, we measured the c-di-GMP-specific PDE activity of CC3396 in the presence or absence of different nucleotides (Table II). cAMP, cGMP, and dibutyryl-cGMP did not affect PDE activity of CC3396. Similarly, AMP, ATP, GMP, and GDP showed no effect. However, when the reaction mixture was supplemented with GTP (100 μM) the initial rate of the reaction increased by about 40-fold to 106.8 ± 1.5 μmol of c-di-GMP formed per μmol of protein and minute (Table II, Fig. 2B). The same positive effect was observed for an equimolar mixture of either GTP and GDP or GTP and GMP, arguing that both GDP and GMP do not counteract the positive effect of GTP. Interestingly, the GTP-activated form of CC3396 quantitatively converted c-di-GMP into the linear form pGpG, but failed to produce substantial amounts of GMP (Fig. 2, A and B, Table I). Together this suggested that the enzymatic activity of CC3396 responsible for the cleavage of c-di-GMP into pGpG is positively controlled

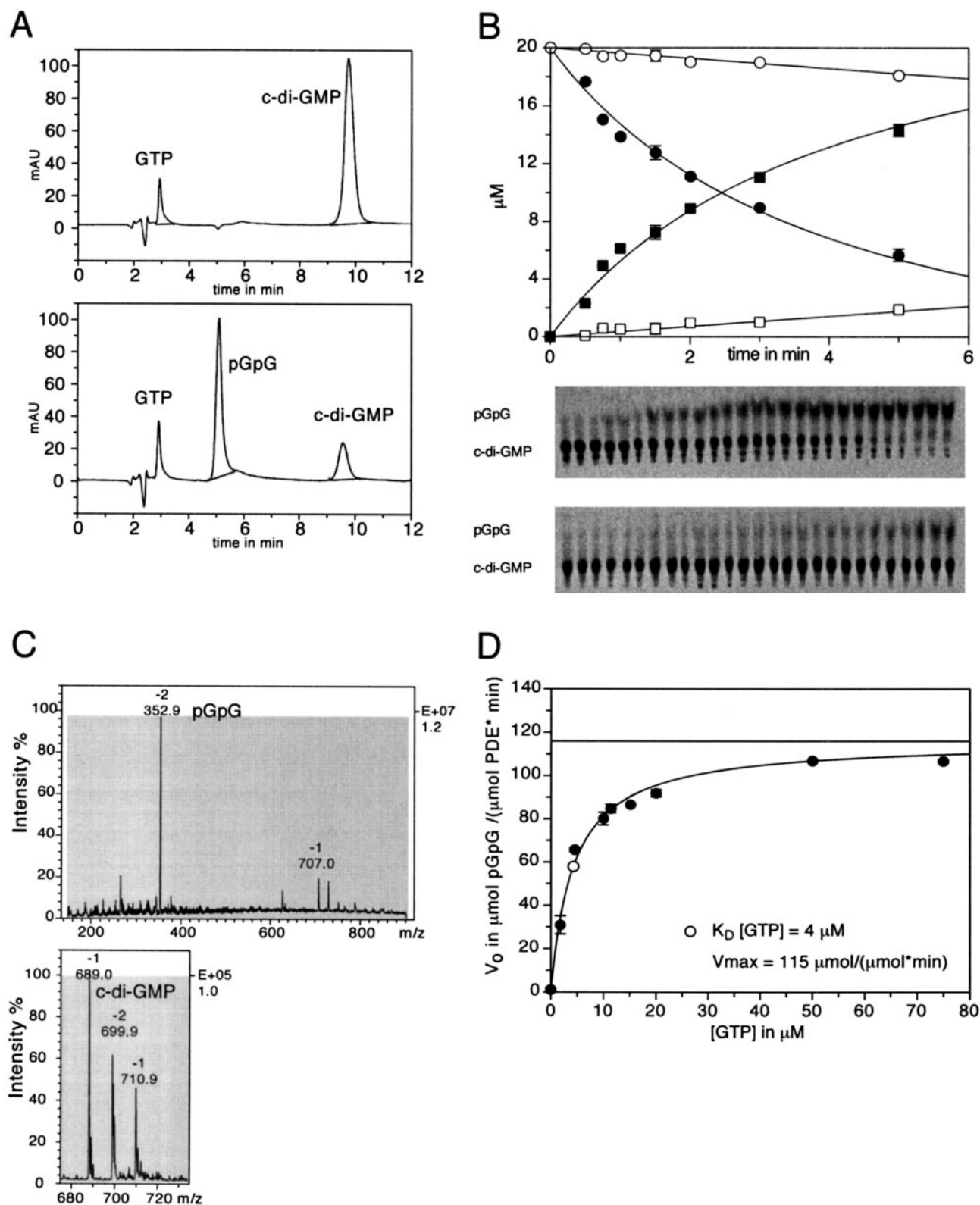


FIG. 2. *C. crescentus* protein CC3396 is a phosphodiesterase. **A**, HPLC analysis of the PDE reaction products. Purified CC3396 protein (5  $\mu\text{M}$ ) was incubated for 1 min with 100  $\mu\text{M}$  *c*-di-GMP, and 4  $\mu\text{M}$  GTP. Nucleotides were separated on a RP-18 column before (top panel) and after the enzymatic reaction (bottom panel), and fractions were analyzed by ESI-MS. GTP, which was added to activate the reaction, was not hydrolyzed. **B**, PDE activity of CC3396 in the absence (open symbols) or presence of GTP (4  $\mu\text{M}$  GTP, closed symbols). The *c*-di-GMP hydrolysis activity of purified CC3396 is indicated as a function of the absolute concentrations of *c*-di-GMP (circles) and pGpG (squares) as determined by thin layer chromatography. Reactions included 150 nM purified CC3396 protein and 20  $\mu\text{M}$  *c*-di-GMP and were incubated at 30  $^\circ\text{C}$  in buffer as described under "Materials and Methods." The polyethyleneimine-cellulose thin layer chromatogram with the raw data is shown below the graph with each time point spotted in triplicate (upper panel, with GTP; lower panel without GTP). **C**, mass spectrometry analysis of the reaction products of the CC3396 PDE. Mass spectrometry analysis of the reaction product of the PDE (top panel) and *c*-di-GMP (bottom panel) as shown in **A** and **B**. Top panel, ESI-MS of pGpG ( $m/z$  -) 352.9 (pGpG) $^{2-}$ , and 707.0 (pGpG) $^{-}$ . Bottom panel, ESI-MS of *c*-di-GMP  $m/z$  - 689.0 [*c*-di-GMP\*H] $^{-}$ ,  $m/z$  - 699.9 [(*c*-di-GMP) $_2$ \*H\*Na] $^{2-}$ ,  $m/z$  - 710.9 [*c*-di-GMP\*Na] $^{-}$ . **D**, determination of the equilibrium constant for GTP. Initial velocities of the PDE reaction were measured at increasing concentrations of GTP and  $V_{\text{max}}/2$  was determined to be 4  $\mu\text{M}$ .

TABLE II  
Activation of c-di-GMP-specific PDE by GTP

Specific activity (initial velocities) of purified CC3396 was determined in the presence of 10  $\mu\text{M}$  c-di-GMP and one additional nucleotide (100  $\mu\text{M}$ ). All reaction mixtures (except the no  $\text{Mg}^{2+}$  control) contained 10 mM  $\text{Mg}^{2+}$  and 10 mM  $\text{Ca}^{2+}$  that were used to show PDE inhibition by calcium ions.

Nucleotide	PDE activity $\mu\text{mol c-di-GMP}/\mu\text{mol min}$
AMP	1.93 $\pm$ 0.08
ATP	2.09 $\pm$ 0.22
cAMP	1.17 $\pm$ 0.46
cGMP	2.13 $\pm$ 0.32
dibu-cGMP <sup>a</sup>	1.79 $\pm$ 0.18
GMP	1.87 $\pm$ 0.20
GDP	1.92 $\pm$ 0.40
GTP	106.8 $\pm$ 1.5
GTP + GDP	113.2 $\pm$ 1.9
GTP + GMP	97.2 $\pm$ 1.5
GTP, no Mg	0.23 $\pm$ 0.10
GTP + Ca	1.61 $\pm$ 0.37

<sup>a</sup> 200  $\mu\text{M}$ .

by GTP, whereas the consecutive hydrolysis step, which generates GMP is probably a nonspecific side reaction and not subject to allosteric control by GTP. It is important to note that we found no indication for GTP hydrolysis during the enzymatic reaction in the presence of the inducer (Fig. 2A).

When logarithmically growing cells were analyzed by nucleotide extraction and HPLC, the internal concentration of c-di-GMP was determined to be 1.1  $\mu\text{M}$  ( $\pm$  0.11  $\mu\text{M}$ ) (data not shown). This is well below the  $K_m$  for c-di-GMP, which was determined for the basal level PDE activity of CC3396 ( $>$ 100  $\mu\text{M}$ ). To test if GTP activation substantially lowers the  $K_m$  for c-di-GMP to a physiologically relevant level, PDE activity was determined at different substrate concentrations. The  $K_m$  for c-di-GMP in the presence of 4  $\mu\text{M}$  GTP (at half-maximal PDE activity, see below) was determined to be 420 nM, close to the cellular concentration of c-di-GMP measured in growing cells.

The intracellular concentration of GTP in bacterial cells growing exponentially in rich medium is in the submillimolar range (29, 30) but can drop by 70–80% upon entry into stationary phase (29). To find out if the concentration of GTP required for activation of CC3396 is physiologically relevant, the  $K_D$  for GTP was determined at saturating substrate concentrations. Half-maximal induction of CC3396 was found to occur at a GTP concentration of 4  $\mu\text{M}$ , well below the GTP concentrations normally found in bacterial cells (Fig. 2D). The  $V_{\text{max}}$  of the GTP-activated protein was 115  $\pm$  4  $\mu\text{mol}/(\mu\text{mol min})$  (Fig. 2D). This argues that under physiological conditions promoting cell growth and division, the PDE activity of CC3396 is likely to be fully induced.

**The PDE Activity of CC3396 Resides in the C-terminal EAL Domain**—The observation that CC3396 harbors PDE but lacks DGC activity raised the question of whether the enzymatic activity is entirely comprised within the GGDEF or the EAL domain, or is maybe the result of a catalytic interaction between the two domains. To distinguish between these possibilities, we attempted to separate the two domains by a limited tryptic digest of the full-length CC3396 protein and to determine the enzymatic activities of the individual domains. Treatment with trypsin resulted in the specific cleavage of CC3396 into two distinct peptide fragments of  $\sim$ 30 and 27 kDa in size, according to their migration behavior in polyacrylamide gels (Fig. 3A). Separation of these two cleavage products by gel filtration, followed by mass spectrometry analysis (Fig. 3, C and D) revealed that the slightly larger peptide corresponds to the N-terminal portion of CC3396, which includes the entire GGDEF domain (amino acids 1–279; fractions 8 and 9 in Fig.

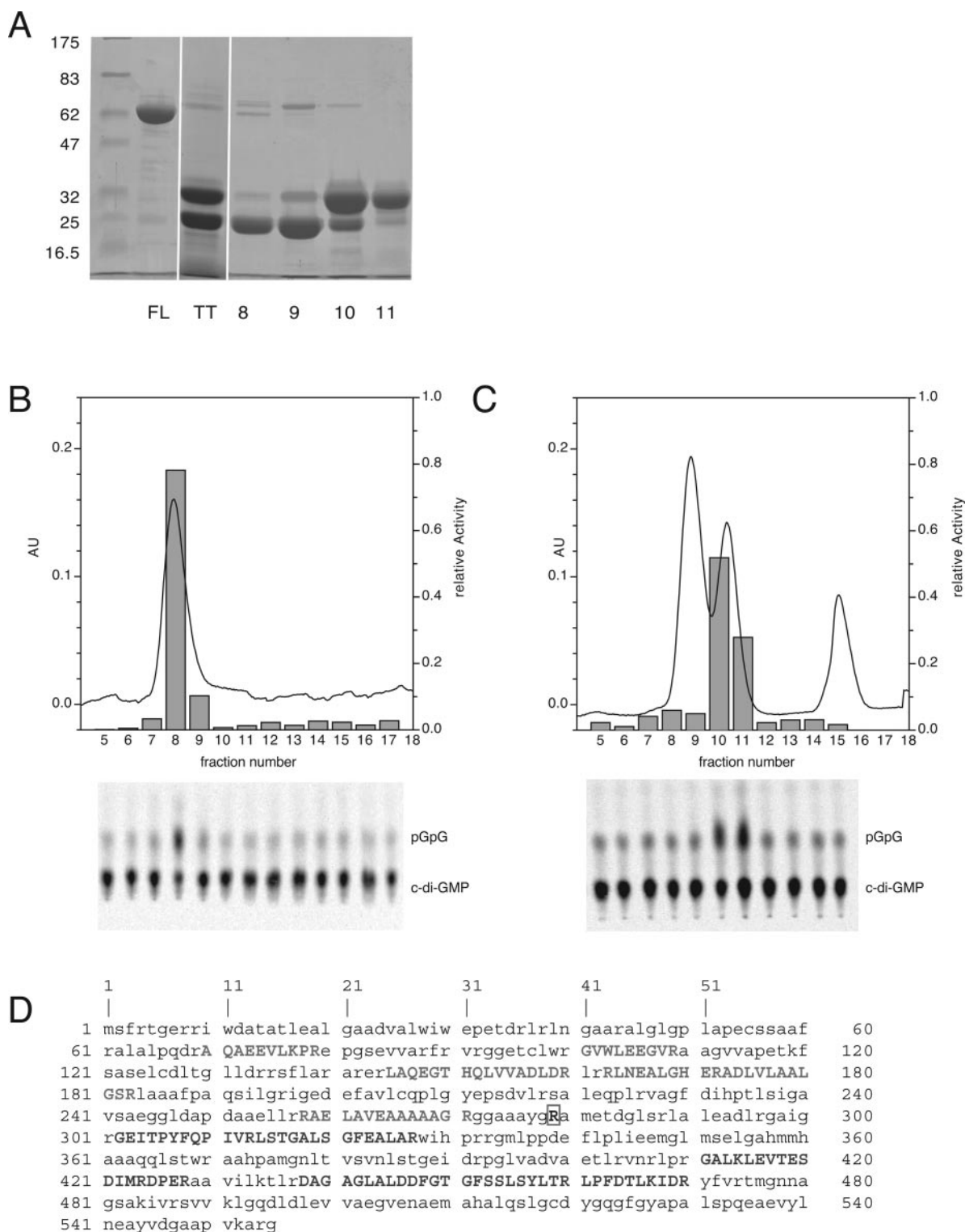
3C), whereas the smaller peptide corresponds exactly to the C-terminal EAL domain (amino acids 280–554; fractions 10 and 11 in Fig. 3C). The cleavage site mapped to the Arg<sup>279</sup> residue positioned in the center of the linker that connects the GGDEF and the EAL domain (Fig. 3D). It is reasonable to assume that the two domains can be separated by proteolysis because this charged residue is easily accessible for the protease because of its position in the flexible inter-domain linker.

PDE activity was found exclusively in fractions 10 and 11 of the gel filtration column used to separate the tryptic digest of CC3396 (Fig. 3C). Because fractions 10 and 11 contain the C-terminal EAL fragment, this strongly supported the view that the c-di-GMP-specific PDE activity is fully contained within the EAL domain. As shown in Table III, the specific activity of the separated EAL domain is similar to the activity found for the full-length CC3396 protein, arguing that the overall PDE activity is not significantly reduced upon separation of the catalytically active EAL from the GGDEF domain. Interestingly, when analyzing a CC3396 mutant with a mutation in the highly conserved aspartic acid residue of the EAL motive (E323Q), we found that both PDE activity and induction by GTP was not affected by this change (Table III). *In vivo* studies with the *Vibrio cholerae* EAL protein VieA had shown that a glutamate to alanine exchange at this position resulted in loss of activity (19). It is possible that the more conservative mutation chosen for CC3396 might still support PDE activity.

**Allosteric Activation of the PDE Activity in EAL Through Binding of GTP to the GGDEF Domain**—Whereas the EAL signature sequence of the C-terminal EAL domain is conserved in CC3396, the GGDEF domain has one of the highly conserved Gly residues of the active site (A-site) motif (24) replaced by Glu (GEDEF) (Fig. 3D). It is possible that this altered A-site in GGDEF is still able to bind GTP but cannot catalyze the diguanylate cyclase reaction. Such an altered domain might have been recruited as a regulatory module for the PDE activity residing in the C-terminal EAL domain. This would be in agreement with the observation that CC3396 has no apparent DGC activity (Table I). Also, a regulatory role for the GGDEF domain would be consistent with the finding that the isolated EAL domain almost fully retained the specific PDE activity of full-length CC3396, but in contrast to the intact protein could not be activated by GTP (Table III).

To obtain evidence in support of this idea we performed UV cross-link experiments with [<sup>33</sup>P]c-di-GMP and [<sup>33</sup>P]GTP using purified full-length CC3396 and the two individual domains separated by trypsin treatment (Fig. 3A). [<sup>33</sup>P]c-di-GMP specifically bound to full-length CC3396 and to the C-terminal EAL domain, but not to the N-terminal GGDEF domain fragment (Fig. 4A). In contrast, [<sup>33</sup>P]GTP, while also cross-linking to the full-length protein, did not bind to the EAL domain fragment but instead specifically reacted with the N-terminal GGDEF domain fragment (Fig. 4B). This suggested that GTP imposes allosteric control on the PDE enzyme activity of CC3396 by binding to its regulatory GGDEF domain.

Catalytically active GGDEF domains bind GTP in their A-site pocket, which in part is formed by a loop structure consisting of the highly conserved GGDEF (often GGEEF) motif (24). One possibility is that the slightly altered A-site motif (GEDEF) of the N-terminal domain of CC3396 has retained the ability to bind GTP and in response activates the associated EAL domain. To test this we generated a mutant CC3396 protein with the A-site motif changed to GQNEF. As shown in Table III, the mutant fully retained its PDE activity. But in contrast to the wild-type protein, the PDE activity was more or less constitutive with a 10-fold higher basal level activity in the absence of GTP as compared with wild-type (Table III). The



**FIG. 3. The PDE activity of CC3396 resides in the C-terminal EAL domain.** **A**, SDS-polyacrylamide gel with purified full-length CC3396 (*FL*), CC3396 after trypsin treatment (see “Materials and Methods”) (*TT*), and elution fractions 8–11 of the gel filtration column used to separate the tryptic fragments (see “Materials and Methods” and *panel C*). Note that *lane TT* was pasted from an independent gel. Samples of undigested (**B**) and trypsin-digested CC3396 protein (**C**) were separated by gel filtration (see “Materials and Methods.”) The TLC plates with the resolved reaction products originating from each fraction are shown *below* the graphs. The *bars* in the graphs indicate the relative activity measured for each fraction, and the *curve* shows the protein concentration as determined by UV spectrometry. The protein peak of fractions 8 and 9 in *panel C* corresponds to the N-terminal GGDEF domain of CC3396, and the protein peak of fractions 10 and 11 (*C*) corresponds to the C-terminal EAL domain of CC3396. Note that on the gel filtration column, the N-terminal GGDEF fragment runs at the position of a dimer, whereas the full-length CC3396 protein and the N-terminal EAL fragment run at the equivalent position of monomers. Fraction 15 corresponds to the cleaved C-terminal His tag, as determined by antibody staining with anti-His antibody. **D**, mass spectrometry analysis of the peptides originating from a tryptic digest of fractions 9 and 10 from *panel C*. A total of seven fragments of the GGDEF domain of CC3396 could be assigned to fraction 9, and a total of six fragments of the EAL domain could be assigned to fraction 10 digest. The corresponding fragments are highlighted in *capital letters*. LC-MS analysis of the undigested sample of fraction 10 revealed a mass of 29650.86 ( $\Delta$ Da 4.16) (amino acids 280–554, theoretical mass: 29655.0). The proposed trypsin cleavage site (Arg<sup>279</sup>) is highlighted.



TABLE III  
Activation of CC3396 wild-type and mutant forms by GTP

Protein	c-di-GMP-specific PDE activity <sup>a</sup>	
	10 $\mu\text{M}$ c-di-GMP	4 $\mu\text{M}$ GTP
CC3396	2.42 $\pm$ 0.28	57.9 $\pm$ 5.9
EAL domain <sup>b</sup>	1.32 $\pm$ 0.33	2.54 $\pm$ 1.10
E323Q	1.2 $\pm$ 4.2	76.2 $\pm$ 8.9
ED213QN	26.9 $\pm$ 3.8	77.3 $\pm$ 7.7

<sup>a</sup> PDE activity (initial velocities) was measured in the presence of 10  $\mu\text{M}$  c-di-GMP and in the presence or absence of 4  $\mu\text{M}$  GTP.

<sup>b</sup> The isolated EAL domain of CC3396 corresponds to fraction 10 of Fig. 3C.

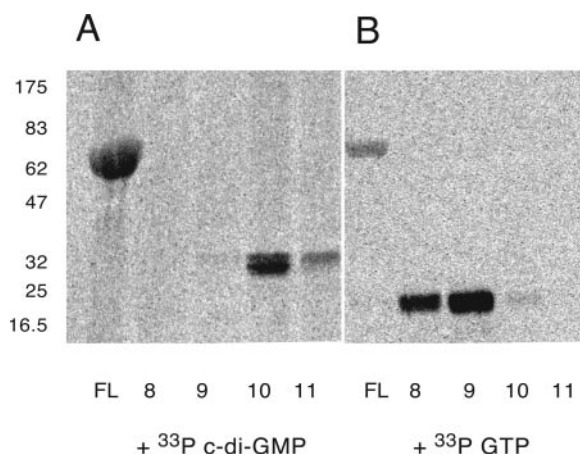


FIG. 4. GGDEF of CC3396 is a GTP binding regulatory domain. Full-length CC3396 (FL) and protein from elution fractions 8–11 of the gel filtration column used to separate the tryptic fragments were separated by SDS-PAGE (see Fig. 3A) and were used to UV cross-link with [<sup>33</sup>P]c-di-GMP (A) or [<sup>33</sup>P]GTP (B) as outlined under “Materials and Methods.” Samples were separated by SDS-PAGE, and the dried gels were analyzed by autoradiography.

addition of GTP resulted in an only 3-fold activation of the GQNEF mutant and resulted in similar activity as the GTP-induced wild-type protein (Table III). This implied that the amino acid changes in the A-site motif are able to switch this domain into the regulatory ON state and is consistent with the view that in CC3396 a catalytically inactive GGDEF domain imposes allosteric regulation by binding of GTP in its substrate binding pocket (A-site).

#### DISCUSSION

The pioneering work of the late Moshe Benziman and collaborators has not only identified dicyclic guanosine monophosphate as a signaling molecule involved in bacterial metabolism, but has also led to the recognition of proteins containing GGDEF and EAL domains as being involved in the synthesis and breakdown of c-di-GMP (reviewed in Ref. 6). Building on this foundation, an increasing number of genetic studies have in recent years highlighted a global role for c-di-GMP as a signaling molecule in bacteria. Most of these studies have reported mutant and/or overexpression phenotypes of proteins containing GGDEF or EAL domains (9–21). The common pattern appearing from these studies is that genetic changes associated with an increase of the cellular concentration of c-di-GMP negatively modulates cell motility and induce biofilm formation, whereas genetic modifications that led to a presumable decrease of c-di-GMP in the cell had the opposite effect. However, limited information is available on the downstream activities and possible targets of c-di-GMP and on the specific biochemical properties of enzymes involved in synthesis and hydrolysis of c-di-GMP. Genetic studies had predicted that GGDEF domains are DGCs and that EAL domains should harbor the c-di-GMP-specific PDE activity. But whereas many

of the several thousand bacterial GGDEF and EAL proteins listed in the non-redundant data bases have either a GGDEF or an EAL domain fused to other signaling domains, a large fraction combines both domains in the same polypeptide (31). A similar heterogeneity is found for cNMP (cAMP or cGMP)-specific cyclases and PDEs in eukaryotic cells, where several families of each enzyme class vary in ligand and co-factor specificities, in regulatory properties, and in tissue distribution (1, 4). This raised several important questions: Are the enzymatic activities responsible for the “make and break” of c-di-GMP really confined to these highly modular single domains? And if so, do all multidomain proteins that contain both a GGDEF and an EAL domain harbor both activities or have some of these proteins “specialized” in that they catalyze only the synthesis or degradation of c-di-GMP, respectively? The few examples studied so far have either been associated with DGC or PDE activity (25). No bifunctional enzyme has been described as yet. And finally, how would these activities be controlled if no obvious regulatory domains are fused to GGDEF or EAL?

Recent biochemical and structural studies have proposed a catalytic and regulatory mechanism for the synthesis of c-di-GMP by the GGDEF protein PleD (22, 24). Here we show that CC3396, a GGDEF-EAL protein of *C. crescentus* harbors c-di-GMP-specific PDE activity but lacks DGC activity. Analysis of the catalytic activities of the individual domains strongly suggested that the PDE activity of CC3396 is confined to the C-terminal EAL domain, and does not depend on the physical presence of the N-terminal GGDEF domain. To our knowledge, this is the first report that directly links an isolated EAL domain with the ability to catalyze the hydrolysis of c-di-GMP *in vitro*. Our data further propose a regulatory role for the N-terminal GGDEF domain of CC3396. The *in vitro* PDE activity of CC3396 is increased about 40-fold upon addition of GTP. Activation of the PDE activity seems to occur via the reduction of the  $K_m$  for c-di-GMP from above 100  $\mu\text{M}$  in the absence of GTP to 420 nM when GTP was present. Several lines of evidence suggest that GGDEF mediates this allosteric control through an interaction with the associated EAL domain. (i) Whereas the basal level PDE activity of full-length CC3396 and the isolated EAL domain are comparable, GTP activation could only be detected if the GGDEF domain was present. (ii) Compared with the *bona fide* DGC PleD (22), the GGDEF domain of CC3396 has a slightly altered consensus sequence A-site motif (GEDEF). Consistent with this, CC3396 does not seem to possess diguanylate cyclase activity *in vitro*. (iii) GTP specifically binds to the GGDEF but not to the associated catalytic EAL domain. (iv) A defined mutation in the A-site motif of the GGDEF domain (GQNEF) abolished allosteric activation and resulted in a constitutive activity of the associated EAL domain. This last observation implies that the GGDEF domain of CC3396 is a GGDEF-like domain, which is still able to bind GTP in the A-site cavity with a relatively high affinity ( $K_D$  4  $\mu\text{M}$ ) but does not catalyze the formation of c-di-GMP. If so, an original GGDEF domain might have been recruited as sensory domain for GTP through the loss of its catalytic function and the evolution of a regulatory interaction with EAL. If such a regulatory role of a GGDEF domain has indeed evolved from an enzymatically active GGDEF domain, two scenarios are possible. Either the GGDEF domain has lost DGC activity because key catalytic residues are missing, or because, in the context of the GGDEF-EAL composite protein, it is no longer able to form a dimeric structure required to condense two GTP molecules into c-di-GMP (24).

Thus, we propose that GGDEF domains, depending on their sequence conservation or on their oligomeric status, can have

two alternative biological activities and can play different roles in the controlled formation and hydrolysis of c-di-GMP. It is conceivable that at least a subgroup of the large family of bacterial GGDEF-EAL composite proteins represents PDEs with an associated regulatory GGDEF domain that can act as GTP sensor. At the same time, GGDEF-EAL proteins may exist that combine both a GGDEF-born DGC and an EAL-associated PDE activity. And finally it is equally possible that the EAL domain of GGDEF-EAL composite proteins also engages in a regulatory function by controlling the N-terminal DGC activity in response to the prevailing c-di-GMP concentration. Such a regulatory mechanism has been proposed recently for the DGC activity of the PleD response regulator, which is under tight negative allosteric control by its own product, c-di-GMP (24). A direct consequence of our findings is that each GGDEF or EAL domain will first have to be carefully analyzed biochemically before it can be assigned a catalytic or regulatory role.

The model that we propose for catalysis and regulation of the CC3396 PDE is shown in Fig. 1B. The protein architecture with an N-terminal regulatory and a C-terminal catalytic domain is reminiscent of cNMP-specific PDEs found in eukaryotes (e.g. PDE5, a phosphodiesterase highly specific for cGMP has two non-catalytic cGMP binding sites located at the N terminus). Binding of cGMP to these allosteric sites stimulates PDE activity, increases cGMP hydrolysis, and thus forms a negative feedback mechanism regulating the cellular cGMP concentration (32). Other N-terminal regulatory domains of cNMP-specific PDEs can serve as phosphorylation sites, can interact with transducing proteins, or act as an allosteric binding site for  $\text{Ca}^{2+}$ /calmodulin effectors (5). It is reasonable to assume that c-di-GMP-specific PDEs in bacteria are also tightly controlled and that the allosteric control of CC3396 reported here represents a general phenomenon of this class of enzymes.

PDE activity is likely to be a critical component of c-di-GMP signaling in bacterial cells. But why would phosphodiesterase activity be coupled to the cellular concentration of GTP? Römmling and colleagues (18) have reported that upon expression of the DGC protein AdrA in *Salmonella typhimurium*, the cellular GTP to c-di-GMP ratio reverses from about 100:1 to 1:10 (18). Thus, it is possible that when c-di-GMP synthesis is fully induced, uncontrolled hydrolysis of c-di-GMP to pGpG and GMP would deplete the cellular GTP pool. A massive reduction of the cellular GTP concentration has been reported as a consequence of the increased production of the "alarmone" pppGpp upon amino acid starvation in *Bacillus subtilis* (33). Similarly, the GTP concentration decreases considerably upon nitrogen starvation in *C. crescentus* (34). It is possible that to prevent drainage of the cellular GTP pool, specific PDEs are quickly turned off when the GTP concentration drops under a threshold level. Considering that the  $K_D$  for GTP of CC3396 is about 4  $\mu\text{M}$ , one would expect such a threshold GTP concentration to be in the low micromolar range. Together with the observation that DGCs can be subject to tight allosteric feedback inhibition by their own product (24), this could be interpreted as a simple means for flux-controlled sensitivity, which would allow breaching the threshold for signal transduction by either increased production or decreased degradation of the second messenger. Alternatively, the prevailing GTP level of the cell itself could be used as a physiological signal to control the internal concentration of c-di-GMP through the controlled activity of PDEs. A drastic drop of the GTP concentration to the low micromolar range could lead to a rapid and substantial increase of the cellular c-di-GMP concentration through the inhibition of one or several key PDEs, which respond to GTP in a similar manner as observed for CC3396. Whereas such a regulatory role for GTP remains speculative, cellular GTP pools

are known to affect developmental transitions in bacteria. A decrease in the cellular GTP concentration, but not of other purine or pyrimidine nucleotides, correlates with the initiation of morphological differentiation during nutrient starvation of *B. subtilis* and *Streptomyces griseus* (29, 35, 36). The signal responsible for the induction of sporulation is the reduced GTP pool, rather than pppGpp, which is formed under the same starvation conditions (29). The cellular GTP concentration is sensed by CodY, a transcriptional repressor of several sporulation and motility genes, whose repression activity depends on binding of GTP with a  $K_D$  in the physiologically relevant millimolar range (37, 38). It remains to be shown if the GTP concentration plays a similar regulatory role in cellular c-di-GMP signaling.

Finally, what is the physiological role of CC3396? CC3396 substantially contributes to the PDE activity in the soluble fraction of actively growing *C. crescentus* cells. It is possible that this protein adds to a more or less constant and rapid degradation of the freely diffusible cytoplasmic pool of c-di-GMP and would only be turned off under severe depletion of GTP. The cellular concentration of c-di-GMP has been determined to be about 1  $\mu\text{M}$  in growing *C. crescentus* cells (this study) or 5–10  $\mu\text{M}$  in cellulose producing *Acetobacter xylinum* (39). This is in good agreement with a  $K_m$  for c-di-GMP of 420 nM, which was determined for the PDE activity of CC3396 in the presence of GTP. It has been argued that specifically localized DGCs might act as "local pacemakers" of metabolic reactions resulting in cellular gradients of c-di-GMP (6, 40). In such a model, c-di-GMP synthesis and signaling would be locally confined and one would imagine that a strong and constitutive PDE activity is critical to spatially confine different c-di-GMP signaling pathways. Further studies are needed to test this idea more thoroughly.

**Acknowledgments**—We thank Tilman Schirmer and Helma Wennemers for helpful discussions, Thomas Augst and Paul Jenö for mass spectrometry analysis, and Nicholas Amiot for providing a sample of c-di-GMP.

#### REFERENCES

- Lucas, K. A., Pitari, G. M., Kazerounian, S., Ruiz-Stewart, I., Park, J., Schulz, S., Chepenik, K. P., and Waldman, S. A. (2000) *Pharmacol. Rev.* **52**, 375–414
- Kaupp, U. B., and Seifert, R. (2002) *Physiol. Rev.* **82**, 769–824
- Essayan, D. M. (2001) *J. Allergy Clin. Immunol.* **108**, 671–680
- Houslay, M. D., and Milligan, G. (1997) *Trends Biochem. Sci.* **22**, 217–224
- Conti, M., and Jin, S. L. (1999) *Prog. Nucleic Acids Res. Mol. Biol.* **63**, 1–38
- Jenal, U. (2004) *Curr. Opin. Microbiol.* **7**, 185–191
- D'Argenio, D. A., and Miller, S. I. (2004) *Microbiology* **150**, 2497–2502
- Ross, P., Weinhouse, H., Aloni, Y., Michaeli, D., Weinberger-Ohana, P., Mayer, R., Braun, S., de Wroom, E., van der Marel, G. A., van Boom, J. H., and Benziman, M. (1987) *Nature* **325**, 279–281
- Spiers, A. J., Kahn, S. G., Bohannon, J., Travisano, M., and Rainey, P. B. (2002) *Genetics* **161**, 33–46
- Drenkard, E., and Ausubel, F. M. (2002) *Nature* **416**, 740–743
- Aldridge, P., Paul, R., Goymer, P., Rainey, P., and Jenal, U. (2003) *Mol. Microbiol.* **47**, 1695–1708
- Huang, B., Whitechurch, C. B., and Mattick, J. S. (2003) *J. Bacteriol.* **185**, 7068–7076
- Bomchil, N., Watnick, P., and Kolter, R. (2003) *J. Bacteriol.* **185**, 1384–1390
- Guvener, Z. T., and McCarter, L. L. (2003) *J. Bacteriol.* **185**, 5431–5441
- Thomas, C., Andersson, C. R., Canales, S. R., and Golden, S. S. (2004) *Microbiology* **150**, 1031–1040
- Garcia, B., Latasa, C., Solano, C., Garcia-del Portillo, F., Gamazo, C., and Lasa, I. (2004) *Mol. Microbiol.* **54**, 264–277
- Choy, W. K., Zhou, L., Syn, C. K., Zhang, L. H., and Swarup, S. (2004) *J. Bacteriol.* **186**, 7221–7228
- Simm, R., Morr, M., Kader, A., Nitz, M., and Römmling, U. (2004) *Mol. Microbiol.* **53**, 1123–1134
- Tischler, A. D., and Camilli, A. (2004) *Mol. Microbiol.* **53**, 857–869
- Kirilina, O., Fetherston, J. D., Bobrov, A. G., Abney, J., and Perry, R. D. (2004) *Mol. Microbiol.* **54**, 75–88
- Johnson, M. R., Montero, C. I., Connors, S. B., Shockley, K. R., Bridger, S. L., and Kelly, R. M. (2005) *Mol. Microbiol.* **55**, 664–674
- Paul, R., Weiser, S., Amiot, N. C., Chan, C., Schirmer, T., Giese, B., and Jenal, U. (2004) *Genes Dev.* **18**, 1715–1727
- Galperin, M. Y., Nikolskaya, A. N., and Koonin, E. V. (2001) *FEMS Microbiol. Lett.* **203**, 11–21
- Chan, C., Paul, R., Samoray, D., Amiot, N. C., Giese, B., Jenal, U., and

- Schirmer, T. (2004) *Proc. Natl. Acad. Sci. U. S. A.* **101**, 17084–17089
25. Tal, R., Wong, H. C., Calhoun, R., Gelfand, D., Fear, A. L., Volman, G., Mayer, R., Ross, P., Amikam, D., Weinhouse, H., Cohen, A., Sapir, S., Ohana, P., and Benziman, M. (1998) *J. Bacteriol.* **180**, 4416–4425
26. Chang, A. L., Tuckerman, J. R., Gonzalez, G., Mayer, R., Weinhouse, H., Volman, G., Amikam, D., Benziman, M., and Gilles-Gonzalez, M. A. (2001) *Biochemistry* **40**, 3420–3426
27. Galperin, M. Y., Natale, D. A., Aravind, L., and Koonin, E. V. (1999) *J. Mol. Microbiol. Biotechnol.* **1**, 303–305
28. Ely, B. (1991) *Methods Enzymol.* **204**, 372–384
29. Lopez, J. M., Marks, C. L., and Freese, E. (1979) *Biochim. Biophys. Acta* **587**, 238–252
30. Bochner, B. R., and Ames, B. N. (1982) *J. Biol. Chem.* **257**, 9759–9769
31. Galperin, M. Y. (2004) *Environ. Microbiol.* **6**, 543–545
32. Corbin, J. D., and Francis, S. H. (1999) *J. Biol. Chem.* **274**, 13729–13732
33. Ochi, K., Kandala, J., and Freese, E. (1982) *J. Bacteriol.* **151**, 1062–1065
34. Chiaverotti, T. A., Parker, G., Gallant, J., and Agabian, N. (1981) *J. Bacteriol.* **145**, 1463–1465
35. Freese, E., Heinze, J. E., and Galliers, E. M. (1979) *J. Gen. Microbiol.* **115**, 193–205
36. Ochi, K. (1987) *J. Bacteriol.* **169**, 3608–3616
37. Ratnayake-Lecamwasam, M., Serror, P., Wong, K. W., and Sonenshein, A. L. (2001) *Genes Dev.* **15**, 1093–1103
38. Bergara, F., Ibarra, C., Iwamasa, J., Patarroyo, J. C., Aguilera, R., and Marquez-Magana, L. M. (2003) *J. Bacteriol.* **185**, 3118–3126
39. Weinhouse, H., Sapir, S., Amikam, D., Shilo, Y., Volman, G., Ohana, P., and Benziman, M. (1997) *FEBS Lett.* **416**, 207–211
40. Ross, P., Mayer, R., and Benziman, M. (1991) *Microbiol. Rev.* **55**, 35–58
41. Ryjenkov, D. A., Tarutina, M., Moskvina, O. V., and Gomelsky, M. (2005) *J. Bacteriol.* **187**, 1792–1798

### **3.2 Allosteric Control of Cyclic di-GMP Signaling**

B. Christen\*, M. Christen\*, R. Paul, F. Schmid, M. Folcher, P. Jenö, M. Meuwly and U. Jenal

**JBC** 281:32015-32024 (2006)

*\*These authors contributed equally to the work*

## Summary

In this publication we describe an important novel feature of GGDEF proteins, which produce the ubiquitous bacterial signaling molecule c-di-GMP. This paper reports the results of in depth structure-function analysis of an allosteric feedback inhibition mechanism that generally acts to regulate diguanylate cyclase activities in bacteria. The mechanism involves binding of the second messenger product, c-di-GMP at an inhibition site (I-site) that is coupled via a conserved beta-strand to the active site (A-site) of the enzyme. The study involves an array of biochemical and genetic techniques applied on various diguanylate cyclases to establish the sequence determinants of the I-site as well as the in vivo physiological relevance of I-site function. To assist the interpretation of the present data and to provide information on binding induced mobility, atomistically detailed simulations were carried out. Normal mode calculations on ligated and unligated PleD were used to analyze the structural transitions that occur during I-site binding of c-di-GMP. Allosteric product inhibition of diguanylate cyclases turns out to have fundamental functional and physiological implications, including threshold setting for c-di-GMP production by particular GGDEF proteins, which can contribute to precision, robustness, noise reduction and accelerated kinetics of c-di-GMP signaling.

The molecular modeling was performed by Franziska Schmid, kinetic data on PleD activity was provided by Ralf Paul, and the mass spectroscopic analysis of trypsin digested PleD was done by Suzette Moes and Paul Jenö

# Allosteric Control of Cyclic di-GMP Signaling\*<sup>§</sup>

Received for publication, April 13, 2006, and in revised form, June 21, 2006. Published, JBC Papers in Press, August 21, 2006, DOI 10.1074/jbc.M603589200

Beat Christen<sup>†1</sup>, Matthias Christen<sup>†1</sup>, Ralf Paul<sup>‡</sup>, Franziska Schmid<sup>§</sup>, Marc Folcher<sup>‡</sup>, Paul Jenoe<sup>‡</sup>, Markus Meuwly<sup>§</sup>, and Urs Jenal<sup>†2</sup>

From the <sup>†</sup>Biozentrum and the <sup>§</sup>Department of Chemistry, University of Basel, Klingelbergstrasse 70, 4056 Basel, Switzerland

Cyclic di-guanosine monophosphate is a bacterial second messenger that has been implicated in biofilm formation, antibiotic resistance, and persistence of pathogenic bacteria in their animal host. Although the enzymes responsible for the regulation of cellular levels of *c*-di-GMP, diguanylate cyclases (DGC) and phosphodiesterases, have been identified recently, little information is available on the molecular mechanisms involved in controlling the activity of these key enzymes or on the specific interactions of *c*-di-GMP with effector proteins. By using a combination of genetic, biochemical, and modeling techniques we demonstrate that an allosteric binding site for *c*-di-GMP (I-site) is responsible for non-competitive product inhibition of DGCs. The I-site was mapped in both multi- and single domain DGC proteins and is fully contained within the GGDEF domain itself. *In vivo* selection experiments and kinetic analysis of the evolved I-site mutants led to the definition of an RXXD motif as the core *c*-di-GMP binding site. Based on these results and based on the observation that the I-site is conserved in a majority of known and potential DGC proteins, we propose that product inhibition of DGCs is of fundamental importance for *c*-di-GMP signaling and cellular homeostasis. The definition of the I-site binding pocket provides an entry point into unraveling the molecular mechanisms of ligand-protein interactions involved in *c*-di-GMP signaling and makes DGCs a valuable target for drug design to develop new strategies against biofilm-related diseases.

A global signaling network that relies on the production of the second messenger cyclic diguanylic acid has recently been discovered in bacteria (1, 2). The *c*-di-GMP<sup>3</sup> system emerges as a regulatory mastermind orchestrating multicellular behavior and biofilm formation in a wide variety of bacteria (2). In addition, *c*-di-GMP signaling also plays a role in bacterial virulence

and persistence (3–7). The broad importance of this novel signaling molecule in pathogenic and non-pathogenic bacteria calls for careful analysis of the molecular mechanisms that control cellular levels of *c*-di-GMP and regulate its downstream targets. *c*-di-GMP is formed by the condensation of two GTP molecules (8–10) and is hydrolyzed to GMP via the linear intermediate pGpG (11–14). Two widespread and highly conserved bacterial protein domains have been implicated in the synthesis and hydrolysis of *c*-di-GMP, respectively (15). The breakdown of *c*-di-GMP is catalyzed by the EAL domain (12–14), and the diguanylate cyclase (8) activity resides in the GGDEF domain (10, 16). The highly conserved amino acid sequence GG(D/E)EF forms part of the catalytically active site (A-site) of the DGC enzyme (8). In agreement with this, mutations that change the GG(D/E)EF motif generally abolish the activity of the respective proteins (14, 16–18).

GGDEF domains are often found associated with sensor domains, arguing that DGC activity is controlled by direct signal input through these domains (1). The best understood example for controlled activation of a DGC is the response regulator PleD, which constitutes a timing device for *Caulobacter crescentus* pole development (17, 19, 20). PleD is activated during *C. crescentus* development by phosphorylation of an N-terminal receiver domain and, as a result, sequesters to the differentiating cell pole (17, 19). An additional layer of control was suggested by the crystal structure of PleD solved recently in complex with *c*-di-GMP (8) (Fig. 1). A *c*-di-GMP binding site was identified in the crystal, spatially separated from the catalytically active site (A-site). Two mutually intercalating *c*-di-GMP molecules were found tightly bound to this site, at the interface between the GGDEF and the central receiver-like domain of PleD (Fig. 1). Based on the observation that PleD activity shows a strong non-competitive product inhibition, it was proposed that this site might constitute an allosteric binding site (I-site) (8). Based on the observation that functionally important residues of the PleD I-site are highly conserved in a majority of GGDEF proteins listed in the data base, we tested the hypothesis that allosteric product inhibition is a general regulatory principle of bacterial diguanylate cyclases.

## MATERIALS AND METHODS

**Strains, Plasmids, and Media**—*Escherichia coli* and *Salmonella enterica* serovar Typhimurium strains were grown in Luria broth (LB). *C. crescentus* strains were grown in complex peptone yeast extract (21). For DGC activity assays *in vivo*, *E. coli* was plated onto LB Congo Red plates (Sigma, 50 µg/ml). To determine the IPTG induction phenotype, 3 µl of a liquid log phase culture was spotted onto LB Congo Red plates with-

\* This work was supported by Swiss National Science Foundation Fellowship 3100A0-108186 (to U. J.) and by a Swiss National Science Foundation Förderprofessur (to M. M.). The costs of publication of this article were defrayed in part by the payment of page charges. This article must therefore be hereby marked "advertisement" in accordance with 18 U.S.C. Section 1734 solely to indicate this fact.

<sup>§</sup> The on-line version of this article (available at <http://www.jbc.org>) contains supplemental text and Figs. S1–S4.

<sup>†</sup> These authors contributed equally to this work.

<sup>‡</sup> To whom correspondence should be addressed: Tel.: 41-61-267-2135; Fax: 41-61-267-2118; E-mail: [urs.jenal@unibas.ch](mailto:urs.jenal@unibas.ch).

<sup>3</sup> The abbreviations used are: *c*-di-GMP, cyclic diguanylic acid; pGpG, linear diguanylic acid; LB, Luria broth; DGC, diguanylate cyclase; PDE, phosphodiesterase; H6, hexa-histidine tag; rdar, red, dry, and rough; IPTG, isopropyl 1-thio-β-D-galactopyranoside; DgcA, diguanylate cyclase A; PdeA, phosphodiesterase A; CR, Congo Red; AC, adenylate cyclase; GC, guanylate cyclase.

## Diguanylate Cyclase Feedback Control

out and with 1 mM IPTG. Biofilm formation was quantified after overnight growth by staining with 1% Crystal Violet as described (22). Motility phenotypes were determined using LB or peptone yeast extract motility plates containing 0.3% Difco-Agar. The exact procedure of strain and plasmid construction is available on request.

**Random I-site Tetrapeptide Library**—The *dgcA* gene (CC3285) was amplified by PCR using primers #1006 and #1007 (for primer list see supplemental text). The PCR product was digested with NdeI and XhoI and cloned into pET21a (Novagen). In a next step a *dgcA*ΔRESΔ allele with a silent PstI restriction site was generated by splicing with overlapping extension PCR using primers #1129, #670, and #1132. The resulting PCR product was digested with NdeI and XhoI and cloned into pET42b (Novagen) to produce pET42b::*dgcA*ΔRESΔ. The PstI/XhoI fragment of pET42b::*dgcA*ΔRESΔ was replaced by 20 independent PCR products, which had been generated using pET42b::*dgcA*ΔRESΔ as a template and primers #1131 and #670. The resulting 20 independent random libraries were individually transformed into *E. coli* BL21 and screened on Congo Red plates (LB plates supplemented with 50 μg/ml Congo Red). As a control reaction, the deleted I-site was reverted back to the wild-type RESΔ motif by cloning the PCR product generated with primers #1130 and #670 into the PstI and XhoI site of pET42b::*dgcA*ΔRESΔ.

**Diguanylate Cyclase and Phosphodiesterase Activity Assays**—DGC reactions were performed at 30 °C with 0.5 μM purified hexahistidine-tagged DgcA or 5 μM PleD in DGC reaction buffer containing 250 mM NaCl, 25 mM Tris-Cl, pH 8.0, 5 mM β-mercaptoethanol, and 20 mM MgCl<sub>2</sub>. For inhibition assays the protein was preincubated with different concentrations of c-di-GMP (1–100 μM) for 2 min at 30 °C before 100 μM [<sup>33</sup>P]GTP (Amersham Biosciences) was added. The reaction was stopped at regular time intervals by adding an equal volume of 0.5 M EDTA, pH 8.0. DGC/PDE tandem assays were carried out using 1 μM hexahistidine-tagged DgcA, which was preincubated for 2 min in the presence or absence of 4.5 μM hexahistidine-tagged phosphodiesterase PdeA. The reaction was started by adding 100 μM [<sup>33</sup>P]GTP. The reactions were stopped at regular time intervals of 15 s by adding equal volumes of 0.5 M EDTA, pH 8.0, and their nucleotide composition was analyzed as described below.

Initial velocity ( $V_o$ ) and inhibition constants were determined by plotting the corresponding nucleotide concentration *versus* time and by fitting the curve according to allosteric product inhibited Michaelis-Menten kinetics with the program ProFit 5.6.7 (with fit function  $[c\text{-di-GMP}]_t = a(1)^*t/(a(2) + t)$ , where the initial velocity  $V_o$  is defined as  $a(1)/a(2)$ ) using the Levenberg-Marquardt algorithm.  $K_i$  values were determined by plotting  $V_o$  *versus* c-di-GMP concentration and using the following fit function,  $V_{o[c\text{-di-GMP}]} = V_{o[c\text{-di-GMP}] = 0} * (1 - ([c\text{-di-GMP}]/(K_i + [c\text{-di-GMP}])))$ .

**Polyethyleneimine Cellulose Chromatography**—Samples were dissolved in 5 μl of running buffer containing 1:1.5 (v/v) saturated NH<sub>4</sub>SO<sub>4</sub> and 1.5 M KH<sub>2</sub>PO<sub>4</sub>, pH 3.60, and blotted on Polygram® CEL 300 polyethyleneimine cellulose TLC plates (Macherey-Nagel). Plates were developed in 1:1.5 (v/v) saturated NH<sub>4</sub>SO<sub>4</sub> and 1.5 M KH<sub>2</sub>PO<sub>4</sub>, pH 3.60 ( $R_f(c\text{-di-GMP})$  0.2,

$R_f(pGpG)$  0.4), dried, and exposed on a storage phosphor imaging screen (Amersham Biosciences). The intensity of the various radioactive species was calculated by quantifying the intensities of the relevant spots using ImageJ software version 1.33.  $V_o$  and  $K_i$  were determined with the Software ProFit 5.6.7.

**UV Cross-linking with [<sup>33</sup>P]c-di-GMP**—The <sup>33</sup>P-labeled c-di-GMP was produced enzymatically using [<sup>33</sup>P]GTP (3000 Ci/mmol) and purified according to a previous study (14). Protein samples were incubated for 10 min on ice in DGC reaction buffer (25 mM Tris-HCl, pH 8.0, 250 mM NaCl, 10 mM MgCl<sub>2</sub>, 5 mM β-mercaptoethanol) together with 1 μM c-di-GMP and <sup>33</sup>P-radiolabeled c-di-GMP (0.75 μCi, 6000 Ci/mmol). Samples were then irradiated at 254 nm for 20 min in an ice-cooled, parafilm-wrapped 96-well aluminum block in an RPR-100 photochemical reactor with a UV lamp RPR-3500 (Southern New England Ultraviolet Co.). After irradiation, samples were mixed with 2× SDS-PAGE sample buffer (250 mM Tris-HCl at pH 6.8, 40% glycerol, 8% SDS, 2.4 M β-mercaptoethanol, 0.06% bromophenol blue, 40 mM EDTA) and heated for 5 min at 95 °C. Labeled proteins were separated by SDS-PAGE and quantified by autoradiography.

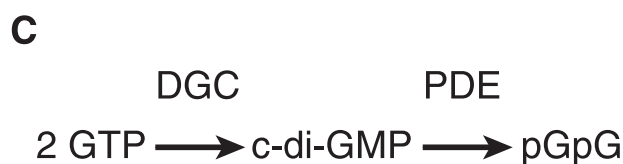
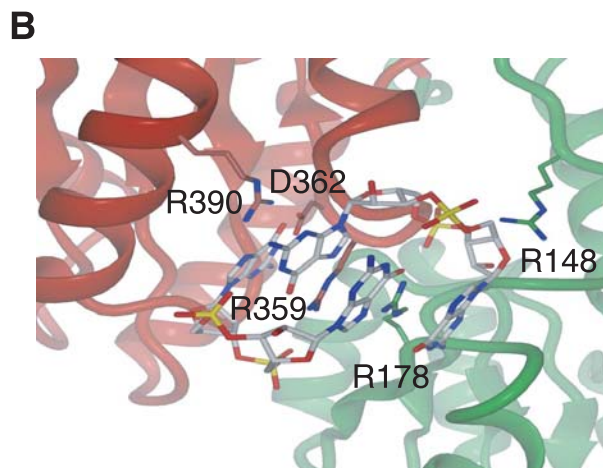
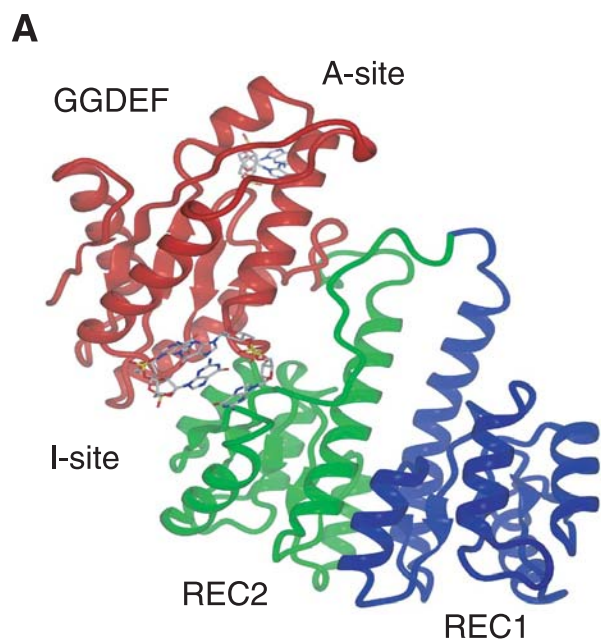
**Nucleotide Extraction and Analysis**—2.0 ml of *E. coli* cell cultures ( $A_{600}$  0.4) were harvested by centrifugation, and supernatant was discarded. The cell pellet was dissolved in 200 μl of 0.5 M formic acid, and nucleotides were extracted for 10 min at 4 °C. Insoluble cell components were then pelleted, and the supernatant was directly analyzed by chromatography. Nucleotides were extracted and separated according to a previous study (23) on a 125/4 Nucleosil 4000-1 polyethyleneimine column (Macherey-Nagel) using the SMART-System (Amersham Biosciences). The nucleotide peak corresponding to c-di-GMP was verified by co-elution with a chemically synthesized c-di-GMP standard.

**DgcA Protein Expression Levels**—DgcA protein expression levels in *E. coli* BL21 were determined by Western blot analysis using Anti-His(C-Term) antibody (Invitrogen) and horseradish peroxidase conjugate of goat anti-mouse IgG (Invitrogen) as secondary antibody. The protein concentration was determined by measuring the intensities of the relevant spots using ImageJ software version 1.33. Signals were calibrated to defined concentrations of purified wild-type DgcA.

**Molecular Modeling of PleD**—All-atom simulations were carried out using the CHARMM (24) program and the CHARMM22/27 force field (25). For additional information see the supplemental material.

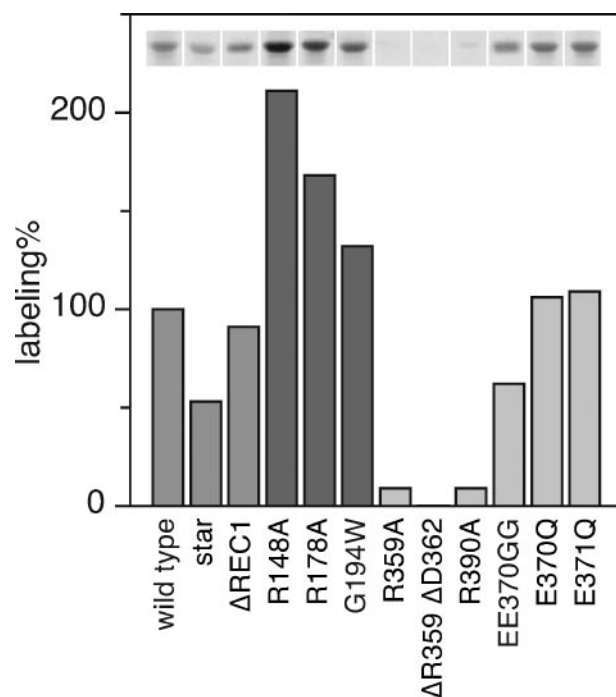
## RESULTS

**Feedback Inhibition of the PleD Diguanylate Cyclase Requires Binding of c-di-GMP to the I-site**—The PleD crystal structure indicated the existence of an allosteric binding pocket (I-site) at the interface of the GGDEF and REC2 domains (8). Binding of a c-di-GMP dimer in the I-site is mediated by specific electrostatic interactions with charged residues of the GGDEF and REC2 domain (Fig. 1). To provide evidence for c-di-GMP binding to the I-site pocket in solution, trypsin digests were performed with purified PleD protein (5 μM) in the presence or absence of c-di-GMP (25 μM). The resulting peptide fragments were separated on a C18 column and analyzed by matrix-as-



**FIGURE 1. Crystal structure of the response regulator PleD.** *A*, domain architecture of PleD with receiver domain REC1 (blue), receiver domain REC2 (green), and GGDEF domain harboring diguanylate cyclase activity (red). The active site (A-site) loop and the allosteric binding site (I-site) are indicated. *B*, zoom in view of the I-site pocket with a bound dimer of c-di-GMP with intercalated purine bases. Residues Arg-148 and Arg-178 (green) from the REC2 domain and residues Arg-359, Asp-362, and Arg-390 (red) from the GGDEF domain make specific contacts to the ligand in the crystal structure. *C*, schematic of c-di-GMP synthesis and degradation reactions.

sisted laser desorption ionization time-of-flight. Both chromatograms were identical, with the exception of two peaks that were only detected in the absence of ligand but were protected when c-di-GMP present during tryptic digest (supplemental Fig. S1). One of the two peptides (T47, retention time 25.6 min) was identified by mass spectrometry and corresponds to the amino acids 354–359 (supplemental Fig. S1), arguing that c-di-GMP specifically protects from trypsin cleavage at Arg-359. To



**FIGURE 2. c-di-GMP labeling efficiency of different PleD mutants.** The upper lane shows autoradiographs of [ $^{33}$ P]c-di-GMP UV cross-linked hexahistidine-tagged PleD mutant proteins separated by SDS-PAGE. Relative labeling efficiency with c-di-GMP is shown below with wild-type PleD corresponding to 100%. Specific mutants in different domains are colored in gray (REC1), dark gray (REC2) and light gray (GGDEF).

provide additional evidence for ligand binding in solution, we performed UV cross-linking assays using  $^{33}$ P-labeled c-di-GMP (14). Residues Arg-148 and Arg-178 of the REC2 domain and Arg-359, Asp-362, and Arg-390 of the GGDEF domain were replaced with alanine, and the resulting protein variants were analyzed. As shown in Fig. 2, mutating I-site residues of the GGDEF domain abolished ( $\Delta$ R359 $\Delta$ D362) or strongly reduced (R359A and R390A) c-di-GMP binding. In contrast, mutations in the A-site (E370Q, E371Q, and EE370GG), which completely abolished enzymatic activity (Table 1), had no effect on c-di-GMP binding (Fig. 2), indicating that labeling with radioactive c-di-GMP results from ligand binding at the I-site. Although mutations R359A, R359V,  $\Delta$ R359 $\Delta$ D362, and D362A all showed a dramatically reduced or complete loss of enzymatic activity, mutant R390A showed wild-type-like DGC activity (Table 1). In agreement with the reduced binding of c-di-GMP (Fig. 2), the  $K_i$  of mutant R390A was increased  $\sim$ 20-fold (Table 1). PleD proteins harboring mutations in the REC2 portion of the I-site (R148A and R178A) showed an increased binding of c-di-GMP (Fig. 2) and slightly lower  $K_i$  values than wild type (Table 1). Surprisingly, R148A/R178A single and double mutants displayed a 5- to 20-fold higher DGC activity compared with wild-type PleD (Table 1). Finally, c-di-GMP binding was normal in mutant proteins that either lacked the REC1 receiver domain or had a bulky tryptophan residue introduced at the REC2-GGDEF interface (G194W, Fig. 2). Together these results implied that the structural requirements for c-di-GMP binding are contained within the GGDEF domain of PleD and that residues Arg-359, Asp-362, and Arg-390 form the core of an allosteric binding pocket for c-di-GMP.



## Diguanylate Cyclase Feedback Control

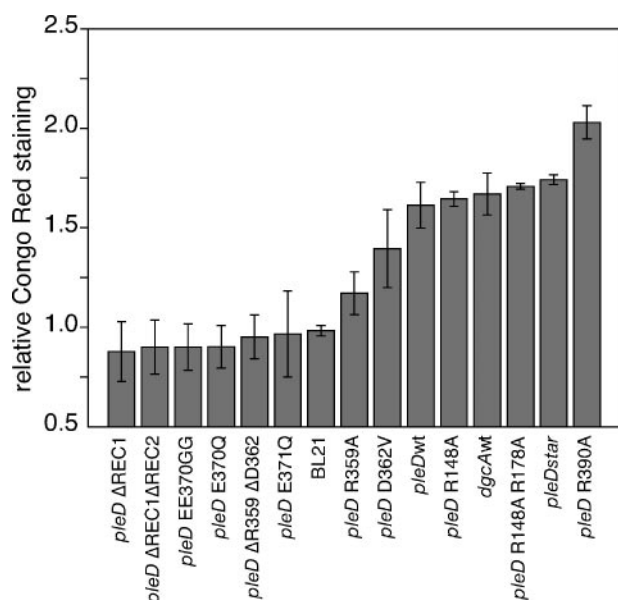


FIGURE 3. *In vivo* activity of different PleD and DgcA mutant proteins. *E. coli* BL21 strains expressing different *pleD* alleles and *dgcA* wild type were spotted onto Congo Red plates. Relative Congo Red binding was determined using imageJ software with BL21 corresponding to 100%.

*Evidence for an in Vivo Role of I-site-mediated Feedback Control*—To test a possible role for feedback inhibition of diguanylate cyclases *in vivo*, we developed a simple assay based on the observation that in *E. coli* and other *Enterobacteriaceae* increased cellular levels of *c*-di-GMP correlate with Congo Red (CR) staining of colonies on plates (28). Low level expression (in the absence of the inducer IPTG) of active *pleD* alleles caused a red colony phenotype in the *E. coli* B strain BL21, whereas cells expressing inactive *pleD* alleles under the same conditions stained white (Fig. 3). Interestingly, PleD mutants with dramatically different diguanylate cyclase activities *in vitro* showed only minor differences of CR staining *in vivo*. For instance, PleDR148A/R178A, which showed a 20-fold increased activity (Table 1), or PleD\*, a constitutively active mutant of PleD several 100-fold more active than wild-type (9), caused virtually identical CR values like PleD wild type (Fig. 3). In contrast, expression of the feedback inhibition mutant PleDR390A resulted in a significantly higher CR staining even though its *in vitro* DGC activity was lower than wild-type PleD (Table 1). This argued that *in vivo* steady-state concentrations of *c*-di-GMP were determined mainly by the PleD inhibition constant (as opposed to the overall activity of the enzyme) and that a functional I-site is critical for DGC control *in vivo*.

*DgcA, a Single Domain Diguanylate Cyclase, Is Subject to Allosteric Product Inhibition*—Sequence alignments of >1000 annotated GGDEF domain proteins revealed that that I-site residues Arg-359 and Asp-362 of PleD are highly conserved. 57% of the proteins containing a GGDEF domain and 27% of GGDEF/EAL composite proteins possess this motif. This suggested that *c*-di-GMP product inhibition could be a general regulatory mechanism of bacterial diguanylate cyclases. To test this, hexahistidine-tagged derivatives of two *C. crescentus* GGDEF domain proteins were analyzed biochemically with respect to their DGC activities and *c*-di-GMP binding proper-

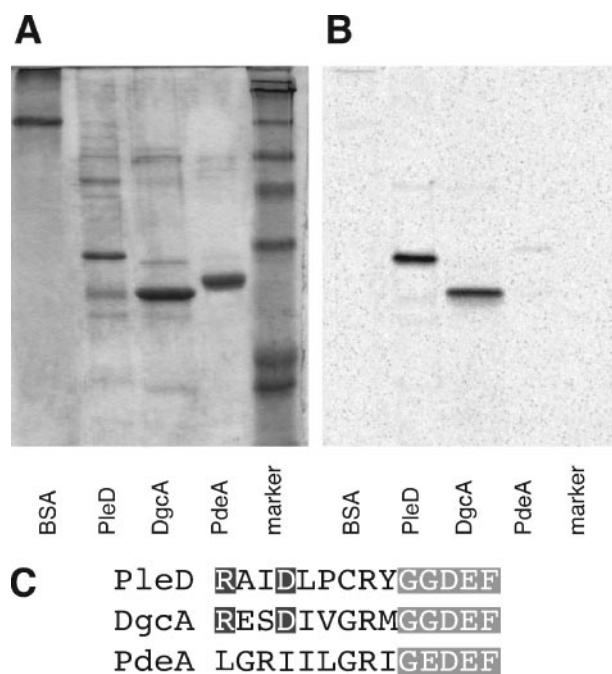


FIGURE 4. UV cross-linking of different GGDEF domains with <sup>33</sup>P-labeled *c*-di-GMP. A, Coomassie-stained SDS-PAGE and B, autoradiograph of BSA (control), PleDΔREC1, DgcA, and the isolated GGDEF domain of the *c*-di-GMP-specific phosphodiesterase PdeA (CC3396) after UV cross-linking with [<sup>33</sup>P]*c*-di-GMP. C, alignment of I- and A-site sequence of PleD, DgcA, and PdeA. I-site (RXXD) and A-site residues (GGDEF) are marked in black and gray, respectively.

ties. Purified DgcA (diguanylate cyclase A, CC3285), a soluble, single domain GGDEF protein that lacks an obvious N-terminal input domain, showed strong diguanylate cyclase activity (Fig. 5A). DgcA has an RESD motive five amino acids upstream of the conserved GGDEF active site and was readily labeled with [<sup>33</sup>P]*c*-di-GMP in a cross-linking experiment (Fig. 4). Consistent with this, DgcA showed strong feedback inhibition (Fig. 5A) with its  $K_i$  (1  $\mu$ M) being in the same range as the inhibition constant determined for PleD (8). In contrast, the GGDEF domain of PdeA (phosphodiesterase A, CC3396), which lacks catalytic activity (14), had no conserved I-site residues and did not bind radiolabeled *c*-di-GMP (Fig. 4). Thus, specific binding of *c*-di-GMP correlated with the presence of a conserved I-site motif RXXD (Fig. 4).

Diguanylate cyclase activity assays revealed strong and rapid product inhibition of DgcA. DgcA alone was able to convert only a small fraction of the available GTP substrate pool into the product *c*-di-GMP ( $V_o = 2.8 \mu$ mol of *c*-di-GMP  $\mu$ mol protein<sup>-1</sup> min<sup>-1</sup>) (Fig. 5B). In contrast, GTP consumption and conversion into *c*-di-GMP and pGpG was rapid ( $V_o = 43.0 \mu$ mol of *c*-di-GMP  $\mu$ mol protein<sup>-1</sup> min<sup>-1</sup>) and almost complete when the PDE CC3396 was added in excess to the enzymatic reaction (Fig. 5B). This argued that *c*-di-GMP feedback inhibition is abolished in a sequential DGC-PDE reaction, because the steady-state concentration of the inhibitor *c*-di-GMP is kept low by continuous degradation of *c*-di-GMP into the linear dinucleotide pGpG. As a consequence of rapid feedback inhibition, the experimentally determined  $V_o$  values of the DGC reaction are generally underestimated. In conclusion, these results strengthen the view that allosteric product inhibi-

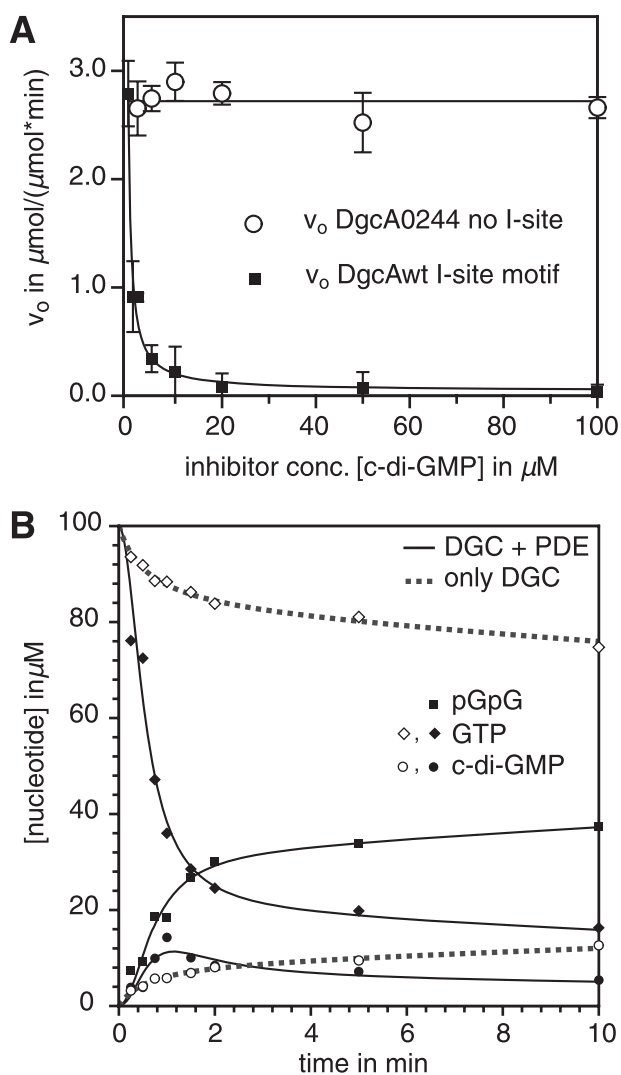


FIGURE 5. ***c*-di-GMP product inhibition of DgcA.** A, initial velocities of the wild-type diguanylate cyclase DgcA (*squares*) and the non-feedback-inhibited I-site mutant DgcA0244 (*circles*) in the presence of increasing concentrations of *c*-di-GMP. B, conversion of GTP into *c*-di-GMP by DgcA (*dashed lines*) and accelerated GTP consumption, *c*-di-GMP synthesis, and cleavage into pGpG by a diguanylate cyclase-phosphodiesterase tandem reaction (*plain lines*).

tion is a general principle of diguanylate cyclases and that high affinity binding of *c*-di-GMP requires an RXXD I-site motif positioned in close proximity to the active site.

**Development of an *in Vivo* Assay to Genetically Probe Allosteric Control of DgcA**—DGCs from different bacterial species have been shown to be functionally interchangeable (17, 26, 27). To determine if DgcA is active *in vivo* we expressed a plasmid-based copy of the *dgcA* gene in *C. crescentus*, *S. enterica*, and *Escherichia coli* B and tested the respective strains for the phenotypes known to result from increased cellular levels of *c*-di-GMP (17, 26, 27). Consistent with these earlier findings, expression of *dgcA* strongly inhibited flagellar-based motility in all three organisms, dramatically increased the ability of *S. enterica* and *E. coli* for surface colonization, and produced the characteristic red, dry, and rough (rdar) colony morphotype when plated on CR plates (Fig. 6, A–F) (29). The red phenotype provided the basis for a visual genetic screen on CR plates. Under these conditions, cells producing active DgcA variants would

produce dark red single colonies, whereas cells producing inactive DgcA mutants would remain white. This prompted us to use the CR screen to isolate *dgcA* mutants, which had a specific defect in feedback regulation, and to define the minimal requirements for product inhibition of this class of enzymes.

**Randomization of *c*-di-GMP Binding Pocket Reveals Three Mutant Classes**—To probe the minimal requirements of the I-site for *c*-di-GMP binding and product inhibition, a *dgcA* mutant library was constructed with the RESD signature replaced by a randomized tetrapeptide sequence (see “Materials and Methods”). In short, a *dgcA* gene, which carried a deletion of the four I-site codons, was used as template for a PCR reaction. For the amplification step a primer complementary to the 3'-end of *dgcA* was used in combination with a mixture of oligonucleotides that spanned the deletion site and contained 12 randomized base pairs at the position coding for the deleted amino acids. The resulting PCR fragments were fused in-frame with the 5'-end of *dgcA* in the expression plasmid pET42b and were transformed into *E. coli* BL21. The resulting gene library contains a theoretical number of  $1.67 \times 10^7$  ( $4^{12}$ ) different *dgcA* alleles, coding for DgcA variants with different combinations of I-site residues.

When plated on CR plates, colonies transformed with a wild-type *dgcA* allele showed the typical rdar colony morphology (Fig. 6G). Transformation of *E. coli* BL21 with a plasmid expressing a mutant DgcA, which lacked the four amino acids of the I-site (DgcA $\Delta$ RESD), produced white colonies on CR plates (Fig. 6H), indicating that this mutant form had lost DGC activity. About 10% of the clones with random tetrapeptide insertions stained red on CR plates and thus had retained DGC activity (Fig. 6I). This result is consistent with the observation that alanine scanning of the PleD I-site almost exclusively produced non-active enzyme variants (Table 1) and argues that the majority of amino acid substitutions introduced at the I-site are detrimental for the catalytic activity of the DGC. To further characterize active DgcA I-site variants, a total of 800 red colonies was isolated and patched onto CR plates without (Fig. 6, J and K) or with the inducer IPTG (Fig. 6, L and M). This secondary screen was based on the observation that IPTG-induced expression of the *pleDR390A* allele (Table 1), but not of the *pleD* wild-type allele, abolished growth of *E. coli* BL21 (data not shown). This suggested that at elevated protein levels, DGCs that lack feedback control are toxic *in vivo* (see below). The majority of the I-site library clones tested failed to grow on plates containing IPTG, indicating that their activity is no longer controlled by product inhibition (Fig. 6, L and M). Only 7 mutants (out of 9000 colonies screened) showed a wild-type-like behavior in that they stained dark red on CR plates and tolerated the presence of the inducer IPTG (Fig. 6, L and M).

This genetic screen led to the isolation of three different I-site mutant classes with the following characteristics: 1) catalytically inactive mutants ( $A^-$ , frequency  $\sim 90\%$ ); 2) feedback control negative mutants ( $I^-A^+$ , frequency  $\sim 10\%$ ); and wild-type-like mutants ( $I^+A^+$ , frequency  $\sim 0.1\%$ ). A subset of class 1 and 2 mutants and all seven class 3 mutants were selected, and hexahistidine-tagged forms of the respective proteins were purified for biochemical characterization. Kinetic parameters of activity ( $V_0$ ) and feedback inhibition ( $K_i$ ) were determined

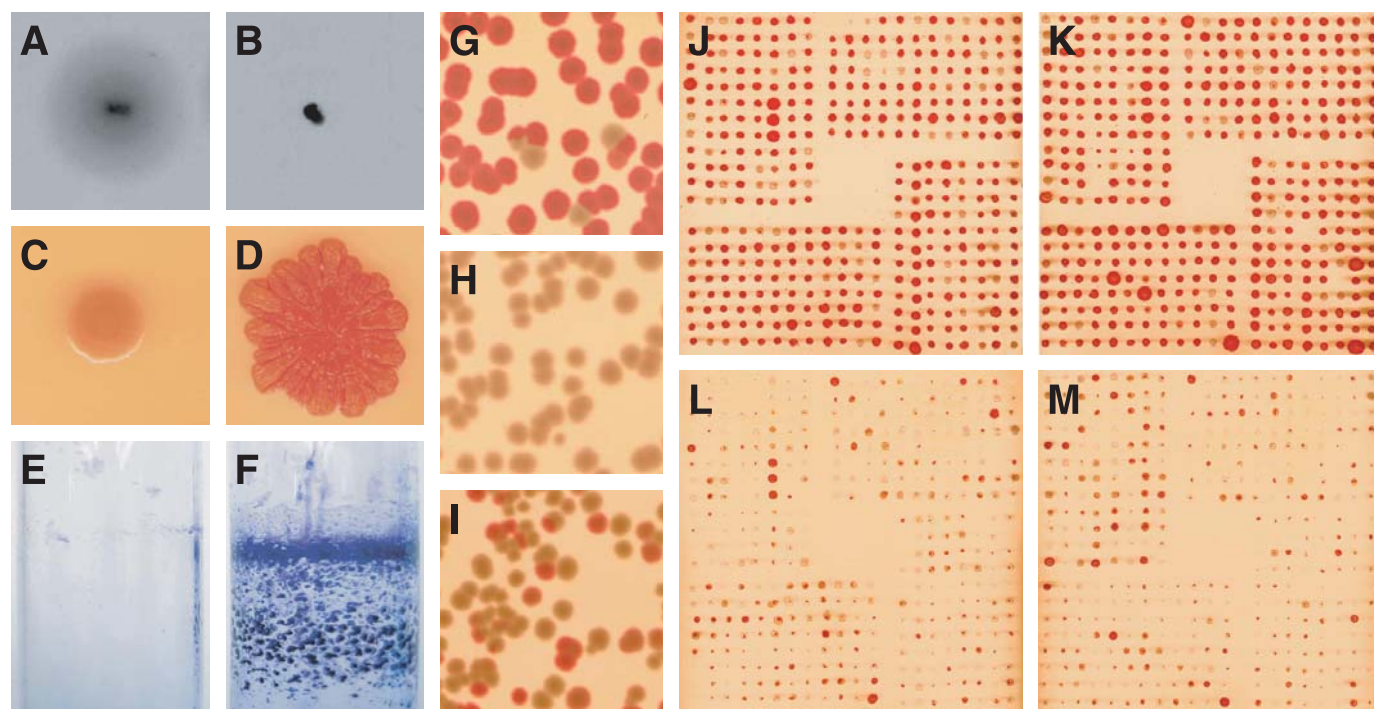


FIGURE 6. Phenotypic characterization of ectopically expressed diguanylate cyclase *dgca* in *E. coli* and *S. enterica*. Behavior of *E. coli* strain BL21 with empty pET42b plasmid (A) and pET42b::*dgca* (B) on motility plates. Colony morphology of *E. coli* strain BL21 with empty pET42b plasmid (C) and with pET42b::*dgca* (D) on Congo Red plates. Biofilm formation of *S. enterica* serovar Typhimurium *trp::T7RNAP* with empty pET42b (E) and pET42b::*dgca* (F) grown in liquid culture and stained with crystal violet. *E. coli* BL21 transformed with PCR-restored *dgca* wild type on pET42b::*dgca* (G), with the inactive allele *dgca*ΔRESΔ (pET42b::*dgca*ΔRESΔ) (H), and with a library of random tetrapeptide insertions in the I-site (pET42b::*dgca*AXXX) (I) and plated on Congo Red plates. *E. coli* BL21 expressing different I-site mutant alleles were spotted onto Congo Red plates without (J and K) and with 1 mM IPTG (L and M) to screen for feedback inhibition *dgca* alleles.

TABLE 1  
Kinetic analysis of PleD mutants

Protein	$V_o$	$\Delta V_o$	$K_i$	$\Delta K_i$
	$\mu\text{mol c-di-GMP}/$ $(\mu\text{mol protein} \cdot \text{min})$		$\mu\text{M}$	
PleD wild type	0.202	$\pm 0.023$	5.8	$\pm 1.0$
PleDR359A	0.005	ND <sup>a</sup>	>100	ND
PleDR359V	0.0	ND		
PleDΔ359Δ362	0.0	ND		
PleDD362A	0.0	ND		
PleDR390A	0.076	$\pm 0.007$	115.0	$\pm 18.1$
PleDR148A	0.822	$\pm 0.020$	2.8	$\pm 1.2$
PleDR178A	0.918	$\pm 0.292$	3.6	$\pm 0.1$
PleDR148AR178A	3.75	$\pm 0.43$	2.9	$\pm 0.6$
PleDG194W	0.161	$\pm 0.005$	6.3	$\pm 1.9$
PleDEE370GG	0.0	ND		
PleDE370Q	0.0	ND		
PleDE371Q	0.0	ND		

<sup>a</sup> ND, not determined.

individually using an *in vitro* diguanylate cyclase activity assay (16). Consistent with their rdar-like *in vivo* phenotype, only class 2 and class 3 mutants showed detectable diguanylate cyclase activity with an initial velocity between 1.93 and 14.21  $\mu\text{mol}$  of c-di-GMP  $\mu\text{mol protein}^{-1} \text{min}^{-1}$  (Table 2). Only mutant proteins from the IPTG tolerant class 3 showed product inhibition with  $K_i$  values close to 1  $\mu\text{M}$  (Table 2). In contrast, all proteins from class 2 mutants showed no feedback inhibition *in vitro*, arguing that their *in vivo* toxicity is the result of uncontrolled run-off DGC activity (Fig. 5A and Table 2). Support for this hypothesis comes from experiments determining the cellular concentration of c-di-GMP and DgcA protein expression levels in *E. coli* BL21 carrying selected *dgca* alleles on plasmid pET42b (see "Materials and Methods"). Alleles *dgcaA0244*,

*dgcaA1229*, and *dgcaA1250* were chosen, because the DGC activity of these enzymes is similar to wild type DgcA (Table 2). Basal level expression (no IPTG) of *dgcaA0244*, the allele coding for a DGC that completely lacks feedback inhibition, resulted in a more than 100-fold increased cellular level of c-di-GMP as compared with cells expressing wild-type *dgca* (Table 3). This was due to an almost 100-fold higher overall turnover of the mutant enzyme as compared with wild type (Table 3). In contrast, enzymatic turnover and cellular concentration of c-di-GMP was increased only marginally in *E. coli* cells expressing alleles *dgcaA1229*, and *dgcaA1250* with restored feedback inhibition control (Table 3).

Sequence analysis of the tetrapeptide insertions of class 2 and class 3 mutants revealed several important characteristics of a functional allosteric I-site binding pocket. All catalytically active and feedback inhibition competent mutants restored the wild-type Arg and Asp residues at positions one and four of the RXXD motive (Table 2). Whereas most of the mutants that had lost feedback inhibition had altered either one or both of these charged residues (Table 2) only two feedback inhibition mutants had retained both charges with changes in the intervening residues (Table 2). Obviously, Arg and Asp, while being strictly required for feedback inhibition, need to be placed in the appropriate sequence context of the I-site loop. These experiments define the minimal requirements of the I-site core region and demonstrate that the Arg and Asp residues that make direct contacts to the c-di-GMP ligand in the crystal structure are of critical functional importance for DGC feedback inhibition *in vivo* and *in vitro*. This provides a plausible

**TABLE 2**  
Diguanylate cyclase activity and inhibition constant of DgcA I-site mutant proteins

Protein	Motif	$V_o$ $\mu\text{mol } c\text{-di-GMP}/$ $(\mu\text{mol protein}\cdot\text{min})$	$\Delta V_o$	$K_i$ $\mu\text{M}$	$\Delta K_i$
DgcA wt	RES D	2.79	$\pm 0.01$	0.96	$\pm 0.09$
DgcA1406	RQGD	5.35	$\pm 0.05$	7.02	$\pm 2.92$
DgcA1040	RLVD	4.92	$\pm 0.19$	4.52	$\pm 1.81$
DgcA1229	RGAD	2.03	$\pm 0.01$	1.84	$\pm 0.26$
DgcA1524	RSAD	3.70	$\pm 0.13$	7.36	$\pm 2.69$
DgcA1529	RLAD	2.79	$\pm 0.04$	1.01	$\pm 0.23$
DgcA0751	RCAD	3.65	$\pm 0.10$	3.51	$\pm 0.52$
DgcA1250	RGGD	2.07	$\pm 0.02$	2.24	$\pm 0.49$
DgcA $\Delta$ RES D		0.14	$\pm 0.06$		ND <sup>a</sup>
DgcA0207	GMGG	14.21	$\pm 0.54$	No inhibition	
DgcA0244	VMGG	2.57	$\pm 0.05$	No inhibition	
DgcA0613	GGVA	4.29	$\pm 0.06$	No inhibition	
DgcA0646	GRDC	8.90	$\pm 0.10$	No inhibition	
DgcA0913	GVDG	3.81	$\pm 0.04$	No inhibition	
DgcA1300	MEGD	0.87	$\pm 0.02$	No inhibition	
DgcA1733	GGNH	11.47	$\pm 0.17$	No inhibition	
DgcA3018	RESE	11.1	$\pm 0.11$	No inhibition	
DgcA0230	RNRD	3.02	$\pm 0.06$	No inhibition	
DgcA0642	RVDS	4.17	$\pm 0.08$	No inhibition	
DgcA1007	RAGG	6.06	$\pm 0.05$	No inhibition	
DgcA2006	RGQD	1.93	$\pm 0.01$	No inhibition	

<sup>a</sup> ND, not determined.

**TABLE 3**  
DgcA protein levels and cellular c-di-GMP concentrations in the absence or presence of IPTG induction at 1 mM

	Protein conc. <sup>a</sup>		c-di-GMP conc.		Turnover <sup>b</sup>	
	No induction	1 mM IPTG	No induction	1 mM IPTG	No induction	1 mM IPTG
	<i>pmol protein/mg dry weight</i>		<i>pmol c-di-GMP/mg dry weight</i>		<i>pmol c-di-GMP per pmol protein</i>	
DgcA0244	4.1	22	1466.3	1570.7	357.6	71.4
DgcA1229	3.5	31	87.6	139.5	25.0	4.5
DgcA1250	2.7	43	24.2	305.4	9.0	7.1
DgcA wt	2.9	33	13.75	189.4	4.7	5.7
DgcA $\Delta$ RES D	3.5	23	ND <sup>c</sup>	ND	NA <sup>d</sup>	NA

<sup>a</sup> See "Materials and Methods."

<sup>b</sup> As derived from the cellular c-di-GMP concentration divided by the cellular protein concentration.

<sup>c</sup> ND, not detectable.

<sup>d</sup> NA, not applicable.

explanation for the strong conservation of the RXXD motif in GGDEF domains.

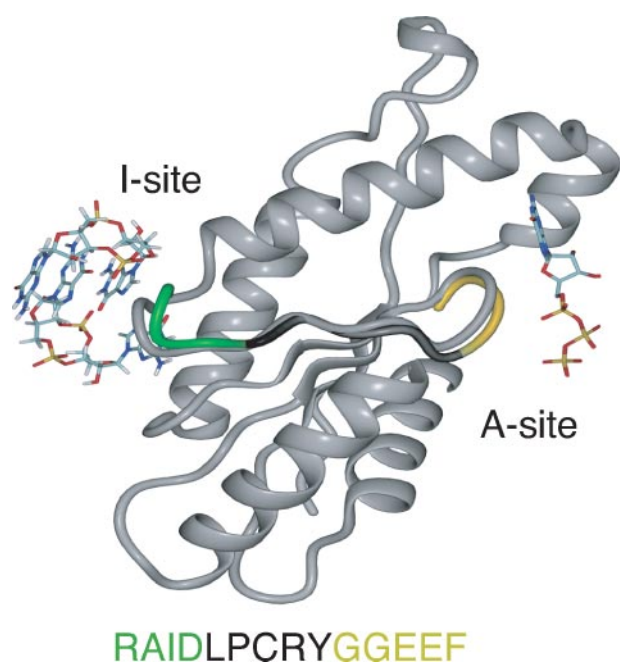
The molecular mechanism of product inhibition through I-site binding remains unclear. To assist the interpretation of the present data and provide information on binding induced mobility, atomistically detailed simulations were carried out. Normal mode calculations on ligated and unligated PleD were used to analyze the structural transitions that occur during I-site binding of c-di-GMP. Normal mode calculations on the optimized structures yielded no imaginary frequencies, and translational and rotational frequencies were close to zero ( $|\omega| \leq 0.02 \text{ cm}^{-1}$ ). This indicated that the minimized structures correspond to real minima on the potential energy surface. The displacements calculated for the ligated and the unligated protein showed a significant decrease in mobility for both I- and A-site residues upon complexation (supplemental Figs. S2 and S3). Whereas motion in the I-site is suppressed due to steric interactions upon ligand insertion, quenching of the A-site residues suggested that the two sites might be dynamically coupled via the short connecting  $\beta$ -strand ( $\beta_2$ ). Backbone C $\alpha$ -atoms and side chains of the I-site and A-site loops were displaced by an average of 1–4 Å in opposite directions, arguing that a balance-like movement centered around  $\beta_2$  could be responsible for direct information transfer between the two sites (Fig. 7). The cumulated displacements per residue over all 147 modes

(supplemental Fig. S3) showed different mobilities in additional regions of the protein. The C $\alpha$  atoms of residues exhibiting large changes in flexibility upon ligand binding are depicted as *spheres* in supplemental Fig. S3. Reduced flexibility (*yellow spheres*) is found at the I-site, A-site, phosphorylation site, and the dimer interface, whereas the flexibility is enhanced (*black spheres*) at the REC1/REC2 interface. In summary, these simulations show that I-site binding of c-di-GMP not only reduced the mobility around the RXXD motif but also of the residues of the A-site loop.

**DISCUSSION**

*Feedback Inhibition Is a General Control Mechanism of Diguanylate Cyclases*—The data presented here propose a general mechanism to regulate the activity of diguanylate cyclases (DGCs), key enzymes of c-di-GMP-based signal transduction in bacteria. High affinity binding of c-di-GMP to a site distant from the catalytic pocket (I-site) efficiently blocks enzymatic activity in a non-competitive manner. Mutational analysis of multi- and single-domain DGC proteins has provided convincing evidence for the role of several charged amino acids in c-di-GMP binding and allosteric regulation. Furthermore, these experiments indicated that the allosteric binding site is functionally contained within the GGDEF domain. An *in vivo* selection experiment using a random tetrapeptide library, and

Downloaded from www.jbc.org at MEDIZINBLIBLIOTHEK on October 17, 2006



**FIGURE 7. Comparison of the energy-minimized structures of the PleD GGDEF domain with and without ligand bound to the I-site.** For improved clarity, the domain is sliced through the I-site loop/ $\beta$ 2/A-site loop plane. The unligated protein is shown in gray and the I-site loop (green),  $\beta$ 2 (black), and A-site loop (gold) of the bound structure are shown as an overlay. GTP bound to the active site is modeled according to the orientation of c-di-GMP bound to the A-site in the crystal structure. The PleD amino acid sequence of I-site,  $\beta$ 2, and A-site is indicated below.

designed to re-engineer the I-site has led to the definition of a highly conserved RXXD core motif of the c-di-GMP binding pocket. The RXXD motif forms a turn at the end of a short five-amino acid  $\beta$ -sheet that directly connects the I-site with the conserved catalytic A-site motif, GG(D/E)EF (Fig. 7). This raised the question of how I-site ligand binding modulates DGC enzyme activity. In the multidomain protein PleD, c-di-GMP bound to the I-site physically connects the GGDEF domain with the REC1-REC2 dimerization stem. It was speculated that product inhibition occurs by domain immobilization, which would prevent the encounter of the two DGC substrate binding sites (8). Several observations argue in favor of a more direct communication between I- and A-sites. First, with a large variety of domains found to be associated with GGDEF domains, it seems unlikely that functional I-sites are generally formed by the interface of a GGDEF with its neighboring domain (2). In agreement with this, residues of the PleD REC2 domain are not required for c-di-GMP binding and feedback inhibition. Second, the single domain DGC protein, DgcA, shows I-site-dependent allosteric control with a  $K_i$  of  $1 \mu\text{M}$ . Third, the introduction of a bulky tryptophan residue (G194W) at the GGDEF-REC2 interface did not affect activity, I-site binding, or feedback inhibition of PleD (Fig. 2 and Table 1). Fourth, atomistic simulations of ligated and unligated PleD predicted a marked drop in flexibility of  $C\alpha$ -atoms both in the I- and A-site upon ligand binding. Simultaneous with motion quenching,  $\beta$ 2 and its flanking I- and A-loops undergo a balance-like movement that repositions A-site residues in the catalytic active site (Fig. 7). This is consistent with the idea that structural changes within the GGDEF domain upon binding of c-di-GMP at the

I-site lead to repositioning of active site residues and possibly altered kinetic parameters. Thus, we propose that c-di-GMP binding and allosteric control represents an intrinsic regulatory property of DGCs that contain an RXXD motif.

Like guanylate and adenylate cyclases (GCs and ACs) and DNA polymerases, DGCs catalyze the nucleophilic attack of the 3'-hydroxyl group on the  $\alpha$ -phosphate of a nucleoside triphosphate. Despite the lack of obvious sequence similarities, the PleD x-ray structure revealed that DGCs possess a similar domain architecture like ACs and GCs (8, 30). Based on mutational analysis (8, 14, 16) and on structural comparisons between DGC, AC, GC, and DNA polymerases (31–34), a model for DGC catalysis can be proposed. In contrast to the heterodimeric ACs and GCs, DGCs form homodimers, with a GTP molecule bound within the catalytic core of each DGC monomer (8). Two  $\text{Mg}^{2+}$  ions are coordinated by the highly conserved glutamic acid residue Glu-371, which is part of the GGDEF motif, and possibly by Asp-327 on the opposing  $\beta$ -sheet. The divalent  $\text{Mg}^{2+}$  carboxyl complex coordinates the triphosphate moiety of GTP and activates the 3'-hydroxyl group for intermolecular nucleophilic attack. Substrate specificity of AC and GC can be interchanged by converting a few key residues involved in purine recognition (31, 34, 35). This includes an arginine residue, which in PleD corresponds to the highly conserved Arg-366 located in the  $\beta$ -sheet connecting the I- and A-sites. Based on the active site model, two alternative inhibition mechanisms can be envisaged. In a first scenario, binding of c-di-GMP to the I-site would change the orientation of Arg-366 and would thereby disturb the guanine binding pocket resulting in an increased  $K_m$  for GTP. Alternatively, inhibitor binding could rearrange the  $\text{Mg}^{2+}$  carboxyl complex and thus destabilize the active state.

*In Silico Analysis of the GGDEF Protein Family Indicates That Product Inhibition Is a General Regulatory Mechanism*—DGC activity of GGDEF domain proteins seems to strictly depend on conserved GGDEF or GGEEF motifs in the active site (10, 16, 18, 36–38). Consistent with this,  $\sim 90\%$  of the GGDEF and 62% of the GGDEF/EAL composite proteins show a conserved GG(D/E)EF A-site motif. Of the GGDEF proteins with a highly conserved A-site motif,  $>60\%$  have conserved RXXD I-site residues and a conserved spacer length between I- and A-site, arguing that the three-dimensional arrangement of catalytic and allosteric pocket is likely to be similar in all DGCs. From a total of 19 GGDEF proteins, for which convincing evidence for a DGC activity exists, 14 have a conserved I-site (supplemental Fig. S4). Ryjenkov and coworkers (10) reported severe toxicity problems when expressing diguanylate cyclases lacking I-site residues in *E. coli* BL21. This is consistent with the growth defect observed upon expression of *dgcA* feedback inhibition mutants in *E. coli* BL21 and argues that these proteins are not feedback-controlled. The molecular basis of growth interference under these conditions is unclear. It is possible that depletion of the GTP pool or adverse effects of unphysiologically high levels of c-di-GMP are responsible for this effect. Although the experiments presented here define a role for the I-site in DGC feedback inhibition, the c-di-GMP binding pocket could also be exploited for other roles in c-di-GMP signaling. It has been proposed recently that non-catalytic GGDEF

domains with variant A-site motifs can fulfill regulatory functions (14). It is attractive to speculate that a subgroup of GGDEF proteins that has degenerate catalytic A-sites but conserved c-di-GMP binding pockets, represents a novel class of c-di-GMP effector proteins that regulate cellular functions in response to c-di-GMP binding.

**Regulatory Significance of DGC Feedback Control**—GGDEF domains are often associated with sensory domains in one- or two-component signaling systems (39, 40). Thus it is reasonable to assume that in most cases DGC activity is controlled by direct signal input through these domains. But why then would a substantial portion of these enzymes also be subject to feedback inhibition? There are several possibilities, which among themselves are not mutually exclusive. Given the anticipated regulatory complexity of the c-di-GMP signaling network (2, 39) and the potentially dramatic changes in cellular physiology and behavior caused by fluctuating levels of c-di-GMP, it is in the cell's best interest to rigorously control the production of the second messenger. Product inhibition of DGCs allows the establishment of precise threshold concentrations of the second messenger, or, in combination with counteracting PDEs, could produce short spikes or even generate oscillations of c-di-GMP. In addition, negative feedback loops have been implicated in neutralizing noise and providing robustness in genetic networks by limiting the range over which the concentrations of the network components fluctuate (41, 42). Similarly, product inhibition of DGCs could contribute to the reduction of stochastic perturbations and increase the stability of the c-di-GMP circuitry by keeping c-di-GMP levels in defined concentration windows. Alternatively, DGC autoregulation may influence the kinetics of c-di-GMP signaling. Mathematical modeling and experimental evidence suggested that negative autoregulation in combination with strong promoters substantially shortens the rise-time of transcription responses (43–45). In analogy, a desired steady-state concentration of c-di-GMP can in principle be achieved by two regulatory designs: (a) a low activity DGC with no product inhibition, and (b) a high activity DGC with built-in negative autoregulation. In cases where circuits have been optimized for fast up-kinetics, design B will be superior. It is plausible that DGCs with or without I-site motifs can be divided into these two kinetically different classes.

This study contributes to the emerging understanding of the c-di-GMP regulatory network in bacteria. The current emphasis lies on the identification of effector molecules, regulatory mechanisms, and processes controlled by c-di-GMP. With the long term goal in mind of approaching a detailed systems-level understanding of c-di-GMP signaling, kinetic parameters of signaling mechanisms will require our particular attention. Our experiments provide an entry point into the kinetic analysis of individual DGCs and the quantitative assessment of the c-di-GMP circuitry.

**Acknowledgments**—We thank Tilman Schirmer for helpful discussions and students of the Microbiology and Immunology Course (Biozentrum of the University of Basel, 2005) and of the Advanced Bacterial Genetics Course (Cold Spring Harbor, 2005) for their help in mutant screening.

## REFERENCES

- Jenal, U. (2004) *Curr. Opin. Microbiol.* **7**, 185–191
- Romling, U., Gomelsky, M., and Galperin, M. Y. (2005) *Mol. Microbiol.* **57**, 629–639
- Brouillette, E., Hyodo, M., Hayakawa, Y., Karaolis, D. K. R., and Malouin, F. (2005) *Antimicrob. Agents Chemother.* **49**, 3109–3113
- Hisert, K. B., MacCoss, M., Shiloh, M. U., Darwin, K. H., Singh, S., Jones, R. A., Ehrt, S., Zhang, Z. Y., Gaffney, B. L., Gandotra, S., Holden, D. W., Murray, D., and Nathan, C. (2005) *Mol. Microbiol.* **56**, 1234–1245
- Kulesekara, H., Lee, V., Brencic, A., Liberati, N., Urbach, J., Miyata, S., Lee, D. G., Neely, A. N., Hyodo, M., Hayakawa, Y., Ausubel, F. M., and Lory, S. (2006) *Proc. Natl. Acad. Sci. U. S. A.* **103**, 2839–2844
- Lestrade, P., Dricot, A., Delrue, R. M., Lambert, C., Martinelli, V., De Bolle, X., Letesson, J. J., and Tibor, A. (2003) *Infect. Immun.* **71**, 7053–7060
- Tischler, A. D., Lee, S. H., and Camilli, A. (2002) *J. Bacteriol.* **184**, 4104–4113
- Chan, C., Paul, R., Samoray, D., Amiot, N. C., Giese, B., Jenal, U., and Schirmer, T. (2004) *Proc. Natl. Acad. Sci. U. S. A.* **101**, 17084–17089
- Ross, P., Weinhouse, H., Aloni, Y., Michaeli, D., Weinbergerohana, P., Mayer, R., Braun, S., Devroom, E., Vandermarel, G. A., Vanboom, J. H., and Benziman, M. (1987) *Nature* **325**, 279–281
- Ryjenkov, D. A., Tarutina, M., Moskvina, O. V., and Gomelsky, M. (2005) *J. Bacteriol.* **187**, 1792–1798
- Ross, P., Mayer, R., and Benziman, M. (1991) *Microbiol. Rev.* **55**, 35–58
- Schmidt, A. J., Ryjenkov, D. A., and Gomelsky, M. (2005) *J. Bacteriol.* **187**, 4774–4781
- Tamayo, R., Tischler, A. D., and Camilli, A. (2005) *J. Biol. Chem.* **280**, 33324–33330
- Christen, M., Christen, B., Folcher, M., Schauerte, A., and Jenal, U. (2005) *J. Biol. Chem.* **280**, 30829–30837
- Tal, R., Wong, H. C., Calhoon, R., Gelfand, D., Fear, A. L., Volman, G., Mayer, R., Ross, P., Amikam, D., Weinhouse, H., Cohen, A., Sapir, S., Ohana, P., and Benziman, M. (1998) *J. Bacteriol.* **180**, 4416–4425
- Paul, R., Weiser, S., Amiot, N. C., Chan, C., Schirmer, T., Giese, B., and Jenal, U. (2004) *Genes Dev.* **18**, 715–727
- Aldridge, P., Paul, R., Goymer, P., Rainey, P., and Jenal, U. (2003) *Mol. Microbiol.* **47**, 1695–1708
- Kirillina, O., Fetherston, J. D., Bobrov, A. G., Abney, J., and Perry, R. D. (2004) *Mol. Microbiol.* **54**, 75–88
- Aldridge, P., and Jenal, U. (1999) *Mol. Microbiol.* **32**, 379–391
- Hecht, G. B., and Newton, A. (1995) *J. Bacteriol.* **177**, 6223–6229
- Ely, B. (1991) *Methods Enzymol.* **204**, 372–384
- O'Toole, G. A., Pratt, L. A., Watnick, P. I., Newman, D. K., Weaver, V. B., and Kolter, R. (1999) *Methods Enzymol.* **34**, 586–595
- Ochi, Y., Hosoda, S., Hachiya, T., Yoshimura, M., Miyazaki, T., and Kajita, Y. (1981) *Acta Endocrinol.* **98**, 62–67
- Brooks, B. R., Bruccoleri, R. E., Olafson, B. D., States, D. J., Swaminathan, S., and Karplus, M. (1983) *J. Comput. Chem.* **4**, 187–217
- MacKerell, A. D., Bashford, D., Bellott, M., Dunbrack, R. L., Evanseck, J. D., Field, M. J., Fischer, S., Gao, J., Guo, H., Ha, S., Joseph-McCarthy, D., Kuchnir, L., Kuczera, K., Lau, F. T. K., Mattos, C., Michnick, S., Ngo, T., Nguyen, D. T., Prodhom, B., Reiher, W. E., Roux, B., Schlenkerich, M., Smith, J. C., Stote, R., Straub, J., Watanabe, M., Wiorkiewicz-Kuczera, J., Yin, D., and Karplus, M. (1998) *J. Phys. Chem. B* **102**, 3586–3616
- Ausmees, N., Mayer, R., Weinhouse, H., Volman, G., Amikam, D., Benziman, M., and Lindberg, M. (2001) *FEMS Microbiol. Lett.* **204**, 163–167
- Simm, R., Fetherston, J. D., Kader, A., Romling, U., and Perry, R. D. (2005) *J. Bacteriol.* **187**, 6816–6823
- Garcia, B., Latasa, C., Solano, C., Portillo, F. G., Gamazo, C., and Lasa, I. (2004) *Mol. Microbiol.* **54**, 264–277
- Zogaj, X., Nimtz, M., Rohde, M., Bokranz, W., and Romling, U. (2001) *Mol. Microbiol.* **39**, 1452–1463
- Pei, J., and Grishin, N. V. (2001) *Proteins* **42**, 210–216
- Tucker, C. L., Hurley, J. H., Miller, T. R., and Hurley, J. B. (1998) *Proc. Natl. Acad. Sci. U. S. A.* **95**, 5993–5997
- Zhang, G. Y., Liu, Y., Ruoho, A. E., and Hurley, J. H. (1997) *Nature* **388**, 204 (Erratum)

## Diguanylate Cyclase Feedback Control

33. Tesmer, J. J., Sunahara, R. K., Johnson, R. A., Gosselin, G., Gilman, A. G., and Sprang, S. R. (1999) *Science* **285**, 756–760
34. Sunahara, R. K., Beuve, A., Tesmer, J. J. G., Sprang, S. R., Garbers, D. L., and Gilman, A. G. (1998) *J. Biol. Chem.* **273**, 16332–16338
35. Baker, D. A., and Kelly, J. M. (2004) *Mol. Microbiol.* **52**, 1229–1242
36. Hickman, J. W., Tifrea, D. F., and Harwood, C. S. (2005) *Proc. Natl. Acad. Sci. U. S. A.* **102**, 14422–14427
37. Mendez-Ortiz, M. M., Hyodo, M., Hayakawa, Y., and Membrillo-Hernandez, J. (2006) *J. Biol. Chem.* **281**, 8090–8099
38. Simm, R., Morr, M., Kader, A., Nimtz, M., and Romling, U. (2004) *Mol. Microbiol.* **53**, 1123–1134
39. Galperin, M. Y., Nikolskaya, A. N., and Koonin, E. V. (2001) *FEMS Microbiol. Lett.* **204**, 213–214
40. Ulrich, L. E., Koonin, E. V., and Zhulin, I. B. (2005) *Trends Microbiol.* **13**, 52–56
41. Becskei, A., and Serrano, L. (2000) *Nature* **405**, 590–593
42. Gardner, T. S., Cantor, C. R., and Collins, J. J. (2000) *Nature* **403**, 339–342
43. McAdams, H. H., and Arkin, A. (1997) *Proc. Natl. Acad. Sci. U. S. A.* **94**, 814–819
44. Rosenfeld, N., Elowitz, M. B., and Alon, U. (2002) *J. Mol. Biol.* **323**, 785–793



## SUPPLEMENTAL MATERIAL:

### MATERIALS AND METHODS:

*Purification of His-tagged proteins* - *E. coli* BL21 cells carrying the respective expression plasmid were grown in LB medium with ampicillin (100 $\mu$ g/ml) or kanamycin (30 $\mu$ g/ml) and expression was induced by adding IPTG at OD<sub>600</sub> 0.4 to a final concentration of 0.4 mM. After harvesting by centrifugation, cells were resuspended in buffer containing 50 mM Tris-HCl, pH 8.0, 250 mM NaCl, 5 mM  $\beta$ -mercaptoethanol, lysed by passage through a French pressure cell, and the suspension was clarified by centrifugation for 10 min at 5,000 x g. Soluble and insoluble protein fractions were separated by a high-spin centrifugation step (100,000 x g, 1 h). The supernatant was loaded onto Ni-NTA affinity resin (Qiagen), washed with buffer, and eluted with an imidazol-gradient as recommended by the manufacturer. Protein preparations were examined for purity by SDS-PAGE and fractions containing pure protein were pooled and dialyzed for 12 h at 4°C.

### *Molecular modeling of PleD*

All-atom simulations were carried out using the CHARMM (25) program and the CHARMM22/27 force field (26). The A chain of the X-ray dimer structure (PDB entry: 1W25 (17)) was used. All titratable side chains were generated in their standard protonation state at pH 7. Parameters and partial charges for the non-standard residue c-di-GMP were adopted from the extended CHARMM parameter sets for nucleic acids. The structure of the ligated (intercalated c-di-GMP bound to the I-site) and the unligated protein, to which hydrogen atoms were added, were minimized using a distance-dependent dielectric with  $\epsilon=4$  and a cutoff of 12 Å for non-bonded interactions. 5000 steps of steepest descent minimization were followed by adopted Newton Raphson minimization until a RMS gradient of 10<sup>-7</sup> kcal/mol·Å was reached. Such a threshold is found to be sufficient for normal mode calculations (49). Normal modes were calculated with the diagonalization in a mixed basis (DIMB) method, as implemented in CHARMM. The DIMB method is an approximate scheme retaining the full atomistic description of the protein, where the Hessian is approximated iteratively. The total number of basis functions was 153 and cumulated displacements were calculated for  $T = 300$  K.

For ligated PleD motion is suppressed at L( $\beta$ 1, $\alpha$ 1) (res.10-12), L( $\beta$ 3, $\alpha$ 3) domain REC1, the C-terminal end of  $\alpha$ 3 (res. 220-224) of domain REC2, the unstructured linker between REC2 and GGDEF domain (res. 282-284), the residues forming the A-site (res. 352), L( $\alpha$ 2, $\beta$ 2) (res. 357-



360, I-site), L( $\beta$ 2, $\beta$ 3) (res. 367-373, A-site) and at the C-terminal end of  $\alpha$ 3 (res. 396-398) of the GGDEF domain. By contrast upon ligand binding mobility increases for  $\alpha$ 1 (res. 24),  $\alpha$ 4 (res. 96-99) of domain REC1, residues (res. 149, 175), L( $\beta$ 2, $\alpha$ 2) (res. 205-207), L( $\beta$ 5, $\alpha$ 5) (res. 254-257) of domain REC2 and residues L( $\beta$ 3', $\beta$ 3'') (res. 404-407) and L( $\beta$ 4, $\alpha$ 4) (res. 422-424) of the GGDEF domain.

*Primer list*

The following primers were used: #1006, ACA CGC TAC ATA TGA AAA TCT CAG GCG CCC GGA C; #1007, ACT CTC GAG AGC GCT CCT GCG CTT; #1129, CAA GCG GCT GCA GGC CAA TGT GAT CGT CGG CCG CAT GGG TGG TGA; #670, TGC TAG TTA TTG CTC AGC GG; #1006 ACA CGC TAC ATA TGA AAA TCT CAG GCG CCC GGA C; #1130, CAA GCG GCT GCA GGC CAA TGT GCG CGA AAG CGA CAT CGT CGG CCG CAT GGG TGG TGA; #1132, CAC ATT GGC CTG CAG CCG CTT GGC GAC; #1131, CAA GCG GCT GCA GGC CAA TGT GNN NNN NNN NNN NAT CGT CGG CCG CAT GGG TGG TGA.

FIGURE LEGENDS:

**Figure S1: Separation of peptides yielded from tryptic digest of PleD in the presence (red chromatogram) or absence of c-di-GMP (black chromatogram) on a C18 column.** Peaks identified by ESI-MS: c-di-GMP  $m/z$  691,  $t_R$  7.70 min, T47 (amino acids 354-359)  $m/z$  659.3  $t_R$  25.64 min. T49 (amino acids 367-386)  $m/z$  2167.7  $t_R$  47.73 min.

**Figure S2: Normal modes of PleD I-site and A-site residues.** The displacements for each mode of the ligated and unligated structures are shown in Å for the residues of the REC2 domain (green) and the GGDEF domain (red). Insertion of intercalated c-di-GMP in the I-site quenches motion in both the I-site (R359-D362, R390) and the A-site (G368-E371), suggesting that the two sites are dynamically coupled.

**Figure S3: Representation of the PleD protein (blue: REC1, green: REC2, red: DGC) with c-di-GMP bound to the I-site.**  $C\alpha$ -atoms at positions of considerable changes in flexibility upon ligand binding are shown as spheres; reduced flexibility (yellow) and enhanced flexibility (black). Note that binding of c-di-GMP at the I-site (I) affects mobility not only in the I-site, but also in other regions of the protein, e.g. A-site (A), phosphorylation site (P) and dimer interface.

**Figure S4: Alignment of I- and A-site sequence of biochemically characterized diguanylate cyclases.** I-site residues (RXXD) are underlined in green and A-site residues (GGDEF) are underlined in yellow.

FIGURE LEGENDS:

**Figure S1: Separation of peptides yielded from tryptic digest of PleD in the presence (red chromatogram) or absence of c-di-GMP (black chromatogram) on a C18 column.** Peaks identified by ESI-MS: c-di-GMP  $m/z$  691,  $t_R$  7.70 min, T47 (amino acids 354-359)  $m/z$  659.3  $t_R$  25.64 min. T49 (amino acids 367-386)  $m/z$  2167.7  $t_R$  47.73 min.

**Figure S2: Normal modes of PleD I-site and A-site residues.** The displacements for each mode of the ligated and unligated structures are shown in Å for the residues of the REC2 domain (green) and the GGDEF domain (red). Insertion of intercalated c-di-GMP in the I-site quenches motion in both the I-site (R359-D362, R390) and the A-site (G368-E371), suggesting that the two sites are dynamically coupled.

**Figure S3: Representation of the PleD protein (blue: REC1, green: REC2, red: DGC) with c-di-GMP bound to the I-site.**  $C\alpha$ -atoms at positions of considerable changes in flexibility upon ligand binding are shown as spheres; reduced flexibility (yellow) and enhanced flexibility (black). Note that binding of c-di-GMP at the I-site (I) affects mobility not only in the I-site, but also in other regions of the protein, e.g. A-site (A), phosphorylation site (P) and dimer interface.

**Figure S4: Alignment of I- and A-site sequence of biochemically characterized diguanylate cyclases.** I-site residues (RXXD) are underlined in green and A-site residues (GGDEF) are underlined in yellow.

Figure S1

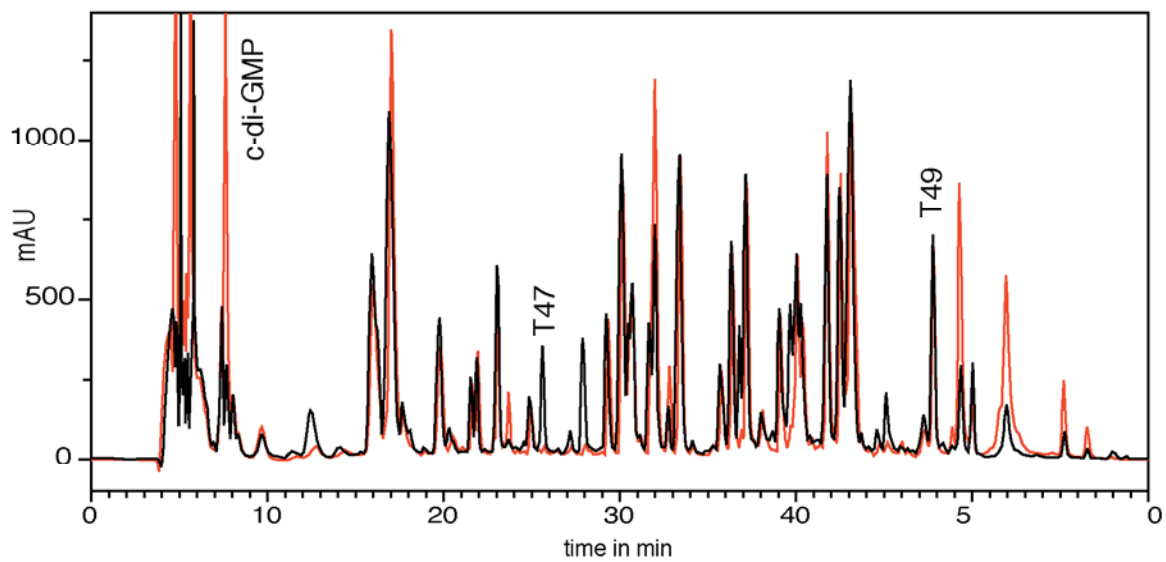


Figure S2

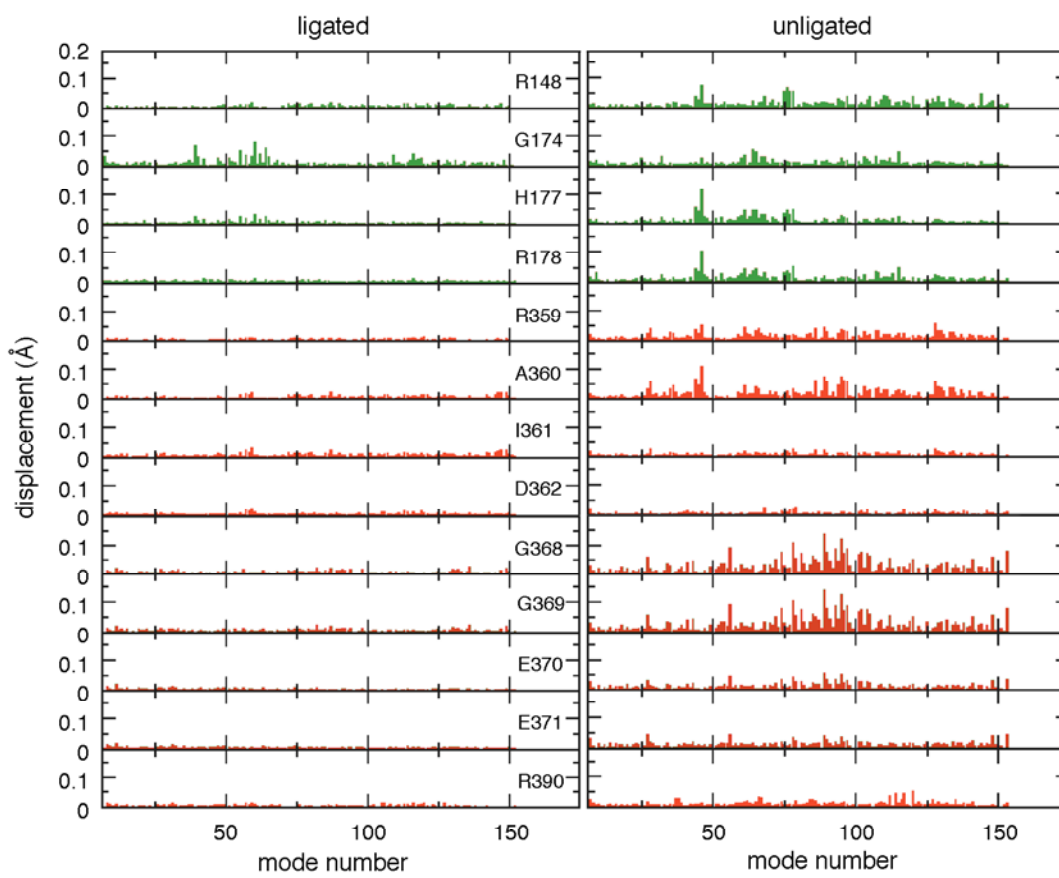


Figure S3

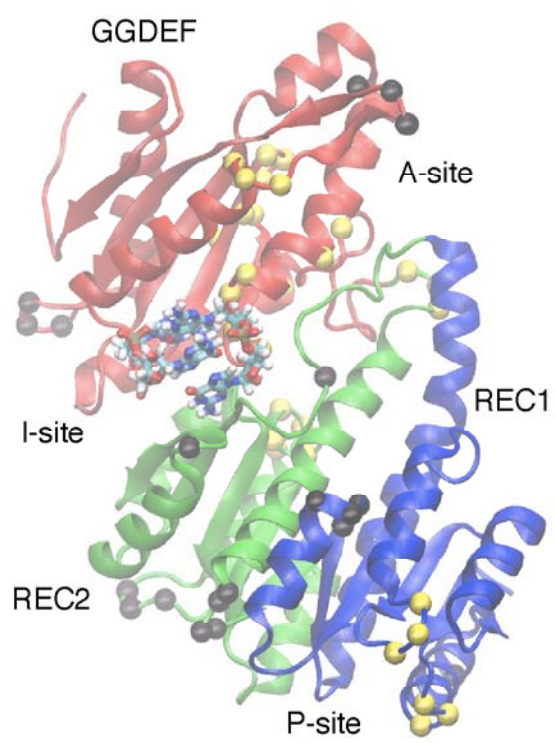


Figure S4

Gene	Sequence	Reference
BORBU_BB0419	LKYKIDVARYGGEEFI	(Ryjenkov et al, 2005)
CAUCR_DgcA	VRESDIVGRMGDEFA	- this study
CAUCR_PleD	VRAIDLPCRYGGEEFV	(Paul et al, 2004)
DEIRA_DRB0044	LPGGASLYRVGGDEFV	(Ryjenkov et al, 2005)
ECOLI_YddV	VRSSDYVFRYGGDEFI	(Mendez-Ortiz, 2006)
ECOLI_YeaP	QQNGEVIGRLGGDEFL	(Ryjenkov et al, 2005)
PSEAE_PA1107	TRSSDSVARLGGEEFL	(Kulesekara et al, 2006)
PSEAE_PA1120	LRESDLVARLGGDEFA	(Kulesekara et al, 2006)
PSEAE_PA1727	VRAQDTIARLGGDEFV	(Kulesekara et al, 2006)
PSEAE_PA2870	LREVDLLGRLGGEEFA	(Kulesekara et al, 2006)
PSEAE_PA3343	RRPLDMAVRLGGEEFA	(Kulesekara et al, 2006)
PSEAE_WspR	SRSSDLAARYGGEEFA	(Hickman et al, 2005)
PSEPA_PA0847	LRQPKAYRLGGDEFA	(Kulesekara et al, 2006)
RHOSP_Rsp3513	LGPADALGRIGGEEFA	(Ryjenkov et al, 2005)
SALTY_AdrA	LRGSDIIGRFGGDEFA	(Simm et al, 2005)
SYNY3_Slr1143	LRSYDILGRWGGDEFM	(Ryjenkov et al, 2005)
THEMA_TM1163	VRESDLVFRYGGDEFL	(Ryjenkov et al, 2005)
VIBCH_VCA096	CRDGVTAYRYGGEEFA	(Ryjenkov et al, 2005)
YERPS_HmsT	VRSRDIVVRYGGEEFL	(Simm et al, 2005)
Consensus	r d R GG#EF	

### **3.3 DgrA is a member of a new family of cyclic di-GMP receptors and controls flagellar motor functions in *Caulobacter crescentus***

M. Christen\*, B. Christen\*, M. G. Allan, M. Folcher, S. Moes, P. Jenö, S. Grsziek, and U. Jenal

**PNAS** (2007)

*\*These authors contributed equally to the work*



## Summary

In this publication we enlighten the signal transduction mechanism of the bacterial second messenger c-di-GMP and demonstrate the existence of diguanylate receptor proteins. We report the biochemical purification of c-di-GMP receptor proteins from *C. crescentus* crude extract and describe their physiological role in c-di-GMP dependent repression of cell motility. A multitude of biochemical, genetic and NMR experiments was used to characterize these effector proteins and homologs from *S. enterica* and *P. aeruginosa* down to molecular level. In particular we used [<sup>33</sup>P] c-di-GMP UV cross linking studies to demonstrate that these receptors specifically bind c-di-GMP in the sub micro molar range and, in combination with NMR spectrometry, to elicit determinants for c-di-GMP binding. Further more, we performed genetic suppressor analysis and epistasis experiments with receptor deletion and point mutants, to corroborate that the identified diguanylate receptors from *C. crescentus* act in vivo downstream of the second messenger c-di-GMP.

**DgrA is a member of a new family of cyclic di-GMP receptors and controls flagellar motor function in *Caulobacter crescentus***

Matthias Christen<sup>¶</sup>, Beat Christen<sup>¶</sup>, Martin G. Allan, Marc Folcher, Paul Jenö Stephan Grzesiek, and Urs Jenal<sup>§</sup>

Biozentrum, University of Basel, Klingelbergstrasse 70,

CH-4056 Basel, Switzerland

= These authors contributed equally to this work

<sup>§</sup> For correspondence:

Urs Jenal, Division of Molecular Microbiology, Biozentrum, University of Basel, Klingelbergstrasse 70, CH-4056 Basel, Switzerland, Telephone +41-61-267-2135, Fax +41-61-267-2118, E-mail [urs.jenal@unibas.ch](mailto:urs.jenal@unibas.ch)

Number of text pages: 16

Number of figures: 6

Number of tables: 1

Number of words in abstract: 185

Characters in text: 34.383

Total number of characters: 46983

Key words: c-di-GMP, PilZ, diguanylate receptor, *Caulobacter*, motility

## Abstract

Bacteria are able to switch between two mutually exclusive lifestyles, motile single cells and sedentary multicellular communities that colonize surfaces. These behavioral changes contribute to an increased fitness in structured environments and are controlled by the ubiquitous bacterial second messenger cyclic di-GMP. In response to changing environments, fluctuating levels of c-di-GMP inversely regulate cell motility and cell surface adhesins. Whereas the synthesis and breakdown of c-di-GMP has been studied in detail, little is known about the downstream effector mechanisms. Using affinity chromatography we have isolated several c-di-GMP binding proteins from *Caulobacter crescentus*. One of these proteins, DgrA, is a PilZ homolog involved in mediating c-di-GMP-dependent control of *C. crescentus* cell motility. Biochemical and structural analysis of DgrA and homologs from *C. crescentus*, *Salmonella typhimurium* and *Pseudomonas aeruginosa* demonstrated that this protein family represents a class of specific diguanylate receptors and suggested a general mechanism for c-di-GMP binding and signal transduction. Increased concentrations of c-di-GMP or DgrA blocked motility in *C. crescentus* by interfering with motor function rather than flagellar assembly. We present preliminary evidence implicating the flagellar motor protein FliL in DgrA-dependent cell motility control.

Cyclic purine nucleotides are ubiquitous second messengers involved in cell signaling. They are produced through the action of growth factors, hormones or neurotransmitters and elicit their response by acting on a range of downstream effector proteins like protein kinases, transcription regulators, gated ion channels, or GTPase nucleotide exchange factors. Whereas cAMP is widespread through all kingdoms of life, cGMP seems to be restricted to signaling in eukaryotes. Recently, a third major cyclic nucleotide messenger, cyclic di-guanosine-monophosphate (c-di-GMP) has emerged as a ubiquitous signaling molecule in prokaryotes, where it antagonistically controls motility and virulence of planktonic cells on one hand and cell adhesion and persistence of multicellular communities on the other (1, 2) (supplemental Fig. 7). C-di-GMP is synthesized from two molecules of GTP and degraded into the linear dinucleotide pGpG by the opposing activities of diguanylate cyclases (DGC) and c-di-GMP-specific phosphodiesterases (PDE). DGC and PDE activities are comprised in GGDEF and EAL domains, respectively (3-8), which represent two large families of output domains found in bacterial one- and two-component signal transduction systems (9, 10).

The molecular principles of c-di-GMP signaling have been studied in the model organism *Caulobacter crescentus*, where c-di-GMP coordinates the developmental transition from a motile swarmer cell to a surface attached, replication competent stalked cell. Both acquisition of flagellar motility in the predivisional cell and its replacement by an adhesive organelle later in development are controlled by c-di-GMP. TipF, an EAL domain protein, is required for an early step of flagellum assembly in the predivisional cell (11), whereas the diguanylate cyclase PleD is involved in flagellum ejection and subsequent steps in pole remodeling (3, 12-15). Similarly, the second messenger c-di-GMP regulates motility, adhesion factors and biofilm formation in a wide variety of bacterial pathogens including *Yersinia*, *Pseudomonas*, *Vibrio* and *Salmonella* (1, 2). C-di-GMP influences flagellar motility as a function of growth (16) or adaptation to surfaces (17), affects pili assembly (18), and controls the production of surface structures like fimbriae and exopolysaccharide matrices (19). The wide variety of cellular functions that are affected by c-di-GMP calls for multiple receptors and signaling mechanisms. However, little information is available on specific targets of c-di-GMP action. With the exception of a component of the cellulose synthase complex from *Gluconacetobacter* (20, 21) and the recent prediction of a candidate c-di-GMP binding domain (22, 23), no c-di-GMP effector proteins have been reported. We have

designed a biochemical approach to purify and characterize c-di-GMP effector molecules from *Caulobacter crescentus* crude cell extracts.

## Results:

**Purification of c-di-GMP binding proteins from *C. crescentus*.** Based on the assumption that c-di-GMP signal transduction depends on specific receptor proteins, we designed a biochemical purification strategy to identify such components. C-di-GMP binding proteins from *C. crescentus* were purified by two consecutive chromatography steps using BlueSepharose<sup>®</sup> CL-6B and affinity chromatography with GTP immobilized on Epoxy activated Sepharose 4B (Pharmacia). UV crosslinking with [<sup>33</sup>P]c-di-GMP was used to identify proteins with specific binding activity for c-di-GMP (see Materials and Methods and supplemental Table II). Two binding proteins with apparent molecular weights of 47 kDa and 36 kDa were detected in the 0.4 – 0.7 M NaCl eluate of the BlueSepharose<sup>®</sup> column (Fig. 1A, B, lane 3) and the 0.7 – 0.9 M NaCl fraction contained several small c-di-GMP binding proteins with apparent molecular weights of 8-12 kDa (Fig. 1A, B, lanes 4-5; Fig. 1C). The latter fraction was dialyzed, concentrated and separated on a GTP Epoxy-Sepharose 4B affinity column (Fig. 1A,B lane 4 and Fig. C). One of these (labeled c in Fig. 1C) was identified by MS/MS as the product of gene CC1599, a conserved hypothetical 12.5 kDa protein that we consequently renamed as diguanylate receptor A (DgrA). Sequence comparison disclosed DgrA as a member of the PilZ protein family, members of which have recently been proposed by bioinformatics to be c-di-GMP effector proteins (22).

**DgrA is a diguanylate receptor protein.** In order to confirm that the identified protein is a c-di-GMP receptor, *dgrA* was subcloned into the expression vector pET-42b and the recombinant hexahistidine-tagged protein was purified by Ni-NTA-affinity chromatography. Like the semi-purified protein from *C. crescentus* (Fig. 1C), the recombinant protein showed strong labeling upon UV crosslinking with [<sup>33</sup>P]c-di-GMP (Fig. 2A), confirming that DgrA is a c-di-GMP receptor protein. UV crosslinking experiments with DgrA in the presence of 60 nM <sup>33</sup>P labeled c-di-GMP and increasing concentrations of cold c-di-GMP, GTP (200 μM), or pGpG (200 μM) indicated that DgrA binds c-di-GMP with high affinity and specificity (Fig. 2B). Furthermore, c-di-GMP seems to bind to DgrA in a non-covalent manner since no radiolabeled c-di-GMP was incorporated without UV irradiation (Fig. 2B). The dissociation constant for c-di-GMP of the recombinant DgrA was determined using the UV

crosslinking assay (Table I). Saturated incorporation of radiolabeled c-di-GMP was already observed at 50 nM, indicating that the  $K_D$  of DgrA for c-di-GMP is below 50 nM.

To test if other members of the PilZ protein family also bind c-di-GMP we analyzed several ortho- or paralogs of DgrA, including CC3165 (renamed as DgrB), YcgR from *S. typhimurium* (24) and PA4608 from *P. aeruginosa* (Fig. 6). As shown in Fig. 2A all four proteins were efficiently labeled with  $^{33}\text{P}$  c-di-GMP upon UV crosslinking, whereas the control protein BSA did not incorporate c-di-GMP. The c-di-GMP binding constants of DgrB, YcgR and PA4608 were determined by performing UV crosslinking experiments with 50 nM receptor protein in the presence of increasing concentrations of  $^{33}\text{P}$  labeled c-di-GMP (50 - 1000 nM). All wild type diguanylate receptor proteins exhibit a binding affinity in the nanomolar range (Table I). Taken together, these data demonstrate that DgrA and its homologs containing a PilZ domain are members of a class of small diguanylate receptor proteins, which bind c-di-GMP, but not other guanine nucleotides, with high affinity. Thus, these proteins represent bona fide diguanylate receptor proteins and may be involved in the response of specific cell functions to fluctuating concentrations of c-di-GMP (2).

**DgrA and DgrB mediate c-di-GMP-dependent motility control in *C. crescentus*.** Low concentrations of c-di-GMP are generally associated with flagella or pili based motility of single planktonic cells, whereas increased concentrations of c-di-GMP promote multicellular traits and efficiently block cell motility (2). In agreement with this, *C. crescentus* cells are non-motile in the presence of a plasmid-borne copy of *dgcA*, which encodes a highly active, soluble diguanylate cyclase (15) (Fig. 3A). Electron micrographs and immunoblot experiments showed that these cells were flagellated and expressed similar level of flagellins (data not shown), arguing that increased c-di-GMP concentrations interfere with flagellar function rather than with the expression or assembly of flagellar components. To test if motility control by c-di-GMP involves *dgrA* or *dgrB*, single and double in frame deletion mutants were generated using a two-step homologous recombination procedure (see supplemental materials). In contrast to *C. crescentus* wild type,  $\Delta dgrA$  and  $\Delta dgrB$  mutants were motile even in the presence of the *dgcA* plasmid (Fig. 3A strains). This was not due to a reduction of the c-di-GMP concentration, as cellular levels of c-di-GMP in these mutants were indistinguishably high (data not shown). At low cellular concentrations of c-di-GMP, motility phenotypes were not significantly altered in the deletion mutants (data not shown), indicating that

DgrA and DgrB interact with cell motility primarily at conditions where the level of c-di-GMP is elevated. Together, these data suggested that the c-di-GMP binding proteins DgrA and DgrB are part of a signal transduction pathway that interferes with flagellar function in response to increasing concentrations of c-di-GMP. In agreement with this, overexpression of *dgrA* or *dgrB* from a plasmid efficiently blocked motility on swarmer plates (Fig. 3B) and in liquid media as observed microscopically (data not shown).

**Analysis of c-di-GMP binding to the diguanylate receptor by NMR spectroscopy.** The available NMR structure and resonance assignments of the DgrA homolog PA4608 from *P. aeruginosa* (25) (PDB 1YWU; BMRB 6514) provided an opportunity to characterize the ligand binding site on a molecular level and to investigate the structural consequences of ligand binding. PA4608 carrying an N-terminal hexahistidine tag was produced in uniformly  $^{15}\text{N}$ - and  $^{13}\text{C}$ -labeled form for NMR spectroscopy. The  $^1\text{H}$  and  $^{15}\text{N}$  chemical shifts observed for pure PA4608 were in good agreement with those reported in BMRB entry 6514. When c-di-GMP was added to the protein,  $^1\text{H}$ - $^{15}\text{N}$ -HSQC spectra changed dramatically (supplemental Fig. 8). Free and ligand-bound PA4608 were in slow exchange on the NMR chemical shift time scale, and titration curves were in agreement with a  $K_D$  in the sub- $\mu\text{M}$  range (data not shown). In order to assign resonances of the PA4608\*c-di-GMP complex, exchange (EXSY) spectra were recorded on a roughly 3:1 mixture of free and c-di-GMP-bound PA4608; exchange within a mixing time of 800 ms was only observed after heating to 313 K. Standard triple-resonance NMR spectra recorded on PA4608 saturated with c-di-GMP were used to complete the backbone resonance assignments. No resonances were observed for residues M3-H12 (hexahistidine tag), H22, F33-I36, G73, I91, E125, L128, and D130-L138<sup>1</sup>. Probably, these residues are flexible on a  $\mu\text{s}$  to ms time scale, and peaks are broadened beyond detection due to intermediate chemical exchange. Secondary  $^{13}\text{C}^\alpha$  and  $^{13}\text{C}^\beta$  shifts (26) showed that the secondary structure of PA4608 remained essentially unchanged after ligand binding (supplemental Fig. 9).

In order to localize the ligand binding site on the protein surface, backbone amide  $^1\text{H}$  and  $^{15}\text{N}$  chemical shifts of the PA4608\*c-di-GMP complex were compared to those of the free protein, and the differences were mapped

---

<sup>1</sup> Residue numbering for PA4608 as in BMRB entry 6514, which differs from that in PDB structure 1YWU by +22, is used throughout this text.



on the structure of the free protein (Figs. 5, 8). Large shift differences are found on one face of the  $\beta$  barrel (around V58, I63), in the C-terminus (V142, A144), and in the N-terminus (R30-D39). We conclude that c-di-GMP binds to the outside of the  $\beta$  barrel close to V58, and that the termini, which are partially flexible in the apo form, fold around the bound ligand. Presumably the side chain N-H group of W99 forms a hydrogen bond with the ligand, since the  $^{15}\text{N}^{\epsilon 1}$  and  $^1\text{H}^{\epsilon 1}$  resonances strongly shift towards higher chemical shifts by 8.24 and 1.66 ppm, respectively.

Due to their distinct chemical shifts ( $>10.7$  ppm), the H1 imino hydrogens of guanine in c-di-GMP could be identified once the assignment of protein backbone  $^1\text{H}^{\text{N}}$  and tryptophan  $^1\text{H}^{\epsilon 1}$  resonances had been completed. Since four separate H1 resonances of about equal intensity are observed for c-di-GMP in complex with PA4608, and each molecule of c-di-GMP contains two guanine bases, c-di-GMP binds to PA4608 as a dimer. Consistent with the ligand-binding site outlined above, two of these H1 imino resonances show intermolecular NOEs to L64 and W99 (supplemental Fig. 10).

Amide  $^{15}\text{N}$   $T_1$  and  $T_2$  relaxation times and heteronuclear  $\{^1\text{H}\}$ - $^{15}\text{N}$  NOEs were measured at 20°C for free and c-di-GMP-bound PA4608 (data not shown). Isotropic rotational correlation times ( $\tau_c$ ) were determined from these data with the program TENSOR (27) as 11.3 and 12.3 ns for free and ligand-bound protein, respectively. These  $\tau_c$  are in reasonable agreement with values expected for monomeric apo-PA4608 (16.7 kDa, 9.8 ns) and c-di-GMP-bound PA4608 (18.1 kDa, 10.6 ns). Thus, PA4608 is a monomer before and after ligand binding.

**C-di-GMP binding mutants of DgrA are unable to control motility.** Alignments of the amino acid sequences of PA4608, DgrA, DgrB, and YcgR revealed that the key residues that, based on NMR data, were postulated to be involved in c-di-GMP binding to PA4608, are conserved among other diguanylate receptor proteins (Fig. 6). To probe the c-di-GMP binding site of DgrA and to define the minimal requirements for c-di-GMP binding, residues R11, R12, D38, and W75 were replaced with Ala and the mutant proteins were analyzed for c-di-GMP binding. Mutants R11AR12A and W75A strongly reduce c-di-GMP binding, whereas mutant D38A is still able to bind c-di-GMP (Fig. 5A). In agreement with this, the binding constant for the D38A mutant was marginally increased to 740 nM, whereas the  $K_D$  for the W75A mutant (6.4  $\mu\text{M}$ ) was increased 100-1000 fold as compared to wild type (Table I). Binding of c-di-GMP was completely abolished in the R11AR12A mutant. To analyze the

importance of c-di-GMP binding for DgrA mediated signaling, the *dgrA* mutant alleles were tested for functionality *in vivo*. As indicated above, overexpression of wild type *dgrA* renders cells non-motile (Figs. 4B, 6B). In contrast, overexpression of *dgrAD38A*, *dgrAR11AR12A*, or *dgrAW75A* only partially affected motility (Fig. 5B). In particular, changing W75 to Ala almost completely abolished the ability of DgrA to block motility under these conditions (Fig. 5B). Similarly, when the *dgrAW75A* mutant allele was expressed in single copy from its original chromosomal locus, cells were fully motile even in the presence of the *dgcA* plasmid, arguing that DgrAW75A can no longer control motility in response to increased c-di-GMP levels (Fig. 3). We isolated suppressors that alleviated the *dgrA*-mediated motility block (see Materials and Methods). One of the intragenic *dms* (diguanylate receptor motility suppressors) mutations mapped to V74, in the immediate vicinity of the Trp residue critical for c-di-GMP binding (Fig. 5B, Fig. 6). Other intragenic *dms* mutations (D62, G82) mapped to conserved residues of DgrA, emphasizing the functional importance of these residues (Fig. 6). In conclusion, these results support the view that ligand binding is essential for the regulatory function of the diguanylate receptor and suggest that DgrA blocks motility in its c-di-GMP bound state.

**Motility control by DgrA correlates with cellular levels of the FliL motor protein.** Immunoblot analysis revealed that overexpression of *dgrA* or *dgrB* blocks motility without interfering with the expression of known class II, class III or class IV components of the flagellar hierarchy (Fig. 3C). Because the expression of each class of genes depends on the successful expression and assembly of components of the preceding class of the hierarchy (28), this result suggested that flagella are assembled normally in cells overexpressing *dgrA* or *dgrB*. In agreement with this, flagella were readily observed by electron microscopy in these non-motile cells (data not shown). The only flagellar protein whose concentration was severely affected in cells overexpressing *dgrA* was FliL (Fig. 3C). The *C. crescentus fliL* gene is not part of the flagellar hierarchy and its product is not assembled into the flagellar structure (29). However, *fliL* is required for flagellar rotation (29). To examine if reduced FliL levels are linked to motility we screened the pool of *dms* mutants (see above) for extragenic suppressors (see Materials and Methods). From a total of 120 independently isolated motile suppressors, only one mapped to the chromosome. This suppressor mutation (*dms0541*), which mapped to gene CC3587 coding for the ribosomal protein S1, not only restored motility but also re-established normal levels of FliL (Fig. 3C).

## Discussion:

Motility control by c-di-GMP is implemented through gene expression, organelle assembly, or motor function (2). In *C. crescentus*, increased cellular concentrations of c-di-GMP block motility by interfering with motor function rather than by altering expression or assembly of structural components of the flagellum (13). How are increased levels of c-di-GMP sensed and how is this information transmitted to the flagellar motor? The data presented here suggest that DgrA and DgrB are high affinity receptors for c-di-GMP that, in a ligand-bound form, interfere with the flagellar motor either directly or indirectly. Motor control by DgrA-like proteins is not unique to *Caulobacter*. *E. coli* H-NS mutants lack flagella because the expression of the flagellar master control operon *flhCD* is reduced. Ectopic expression of *flhCD* restores flagellation but leaves the motors partially paralyzed (24). Under these conditions flagellar function can be restored either by a mutation in *ycgR*, coding for the *E. coli* DgrA homolog, or by providing multiple copies of *yhjH*, which encodes a presumable c-di-GMP specific phosphodiesterase (24). Together with our data demonstrating that the *Salmonella* YcgR protein specifically binds c-di-GMP, this suggests that in *C. crescentus* and in enteric bacteria flagellar motor function might be controlled by c-di-GMP via similar mechanisms.

But how would DgrA or YcgR interfere with the function of the flagellum? Our data propose the FliL protein as a candidate for such a role. FliL was the only flagellar protein that showed significantly reduced levels in non-motile cells overexpressing *dgrA*. In *C. crescentus* the FliL protein is not part of the flagellar structure but is required for flagellar rotation (29). Intriguingly, *fliL* mutant strains exhibit an identical motility phenotype like cells that have high levels of c-di-GMP or overexpress *dgrA* (29). Because the expression of *fliM*, the gene located immediately downstream of *fliL* in the same operon (30), was not affected by DgrA, FliL changes must be the result of altered translation or protein stability. An extragenic suppressor mutation that restored motility under these conditions also re-established normal FliL concentrations, indicating that the two phenotypes are linked. The simplest model that is in agreement with these results predicts that DgrA, upon binding of c-di-GMP, represses FliL by a so far unknown mechanism and through this blocks motor function. The extragenic suppressor mutation restoring FliL levels was mapped to the coding region of *rpsA* (*ribosomal protein S1*). RpsA enhances translation initiation by binding to mRNA regions upstream of the Shine-Dalgarno sequence and by

tethering the mRNAs on the 30S subunit of the ribosome (31-33). We are currently investigating how DgrA and its ligand c-di-GMP modulate FliL levels. Recently, FliL was reported to be involved in surface sensing and virulence gene expression in the urinary tract pathogen *Proteus mirabilis* (34). Thus, it is possible that FliL has a more general role in controlling the switch between a planktonic and a surface-associated lifestyle.

A bioinformatics study originally proposed that the PilZ domain is a specific c-di-GMP binding module (22). This was recently substantiated by the demonstration that YcgR, a PilZ protein from *E. coli*, is able to bind c-di-GMP (23). Here we presented genetic, biochemical, and structural evidence that further validate this hypothesis and propose a model for ligand binding and activation of proteins containing a PilZ domain. NMR studies with the DgrA homolog PA4608 showed that a dimer of c-di-GMP binds to a well-defined binding site on the surface of the  $\beta$ -barrel (Fig. 4). Large chemical shift differences between free and ligand-bound PA4608, which indicate changes in the local environment, were also observed in both termini of the protein, with the largest differences observed for residues R30-R32, V142, and A144. These regions are structurally ill defined in the absence of ligand (25) and are probably flexible. The observed chemical shift differences indicate that these regions come in direct contact with the ligand after complex formation. The N-terminal part of PA4608 contains three consecutive Arg residues, which are conserved in most PilZ domains (22) (Fig. 6). Arg side chains are likely to be involved in hydrogen bonds or in electrostatic or  $\pi$  stacking interactions with c-di-GMP, as has been shown for the allosteric binding site of the diguanylate cyclases PleD and DgcA (15, 35). Furthermore, it is conceivable that the positively charged head groups of Arg are sufficient for transient binding to the phosphate groups of c-di-GMP and that their position on the flexible N-terminus increases the ligand capture radius of the protein, as in the “fly-casting mechanism” proposed in (36). Alternatively, the observed folding of previously flexible parts of the protein may be responsible for communication of the c-di-GMP signal to downstream elements, either by forming new interaction surfaces or by determining the relative position of neighboring domains. Similarly, the chemical shift differences of the C-terminal part of PA4608 could be explained by a specific role in ligand binding. However, the fact that residues V142 and A144, which showed the largest chemical shift differences are not conserved, argues against this possibility. Several of the motile *dgrA* loss of function suppressors that were isolated had frameshift mutations in the very C-terminus of DgrA (Fig. 6), suggesting that this part of the protein is critical for its *in vivo* function. One possibility is that the C-terminus

contributes to the specific readout mechanism of this protein family. Upon c-di-GMP binding to the  $\beta$ -barrel surface, the C-terminus could be untied to interact with downstream components. In accordance with such a view, the very C-terminus of the *P. aeruginosa* PilZ protein has recently been proposed to interact with the PilF protein required for type 4-pilus assembly (37). To complement our picture of the c-di-GMP circuitry, future studies will have to focus on interaction partners of DgrA and related PilZ domain proteins.

It is intriguing that genetic and biochemical studies of the *C. crescentus* DgrA protein and structural analysis of PA4608 from *P. aeruginosa* identified the same set of key amino acids involved in c-di-GMP binding (Fig. 6). This finding is a strong indication that these proteins bind c-di-GMP in a similar way and suggests that they may share a common signaling mechanism. Based on these results we postulate that most or all PilZ domain proteins function as diguanylate receptor proteins.

## Materials and Methods:

**Strains, plasmids and media.** *E. coli* strains were grown in Luria Broth (LB). *C. crescentus* strains were grown in complex peptone yeast extract (PYE) (38) supplemented with antibiotics, where necessary. For the exact procedure of strain and plasmid construction see supplemental material.

**UV cross-linking with [<sup>33</sup>P]c-di-GMP, and isolation of DgrA.** Procedures for enzymatic production of [<sup>33</sup>P]c-di-GMP and, UV cross-linking with [<sup>33</sup>P]c-di-GMP were published earlier (6, 39). For a detailed protocol used for the isolation of DgrA see supplemental material.

**Preparation of isotope-labeled protein, NMR samples and NMR spectroscopy.** The detailed procedures for overexpression and <sup>13</sup>C, <sup>15</sup>N- double-labeling of PA4608 are described in supplemental material. NMR samples (Shigemi microtubes) were prepared as 0.8 mM U-<sup>13</sup>C/<sup>15</sup>N-labeled protein in 300 μl 95 % H<sub>2</sub>O/5% D<sub>2</sub>O, 250 mM NaCl, 10 mM DTT, 1 mM sodium azide, 10 mM Tris at pH 7.1. C-di-GMP was added at suitable molar ratios from a 7.7 mM stock solution. NMR spectra were recorded on Bruker DRX 600 and 800 MHz spectrometers at 293 K (20°C) with the exception of EXSY spectra that were recorded at 313 K for faster exchange. Standard 1D, 2D and 3D spectra were recorded and processed as described elsewhere (40).

**Isolation and mapping of motile *dgrA* suppressors.** A plasmid carrying *dgrA* (pBBR::*dgrA*) was conjugated into a *C. crescentus recA* mutant strain and 150 individual transconjugants were patched onto PYE swarmer plates. Motile *dms* (diguanylate receptor motility suppressors) mutants were isolated and analyzed by immunoblot using an α-DgrA antibody. Mutants with reduced DgrA levels were discarded. The rest was analyzed by retransforming plasmids into the *recA* mutant strain in order to distinguish between intra- and extragenic suppressors. Intragenic mutations were identified by sequencing.. The extragenic suppressor (*dms0541*) was mapped by *Tn5* linkage (41) and co-transduction with phage ΦCR30, and identified by sequencing.

## **Acknowledgments**

We would like to thank Suzette Moes for handling of MS samples, Martha Gerber and Flora Mauch for help with the suppressor screen, Jacob Malone for a gift of *P. aeruginosa* DNA, and Colin Manoil for providing plasmid pIT2. This work was supported by Swiss National Science Foundation Fellowships 3100A0-108186 to U.J. and 31-109712 to S.G.

## References:

1. Kolter, R. & Greenberg, E. P. (2006) *Nature* **441**, 300-302.
2. Jenal, U. & Malone, J. (2006) *Annual Review of Genetics* **40**, 385-407.
3. Paul, R., Weiser, S., Amiot, N. C., Chan, C., Schirmer, T., Giese, B. & Jenal, U. (2004) *Genes Dev* **18**, 715-727.
4. Ryjenkov, D. A., Tarutina, M., Moskvina, O. V. & Gomelsky, M. (2005) *J Bacteriol* **187**, 1792-8.
5. Schmidt, A. J., Ryjenkov, D. A. & Gomelsky, M. (2005) *J Bacteriol* **187**, 4774-81.
6. Christen, M., Christen, B., Folcher, M., Schauerte, A. & Jenal, U. (2005) *J Biol Chem* **280**, 30829-37.
7. Bobrov, A. G., Kirillina, O. & Perry, R. D. (2005) *FEMS Microbiol Lett* **247**, 123-30.
8. Tamayo, R., Tischler, A. D. & Camilli, A. (2005) *J Biol Chem* **280**, 33324-3.
9. Galperin, M. Y., Nikolskaya, A. N. & Koonin, E. V. (2001) *FEMS Microbiol Lett* **203**, 11-21.
10. Ulrich, L. E., Koonin, E. V. & Zhulin, I. B. (2005) *Trends Microbiol* **13**, 52-6.
11. Huitema, E., Pritchard, S., Matteson, D., Radhakrishnan, S. K. & Viollier, P. H. (2006) *Cell* **124**, 1025-37.
12. Aldridge, P. & Jenal, U. (1999) *Mol Microbiol* **32**, 379-91.
13. Aldridge, P., Paul, R., Goymer, P., Rainey, P. & Jenal, U. (2003) *Mol Microbiol* **47**, 1695-708.
14. Levi, A. & Jenal, U. (2006) *J Bacteriol* **188**, 5315-8.
15. Christen, B., Christen, M., Paul, R., Schmid, F., Folcher, M., Jenoe, P., Meuwly, M. & Jenal, U. (2006) *Journal of Biological Chemistry*.
16. Choy, W. K., Zhou, L., Syn, C. K., Zhang, L. H. & Swarup, S. (2004) *J Bacteriol* **186**, 7221-8.
17. Boles, B. R. & McCarter, L. L. (2002) *J Bacteriol* **184**, 5946-54.
18. Kazmierczak, B. I., Lebron, M. B. & Murray, T. S. (2006) *Mol Microbiol* **60**, 1026-43.
19. Kader, A., Simm, R., Gerstel, U., Morr, M. & Romling, U. (2006) *Mol Microbiol* **60**, 602-16.
20. Ross, P., Mayer, R., Weinhouse, H., Amikam, D., Huggirat, Y., Benziman, M., de Vroom, E., Fidder, A., de Paus, P., Sliedregt, L. A. & et al. (1990) *J Biol Chem* **265**, 18933-43.
21. Weinhouse, H., Sapir, S., Amikam, D., Shilo, Y., Volman, G., Ohana, P. & Benziman, M. (1997) *FEBS Lett* **416**, 207-11.
22. Amikam, D. & Galperin, M. Y. (2006) *Bioinformatics* **22**, 3-6.
23. Ryjenkov, D. A., Simm, R., Romling, U. & Gomelsky, M. (2006) *J Biol Chem* **281**, 30310-4.
24. Ko, M. & Park, C. (2000) *J Mol Biol* **303**, 371-82.
25. Ramelot, T. A., Yee, A., Cort, J. R., Semesi, A., Arrowsmith, C. H. & Kennedy, M. A. (2006) *Proteins*.
26. Spera, S. & Bax, A. (1991) *Journal of the American Chemical Society* **113**, 5490-5492.
27. Dosset, P., Hus, J.-C., Blackledge, M. & Marion, D. (2000) *J. Biomol. NMR* **16**, 23-28.
28. Gober, J. W. a. E., J.C. (2000) in *Prokaryotic development*, ed. Shimkets, Y. V. B. a. L. J. (ASM Press, Washington, DC), pp. 319-339.
29. Jenal, U., White, J. & Shapiro, L. (1994) *J Mol Biol* **243**, 227-44.
30. Yu, J. & Shapiro, L. (1992) *J Bacteriol* **174**, 3327-38.
31. Sengupta, J., Agrawal, R. K. & Frank, J. (2001) *Proc Natl Acad Sci U S A* **98**, 11991-6.
32. Komarova, A. V., Tchufistova, L. S., Supina, E. V. & Boni, I. V. (2002) *Rna* **8**, 1137-47.
33. Sorensen, M. A., Fricke, J. & Pedersen, S. (1998) *J Mol Biol* **280**, 561-9.
34. Belas, R. & Suvanasuthi, R. (2005) *J Bacteriol* **187**, 6789-803.
35. Chan, C., Paul, R., Samoray, D., Amiot, N. C., Giese, B., Jenal, U. & Schirmer, T. (2004) *Proc Natl Acad Sci U S A* **101**, 17084-9.
36. Shoemaker, B. A., Portman, J. J. & Wolynes, P. G. (2000) *Proceedings of the National Academy of Sciences of the United States of America* **97**, 8868-+.
37. Kim, K., Oh, J., Han, D., Kim, E. E., Lee, B. & Kim, Y. (2006) *Biochemical and Biophysical Research Communications* **340**, 1028-1038.
38. Ely, B. (1991) *Methods Enzymol* **204**, 372-84.
39. Christen, B., Christen, M., Paul, R., Schmid, F., Folcher, M., Jenoe, P., Meuwly, M. & Jenal, U. (2006) *J Biol Chem* **281**, 32015-24.
40. Grzesiek, S., Bax, A., Hu, J. S., Kaufman, J., Palmer, I., Stahl, S. J., Tjandra, N. & Wingfield, P. T. (1997) *Protein Science* **6**, 1248-1263.



41. Jacobs, M. A., Alwood, A., Thaipisuttikul, I., Spencer, D., Haugen, E., Ernst, S., Will, O., Kaul, R., Raymond, C., Levy, R., Chun-Rong, L., Guenther, D., Bovee, D., Olson, M. V. & Manoil, C. (2003) *PNAS* **100**, 14339-14344.

**Fig. 1.** Isolation of c-di-GMP binding proteins from *C. crescentus*. A) Coomassie stained SDS-PAGE gel with protein fractions used for UV-crosslinking with [<sup>33</sup>P]c-di-GMP. Lane 1: 100.000 × g supernatant, lane 2: 60% ammonium sulfate precipitation, lane 3: 0.4 - 0.7 M NaCl eluate from Blue Sepharose<sup>®</sup>, lane 4: 0.7 - 0.9 M NaCl eluate from Blue Sepharose<sup>®</sup> and lane 5: 125 mM NaCl eluate from GTP-sepharose column. B) Autoradiograph of SDS-PAGE gel shown in A. C-di-GMP binding proteins a, b, and c were identified by MS/MS and their role in c-di-GMP signaling is under investigation. Protein c was identified by MS/MS as hypothetical protein CC1599 and was renamed DgrA (Diguanylate receptor protein A).

**Fig. 2.** DgrA is a member of a novel family of c-di-GMP binding proteins. A) UV crosslinking of purified hexahistidine-tagged diguanylate receptor proteins with [<sup>33</sup>P]c-di-GMP. The following proteins were used: DgrA (CC1599; *C. crescentus*), DgrB (CC3165; *C. crescentus*), PA4608 (*P. aeruginosa*), YcgR (*S. typhimurium*), and BSA (control). The Coomassie-stained gel (left) and the autoradiograph (right) are shown. B) UV crosslinking of 10 μM DgrA in the presence of 60 nM of <sup>33</sup>P labeled c-di-GMP. Samples were supplemented with increasing concentrations of non-labeled nucleotides as indicated. Controls carried out in the absence of UV irradiation or with BSA are shown on the right.

**Fig. 3.** DgrA and DgrB are involved in motility control by c-di-GMP. Motility behavior of *C. crescentus* wild type strain CB15 and mutants are shown on semisolid agar plates. Three different colonies from independent conjugation experiment are shown. A) The following strains containing plasmid pUJ142::*dgcA* or control plasmid pUJ142 were analyzed: CB15/pUJ142::*dgcA* (a), CB15Δ*dgrA*/pUJ142::*dgcA* (b), CB15*dgrAW75A*/pUJ142::*dgcA* (c), CB15Δ*dgrB*/pUJ142::*dgcA* (d), CB15Δ*dgrA*Δ*dgrB*/pUJ142::*dgcA* (e), CB15/pUJ142 (f). B) Overexpression of *dgrA* or *dgrB* from the lactose promoter (Plac) repressed *C. crescentus* motility. CB15/pBBR (vector control) (a), CB15/pBBR::*dgrA* (b), CB15/pBBR::*dgrB* (c). C) Levels of class II, class III, and class IV structural components of the *C. crescentus* flagellum were determined by immunoblot analysis for the following strains: CB15/pBBR (wild-type), CB15/pBBR::*dgrA* (DgrA), CB15/pBBR::*dgrB* (DgrB) and the extragenic diguanylate receptor motility suppressors CB15*dms0541* pBBR::*dgrA* (*dms0541*). The motility behavior of each strain is shown on top of the graph.

**Fig. 4.** Combined amide  $^1\text{H}$  and  $^{15}\text{N}$  shift differences ( $\Delta\delta$ ) between PA4608 in its free and ligand-bound form. Shift differences are color-coded on the structure of free PA4608 (PDB 1YWU, model 12). Combined chemical shift differences were calculated as  $\Delta\delta = \text{sqrt}([(\Delta\delta_{\text{H}})^2 + (\Delta\delta_{\text{N}}/5)^2]/2)$ . These data are also shown in supplemental Fig. 8. Residue W99 is shown as sticks, and  $\text{N}^{\text{e1}}$  and  $\text{H}^{\text{e1}}$  are shown in red to highlight the large  $\Delta\delta$  value (1.67 ppm) for these atoms.

**Fig. 5.** C-di-GMP binding and motility control of DgrA mutants. A) UV crosslinking of different DgrA mutant proteins with [ $^{33}\text{P}$ ]c-di-GMP. Coomassie stained SDS-PAGE (top) and autoradiograph (bottom) with purified wild-type and mutant DgrA proteins (10  $\mu\text{M}$ ). B) Motility behavior of *C. crescentus* wild type CB15 overexpressing different *dgrA* alleles. CB15/pBBR::*dgrA* (a), CB15/pBBR::*dgrAR11AR12A* (b), CB15/pBBR::*dgrAD38A* (c), CB15/pBBR::*dgrAV74A* (d), CB15/pBBR::*dgrAR11AR12AV74A* (e), CB15/pBBR::*dgrAW75A* (f), CB15/pBBR (vector control) (g). Three different colonies from independent conjugation experiment are shown.

**Fig. 6.** Sequence alignment of the c-di-GMP binding proteins DgrA, DgrB, YcgR and PA4608 according to the PilZ PFAM entry PF07238. The PilZ domain is highlighted in green. DgrA residues shown to be important for c-di-GMP binding and *in vivo* function (red) and the positions of intragenic *dms* suppressor mutations (black) are highlighted above the alignment. Residues of PA4608 with large chemical shift differences upon c-di-GMP binding (blue) are indicated below the alignment.

Table I:  
Binding constants of diguanylate receptor proteins determined by UV crosslinking with <sup>33</sup>P c-di-GMP

Organism	Protein	K <sub>D</sub> in nM	ΔK <sub>D</sub>	
<i>C. crescentus</i>	DgrB	132	36	
	DgrA	wt <sup>*</sup>	< 50	14
		RR11AA	N. D. <sup>**</sup>	-
		D38A	761	149
		W75A	6200	496
<i>S. typhimurium</i>	YcgR	182	29	
<i>P. aeruginosa</i>	PA4608	< 50	27	

protein concentrations used for binding assay: 50 nM

<sup>\*</sup> wt, wild type

<sup>\*\*</sup> N.D. not detectable

Table II:  
Purification of c-di-GMP binding proteins from *C. crescentus* CB15 crude extracts

Sample	Total yield of protein		Total yield of binding activity	Purification
	$\mu g$	%	%	<i>fold</i>
100.000 x g supernatant	680.000	100	100	1
60 % (NH <sub>4</sub> ) <sub>2</sub> SO <sub>4</sub> precipitation	323,000	47.5	95	2
BlueSepharose 0.4 - 0.7 M NaCl	10.800	1.59	40	26
BlueSepharose 0.7 - 0.9 M NaCl	7.800	1.15	41	35
GTP Sepharose 125 mM NaCl	24	0.0035	11	3200

Figure 1

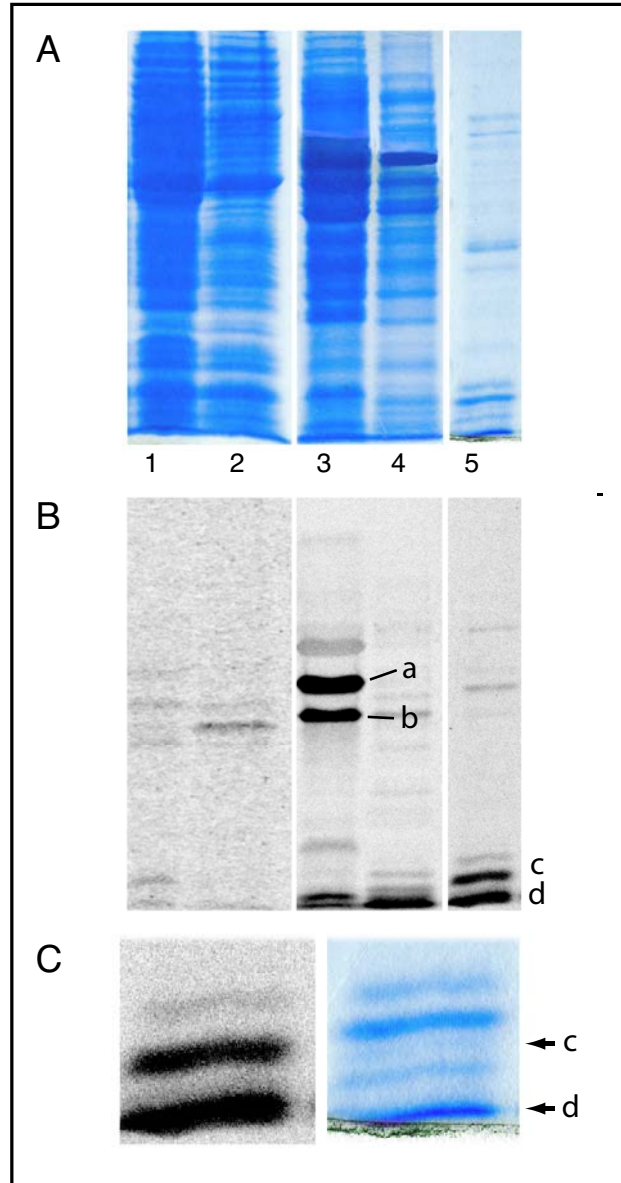


Figure 2

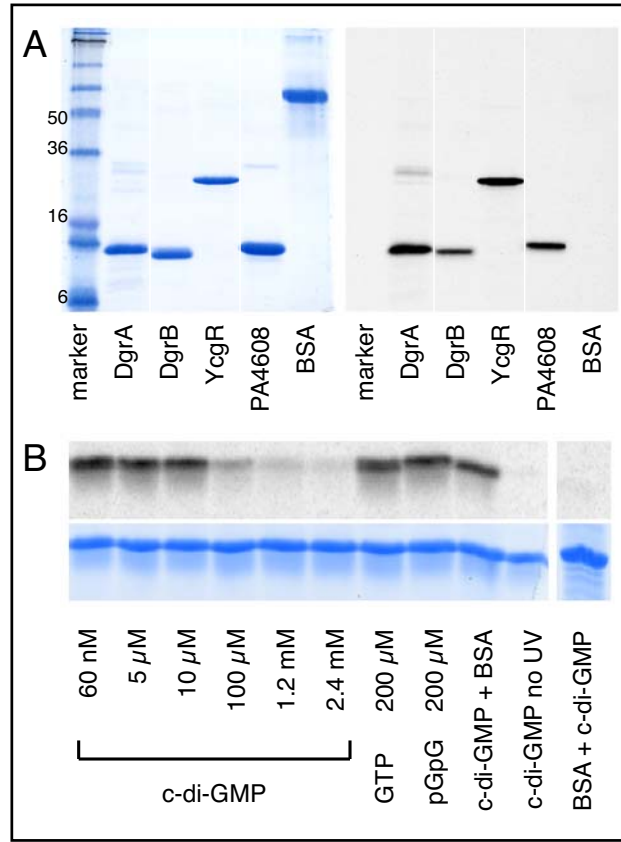


Figure 3

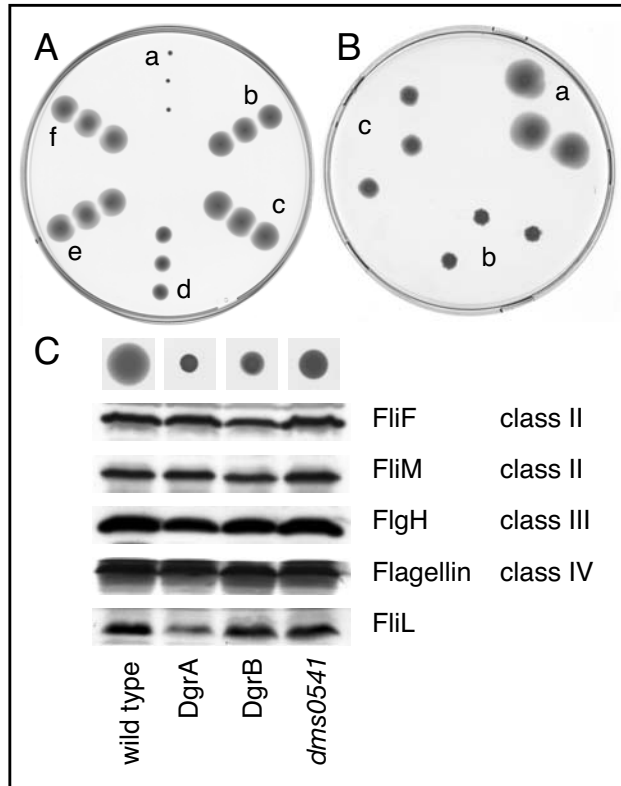




Figure 4

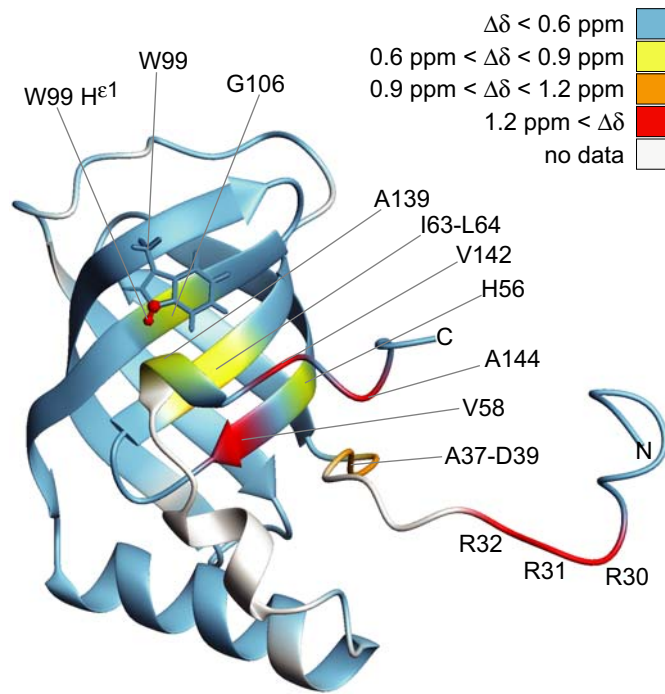


Figure 5

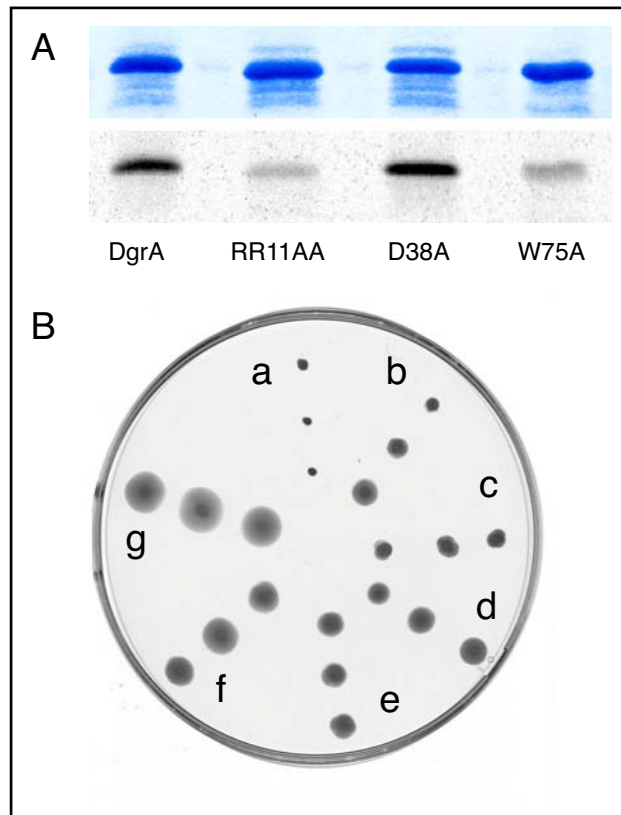


Figure 6

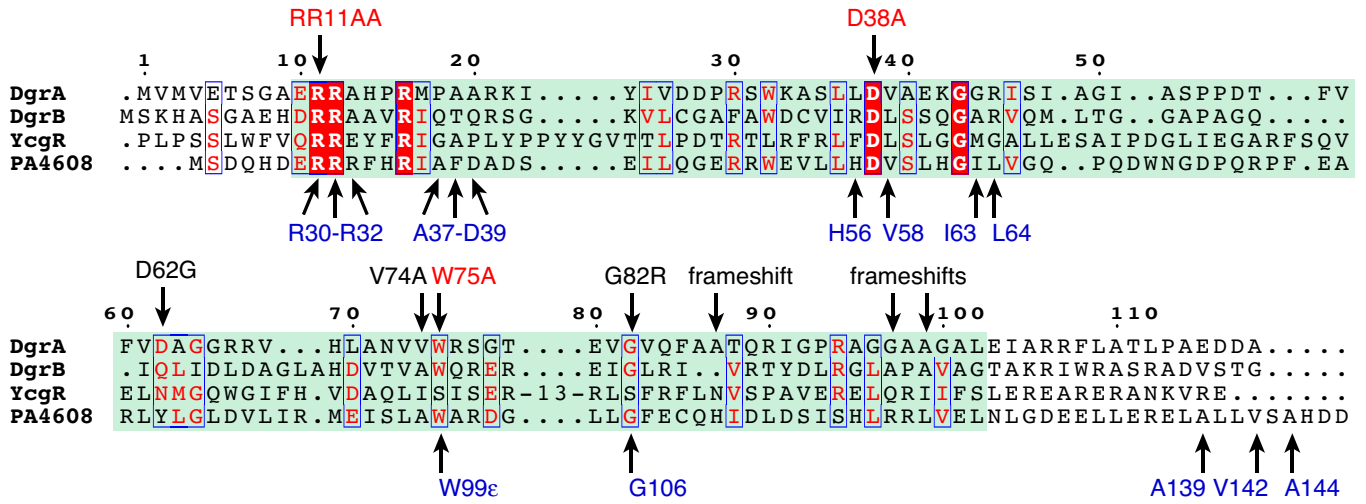


Figure 7

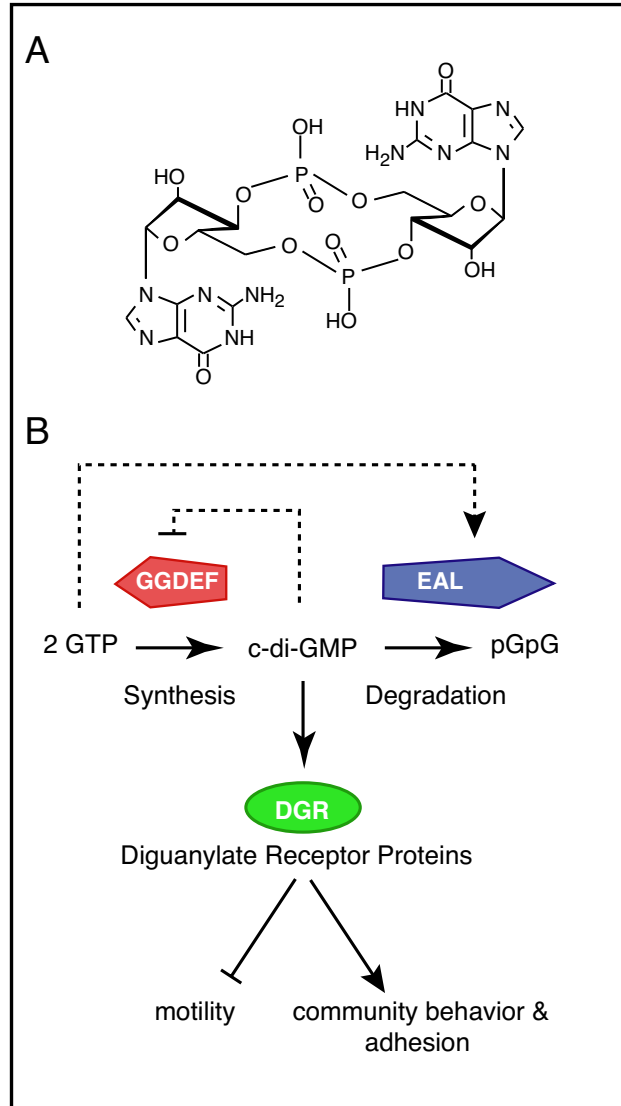


Figure 8

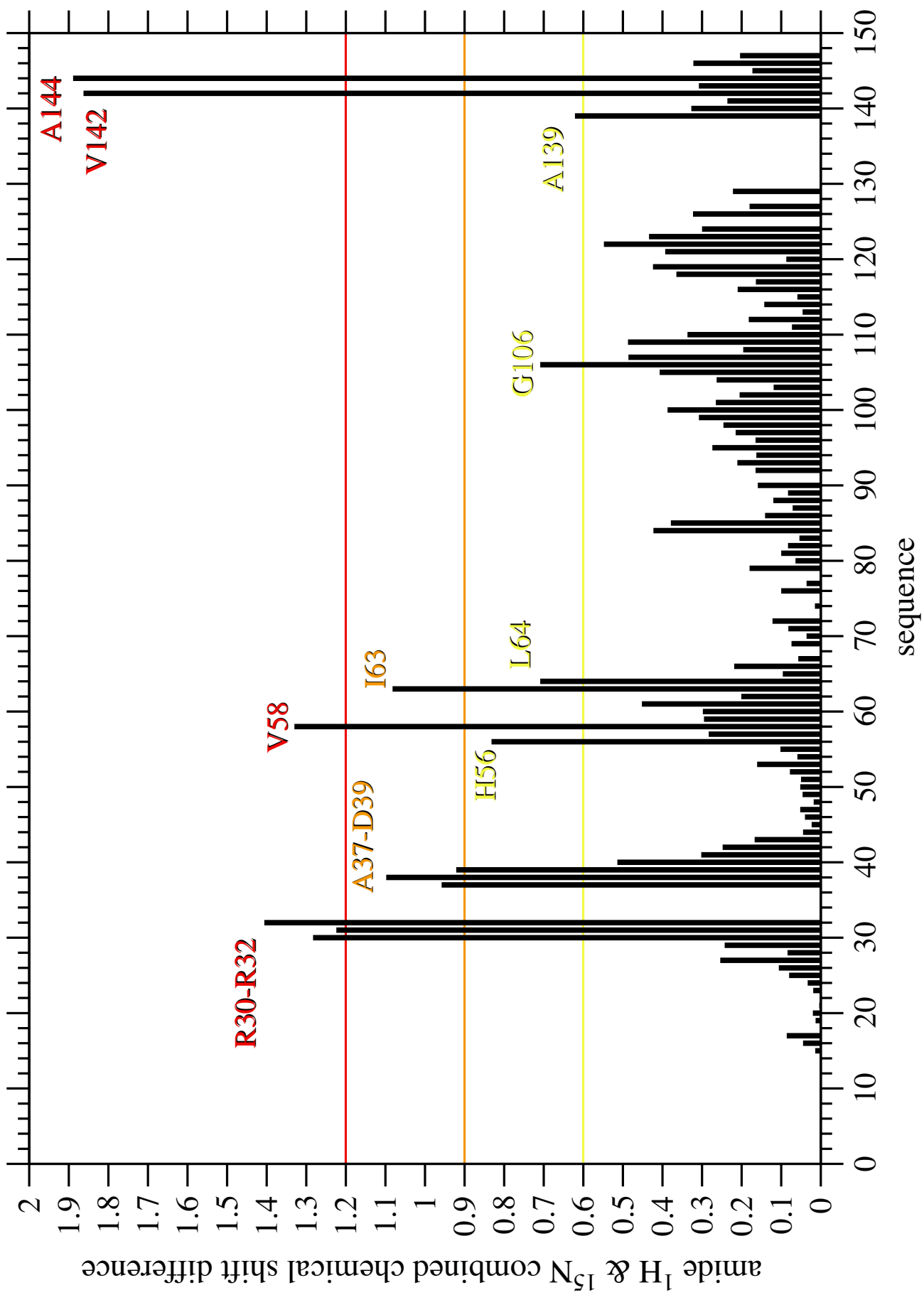


Figure 9

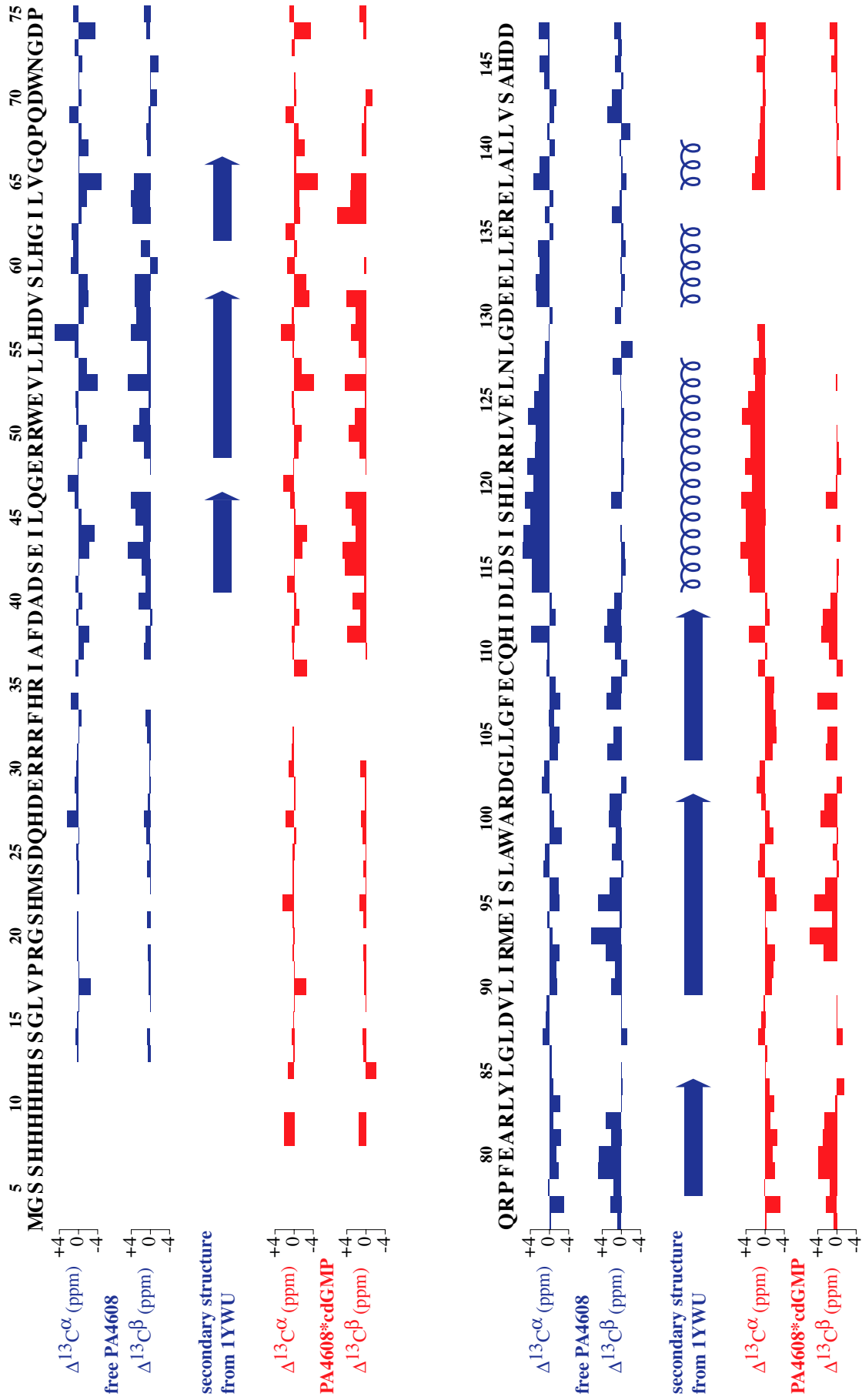
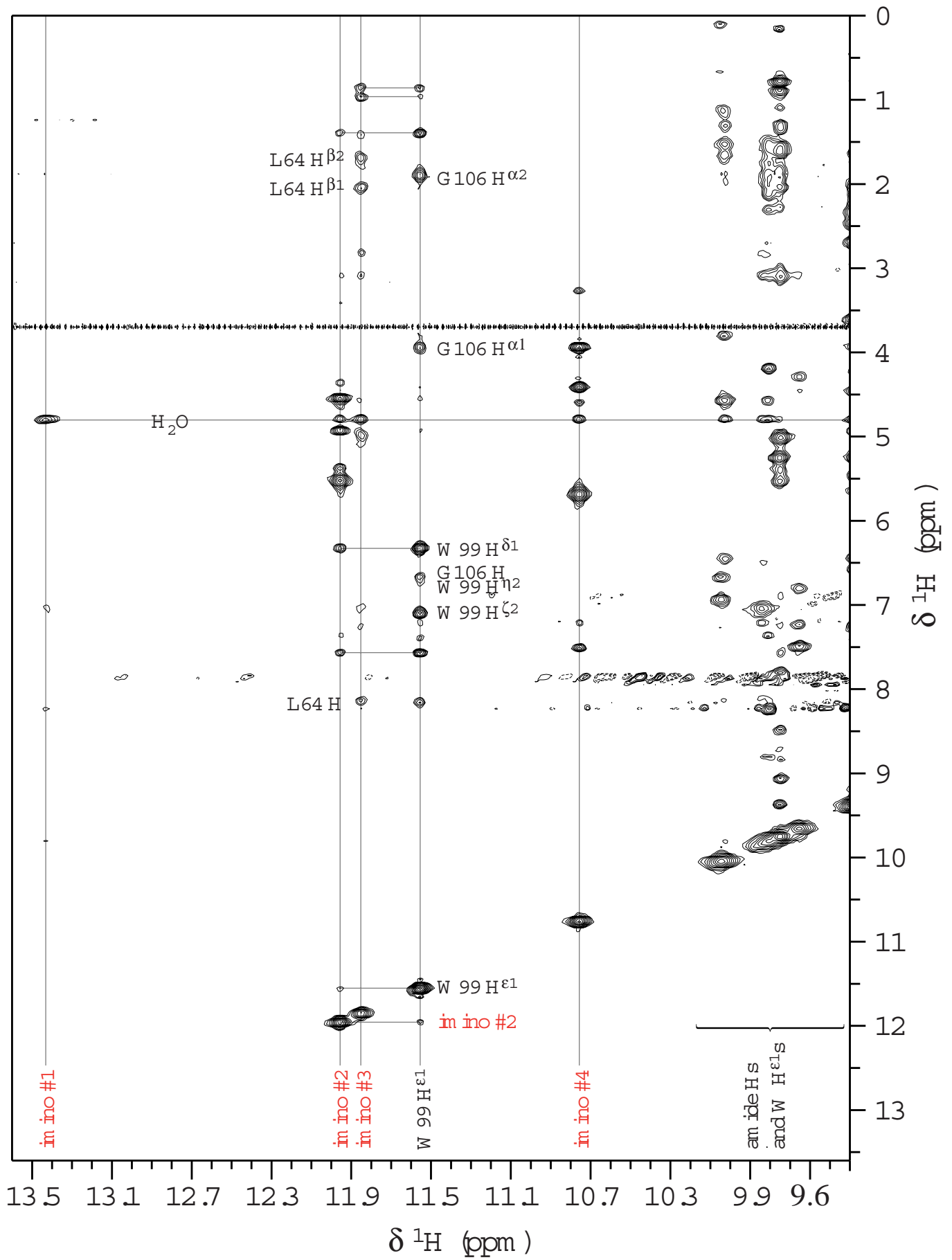


Figure 10



### **3.4 The structure-function relationship of WspR; a *Pseudomonas fluorescens* response regulator with a GGDEF output domain**

Malone, J. G., Williams, R., Christen, M., Jenal, U., Spiers, A.J., and Rainey, P.B.,  
**Microbiology** manuscript accepted (dec. 2006)



## Summary

The GGDEF response regulator WspR couples the chemosensory Wsp pathway to the overproduction of acetylated cellulose and cell attachment in the niche-specialist *Pseudomonas fluorescens* SBW25 wrinkly spreader (WS) genotype. This paper demonstrates biochemically that WspR is a diguanylate cyclase (DGC), and that DGC activity is elevated in the WS genotype compared to the ancestral smooth (SM) genotype. The work described uses two distinct mutagenesis strategies to probe in detail the structure-function relationship of WspR. In the first of these, short, in-frame stretches of DNA were introduced at positions throughout *wspR*. In the second, the amino-acid residues of the RYGGEEF active site motif (A-site) were substituted via extensive site-specific mutagenesis. The resulting library of *wspR* mutant alleles was analyzed with perspective to surface attachment, cellulose production and colony morphology.

## Statement of my work

This paper has been developed within a scientific collaboration with the laboratories of P. Rainey and U. Jenal. Whereas most of the scientific work was done within the scope of the PhD thesis of J. Malone, I contributed to this paper by synthesizing and providing [<sup>33</sup>P] labeled c-di-GMP as reference compound and by performing and teaching the procedure of DGC activity assays with His-tag purified WspR and various *Pseudomonas fluorescens* mutant strains (see figure 1).

1           **The structure-function relationship of WspR; a *Pseudomonas fluorescens***  
2                           **response regulator with a GGDEF output domain**

3           Malone, J.G.<sup>1,2</sup>, Williams, R.<sup>2</sup>, Christen, M.<sup>1</sup>, Jenal, U.<sup>1</sup>, Spiers, A.J.<sup>2,4</sup>, and Rainey, P.B.<sup>2,3\*</sup>

4  
5

6   Working title:

7   A structure-function analysis of *P. fluorescens* WspR

8

9   Contents category:

10   Biochemistry and Molecular Biology

11

12

13

14

15

16

17

18

19

20

21

22

23

24

25   \* Corresponding author, email: p.rainey@auckland.ac.nz

26   1. Division of Molecular Microbiology, Biozentrum, Klingelbergstrasse 50-70, 4056 Basel, C.H.

27       Tel. + 41 61 267 2129, Fax + 41 61 267 2118

28   2. Department of Plant Sciences, Oxford University, South Parks Road, Oxford, OX13RB, U.K.

29       Tel. + 44 1865 275 000, Fax + 44 1865 275 074

30   3. School of Biological Sciences, University of Auckland, Auckland, N.Z.

31       Tel. + 64 9 3737599, Fax. + 64 9 3737946

32   4. Centre for Ecology and Hydrology, Mansfield Road, Oxford, OX13SR, U.K.

1 **Summary**

2 The GGDEF response regulator WspR couples the chemosensory Wsp pathway to the  
3 overproduction of acetylated cellulose and cell attachment in the niche-specialist  
4 *Pseudomonas fluorescens* SBW25 wrinkly spreader (WS) genotype. Here we show that  
5 WspR is a diguanylate cyclase (DGC), and that DGC activity is elevated in the WS genotype  
6 compared to the ancestral smooth (SM) genotype. A structure-function analysis of 120 *wspR*  
7 mutant alleles was employed to gain insight into the regulation and activity of WspR. Firstly,  
8 44 random and defined pentapeptide insertions were produced in WspR, and the effects  
9 determined using assays based on colony morphology, attachment to surfaces and cellulose  
10 production. The effects of mutations within WspR were interpreted using a homology model,  
11 based on the crystal structure of *Caulobacter crescentus* PleD. Mutational analyses indicate  
12 that WspR activation occurs as a result of disruption of the interdomain interface, leading to  
13 the release of effector domain repression by the N-terminal receiver domain. Quantification of  
14 WspR variant function suggests that regulation of cellulose production and surface attachment  
15 proceed *via* two separate pathways. The conserved RYGGEF motif of WspR was also  
16 subjected to mutational analysis and the effects of 76 single amino acid residue substitutions  
17 tested for their effects on WspR function. The RYGGEF motif of WspR is functionally  
18 conserved, with almost every mutation abolishing function.

19

20

21

22

23

24

25

26

27

28

## 1 **Introduction**

2 Investigations into the regulation of surface colonization and aggregative behaviour in  
3 prokaryotes have established the central role of the second messenger cyclic-di-GMP (c-di-  
4 GMP) (Jenal, 2004; D'Argenio & Miller, 2004; Römling *et al.*, 2005). Though the biological  
5 pathways through which c-di-GMP regulates persistence, cell aggregation and the switch to  
6 the commensal lifestyle are currently poorly understood, the proteins responsible for c-di-  
7 GMP synthesis and degradation have been determined, and at least partially characterised.  
8 Bacterial di-guanylate cyclase (DGC) activity is found in GGDEF domain-containing proteins  
9 (Paul *et al.*, 2004; Ryjenkov *et al.*, 2005; Hickman *et al.*, 2005; Kulesekara *et al.*, 2006),  
10 whilst EAL domains have been shown to have c-di-GMP-specific phosphodiesterase (PDE)  
11 activity (Bobrov *et al.*, 2005; Christen *et al.*, 2005; Schmidt *et al.*, 2005; Kulesekara *et al.*,  
12 2006).

13  
14 Despite the publication of much biological data concerning GGDEF domains, biochemical  
15 demonstration of DGC activity (Paul *et al.*, 2004; Ryjenkov *et al.*, 2005), and the solution of  
16 the crystal structure of the GGDEF response regulator PleD (Chan *et al.*, 2004), detailed  
17 structure-function analyses of GGDEF proteins are scarce. Site-specific mutagenesis studies  
18 to date have focussed on single residues of interest (Kirillina *et al.*, 2004; Garcia *et al.*, 2004;  
19 Goymer *et al.*, 2006), and systematic mutagenesis has yet to be described. Such analyses  
20 stand to contribute insights into various issues, including the role of the GGDEF motif, the  
21 mode of activation of individual GGDEF proteins, and potential alternative mechanisms of  
22 downstream signal transduction.

23  
24 The GGDEF domain was first recognised in PleD, a response regulator responsible for  
25 mediating the swarmer-to-stalked cell transition in *Caulobacter crescentus* (Hecht & Newton,  
26 1995), and has since been identified in large numbers in many bacterial species (Galperin *et al.*  
27 *al.*, 1999; 2001; Galperin, 2005). GGDEF domains are often associated with receiver, PAS

1 and GAF sensor domains, and are frequently paired with EAL domains (Galperin *et al.*,  
2 2001).

3  
4 Numerous studies in diverse species have linked GGDEF domain proteins to processes  
5 involved in biofilm formation and aggregative behaviour (reviewed in Römling, 2005;  
6 Römling *et al.*, 2005). The effects of GGDEF proteins on exopolysaccharide levels have been  
7 probed *via* genetic studies in numerous species, including *Pseudomonas putida* (Gjermansen  
8 *et al.*, 2005; Ude *et al.*, 2006), *P. fluorescens* SBW25 (Spiers *et al.*, 2002; 2003; Goymer *et*  
9 *al.*, 2006; Ude *et al.*, 2006), *Salmonella typhimurium* (Simm *et al.*, 2004; Garcia *et al.*, 2004;  
10 Simm *et al.*, 2005), *Thermotoga maritima* (Johnson *et al.*, 2005), and *Vibrio cholerae*  
11 (Bomchil *et al.*, 2003; Rashid *et al.*, 2003; Kovacikova *et al.*, 2005).

12  
13 In addition, GGDEF-containing proteins have been repeatedly implicated in the regulation of  
14 cell motility, attachment and virulence (reviewed in Jenal, 2004; D'Argenio & Miller, 2004;  
15 Römling, 2005). For example, PleD controls the onset of motility during the *C. crescentus*  
16 cell cycle (Aldridge *et al.*, 2003; Paul *et al.*, 2004). In *Pseudomonas aeruginosa*, auto-  
17 aggregation is controlled by the GGDEF response regulator WspR (D'Argenio *et al.*, 2002;  
18 Hickman *et al.*, 2005), and twitching motility by FimX, which contains GGDEF and EAL  
19 domains (Huang *et al.*, 2003; Kazmierczak *et al.*, 2006). Additional examples of the effects of  
20 GGDEF domains on cell attachment and motility include ScrC regulation of attachment  
21 factors in *Vibrio parahaemolyticus* (Boles & McCarter, 2002), control of curli fimbriae by  
22 AdrA in *S. typhimurium* (Simm *et al.*, 2004), and RocS effects on *V. cholerae* motility  
23 (Rashid *et al.*, 2003). A recent survey of all GGDEF-containing genes in *P. aeruginosa* PA14  
24 showed that in several cases over-expression or inactivation had profound effects on cell  
25 attachment to surfaces and virulence (Kulesekara *et al.*, 2006).

26  
27 The GGDEF response regulator WspR was initially discovered as a consequence of  
28 investigation into the genetic causes of adaptive radiation in experimental populations of *P.*

1 *fluorescens* SBW25 (Rainey & Travisano, 1998; Spiers et al., 2002). One class of derived  
2 genotype colonises the air-liquid interface of static broth microcosms: these genotypes  
3 produce distinctive wrinkled colonies on agar plates and are termed wrinkly spreaders (WS).  
4 Transposon mutagenesis was used to identify genes that determine WS phenotype, focussing  
5 initially on a single WS genotype, the LSWS genotype. Two major gene clusters were  
6 identified: the *wrinkly spreader structural* (*wss*) and *wrinkly spreader phenotype* (*wsp*)  
7 operons (Spiers et al., 2002; Goymer et al., 2006). The *wss* operon encodes proteins involved  
8 in cellulose synthesis and acetylation (Spiers et al., 2002; 2003), whilst the *wsp* operon  
9 encodes a chemosensory system with homology to the chemotaxis system of *Escherichia coli*  
10 (P.B. Rainey, E. Bantinaki, R. Kassen, C.G. Knight, Z. Robinson & A.J. Spiers, unpublished).

11  
12 WspR is the final gene product, and primary output component of the Wsp pathway, and is  
13 activated by a currently unknown signal processed by the rest of the Wsp complex (Spiers et  
14 al. 2002). A *wspR::mini-Tn5* WS mutant displays a smooth colony morphology (Spiers et al.  
15 2002), and does not produce cellulose or attach to surfaces (Spiers et al. 2003). Expression of  
16 *wspR in trans* stimulates attachment and exopolysaccharide synthesis in various species  
17 (Aldridge et al., 2003; Goymer et al., 2006; Ude et al., 2006). The evolutionary cause of  
18 LSWS is a single point mutation in the gene encoding the WspF methyltransferase which results  
19 in over-activation of the WspE kinase and constitutive activation of the primary output  
20 component of the Wsp pathway, WspR (P.B. Rainey, E. Bantinaki, R. Kassen, C.G. Knight,  
21 Z. Robinson & A.J. Spiers, unpublished).

22  
23 *P. fluorescens* SBW25 WspR is a 333 residue protein comprising an N-terminal response  
24 regulator receiver domain and a C-terminal GGDEF domain separated by a linker region  
25 (Spiers et al., 2002; 2003). Recently, a combination of random and site-specific mutagenesis  
26 was used to outline basic physical characteristics of WspR (Goymer et al., 2006). Asp 67 was  
27 established as the site of WspR phosphorylation, and WspR activation was shown to be  
28 dependant upon phosphorylation. In addition, constitutively-active (e.g. WspR 19 (R129C),

1 D'Argenio *et al.*, 2002; Aldridge *et al.*, 2003) and dominant-negative (e.g. WspR 9 (G296R))  
2 *wspR* alleles were identified. A model was proposed to explain the dominant-negative effect  
3 seen upon the production of certain WspR variants. In this model, N-terminal receiver  
4 domains without functional C-termini competitively inhibited the interaction of  
5 chromosomally-expressed WspR with the Wsp kinase machinery, and hence ameliorated the  
6 downstream signal (Goymer *et al.*, 2006).

7

8 The work described here expands on the findings of Goymer *et al.* (2006), employing two  
9 distinct mutagenesis strategies to probe in detail the structure-function relationship of WspR.  
10 In the first of these, short, in-frame stretches of DNA were introduced at positions throughout  
11 *wspR*. In the second, the amino-acid residues of the RYGGEEF motif were substituted *via*  
12 site-specific mutagenesis. Following mutagenesis, phenotypic assays were applied to the  
13 libraries of *wspR* mutant alleles. Morphological analysis and assays for surface attachment  
14 and cellulose production were carried out on SBW25 strains expressing the *wspR* insert and  
15 substitution libraries *in trans*, allowing for qualitative, quantitative and *in silico* analysis of  
16 WspR. These data, combined with biochemical analyses of cell extracts and purified protein,  
17 were used to revise and expand upon models for the structure-function relationship of WspR.  
18 More broadly, these models were applied to our understanding of both response regulators  
19 and GGDEF domain-containing proteins.

20

21

22

23

24

25

26

27

28

## 1 **Methods**

### 2 *Strains and growth conditions*

3 Bacterial strains used in this work are listed in Table 3. Bacteria were grown in either KB or  
4 LB media (King *et al.*, 1954; Miller 1972) at 28 °C (*P. fluorescens*) or 37 °C (*E. coli*) with  
5 shaking. KB microcosms contained 6ml KB in 35ml universal glass vials and were used for  
6 attachment and growth assays. Kanamycin was used at a final concentration of 50 µg ml<sup>-1</sup>,  
7 Streptomycin at 100 µg ml<sup>-1</sup> and Tetracycline at 12.5 µg ml<sup>-1</sup>. Oligonucleotide primers used in  
8 this work are listed in Table S3.

9

### 10 *Molecular biology procedures*

11 Cloning was carried out in accordance with standard molecular biology techniques  
12 (Sambrook *et al.*, 1989). The plasmid pME6010-*wspR* was constructed by ligation of *wspR*  
13 excised as a *Bam*HI/*Eco*RI fragment from pWspR12 (Aldridge *et al.*, 2003) between the *Bgl*III  
14 and *Eco*RI sites of pME6010 (Heeb *et al.*, 2000), destroying the *Bgl*III site in the process. The  
15 plasmid pET42b-*wspR* was constructed by ligation of the relevant *wspR* PCR fragment  
16 (amplified with primers WsprPurFor and WsprPurRev from pME6010-*wspR*), between the  
17 *Xho*I and *Nde*I sites of pET42b (Novagen).

18

### 19 *Over-expression and purification of His<sub>6</sub>-WspR*

20 Overnight cell cultures of *E. coli* BL21-(DE3) containing pET14b-*wspR* and pET42b-*wspR*  
21 were used to inoculate LB medium plus ampicillin, to an initial OD<sub>600</sub> of 0.1. Cell cultures  
22 were incubated for 150 min at 37 °C with shaking before protein expression was induced with  
23 IPTG (Sigma) solution at a final concentration of 100 µM for pET14b-*wspR*, 1 mM for  
24 pET42b-*wspR*. Cell cultures were then incubated for an additional 150 min at 30 °C. Cells  
25 were harvested by centrifugation and re-suspended in running buffer (25 mM Tris-HCl pH  
26 8.0, 250 mM NaCl, 1 % β-mercaptoethanol), before lysis by sonication and French press.  
27 Following lysis, the samples were centrifuged (30,000 x g, 15 min, 4 °C) and His<sub>6</sub>-WspR  
28 purified from the supernatant *via* NTA-nickel chromatography according to the



1 manufacturer's protocol (Qiagen). Both His<sub>6</sub>-WspR samples eluted in the 200 mM imidazole  
2 fraction, and N-terminal His<sub>6</sub>-WspR was verified by mass spectrometry. The protein  
3 concentration of samples was determined after Bradford (1976) [N-terminal His<sub>6</sub>-WspR 1.6  
4 mg ml<sup>-1</sup>, C-terminal His<sub>6</sub>-WspR 5.0 mg ml<sup>-1</sup>].

5

#### 6 *Western blotting*

7 Overnight cell cultures were lysed by incubation (95 °C, 5 min) with 1 volume SDS loading  
8 buffer (10 mM Tris-HCl pH 6.8, 0.005 % bromophenol blue, 10 % glycerol, 2 % SDS).  
9 Proteins from the resulting cell extracts were separated on pre-poured 12 % Tris-HCl gels  
10 (BioRad) and blotted onto polyvinylidene difluoride (PVDF) membranes (Millipore). After  
11 overnight incubation in blocking solution (15 mM Tris-HCl pH 7.0, 10 mM KCl, 10 mM  
12 NaCl, 0.01 % Tween20, 10 % glycerol, 5 % milk powder), WspR was detected with a 1/2,500  
13 dilution of WspR-specific polyclonal antiserum (Harlan Seralabs) and a 1/3,000 dilution of  
14 anti-rabbit secondary antibody (Invitrogen). Bound antibodies were visualized with ECL  
15 Chemiluminescent detection reagent (Amersham Biosciences) and photographic film.

16

#### 17 *Assay for DGC activity*

18 Di-guanylate cyclase activity was assayed after Paul *et al.* (2004). Overnight cultures were  
19 grown of SBW25 strains, cells were harvested, re-suspended in running buffer and partially  
20 lysed by gentle sonication. Assays were run in 50 µl (final volume) of running buffer  
21 containing 10 µl cell extract or purified WspR and started by the addition of (final  
22 concentration) 100 µM GTP [18.5 kBq α<sup>32</sup>P-GTP] (Amersham Biosciences). Retardation  
23 Factor (RF) values were recorded as the ratio of spot migration distance to the distance  
24 migrated by the solvent front.

25

#### 26 *Polymerase chain reaction (PCR)*

27 A standard reaction contained 5 µl 2 mM dNTP mix, 2.5 µl 10x polymerase buffer, 1 U *Pfu*  
28 turbo polymerase (Stratagene), 0.4 pmol of each primer, and 10-20 ng template DNA, made

1 up to 25  $\mu$ l with deionised water. Following an initial template denaturation step of 3 min at  
2 94 °C, amplification was performed by 25 cycles of denaturation for 30 sec at 94 °C,  
3 annealing for 30 sec at the appropriate temperature (56 °C – 62 °C depending on the reaction)  
4 and strand extension for 1 min 30 sec at 72 °C. A final extension step for 5 min at 72 °C was  
5 performed before samples were kept at 4 °C.

6

#### 7 *Pentapeptide scanning mutagenesis (PSM)*

8 PSM was used to insert 15 base-pair sections of DNA into pME6010-*wspR* after the method  
9 of Hallet *et al.* (1997), except that a morphological screen was used for transposon insertions  
10 in *wspR*. *P. fluorescens* WS-4 (WS *wspR*::miniTn5) was transformed with pooled pME6010-  
11 *wspR*::Tn4430 DNA and transformant colonies exhibiting a smooth morphology were  
12 selected. These colonies contained constructs unable to complement WS-4; hence they  
13 contained transposon insertions in *wspR*. Following mutagenesis, the site of insertion in each  
14 case was verified by sequencing.

15

#### 16 *Strand overlap extension PCR (SOE-PCR)*

17 SOE-PCR (Ho *et al.*, 1989) was used during the systematic mutagenesis of *wspR*. DNA on  
18 either side of the point of mutation was amplified by a standard PCR reaction with primers  
19 SOEFor/Rev 1-25 that complemented at the site for joining (and containing the altered  
20 nucleotide sequence). PCR products were purified and 1  $\mu$ l of each used as templates in the  
21 subsequent SOE-PCR reaction. The SOE-PCR reaction was carried out with primers  
22 SOEFOR and SOEREV in a final volume 25  $\mu$ l. Following an initial template denaturation  
23 step of 3 min 30 sec at 94 °C, strand extension was carried out in two steps; primer annealing  
24 for 30 sec at 56 °C followed by extension for 2 min at 72 °C. DNA was then amplified under  
25 the conditions described for the standard PCR protocol, with annealing at 56 °C for 30 sec.  
26 SOE-PCR fragments were confirmed by sequencing and ligated between the *Xho*I and *Eco*RI  
27 sites of pME6010.

28

### 1 *Degenerate PCR-based mutagenesis*

2 In order to efficiently mutagenise the GGEEF motif of *wspR*, an upstream restriction site was  
3 required. This allowed mutagenesis to proceed *via* PCR with degenerate primers, and reduced  
4 the size of the inserts produced from 1 kb to approximately 300 bps (the region of *wspR* DNA  
5 between the introduced site and the downstream *EcoRI* site). A *SacI* restriction site  
6 (GAGCTC, coding for E-L) was introduced at positions 339/240 of *wspR* *via* SOE-PCR with  
7 primers *SacI*For and *SacI*Rev. PCR was carried out using the degenerate primers DEG1-14  
8 with the primer SOEREV, and pME6010-*wspR-SacI* as a template. PCR products were  
9 ligated as a pool between the *SacI* and *EcoRI* sites of pME6010-*wspR-SacI*. SM cells were  
10 transformed with the pooled constructs and colony morphology on LB agar determined.  
11 Individual colonies were selected on the basis of morphology and the substituted codon in  
12 each case verified by sequencing.

13

### 14 *DNA sequencing*

15 A 50-100 ng aliquot of plasmid DNA was mixed with 1 pmol of primer SeqFor or SeqRev  
16 and 4 µl Big-Dye ready reaction mix version 3.0 (ABI), in a final volume of 10 µl. Samples  
17 were thermocycled for 25 cycles of 10 sec at 96 °C, 5 sec at 50 °C, and 4 min at 60 °C before  
18 cooling to 4 °C. Following the reaction, samples were ethanol precipitated and submitted for  
19 sequence analysis on an ABI 3100 sequencer.

20

### 21 *Measurement of overnight culture cell density*

22 Assays for attachment and cellulose production described below were inoculated with 24 hour  
23 cell cultures. Accordingly, the effects of *WspR* variants on SM culture growth were  
24 measured. KB microcosms inoculated with 60 µl aliquots of overnight cultures, and with the  
25 lids loosely taped in place were incubated at 28 °C with shaking. All cultures displayed  
26 similar optical densities (OD<sub>600</sub>) after 24 hours growth. A Spectronic-20 spectrometer  
27 (Genesys) was used throughout.

28

1 *Attachment assay*

2 Bacterial attachment was determined quantitatively using Crystal Violet (CV) after Spiers *et*  
3 *al.* (2003). KB microcosms were inoculated with 60 µl aliquots of overnight cultures and  
4 incubated statically at 28 °C for 48 h. Vials were emptied and washed vigorously with  
5 deionised water. 1 ml of 0.05% (w/v) CV (Sigma) was added and mixed for two minutes. The  
6 vials were then emptied and washed with deionised water. CV was eluted in 5 ml ethanol with  
7 vigorous shaking for 1 h and the  $A_{570}$  determined.

8

9 *Congo Red (CR) binding assay*

10 Cellulose expression was measured using a CR binding assay adapted from Spiers *et al.*  
11 (2003). Ten µl drops of overnight cultures were grown on 25 ml KB agar plates for 24 hours  
12 at 28°C. Colonies were re-suspended in 1 ml 0.005% (w/v) CR (Sigma) and incubated for 2 h  
13 at 37°C. Colony material was then pelleted by centrifugation. The amount of CR remaining in  
14 the supernatant was determined by measurement of  $A_{490}$  and comparison with appropriate CR  
15 standards. CR binding was expressed as a fraction of the CR bound by the control strain.

16

17 *Homology modelling*

18 BLAST (Altschul *et al.*, 1997) was used to align the primary sequence of WspR and the  
19 monomeric structure of *Caulobacter crescentus* PleD (Chan *et al.*, 2004, PDB code 1w25B).  
20 Twenty-two residues were deleted from the sequence of WspR and gaps were added where  
21 necessary to give the optimum alignment (Figure S1), which was then used as a template for  
22 SwissModel analysis (Schwede *et al.*, 2003). The resulting WspR homology model was  
23 visualised and manipulated using DeepView / Swiss PDB Viewer v3.7 (Guex & Peitsch  
24 1997). The reliability of the homology model was assessed by comparison of the predicted  
25 secondary structures of WspR and PleD to the known secondary structure of PleD (Chan *et*  
26 *al.*, 2004) using PROFsec from the Predict Protein database (Rost *et al.*, 2004).

27

28

## 1 Results

### 2 WspR functions as a diguanylate cyclase (DGC) *in vitro* and enzymatic activity is 3 increased in a WS background

4 N- and C-terminal His<sub>6</sub>-tagged WspR were over-expressed in *E. coli* BL21-(DE3) and  
5 purified from cell extracts using NTA-Nickel affinity chromatography. For purification of N-  
6 terminal His<sub>6</sub>-WspR (molecular weight 39.1 kilo Daltons (kDa)), the major eluted band  
7 corresponded unambiguously to WspR when tested by mass spectrometry (data not shown).  
8 The smaller, minor band (35 kDa) seen in Figure 1(c) also corresponded to WspR and is  
9 likely to be a degradation fragment of WspR.

10

11 N-terminal His<sub>6</sub>-WspR was supplied to Harlan Seralabs for generation of a WspR-specific  
12 polyclonal antiserum. Western blotting with this antiserum was then used to provide a  
13 qualitative comparison of relative WspR expression levels in the (wild type) SM and WS  
14 genotypes. A sample of purified N-terminal His<sub>6</sub>-tagged WspR was included as a control (Fig.  
15 1c). Approximately equal amounts of WspR were detected in SM and WS cell lysates,  
16 supporting the hypothesis that the WS wrinkled phenotype does not arise primarily as the  
17 result of WspR over-expression, in agreement with previous observations (Spiers *et al.*,  
18 2002).

19

20 Given the sequence homology (74 % identity) between SBW25 and *P. aeruginosa* PA01  
21 WspR (recently shown to function as a DGC (Hickman *et al.*, 2005)) and the fact that WspR  
22 R129C complements PleD activity in *C. crescentus* (Aldridge *et al.*, 2003), it was reasonable  
23 to assume that WspR is a DGC, catalyzing the formation of c-di-GMP from two molecules of  
24 GTP. Nevertheless, it was important to independently verify DGC activity for SBW25 WspR.  
25 N- and C-terminal His<sub>6</sub>-WspR was assayed for DGC activity after the method of Paul *et al.*  
26 (2004). Radio-labelled GTP was incubated with purified His<sub>6</sub>-WspR, and samples removed at  
27 regular intervals. When the nucleotide samples were separated by TLC, a spot corresponding  
28 to c-di-GMP was generated over time by His<sub>6</sub>-WspR, determined by comparison with a c-di-

1 GMP control sample (Christen *et al.*, 2005) (Fig. 1a). The low rate of c-di-GMP formation  
2 suggests that conditions in this assay were sub-optimal for enzyme activity. No DGC activity  
3 was detected for N-terminal His<sub>6</sub>-WspR (data not shown), possibly as a result of disruption of  
4 the active state by the His<sub>6</sub>-tag, similar to that seen for N-terminal His<sub>6</sub>-PleD (R. Paul and U.  
5 Jenal, personal communication).

6

7 To investigate the effects of the WS background on WspR DGC activity, cell extracts from  
8 overnight cultures of SM, WS, and isogenic strains lacking WspR (SM  $\Delta$ wspR and WS  
9  $\Delta$ wspR), and containing pME6010 and pME6010-wspR as indicated, were assayed for DGC  
10 activity (Fig. 1b) in the same way as above. A slow running spot corresponding to c-di-GMP  
11 was generated in WS cell lysates expressing wspR both from pME6010 and from the  
12 chromosome. No c-di-GMP was seen in any other samples. Hence, the WS cell extract  
13 activates WspR DGC activity, whereas the SM cell extract does not.

14

#### 15 **Mutagenesis of WspR**

16 Nineteen wspR mutant alleles were produced by Pentapeptide Scanning Mutagenesis (PSM),  
17 (Hallet *et al.*, 1997), (see supplemental Table S1). The five amino acid residue insert resulting  
18 from PSM differs among mutants depending on the specific site of Tn4430 insertion into  
19 wspR. However, the disruption to protein tertiary structure caused by the insertion of five  
20 amino-acids into the protein was considered likely to outweigh any effects caused by  
21 variation in the amino-acid sequence of the insert, and this latter difference was discounted  
22 (Hayes & Hallet 2000).

23

24 To complement the PSM variants and fully mutagenise wspR, strand-overlap-extension PCR  
25 (SOE-PCR), (Ho *et al.*, 1989) was used to introduce 25 GVPTK insertions at specific  
26 positions throughout wspR (supplemental Table S2). The resulting library (44 variants)  
27 contained approximately one insert for every seven to eight amino-acid residues of WspR,

1 ensuring a high probability of disrupting most elements of secondary structure present in the  
2 protein.

3

4 To determine whether soluble protein was expressed from each pME6010-*wspR* mutant  
5 allele, all alleles were expressed separately in SM  $\Delta$ *wspR*, to allow WspR produced from  
6 pME6010 to be detected by Western blotting. Forty *wspR* mutant alleles produced detectable  
7 amounts of protein, but no WspR was detected for variants with inserts at residue positions  
8 99, 182, 246 and 264 (data not shown), suggesting either that an undetectably small amount  
9 of WspR was present in each case, or that these variants produced highly unstable protein that  
10 was rapidly degraded during sample preparation. However, when expressed in WS these four  
11 variants ameliorated the wrinkled colony morphology (see below): given clear phenotypic  
12 effects these alleles were included in subsequent analyses.

13

#### 14 **Phenotypic characterisation of WspR variants**

15 The WspR variants may be divided into several functional classes; inactive, signal-dependent  
16 (i.e. wild type), signal independent (i.e. dominant or constitutively-active) and dominant-  
17 negative. When wild-type *wspR* is expressed *in trans* in the ancestral SM genotype it causes  
18 development of the WS phenotype. By extension, the activity states of different WspR  
19 variants may be distinguished by their effects in different SBW25 backgrounds (Goymer *et*  
20 *al.*, 2006). Because WspR is activated by the WspE kinase, (P.B. Rainey, E. Bantinaki, R.  
21 Kassen, C.G. Knight, Z. Robinson & A.J. Spiers, unpublished) development of WS  
22 morphology in strains lacking the *wsp* operon (e.g. SM  $\Delta$ *wspA-wspF*) indicates the presence  
23 of constitutively-active WspR. In cases where a WS morphology develops in the presence of  
24 the Wsp machinery (e.g. in SM) but not in a *wsp* deletion background the protein is signal-  
25 dependent and behaves like wild-type WspR. Inactive proteins have no effect in any SBW25  
26 genotype, whilst dominant-negative WspR variants produce a smooth morphology in the WS  
27 genotype. Potential interactions between WspR variants and chromosomal WspR may be

1 investigated by expanding the morphological analysis to include *wspR* deletion strains (e.g.  
2 SM  $\Delta$ *wspA-wspR* and SM/WS  $\Delta$ *wspR*).

3  
4 To fully distinguish between all possible activity states, the *wspR* insert alleles were  
5 expressed in several SBW25 backgrounds: SM, WS, SM  $\Delta$ *wspA-wspF*, SM  $\Delta$ *wspA-wspR*, SM  
6  $\Delta$ *wspR*, and WS  $\Delta$ *wspR* and their effects on colony morphology were determined. In general,  
7 changes in colony morphology conformed to predictions, and allowed one to assign one of the  
8 four activity states described previously to every tested WspR variant (Table 1, and Figure 2).  
9 Morphological analysis provided no evidence for interactions between WspR variants and  
10 chromosomal WspR; little morphological difference was seen upon WspR production in SM  
11 versus SM  $\Delta$ *wspR*, or SM  $\Delta$ *wspA-wspF* versus SM  $\Delta$ *wspA-wspR*.

12  
13 The activation states of the WspR variants correlated with the positions of the inserts  
14 throughout WspR. N-terminal variants displayed all four states, whilst linker variants were all  
15 constitutively-active, and C-terminal variants were either dominant-negative or inactive.  
16 Several WspR variants (marked with an asterisk in Table 1) produced a wrinkled morphology  
17 in WS  $\Delta$ *wspR*, but had no effect in other tested strains. Whilst these variants appeared to have  
18 some residual activity, they were classed as inactive for the purposes of further analysis.  
19 These variants suggested that recovery of the WS phenotype was significantly simpler than  
20 generation of a wrinkled morphology in the SM genotype.

21  
22 The emerging model of WspR function was refined through analysis of the effects of WspR  
23 variants on different aspects of biofilm formation. WspR is known to be essential for the  
24 enhanced levels of attachment seen in the WS (Spiers *et al.*, 2003). Therefore, the effect of  
25 *wspR* mutant allele expression on attachment in SBW25 strains was measured using a  
26 quantitative Crystal Violet assay (Figure 3). To distinguish between the effects of  
27 constitutively-active and signal-dependent variants on attachment, the assay was repeated in  
28 SM and SM  $\Delta$ *wspA-wspR* backgrounds.



1

2 Variations in bacterial attachment corresponded well with the changes seen in colony  
3 morphology. Specifically, constitutively-active WspR variants (e.g. WspR138) produced  
4 raised levels of cell attachment in both tested backgrounds, relative to the plasmid-only  
5 control. Signal-dependent variants produced enhanced levels of attachment in SM only (e.g.  
6 WspR6). Insertions in the N-terminus (residues 1-130) and in the linker region of WspR  
7 (residues 131-163) produced active or constitutively-active proteins, with corresponding  
8 increases in cell attachment. Insertions in the C-terminus (residues 164-333) eliminated WspR  
9 function, and these variants did not affect cell attachment. Several variants produced greatly  
10 enhanced levels of attachment compared with wild-type WspR.

11

12 To determine whether the close correlation between attachment and colony morphology also  
13 applied to cellulose production, the effects of WspR variants on cellulose production in SM  
14 were determined quantitatively using a Congo Red (CR) binding assay after Spiers *et al.*  
15 (2003) (Figure 4). [In addition, the presence or absence of cellulose in each sample was  
16 determined qualitatively by staining with Calcofluor (CF)(Sigma). No major discrepancies  
17 emerged between cellulose seen upon CF staining, and the results of the CR assay (data not  
18 shown)]. In general, increased cellulose production relative to SM pME6010 was seen for  
19 those strains displaying WS colony morphology in SM (Table 1). High levels of cellulose  
20 production (relative to the SM pME6010-*wspR* control) were observed for several N-terminal  
21 and linker region variants, whilst C-terminal variants did not affect cellulose production. The  
22 CR assay results were then compared with the results for attachment in the SM genotype.  
23 Several variants were identified that strongly up-regulated cell attachment, but did not effect a  
24 corresponding large increase in cellulose production (e.g. WspR6), suggesting that WspR  
25 may regulate these two systems *via* distinct and separable mechanisms.

26

27 The solution of the crystal structure of PleD from *C. crescentus* (Chan *et al.*, 2004) made  
28 possible the use of homology modelling software to produce a putative three-dimensional

1 structure for WspR (Figure 5). The PleD structure contains two response regulator receiver  
2 domains and a C-terminal GGDEF domain, which has a similar fold to the adenylyl cyclase  
3 catalytic domain (Zhang *et al.*, 1997), consistent with the earlier predictions of Pei & Grishin  
4 (2001). WspR shares significant sequence homology with PleD across the second response  
5 regulator receiver (R2) and GGDEF (DGC) domains, and the PleD and WspR DGC domains  
6 are functionally interchangeable in *C. crescentus* (Aldridge *et al.*, 2003). Therefore, the PleD  
7 crystal structure represented the best candidate upon which to base the model. The completed  
8 homology model was then used to refine the structure-function models of WspR. The  
9 insertion positions of the N-terminal and linker region WspR variants were mapped onto the  
10 WspR homology model (Figure 5), and the relationship between each insert's position and its  
11 effect on function was analysed.

12

### 13 **The GGEEF motif of WspR is functionally conserved**

14 As a final extension of the structure-function analysis of WspR, single amino-acid residue  
15 substitutions throughout the GGEEF motif, and the preceding two residues RY (residues 246-  
16 252) were produced and analysed. To allow for simple, high throughput mutagenesis, a WspR  
17 variant (WspR-*SacI*, containing the substitutions R239E and P240L) was selected for use in  
18 the substitution mutagenesis. Analysis of colony morphology and biofilm formation indicated  
19 that WspR-*SacI* activity was similar to that of wild-type WspR (Figure 6). Substitution  
20 variants were produced as a random pME6010-*wspR-SacI* plasmid pool in which all residue  
21 substitutions (except tryptophan) were possible throughout RYGGEEF. This pool was used to  
22 transform SM, and WspR substitution variants were recovered and checked. In total, 76  
23 different WspR substitution variants were isolated. Seventy-five of these were from colonies  
24 displaying smooth colony morphology (i.e. those in which the WspR variant was no longer  
25 active) (Table 2). One additional variant, WspRE250D, produced a wrinkled colony  
26 phenotype in SM, suggesting that the protein was active in this case.

27

1 Twenty-one WspR substitution variants were selected for further characterisation on the basis  
2 of the side chain chemistry of the substituted residues. Firstly, the effects of WspR variant  
3 production on WS colony morphology were analysed, and used to predict their activity states  
4 as described previously. All but one of the WspR variants, WspRY247F, produced smooth  
5 colony morphology in WS, indicating dominant-negative activity. WspRY247F was classed  
6 as inactive. Given that most of the tested proteins produced a dominant negative phenotype,  
7 quantitative analysis was used to investigate the properties of this phenotype. Therefore,  
8 assays for cellulose production and attachment were undertaken in the WS genotype.  
9 WspRY247F did not repress WS cellulose production, in contrast with the other substitution  
10 variants. Finally, none of the WspR variants significantly reduced WS attachment levels  
11 (Figure 6), providing additional support for the hypothesis that attachment and  
12 exopolysaccharide production are regulated separately by WspR.

13

14

15

16

17

18

19

20

21

22

23

24

25

26

27

28

1

2 **Discussion**

3 A systematic biological and biochemical analysis was undertaken of the GGDEF domain-  
4 containing protein, WspR, in order to address several unanswered questions concerning  
5 GGDEF proteins in general, and WspR in particular. Firstly, biochemical analysis was carried  
6 out on purified WspR and on SBW25 cell extracts. WspR was shown to function as a DGC  
7 (Figure 1a, 1b), and the WS phenotype was shown to stimulate WspR DGC activity in cell  
8 extracts, in proportion to the level of WspR present. This provided a definite mechanism for  
9 WspR function, and indicates that the WS phenotype arises (at least in part) as the result of  
10 increased levels of WspR activation and concomitant c-di-GMP production.

11

12 Secondly, to probe the mechanisms of WspR activation and regulation, systematic  
13 mutagenesis was used to disrupt WspR at positions throughout its length. The effects of the  
14 resulting WspR insert library on SBW25 colony morphology, attachment and cellulose  
15 production were analysed, and used to determine the activity state of the various WspR  
16 variants. Several distinct observations were made of the relationship between WspR activity  
17 and insert position. Firstly, inserts in the C-terminus (residues 164-333) of WspR always  
18 eliminated enzymatic activity. Whilst several insertions in the N-terminus also eliminated  
19 enzymatic function, the same sensitivity to mutation was not seen in the domain as a whole.  
20 Secondly, a number of constitutively-active WspR variants were found with insertions in the  
21 N-terminus (residues 1-130), and insertions in the linker region (residues 131-163) produced  
22 constitutively-active enzymes in every case (Figure 4). To our knowledge, WspR is the only  
23 GGDEF protein for which a comprehensive structure-function analysis of this kind has been  
24 undertaken.

25

26 Detailed structure-function analysis provides significant insight into the means of protein  
27 regulation, and in this case allowed the construction of a model for WspR activation (Figure  
28 7). In this model, the C-terminal effector domain is inhibited in the inactive state by the N-

1 terminal domain. Regulation through effector domain inhibition occurs in a number of  
2 response regulators including *E. coli* NarL (Baikalov *et al.*, 1996; Eldridge *et al.*, 2002) and  
3 *S. typhimurium* CheB (Djordjevic *et al.*, 1998). Phosphorylation (Figure 7a), or mutation of  
4 the N-terminal domain (Figure 7b) leads to the release of inhibition. This model expands on  
5 the observations of Goymer *et al.* (2006), who noted that mutations in or near the linker  
6 region of WspR mimicked the phosphorylated state of the protein. Biochemical (Ryjenkov *et*  
7 *al.*, 2005) and structural (Chan *et al.*, 2004) evidence suggests that DGCs function as dimers.  
8 Whilst this study provides no direct evidence for WspR dimerisation, it is reasonable to  
9 assume that activation is accompanied by dimerisation. In this case, disruption of the inactive  
10 form of the protein might lead to exposure of the dimer interface, and hence activation  
11 (Figure 7b). These data do not rule out the possibility of an alternative activation mechanism,  
12 where the phosphorylated N-terminal domain stabilizes the DGC activated conformation.  
13 However, it is unlikely that the precise interactions required by such a mechanism would be  
14 reproduced by every activating insertion tested, strongly suggesting that the mechanism of  
15 WspR activation proceeds *via* release of effector domain repression.

16

17 A number of insertions produced a dominant-negative phenotype. In these cases, the activity  
18 of either the Wsp or Wss machinery was adversely affected by *trans*-expressed *wspR* mutant  
19 alleles. This dominant-negative phenotype could arise as a consequence of competitive  
20 inhibition of the Wsp signalling machinery by inactive WspR variants, in agreement with the  
21 model proposed by Goymer *et al.* (2006) for suppression of the WS wrinkled morphology by  
22 the isolated WspR N-terminus. Alternatively, inactive heterodimers, formed between inactive  
23 WspR variants and chromosomal wild-type WspR could interrupt Wsp signalling at the level  
24 of WspR. Neither model for inhibition may be ruled out at this stage. However, the fact that  
25 chromosomal *wspR* appears to have little influence on the behaviour of *trans*-expressed  
26 WspR variants lends support to the competitive model for Wsp inhibition.

27

1 When the positions of the five amino-acid residue inserts were plotted onto the N-terminus  
2 and linker region of the homology model (Figure 5), they clustered according to their effects  
3 on WspR activity, suggesting that each group affected WspR function *via* a common  
4 mechanism. N-terminus insertions producing constitutively-active proteins were found at the  
5 interface between the N- and C-terminal domains and in adjoining loops and helices. These  
6 insertions presumably activated WspR *via* disruption of the interface between the two  
7 domains, a mechanism common to many response regulator activation mechanisms (Eldridge  
8 *et al.*, 2002; Park *et al.*, 2002; Muchova *et al.*, 2004). A comparison of the domain interaction  
9 surfaces of four full-length, two-domain response regulator crystal structures (Robinson *et al.*,  
10 2003) suggested that the activation mechanisms of the different proteins; NarL (Baikalov *et*  
11 *al.*, 1996), CheB (Djordjevic *et al.*, 1998), DrrD (Buckler *et al.*, 2002), and DrrB (Robinson *et*  
12 *al.*, 2003) varied with the extent of their interdomain interfaces.

13

14 Several activating insertions were clustered in the  $\alpha$ -helical section of the linker region  
15 (Figure 5). Mutational analysis of the linker region between the receiver and effector domains  
16 of OmpR by Mattison *et al.* (2002) showed that the composition of the linker region affected  
17 the interplay of the two domains, and hence played a role in transducing the receiver signal to  
18 the effector. In addition, the importance of interdomain linkers in the determination of the  
19 response regulator activation mechanism was shown using OmpR-PhoB hybrid proteins  
20 (Walthers *et al.*, 2003). The linker region appears to play an important role in regulation of  
21 WspR activation. However, studies with NarL assigned little functional significance to the  
22 linker region (Eldridge *et al.*, 2002), suggesting that linker-mediated regulation is not a  
23 universal feature of response regulators.

24

25 Insertions producing inactive and dominant-negative WspR variants were spread over the  
26 surface of the model furthest from the domain interface, surrounding the predicted  
27 phosphorylation site (Figure 5). N-terminal dominant-negative insertions may have disrupted  
28 protein folding without affecting the domain interface or promoting dimerisation in the same

1 manner as was seen for the activating insertions. Alternatively, these insertions could have  
2 affected WspR interaction with the Wsp chemosensory kinase.

3

4 Quantitative analysis of the effects of WspR variants showed that generation of the wrinkled  
5 phenotype in SM strains was associated with increases in levels of both cell attachment and  
6 cellulose production (Figures 2, 3 and 4). An important exception however, was the discovery  
7 of several WspR variants whose expression produced little effect on cellulose production, but  
8 greatly stimulated cell attachment, relative to the other tested WspR variants (e.g. WspR6,  
9 WspR120). In addition, greatly decreased levels of cellulose production in WS were observed  
10 upon expression of the 20 dominant-negative *wspR* substitution mutant alleles. However, cell  
11 attachment to glass in WS strains expressing these *wspR* mutant alleles was not repressed,  
12 relative to results seen with the wild-type control (Figure 6). These findings suggest that  
13 cellulose production and cell attachment are regulated by WspR through two distinct and  
14 separable pathways.

15

16 [For several *wspR* insert variants (e.g. SOE<sub>*wspR130*</sub>) higher levels of attachment were  
17 observed upon expression in SM  $\Delta$ *wspA-wspR* than in SM (Figure 3). This may be related to  
18 the loss of pellicle structure in SM  $\Delta$ *wspA-wspR* compared to SM, allowing more cells to  
19 attach at the meniscus than would be possible for strains producing a structured biofilm.  
20 Similarly, repression of cellulose production, and hence loss of pellicle structure, may explain  
21 why several dominant-negative WspR substitution variants (e.g. SUB<sub>*wspRR246F*</sub>) produced  
22 increased WS attachment levels compared to wild-type WspR (Figure 6).]

23

24 There are two possible alternative explanations for the quantitative data described above. In  
25 both scenarios, WspR functions exclusively as a DGC. In the first, up-regulation of  
26 attachment requires considerably lower levels of c-di-GMP than cellulose production. In this  
27 case, WspR insert variants that up-regulate attachment only (e.g. WspR6) would not produce  
28 enough c-di-GMP to trigger cellulose production. Likewise, inhibition of DGC activity by

1 dominant-negative WspR substitution variants (e.g. WspRR246L) would reduce c-di-GMP  
2 levels to the point where cellulose production, but not attachment is repressed. While further  
3 research is required to fully exclude this possibility, the fact that WspR variants were able to  
4 completely repress cellulose production while having no discernable effect on attachment  
5 (Figure 6) seems more consistent with separate activation pathways than with a graded  
6 response to a single signal.

7

8 In the second case, the Wsp kinase modulates c-di-GMP levels through WspR, but activates  
9 attachment through a second, as yet undiscovered response regulator. An example of a similar  
10 system is the Ple/Div system in *C. crescentus*, where the response regulators PleD and DivK  
11 are jointly controlled by the kinases PleC and DivJ (Paul et al., 2004). Repression of cellulose  
12 production in WS by dominant-negative WspR variants would have no effect on attachment  
13 in this scenario. If a second Wsp-controlled response regulator existed, we would expect to  
14 see high levels of attachment for WS  $\Delta wspR$  relative to SM  $\Delta wspR$ . In fact, attachment levels  
15 in this strain are comparable to SM  $\Delta wspR$  (Figure S2), strongly arguing against this model.

16

17 The separation of WspR regulatory activities is consistent with recent data obtained for the *C.*  
18 *crescentus* protein CC3396 (Christen et al., 2005), in which a domain with a degenerate  
19 GGDEF motif regulates protein function by binding GTP. A similar regulatory function has  
20 also been proposed for *P. aeruginosa* FimX (Kazmierczak et al., 2006). The existence of  
21 additional, non-enzymatic regulatory functions for GGDEF domains provides an explanation  
22 for why many species contain such large numbers of GGDEF containing proteins (Galperin,  
23 2005), a fact that is difficult to reconcile with enzymatic activity alone.

24

25 Finally, the RYGGEF motif of WspR was investigated using site-specific mutagenesis, and  
26 was shown to be highly sensitive to mutation. Substitution of residues 246-252 (RYGGEF),  
27 led to a loss of protein function in almost every tested case. Of the 76 *wspR* substitution  
28 alleles produced, only one produced an active protein (wrinkled morphology in SM). As



1 WspR functions as a DGC, it is reasonable to suggest that the level of functional conservation  
2 seen for the WspR RYGGEEF motif may also apply to other DGCs; that this motif  
3 (GGD/EEF) is absolutely required for DGC activity. [The GGD/EEF motif is not  
4 always required for protein function, however (Christen *et al.*, 2005; Kazmierczak *et al.*,  
5 2006)]. Mutagenesis of single residues in RYGGD/EEF has eliminated protein function in  
6 numerous species (Paul *et al.*, 2004; Simm *et al.*, 2004; Kirillina *et al.*, 2004; Garcia *et al.*,  
7 2004; Goymer *et al.*, 2006), and the crystal structure of PleD places the RYGGEEF motif  
8 close to the ribose group and alpha-phosphate of bound c-di-GMP, suggesting a critical role  
9 in nucleotide binding or catalysis (Chan *et al.*, 2004).

10

11 The single active WspR variant, WspRE250D contained the motif RYGGDEF, rather than  
12 RYGGEEF. An analysis of sequence conservation among GGDEF domains (Galperin *et al.*,  
13 2001) indicated that aspartate and glutamate were found with similar frequency at position  
14 250. It is possible that the conformational constraints on the first glutamate in the RYGGEEF  
15 motif are not so pronounced as for the second, allowing either residue to be present.  
16 Interestingly, tyrosine 247 was absolutely conserved in this study, despite the residue at this  
17 position showing substantial variation across different GGDEF domains (Galperin *et al.*,  
18 2001). When three WspR substitution variants were chosen to represent each position of the  
19 RYGGEEF motif and analysed in more depth, almost every tested variant produced a  
20 dominant-negative effect on WS morphology (Table 5). The only exception was  
21 WspRY247F, which produced an inactive protein. The structural similarity between tyrosine  
22 and phenylalanine suggested that an undefined protein mis-folding event, avoided in the case  
23 of a structurally conserved substitution such as that in WspRY247F, effected the observed  
24 dominant-negative effect of the tested residue substitutions on WspR activity.

25

26 This work sheds light on several previously unanswered aspects of the WspR structure-  
27 function relationship. WspR functions as a DGC, whose enzyme activity is stimulated in the

1 WS genotype compared with the (wild-type) SM genotype. Upon phosphorylation, or  
2 disruption of the linker region or the interdomain interface, activation proceeds *via* release of  
3 effector domain repression by the receiver domain. Quantitative analysis of aspects of biofilm  
4 formation suggested a dual regulatory mechanism for WspR. Finally, the RYGGEEF motif of  
5 WspR is highly functionally conserved, with almost every tested substitution abolishing  
6 function in a dominant-negative fashion. As the time and effort required to produce high-  
7 quality structural models of proteins continues to decrease, this study underlines the  
8 continued utility of systematic mutagenesis to structure-function analyses.

9

10

11

12

13

14

15

16

17

18

19

20

21

22

23

24

25

26

27

## References:

- Aldridge, P., (2003) *Mol Microbiol* **47**, 1695-1708.
- Altschul, S. F. (1997). *Nucleic Acids Res* **25**, 3389-3402.
- Baikalov, I. (1996). *Biochemistry* **35**, 11053-11061.
- Bobrov, A. G., *FEMS Microbiol Lett* **247**, 123-130.
- Boles, B. R.. (2002). *J Bacteriol* **184**, 5946-5954.
- Bomchil, N., *J. Bacteriol* **185**, 1384-1390.
- Bradford, M. M. (1976). *Anal. Biochem* **72**, 248-254.
- Buckler, D. R., *Structure* **10**, 153-164.
- Chan, C., (2004). *Proc Natl Acad Sci U S A* **101**, 17084-17089.
- Christen, M., (2005) *J Biol Chem* **280**, 30829-30837.
- D'Argenio, D. A., *J Bacteriol* **184**, 6481-6489.
- D'Argenio, D. A. (2004). *Microbiology* **150**, 2497-2502.
- Djordjevic, S., (1998). *Proc Natl Acad Sci U S A* **95**, 1381-1386.
- Eldridge, A. M., (2002). *Biochemistry* **41**, 15173-15180.
- Galperin, M. Y. (2005). *BMC Microbiol* **5**, 35.
- Galperin, M. Y., (1999) *J Mol Microbiol Biotechnol* **1**, 303-305.
- Galperin, M. Y., (2001). *FEMS Microbiol Lett* **203**, 11-21.
- Garcia, B., (2004). *Mol Microbiol* **54**, 264-277.
- Gjermansen, M., (2005). *Environ Microbiol* **7**, 894-906.
- Goymer, P., (2006). *Genetics*
- Guex, N. & Peitsch, M. C. (1997). *Electrophoresis* **18**, 2714-2723.
- Hallet, B., (1997). *Nucleic Acids Res* **25**, 1866-1867.
- Hayes, F. & Hallet, B. (2000). *Trends Microbiol* **8**, 571-577.
- Hecht, G. B. & Newton, A. (1995). *J Bacteriol* **177**, 6223-6229.
- Heeb, S., (2000). *Mol Plant Microbe Interact* **13**, 232-237.
- Hickman, J. W., (2005). *Proc Natl Acad Sci U S A* **102**, 14422-14427.
- Ho, S. N., (1989). *Gene* **77**, 51-59.
- Huang, B., (2003). *J Bacteriol* **185**, 7068-7076.
- Jenal, U. (2004). *Curr Opin Microbiol* **7**, 185-191.
- Johnson, M., (2005). *Mol Microbiol* **55**, 664-674.
- Kazmierczak, B. I., (2006). *Mol Microbiol* **60**, 1026-1043.
- King, E. O., (1954). *J Lab Clin Med* **44**, 301-307. 6
- Kirillina, O., (2004). *Mol Microbiol* **54**, 75-88.
- Kovacicova, G., (2005). *Mol Microbiol* **57**, 420-433.
- Kulesekara, H., (2006). *Proc Natl Acad Sci U S A*.
- Mattison, K., (2002). *J Biol Chem* **277**, 32714-32721.
- Miller, J. H. (1972). *Cold Spring Harbor, New York*, 352-355.
- Muchova, K., (2004). *Mol Microbiol* **53**, 829-842.
- Park, S., (2002). *FASEB Journal* **16**, 1964-1966.
- Paul, R., (2004). *Genes Dev* **18**, 715-727.
- Pei, J. (2001). *Proteins* **42**, 210-216.
- Rainey, P. B. (1996). *Mol Microbiol* **3**, 521-533.
- Rainey, P. B. (1998). *Nature* **394**, 69-72.
- Rashid, M. H., (2003). *FEMS Microbiol Lett* **227**, 113-119.
- Robinson, V. L., (2003). *J Bacteriol* **185**, 4186-4194.
- Romling, U. (2005). *Cell Mol Life Sci* **62**, 1234-1246.
- Romling, U., (2005). *Mol Microbiol* **57**, 629-639.
- Rost, B., (2004). *Nucleic Acids Res* **32**, W321-W326.
- Ryjenkov, D. A., (2005). *J Bacteriol* **187**, 1792-1798.
- Schmidt, A. J., (2005). *J Bacteriol* **187**, 4774-4781.
- Schwede, T., (2003). *Nucleic Acids Res* **31**, 3381-3385.
- Simm, R (2004). *Mol Microbiol* **53**, 1123-1134.
- Simm, R., (2005). *J Bacteriol* **187**, 6816-6823.
- Spiers, A. J., (2002). *Genetics* **161**, 33-46.
- Spiers, A. J., (2003). *Mol Microbiol* **50**, 15-27.
- Summers, D. K. (1988). *EMBO J* **7**, 851-858.
- Ude, S., (2006). *Environ Microbiol*. Epub. ahead of print.
- Walthers, D., (2003). *J Bacteriol* **185**, 317-324.
- Woodcock, D. M., (1989). *Nucleic Acids Res* **17**, 3469-3478.
- Zhang, G. Y (1997). *Nature* **388**, 204-204.

## Acknowledgements

This work was supported by the UK Biotechnology and Biological Sciences Research Council (BBSRC).

The authors wish to thank Sripadi Prabhakar for assistance with mass spectroscopy, and Zena Robinson and Julie Stansfield for technical assistance.

**Figure 1: Biochemical analysis of WspR.** (a): WspR was shown to function as a DGC in vitro. C-di-GMP production was observed over time against control lanes (Ctrl) containing  $\alpha$ -<sup>33</sup>P c-di-GMP (Christen et al., 2005). 1(b): DGC activity assays were carried out with whole cell extracts. The furthest migrating spot, thought to correspond to GMP, (retardation factor [RF] value 0.54) predominated in the cell extracts. The second furthest migrating spot ( $R_f$  0.47) was thought to correspond to GDP. These molecules may have been formed through breakdown of GTP ( $R_f$  0.37) by enzymes in the cell lysate. The slowest running spot ( $R_f$  0.25) was present in WS cell lysates expressing wspR either from a plasmid or from the chromosome (Lanes 2 and 6). This spot corresponded to c-di-GMP. 1(c): Protein expression levels were measured for SM and WS cell extracts by Western blotting. WspR expression levels were similar in SM and WS cultures. SBW25 SM  $\Delta$ wspR cell extract, and N-terminal His6-tagged WspR were included as controls. The small, minor band seen in the control lane was shown to correspond to a degradation fragment of WspR by mass spectroscopy.

**Figure 2: The effects of five amino-acid residue insertions on WspR activity.** Morphology data was used to assign activity states to WspR insert variants. The arrows represent the positions of amino-acid inserts, and indicate the resultant activity of the insert as shown. Insertions in the linker region and sections of the N-terminus produced constitutively-active variants, whilst insertions in the C-terminus abolished WspR activity and usually led to suppression of the wrinkled phenotype in WS.

**Figure 3: The effects of *wspR* mutant allele expression on SM and SM  $\Delta$ wspA-*wspR* attachment to glass microcosms** Data show mean A570  $\pm$  standard error for eight replicates. The grey bars represent SM  $\Delta$ wspA-*wspR*, and the white bars SM strains, both containing WspR variants with inserts at the residue positions noted. The bar below the graph represents the domain structure of WspR. The grey section represents the N-terminus, the black section the linker region, and the white section the C-terminus. A two-way ANOVA showed that the effect of the mutation was dependent on whether it was in the N-terminal domain, the linker region, or the C-terminal domain [F2,698 = 118.84, P < 0.0001]. The effect of strain background was not significant [F1,698 = 0.32, P = 0.571], but the interaction effect was highly significant [F2,698 = 12.76, P < 0.0001].

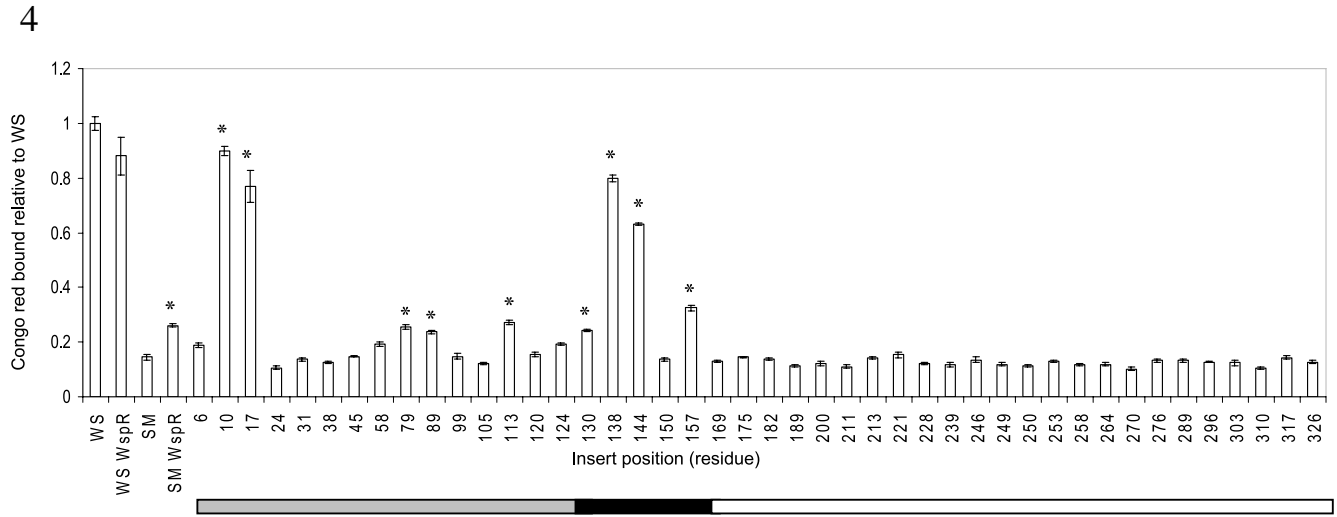
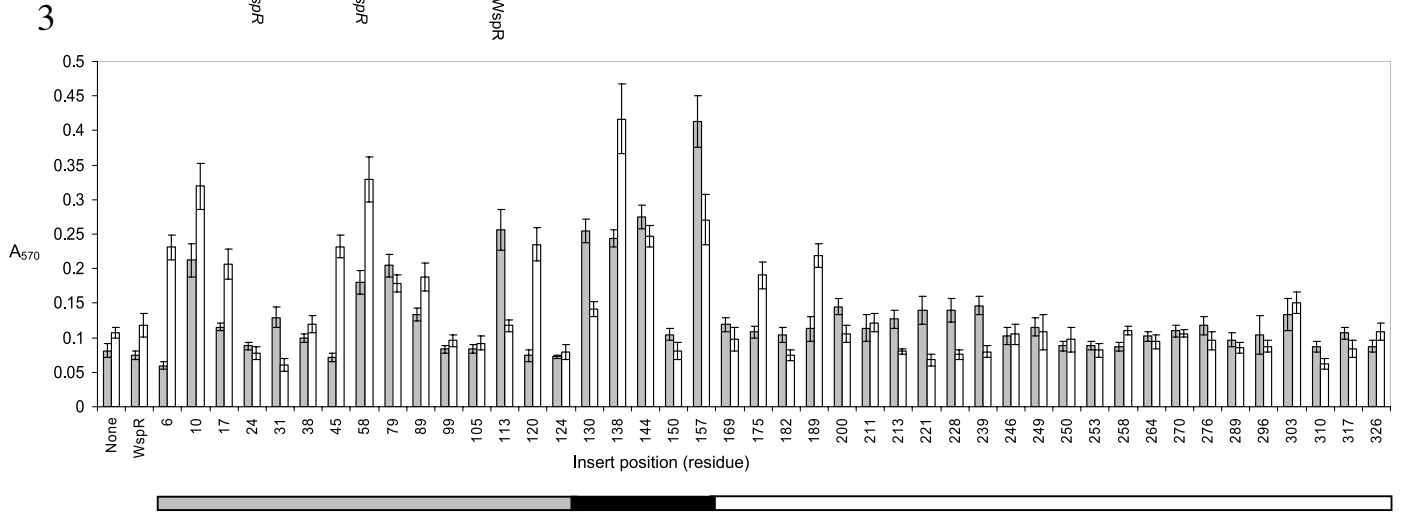
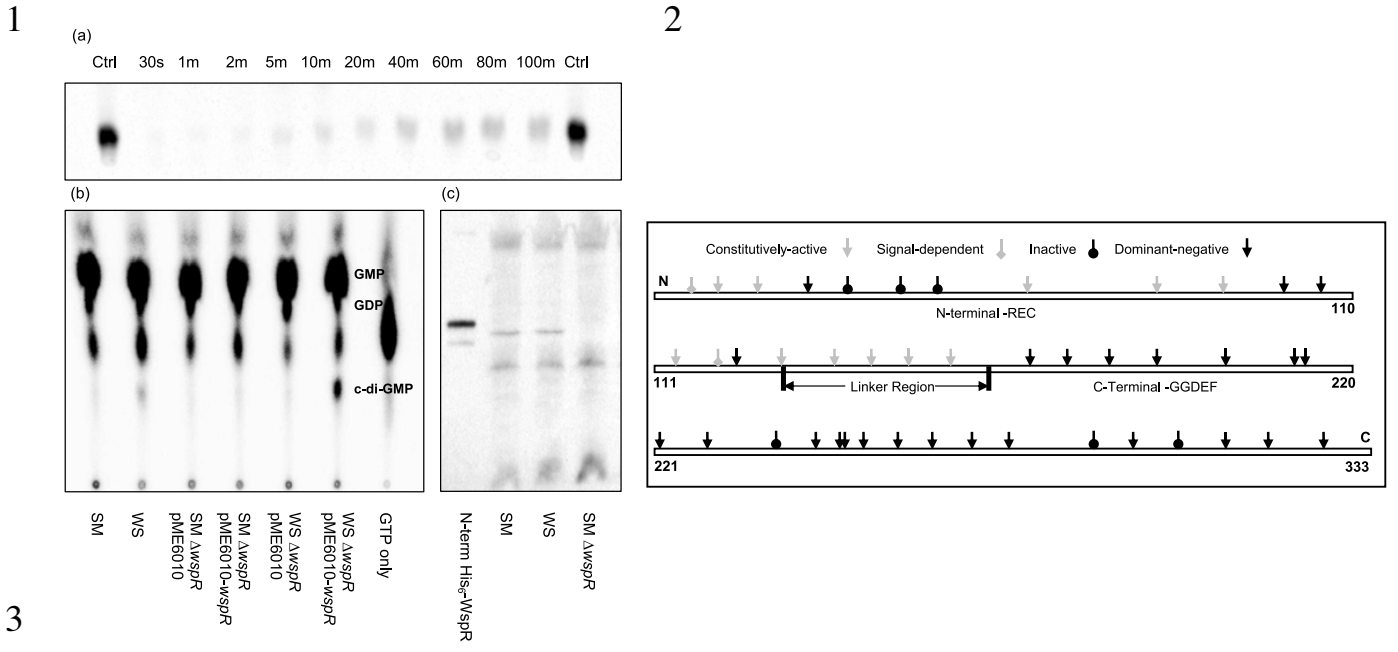
**Figure 4: The effects of *wspR* mutant allele expression on SM and WS binding to Congo Red dye.** Data show mean Congo Red absorbed relative to WS pME6010  $\pm$  standard error for five replicates. The bar below the graph represents the domain structure of WspR. The grey section represents the N-terminus, the black section the linker region, and the white section the C-terminus. One-way ANOVA revealed a highly significant difference among means [F47,192 = 238.00, P < 0.0001]. Dunnett's test was used to identify alleles that gave effects that were significantly greater than the plasmid controls and are indicated by an asterisk.

**Figure 5: Insert positions in the N-terminus and linker region of WspR.** The figure shows the WspR homology model visualised from four different angles. The GGDEF domain is coloured grey. The N-terminal receiver domain and the linker region are coloured green, with the sites of five amino-acid residue insertions highlighted according to their resultant activity state. Constitutively-active = red, signal-dependent = orange, inactive = light blue, dominant-negative = dark blue. Areas of ribbon coloured grey in the N-terminus represent sections with no corresponding WspR sequence.

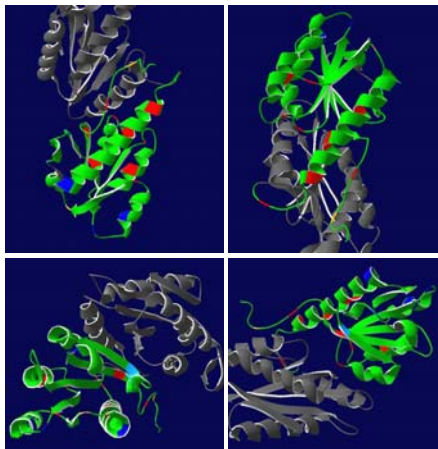
**Figure 6: Effects of WspR substitution variants on WS behaviour.** The effects of 21 WspR substitution variants on (a) cellulose production and (b) attachment in WS were measured. Data show (a) mean A490  $\pm$  standard error for five replicates and (b) mean A570  $\pm$  standard error for

eight replicates respectively. Constructs are named based on the WspR substitution in each case. Wrinkled morphology and cellulose production were repressed in WS upon production of all but one variant protein; WspRY247F. Attachment was not repressed by any WspR variant. A nested ANOVA revealed a significant effect due to substitutions at different positions in the RYGGEEF motif [ $F_{9,168} = 26.96$ ,  $P < 0.0001$ ] and a significant effect of the particular residue at each position [ $F_{14,168} = 4.50$ ,  $P < 0.0001$ ]. Analysis of a priori contrasts in least-squared-means derived from the nested ANOVA model showed highly significant effects of substitutions at positions 246, 247 and 248 ( $P < 0.0001$  in each case), but no significant effect of substitutions at positions 250-252.

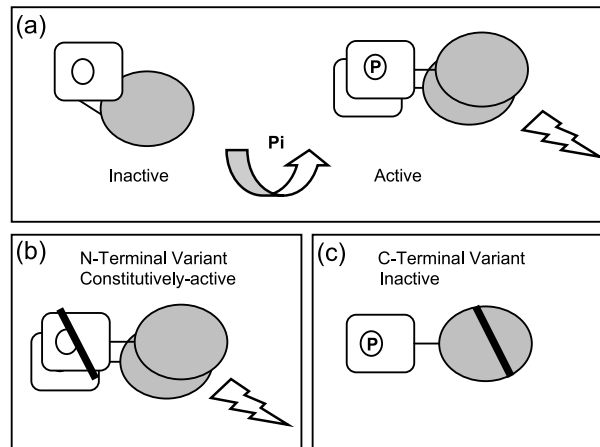
**Figure 7: A model for WspR function.** For wild-type WspR (a), inhibition of the C-terminal effector domain (oval) by the N-terminal receiver domain (square) is relieved upon phosphorylation, allowing WspR to produce a signal, possibly via dimerisation in a similar manner to other GGDEF proteins (Chan et al., 2004, Ryjenkov et al., 2005). Mutation of the N-terminus or linker region (b) may remove this inhibition, as exemplified by constitutively-active WspR variants. Mutation of the C-terminus (c) knocks out function irrespective of the phosphorylation state of WspR, resulting in the inactive or dominant negative state.



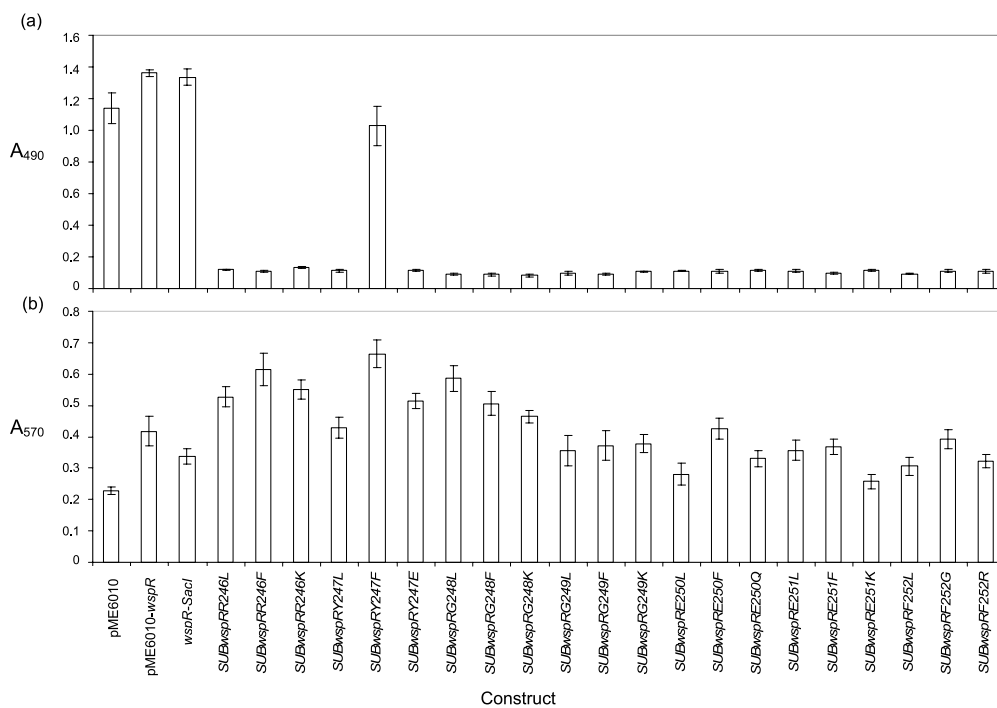
5



7



6



1 **Table 1:** Colony morphologies of SBW25 strains expressing the pME6010-*wspR* insert  
 2 library

Construct <sup>a</sup>	Colony morphology <sup>b</sup>						Activity state <sup>c</sup>
	SM	WS	SM	SM	WS	SM	
			$\Delta wspA-F$	$\Delta wspA-R$	$\Delta wspR$	$\Delta wspR$	
pME6010	SM	WS	SM	SM	SM	SM	I
pME6010- <i>wspR</i>	WS	WS	SM	SM	WS	WS	D
PSM <i>wspR6</i>	WS	WS	SM	SM	WS	WS	D
PSM <i>wspR10</i>	WS	WS	WS	WS	WS	WS	C
SOE <i>wspR17</i>	WS	WS	WS	WS	WS	WS	C
SOE <i>wspR24</i>	SM	SM	SM	SM	SM	SM	N
SOE <i>wspR31</i>	SM	WS	SM	SM	WS	Int.	I*
PSM <i>wspR38</i>	SM	WS	SM	SM	WS	SM	I*
PSM <i>wspR45</i>	SM	WS	SM	SM	SM	Int.	I
SOE <i>wspR58</i>	WS	WS	WS	WS	WS	WS	C
SOE <i>wspR79</i>	WS	WS	WS	WS	WS	WS	C
PSM <i>wspR89</i>	WS	WS	WS	WS	WS	WS	C
PSM <i>wspR99</i>	SM	SM	SM	SM	SM	SM	N
PSM <i>wspR105</i>	SM	SM	SM	SM	SM	SM	N
SOE <i>wspR113</i>	WS	WS	WS	WS	WS	Int.	C
PSM <i>wspR120</i>	WS	WS	SM	SM	WS	WS	D
PSM <i>wspR124</i>	SM	SM	SM	SM	SM	SM	N
SOE <i>wspR130</i>	WS	WS	WS	WS	WS	WS	C
PSM <i>wspR138</i>	WS	WS	WS	WS	WS	WS	C
SOE <i>wspR144</i>	WS	WS	WS	WS	WS	WS	C
SOE <i>wspR150</i>	WS	WS	WS	WS	WS	WS	C
SOE <i>wspR157</i>	WS	WS	WS	WS	WS	WS	C
SOE <i>wspR169</i>	SM	SM	SM	SM	SM	SM	N
PSM <i>wspR175</i>	SM	SM	SM	SM	SM	SM	N
SOE <i>wspR182</i>	SM	SM	SM	SM	SM	SM	N
PSM <i>wspR189</i>	SM	SM	SM	SM	SM	SM	N
SOE <i>wspR200</i>	SM	SM	SM	SM	SM	SM	N
PSM <i>wspR211</i>	SM	SM	SM	SM	SM	SM	N
PSM <i>wspR213</i>	SM	SM	SM	SM	SM	SM	N
SOE <i>wspR221</i>	SM	SM	SM	SM	SM	SM	N
SOE <i>wspR228</i>	SM	SM	SM	SM	SM	SM	N
SOE <i>wspR239</i>	SM	WS	SM	SM	WS	SM	I*
SOE <i>wspR246</i>	SM	SM	SM	SM	SM	SM	N
PSM <i>wspR249</i>	SM	SM	SM	SM	SM	SM	N
PSM <i>wspR250</i>	SM	SM	SM	SM	SM	SM	N
SOE <i>wspR253</i>	SM	SM	SM	SM	SM	SM	N
PSM <i>wspR258</i>	SM	SM	SM	SM	SM	SM	N
SOE <i>wspR264</i>	SM	SM	SM	SM	SM	SM	N



SOE <i>wspR270</i>	SM	SM	SM	SM	SM	SM	N
SOE <i>wspR276</i>	SM	SM	SM	SM	SM	SM	N
SOE <i>wspR289</i>	SM	WS	SM	SM	WS	SM	I*
PSM <i>wspR296</i>	SM	SM	SM	SM	SM	SM	N
SOE <i>wspR303</i>	SM	Int.	SM	SM	SM	SM	I
SOE <i>wspR310</i>	SM	SM	SM	SM	SM	SM	N
SOE <i>wspR317</i>	SM	SM	SM	SM	SM	SM	N
PSM <i>wspR326</i>	SM	SM	SM	SM	SM	SM	N

1

2 <sup>a</sup> Each construct name contains the amino-acid position of the insert.3 <sup>b</sup> Colony morphology on LB agar plates; designated as smooth (SM), wrinkled (WS) or intermediate  
4 (Int.). Strains containing pME6010 and pME6010-*wspR* (wild-type) are included as controls.5 <sup>c</sup> The deduced activity state of each WspR variant is given as either constitutively-active (C), signal-  
6 dependent (D), inactive (I) or dominant-negative (N) (see Figure 2).

7

8

9

10

11

12

13

14

15

16

17

18

19

20

21

22

23

1 **Table 2:** Amino-acid residue substitutions that knock out WspR-SacI activity<sup>a</sup>

Altered residue	No. of substitutions <sup>b</sup>	Substituted residues <sup>c</sup>			
		Aliphatic residues	Aromatic residues	Charged or polar	Aliphatic hydroxyl/sulphur-containing
246 R	11	L, I, V, A	F	K, Q	T, S, C, M
247 Y	11	L, I, V, P	F, H	D, E	T, S, C
248 G	9	L, I, V	F, Y	K, R, Q	T
249 G	10	L, I, V, A	F, Y	K, N	S, C
250 E	11	G, L, I, A, P	F, Y	Q	T, S, C
251 E	13	G, L, I, V, P	F, Y	K, R, N	T, S, C
252 F	10	G, L, I, V		R, D, E, N	S, C

2

3 <sup>a</sup> In every example shown, the ability of the variant protein to produce a wrinkled phenotype in SM  
4 cells grown on LB agar plates was abolished.

5 <sup>b</sup> The number of substitutions is out of a possible 18 residue substitutions at each position.

6 <sup>c</sup> WspR variants are grouped according to the chemistry of the substituted residue side-chain. Standard  
7 amino-acid definitions are used.

8

9

10

11

12

13

14

15

16

17

18

19

20

21

22

1 **Table 3:** Bacterial strains and plasmids

Strain or Plasmid	Description	Reference <sup>a</sup>
<i>P. fluorescens</i> SBW25		
SM	Environmental isolate, wild-type ancestral smooth genotype	42
WS (also LSWS)	Biofilm former, evolved from SBW25 SM	56
SM $\Delta$ <i>wspA-wspF</i>	SM with <i>wspA-wspF</i> deleted	Rainey et al. (unpublished)
SM $\Delta$ <i>wspA-wspR</i>	SM with <i>wspA-wspR</i> deleted	Bantinaki, E. (unpublished)
SM $\Delta$ <i>wspR</i>	SM with <i>wspR</i> deleted	Gehrig, S.M. (unpublished)
WS $\Delta$ <i>wspR</i>	WS with <i>wspR</i> deleted	20
WS-4	WS <i>wspR::miniTn5</i> , Km <sup>R</sup>	56
<i>E. coli</i>		
BL21-(DE3)	Sm <sup>R</sup> , K12 <i>recF143 lacF<sup>l</sup> lacZ<math>\Delta</math>M15, xylA</i>	Novagen
DH5 $\alpha$	<i>endA1, hsdR17</i> (r <sub>K</sub> -m <sub>K</sub> <sup>+</sup> ), <i>supE44, recA1, gyrA</i> (Nal <sup>r</sup> ), <i>relA1, <math>\Delta</math>(lacIZYA-argF)U169, deoR, <math>\Phi</math>80dlac<math>\Delta</math>(lacZ)M15</i>	60
DS941	K12 <i>recF143 lacF<sup>l</sup> lacZ<math>\Delta</math>M15, xylA</i> , Sm <sup>R</sup>	57
FH395	DH5 $\alpha$ containing pFH395, a Km <sup>R</sup> , conjugative F derivative (pOX38Km) containing transposon Tn4430 - inserted <i>in vivo</i>	Hayes, F. (unpublished)
Plasmids		
pET14b- <i>wspR</i>	pET14b with <i>wspR</i> as <i>NdeI-BamHI</i> fragment	Goymer, P.J. (unpublished)
pET42b- <i>wspR</i>	pET42b with <i>wspR</i> as <i>XhoI-NdeI</i> fragment	this study
pME6010	Tet <sup>R</sup> , P <sub>K</sub> , 8.3 kb pVS1 derived shuttle vector	25
pME6010- <i>wspR</i>	pME6010 with <i>wspR BamHI-EcoRI</i> fragment ligated between <i>BglII</i> and <i>EcoRI</i> - <i>BglII</i> site destroyed	this study
PSM <i>wspR</i> alleles	pME6010- <i>wspR</i> with 19 separate 15 bp inserts produced by transposon mutagenesis - see Table S1	this study
SOE <i>wspR</i> alleles	25 <i>wspR-SOE</i> alleles produced by SOE PCR using pME6010- <i>wspR</i> . PCR products ligated between <i>XhoI</i> and <i>EcoRI</i> of pME6010 - see Table S2	this study
pME6010- <i>wspR-SacI</i>	<i>wspR-SacI</i> produced by SOE PCR using pME6010- <i>wspR</i> . PCR product ligated between <i>XhoI</i> and <i>EcoRI</i> of pME6010	this study
SUB- <i>wspR</i> alleles	76 <i>wspR</i> fragments containing substitutions between codons 246 and 252, produced by PCR with degenerate primers using pME6010- <i>wspR-SacI</i> , and ligated between <i>SacI</i> and <i>EcoRI</i> of pME6010- <i>wspR-SacI</i> - see Table 2	this study

2

3 <sup>a</sup> SM  $\Delta$ *wspA-wspR*, SM  $\Delta$ *wspR*, FH395 and pET14b-*wspR* were the kind gifts of E. Bantinaki, S.M.

4 Gehrig, F. Hayes and P.J. Goymer respectively.

5

6

7

### **3.5 Unpublished results**

### 3.5.1 Cyclic di-GMP regulates adenylosuccinate synthetase - a key enzyme in purine biosynthesis pathway

Marc Folcher, Matthias Christen, Beat Christen, Suzette Moes, Paul Jenö and Urs Jenal  
Biozentrum, University of Basel, Klingelbergstrasse 70, CH-4056 Basel, Switzerland

#### Abstract:

C-di-GMP is a bacterial second messenger implicated in biofilm formation, antibiotic resistance, and persistence of pathogenic bacteria in their animal host. The enzymes responsible for the regulation of cellular levels of c-di-GMP, diguanylate cyclases (DGC) and phosphodiesterases (PDE), have been identified and characterized. So far little information is available regarding c-di-GMP effector mechanisms and binding proteins. Using affinity chromatography and a specific assay for c-di-GMP binding, we have identified in *Caulobacter crescentus* extract an adenylosuccinate synthetase (PurA, CC3103) that binds c-di-GMP with high affinity. Using purified recombinant PurA for kinetic analysis and binding studies, we show that c-di-GMP is a potent inhibitor of PurA activity. Initial rate kinetics revealed that c-di-GMP inhibition is competitive with respect to GTP and noncompetitive with respect to IMP. These findings suggest a central role for c-di-GMP as regulator of nucleotide pool. We propose that inhibition of the first step of *de novo* biosynthesis of AMP by c-di-GMP directs IMP towards guanine biosynthesis and thereby prevent the drainage of the guanine pool under conditions of elevated c-di-GMP levels.

## Results

**Purification of c-di-GMP binding proteins from *C. crescentus*.** Based on the assumption that c-di-GMP signal transduction depends on specific receptor proteins, we designed a biochemical purification strategy to identify such components. C-di-GMP binding proteins from *C. crescentus* were purified by two consecutive chromatography steps using BlueSepharose® CL-6B and affinity chromatography with GTP immobilized on Epoxy activated Sepharose 4B (Pharmacia). UV cross-linking with [<sup>33</sup>P]c-di-GMP was used to identify proteins with specific binding activity for c-di-GMP (see Materials and Methods). After ammonium sulfate precipitation of 100.000 × g *C. crescentus* supernatant, 323 mg resolubilized protein was applied to a BlueSepharose® CL-GB column (Pharmacia). Most of the protein was eluted during the first wash step with 0.4 M NaCl. Fractions eluted in subsequent washing steps (0.4 - 0.7 M and 0.7 – 0.9 M NaCl) included most of the specific binding activity. Two binding proteins with apparent molecular weights of 47 kDa and 36 kDa were detected in the 0.4 – 0.7 M NaCl eluate (Figure 3A, B, lane 3) and the 0.7 – 0.9 M NaCl fraction contained several small c-di-GMP binding proteins with apparent molecular weights of 8-12 kDa (Figure 3A, B, lane 4). The 0.4 – 0.7 M NaCl eluate was dialyzed, concentrated and applied to a MiniQ anion exchange column (Amersham Pharmacia Biotech). The column was washed with PBS Buffer, and bound material was eluted with a 0 – 500 mM linear gradient of NaCl in PBS Buffer. Fractions were analyzed by UV cross linking with [<sup>33</sup>P]c-di-GMP, separated by tricine gradient gel and stained with coomassie colloidal blue. The 47 kD c-di-GMP binding protein was eluted in fraction 9 (162-185 mM NaCl) (Figure 3C,D lane 9) and identified by MS/MS analysis as the product of the gene CC3103, the *C. crescentus* homologue of the adenylosuccinate synthetase PurA (EC 6.3.4.4) (Figure 3E).

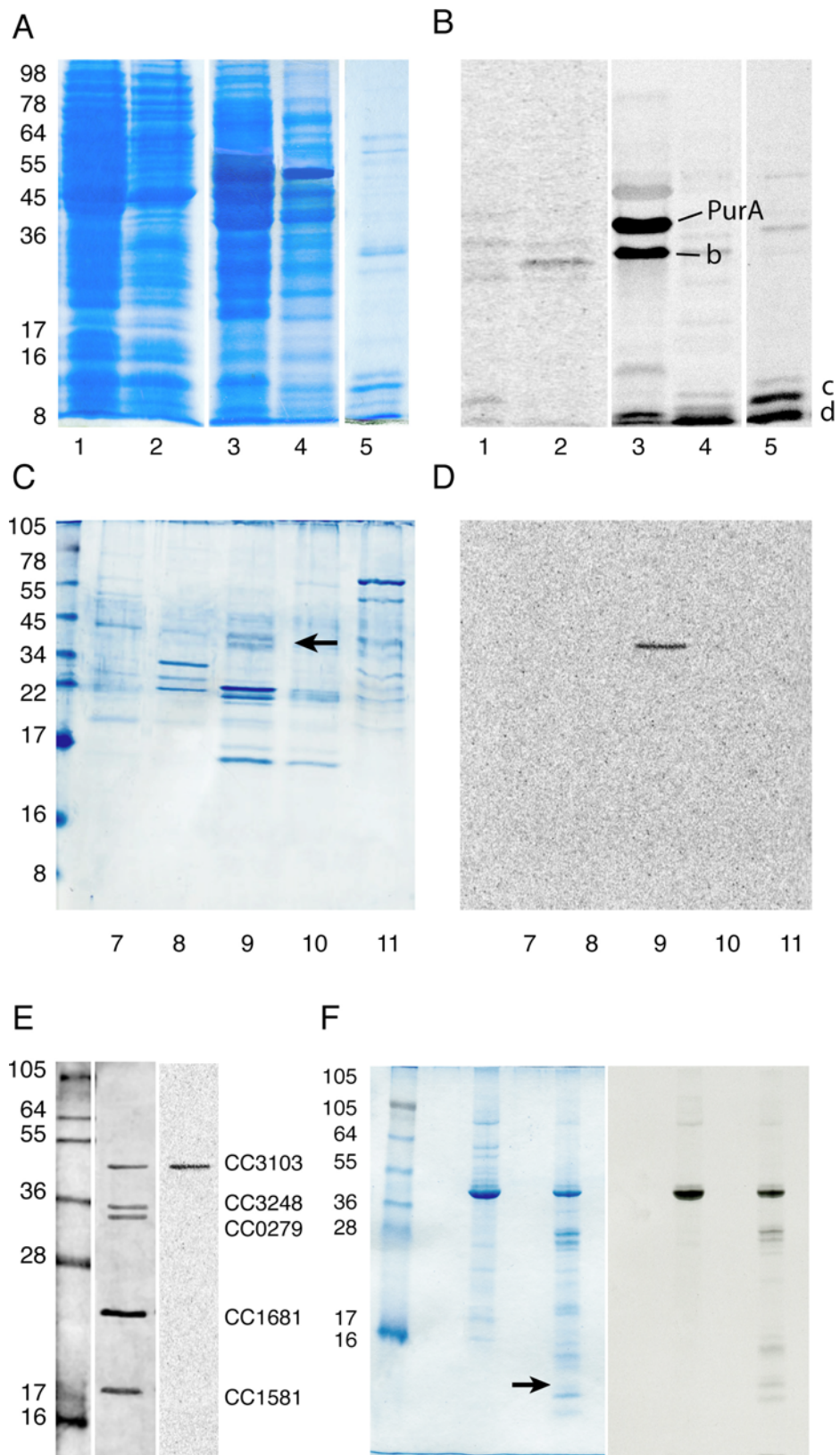


Figure 3 Isolation of c-di-GMP binding proteins from *C. crescentus*.

**A)** Coomassie stained SDS-PAGE gel with protein fractions used for UV cross linking with [<sup>33</sup>P]c-di-GMP. Lane 1: 100.000 × g supernatant of total protein extracts, lane 2: 60% ammonium sulfate precipitation, lane 3: 0.4 - 0.7 M NaCl eluate from Blue Sepharose®, lane 4: 0.7 - 0.9 M NaCl eluate from Blue Sepharose® and lane 5: 125 mM NaCl eluate from GTP-sepharose column. **B)** Autoradiograph of SDS-PAGE gel shown in A. Due to weak incorporation, lanes 1 and 2 were exposed on a phosphoimager screen, whereas lane 3–5 were exposed on X-ray film. Protein a was identified by MS/MS as the *C. crescentus* adenylosuccinate synthetase PurA (CC3103), protein b as translation elongation factor EF-Tu (CC1240, CC3199), protein c as DgrA (Diguanilate receptor protein A, CC1599) the nature of protein d is under investigation. **C)** Coomassie stained tricine gradient gel with protein fractions from the miniQ column used for UV-cross linking with [<sup>33</sup>P]c-di-GMP. The arrow indicates the c-di-GMP binding protein PurA identified by MS/MS analysis. **D)** Autoradiograph of SDS-PAGE gel shown in C. **E)** Coomassie stained tricine gradient gel with protein fraction 9 from the miniQ column labeled with [<sup>33</sup>P]c-di-GMP. left lane: marker, middle lane: coomassie colloidal staining, right lane: radiography. By MS/MS identified proteins: CC3103 adenylosuccinate synthetase, CC3248 glyceraldehyde-3-phosphate dehydrogenase, CC0279 methionyl tRNA formyltransferase, CC1681 guanylate kinase, CC1581 glycosamine 1-phosphate N-acetyltransferase. **F)** UV cross linking of purified hexahistidine-tagged PurA with [<sup>33</sup>P]c-di-GMP. left lane: marker, middle lane: recombinant PurA protein containing a C-terminal His-tag, right lane: tryptic digest of the recombinant PurA protein after UV cross-linking with [<sup>33</sup>P]-c-di-GMP. The arrow indicates the 5 kD N-terminal fragment of PurA which has been identified by MS/MS the peptide fragments AA18-27 K.LALLPSGVVQGK.LMH+= 1181.72 and AA51-68 K.IVDWLSNR.A MH+= 1002.52.

**PurA is a c-di-GMP binding protein.** In order to confirm that the identified protein is c-di-GMP binding, *purA* was sub cloned into the expression vector pET-21b and the recombinant hexahistidine-tagged protein was purified by Ni-NTA-affinity chromatography. Like the semi-purified protein from *C. crescentus* (Figure 3E), the recombinant protein showed strong labeling upon UV cross linking with [<sup>33</sup>P]c-di-GMP (Figure 3F), confirming that PurA is a c-di-GMP binding protein.

**C-di-GMP is a competitive inhibitor towards GTP.** PurA plays an important role in the de novo pathway of purine nucleotide biosynthesis. It catalyzes the committed step of the AMP de novo biosynthesis, the generation of 6-phosphoryl-IMP from GTP and IMP followed by the formation of adenylosuccinate from 6-phosphoryl-IMP and L-aspartate. It has been shown, that PurA is inhibited by a wide variety of nucleotides as by the product adenylosuccinate (34), by AMP (35), the end product of the pathway, but also by different guanine nucleotides. GMP exhibits competitive inhibition towards both GTP and IMP, and GDP and ppGpp are competitive inhibitors toward GTP (36-43). Based on these diverse inhibition properties and based on the finding that PurA binds specific c-di-GMP, we assumed that binding of the guanine nucleotide c-di-GMP might affect PurA activity as well. Therefore, initial rate kinetic studies with the recombinant *C. crescentus* adenylosuccinate synthetase were undertaken, to investigate the role of c-di-GMP binding for PurA activity. The experimental protocol involves varying the concentration of one of the substrate



at several fixed levels of c-di-GMP. The concentrations of the other two substrates are held constant at values above their respective Michaelis-Menten constant but below saturation (39).

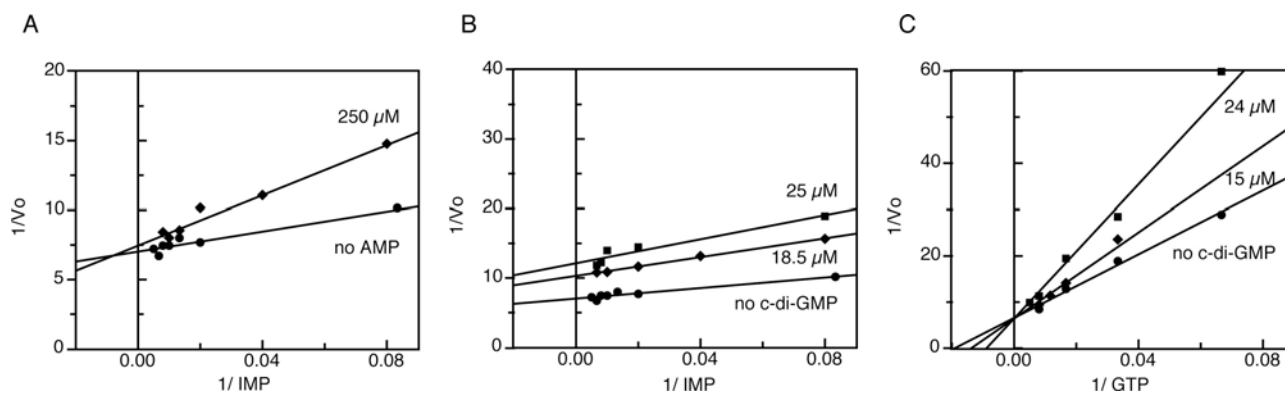


Figure 4 Lineweaver-Burk plots of inhibited adenylosuccinate synthetase.

**A)** Plot of the reciprocal initial velocity (ODU280nm / min) versus the reciprocal molecular concentration of IMP (in  $\mu\text{M}^{-1}$ ). AMP concentrations are 0 and 250  $\mu\text{M}$ , GTP and aspartate concentrations are 125  $\mu\text{M}$  and 2.5 mM. IMP was varied in the range 12.5 to 200  $\mu\text{M}$ . Other experimental details are described in “Experimental procedures”. **B)** Plot of the reciprocal initial velocity (ODU280nm / min) versus the reciprocal molecular concentration of IMP (in  $\mu\text{M}^{-1}$ ). C-di-GMP concentrations are 0, 18.5 and 25  $\mu\text{M}$ , GTP and aspartate concentrations are 125  $\mu\text{M}$  and 2.5 mM. IMP was varied in the range 12.5 to 200  $\mu\text{M}$ . Other experimental details are described in experimental procedures. **C)** Plot of the reciprocal initial velocity (ODU280nm / min) versus the reciprocal molecular concentration of GTP (in  $\mu\text{M}^{-1}$ ). C-di-GMP concentrations are 0, 15 and 24  $\mu\text{M}$ , GTP and aspartate concentrations are 125  $\mu\text{M}$  and 2.5 mM. GTP was varied in the range 25 to 200  $\mu\text{M}$ . Other experimental details are described in experimental procedures.

AMP was found to be a competitive inhibitor towards IMP, as previously reported for the *E. coli* adenylosuccinate synthetase (Figure 4A, (44, 45)), whereas c-di-GMP was found to be a noncompetitive inhibitor towards IMP (Figure 4B) and a competitive inhibitor towards GTP, indicating that c-di-GMP acts as a substrate analog binding at the GTP site. This hypothesis is supported by UV cross-linking experiments with PurA in the presence of 1  $\mu\text{M}$  [ $^{33}\text{P}$ ] labeled c-di-GMP (see material and methods). After trypsin digestion of [ $^{33}\text{P}$ ]c-di-GMP labeled PurA, a [ $^{33}\text{P}$ ]c-di-GMP labeled 5 kD N-terminal trypsin digested fragment including the GTP binding site G12-K18 of PurA was isolated and identified by MS/MS (Figure 3F and Figure 7F), peptide fragments AA18-27 K.IVDWLSNR.A MH<sup>+</sup>= 1002.52 and AA51-68 K.LALLPSGVVQGK.L MH<sup>+</sup>= 1181.72.).

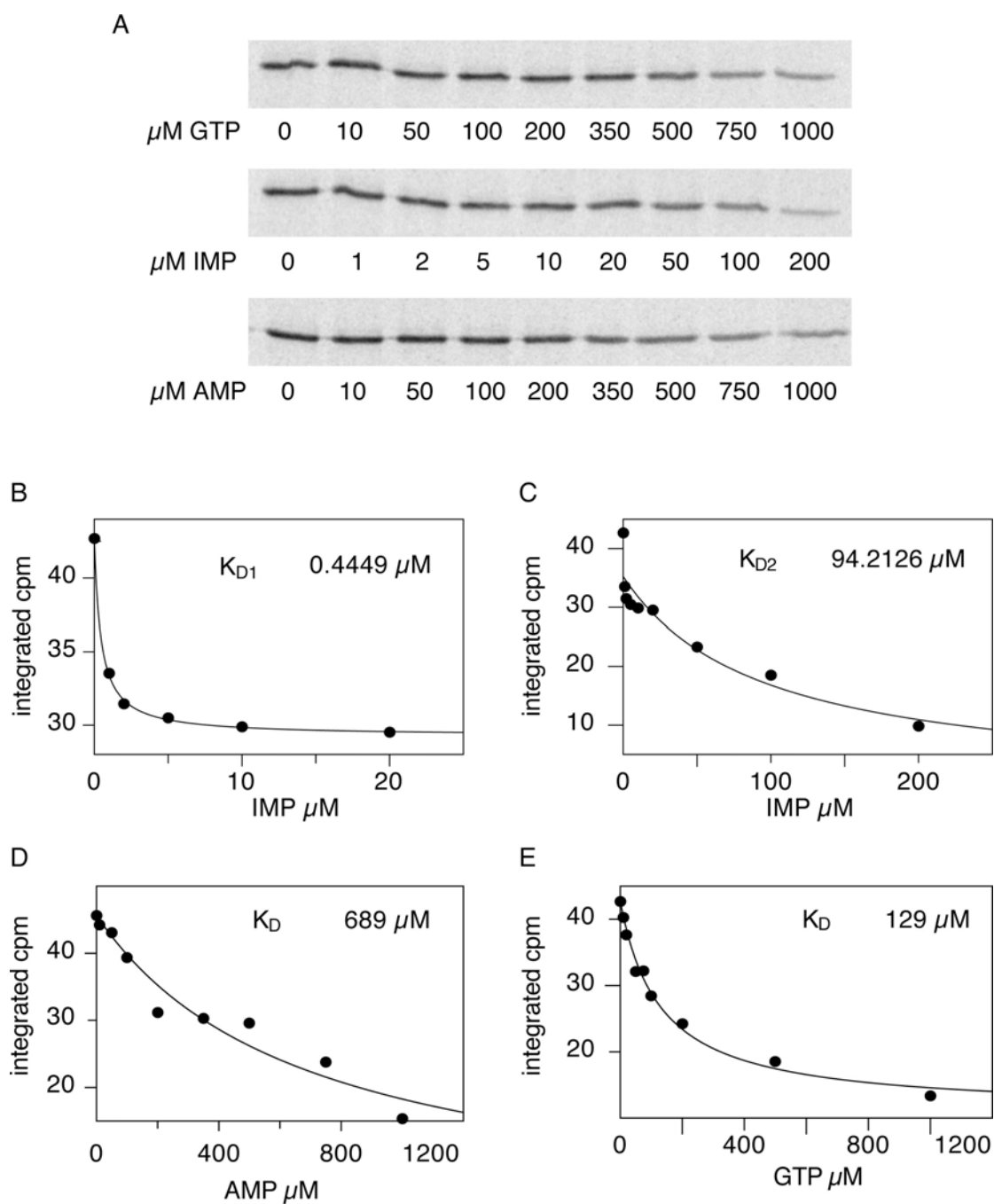


Figure 5 UV cross linking of PurA with  $^{33}\text{P}$ -c-di-GMP in presence of GTP, IMP or AMP.

**A)** Radiography of UV cross linking of 500 nM PurA in the presence of 1  $\mu\text{M}$  of  $^{33}\text{P}$  labeled c-di-GMP and GTP (0, 10, 50, 100, 200, 350, 500, 750 and 1000  $\mu\text{M}$ , upper lane), IMP (0, 1, 2, 5, 10, 20, 50, 100 and 200  $\mu\text{M}$  middle lane), or AMP (0, 10, 50, 100, 200, 350, 500, 750, 1000  $\mu\text{M}$  lower lane). **B-E)** Binding constants for IMP, AMP and GTP derived from the  $^{33}\text{P}$  c-di-GMP-IMP, GTP or AMP competition experiment.

**Competition of C-di-GMP binding by GTP, IMP and AMP.** Competition of C-di-GMP binding by GTP, IMP and AMP was monitored upon UV cross linking PurA in presence of  $1\mu\text{M}$  [ $^{33}\text{P}$ ]c-di-GMP and increasing concentration of cold GTP, IMP or AMP. IMP shows a mixed inhibition profile. At low concentration, IMP competes with a  $K_i$  of  $0,4\mu\text{M}$  for one third of the c-di-GMP binding capacity (Figure 5B) at higher concentration of IMP a second  $K_i$  of  $94\mu\text{M}$  can be observed where IMP is competing with two third of the c-di-GMP binding capacity (Figure 5C). In a similar experiment the indirect binding constants for GTP and AMP were determined to  $690\mu\text{M}$  for AMP and  $130\mu\text{M}$  for GTP. These values are in agreement with the dissociation constants determined by initial rate kinetics ( $K_i > 500\mu\text{M}$  for AMP, a  $K_m$  of  $120\mu\text{M}$  for GTP and  $6.7\mu\text{M}$  for IMP).

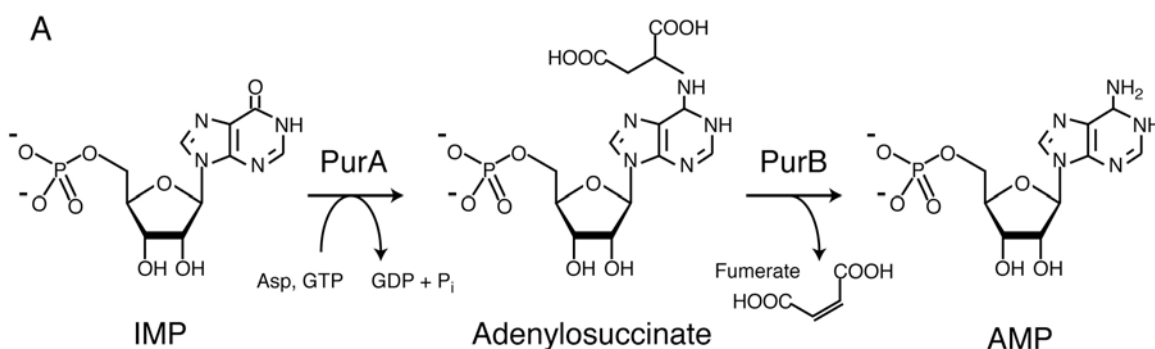


Figure 6 The de novo AMP synthesis from IMP by PurA (EC 6.3.4.4) and PurB (EC 4.3.2.2).

## Discussion

Using affinity chromatography and a specific assay for c-di-GMP binding (46, 47), we have purified and identified in *C. crescentus* extract an adenylosuccinate synthetase (PurA, CC3103) that has high affinity for the bacterial second messenger c-di-GMP. Binding studies and initial rate kinetic studies with purified recombinant were undertaken to clarify the inhibition mechanism of the second messenger c-di-GMP on PurA activity. Enzyme kinetics revealed that c-di-GMP potently inhibits PurA activity and that c-di-GMP inhibition is competitive with respect to GTP and noncompetitive towards IMP. Beside activation of the cellulose synthase complex from *Gluconacetobacter* by c-di-GMP (48, 49) and allosteric product inhibition of diguanylate cyclases, (47) the c-di-GMP mediated regulation of PurA activity represents a novel example of enzyme regulation by this bacterial second messenger.

The catalytic mechanism of the adenylosuccinate synthetase has been investigated intensively by kinetic studies and X-ray crystallographic analysis of various PurA substrate and inhibitor complexes (34, 40, 50-57). Isotope exchange studies at equilibrium by Cooper and Bass (58, 59) support the formation of 6-phosphoryl IMP prior to the nucleophilic attack of aspartate. Based on these investigations a two-step catalytic reaction mechanism, as suggested 60 years ago by Liebermann et al. (60), including the formation of the 6-phosphoryl IMP as an intermediate of the reaction pathway seems to be a valuable model (Figure 7B-D). In detail the catalytic process starts with the proton abstraction from N1 of IMP by Asp13 and generation of the 6-oxoanion, which is stabilized by a hydrogen bond to Gln222. The 6-oxoanion then displaces GDP from the  $\gamma$ -phosphate of GTP (Figure 7B), yielding the 6-phosphoryl IMP intermediate (Figure 7C). In the transition state, His41 and  $Mg^{2+}$  presumably stabilize the charge development on the  $\beta$ - and  $\gamma$ -phosphate of GTP. The second reaction catalyzed by the enzyme involves the nucleophilic substitution of the phosphate from 6-phosphoryl-IMP by the amino group of L-aspartate generating adenylosuccinate and phosphate. The hydrogen bond between the  $\beta$ -carboxylate and  $\alpha$ -amino group of L-aspartate enhances the nucleophilicity of the amino group, meanwhile enhances the hydrogen bond between N1 and Asp13 the electrophilicity of C6 and the hydrogen bond between His41 and the 6-phosphoryl group stabilizes the developing charge on the leaving group.

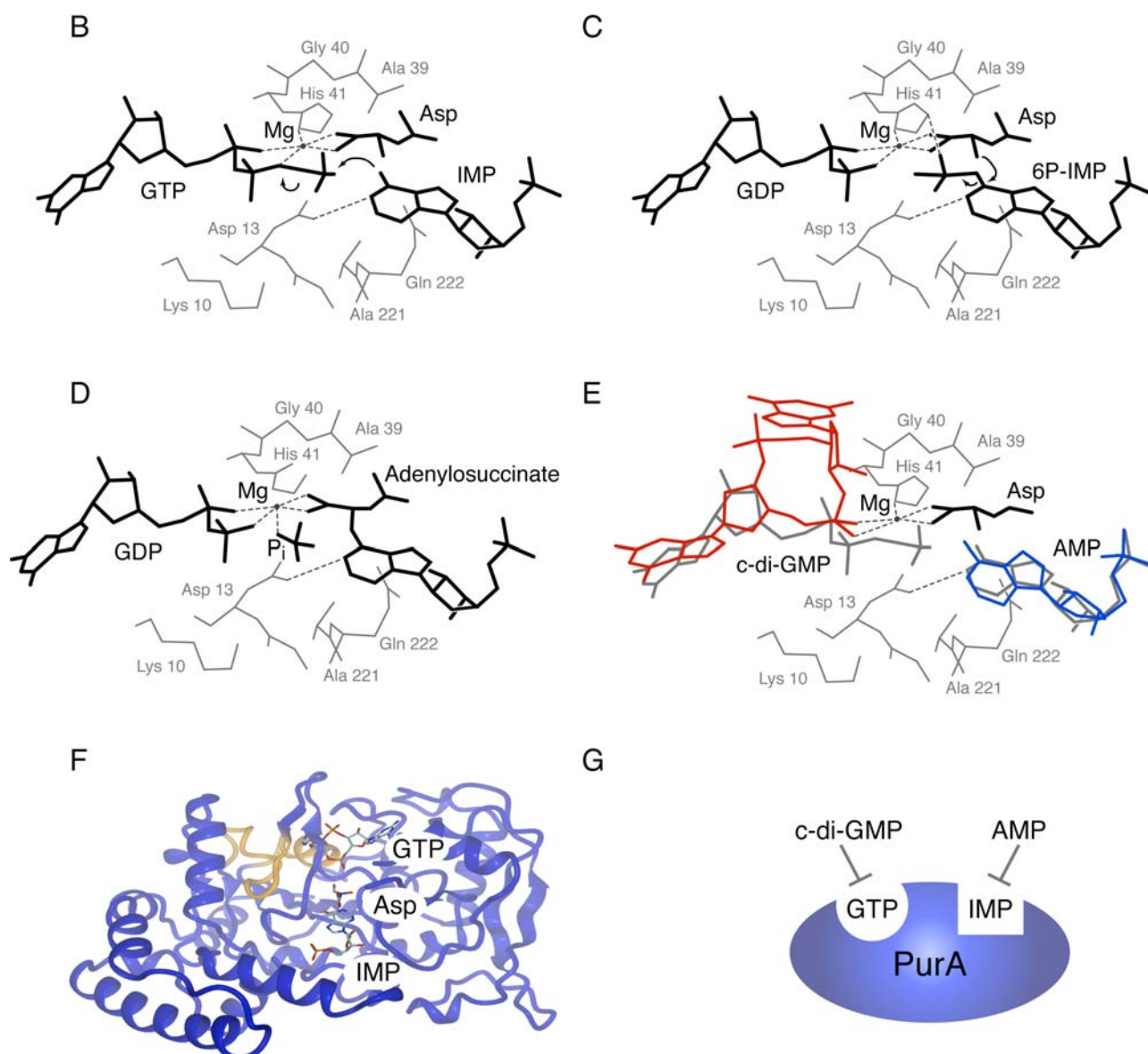


Figure 7 Reaction mechanism of the adenylosuccinate synthetase PurA

**B-D)** Homology model of the nucleotide binding site of the *C. crescentus* adenylosuccinate synthetase (CC3103) generated by Swissmodel with PDB entries 1CH8.pdb, 1CG0.pdb and 1SON.pdb as templates. A model of the reaction mechanism of the adenylosuccinate synthetase is shown according to (Bradley Poland JBC1997, Bradley Poland JMB 1996, Liebermann I JBC 1956). **B)** Proton abstraction at N1 of IMP by the carboxyl moiety of Asp13 is generating the 6-oxoanion of IMP, which then displaces GDP from the g-phosphate of the bound GTP. **C)** Nucleophilic displacement of 6-phosphate from the 6-phosphoryl intermediate by the amino group of Asp and subsequent protonation of N1 via Asp13. **D)** Reaction products adenylosuccinate, GDP and phosphate. **E)** Model for the inhibition of PurA by c-di-GMP (red) and AMP (blue). Our initial rate kinetic studies indicate, that the c-di-GMP inhibition of PurA is competitive with respect to GTP and non-competitive with respect to IMP, suggesting that c-di-GMP binds to the GTP binding site of the enzyme. **F)**

Homology model of the *C. crescentus* PurA with c-di-GMP placed into the GTP binding pocket. Peptides AA18-27 and AA51-68, which have been identified by MS/MS are highlighted in yellow.

It is well known, that the adenylosuccinate synthetase is regulated by a wide variety of guanine nucleotides. For GDP, ppGpp, pppGpp and ppG3':2'p it has been demonstrated that they act as competitive inhibitors towards the GTP binding site of the enzyme (61-63), whereas guanosine monophosphate has been shown to compete with both, GTP and IMP (63, 64). Our results suggest that the cyclic dimeric form of guanosine monophosphate, c-di-GMP, interacts mainly with the GTP binding site and functions as a competitive GTPase inhibitor as shown for the stringent response ppGpp (37, 65).

The cellular function of PurA inhibition by c-di-GMP is unclear. A possible physiological function might be the negative regulation of the *de novo* purine nucleotide synthesis upon induction of c-di-GMP. To maintain cellular homeostasis, nucleotide biosynthesis pathways are subject to tight allosteric control. Because AMP and GMP biosynthesis pathways compete for the same precursor IMP, feedback inhibition of their first enzymatic step (PurA for AMP and GuaB for GMP) not only controls the flux of metabolites but also contributes to balanced purine pools. Increasing c-di-GMP levels upon induction of enzymatic production of c-di-GMP from two molecules of GTP by diguanylate cyclases (DGC's) results in an accelerated consumption of the cellular guanosine pool. However nucleotide analysis by HPLC revealed that under such conditions the intracellular concentration of ATP and GTP are not affected (Figure 15A). A possible physiological function of PurA inhibition by c-di-GMP might be to shift the *de novo* purine biosynthesis towards the guanosine synthesis to maintain the GTP level and counteract the GTP consumption of DGCs. It has been reported, that the synthesis of the second messenger c-di-GMP as well as its degradation are under multiple control by guanine nucleotides (46, 47, 66). The synthesis of c-di-GMP is allosterically inhibited by c-di-GMP itself and it has been reported that the c-di-GMP specific phosphodiesterases PdeA from *C. crescentus* and FimX from *P. aeruginosa* are allosterically activated by GTP (46, 66). In such a context inhibition of PurA by c-di-GMP might be part of a cellular regulation network designated to maintain cellular homeostasis of the guanine pool under conditions of elevated c-di-GMP level.

**Material and methods:**

**Strains, plasmids and media.** *E. coli* strains were grown in Luria Broth (LB). *C. crescentus* strains were grown in complex peptone yeast extract (PYE) (67) supplemented with antibiotics, where necessary. Motility phenotypes were determined using PYE motility plates containing 0.3% Difco-Agar. For the exact procedure of strain and plasmid construction see supplemental material.

**BlueSepharose® CL-6B column.** 50 ml of resuspended and dialyzed 60%  $(\text{NH}_4)_2\text{SO}_4$  precipitate containing 323 mg protein (6.63 mg/ml) were loaded on a BlueSepharose® CL-6B column (Pharmacia) (flow 2 ml/min, 30 ml resin) with buffer A as loading buffer (1x PBS buffer containing 10 % (v/v) glycerol, 1 mM DTT). 151 mg protein was collected in the flow through and additional 160 mg was eluted during washing with 200 ml of buffer A. Bound proteins were eluted with a gradient of 50 - 1000 mM NaCl at a flow rate of 3 ml/min. The following fractions were pooled, dialyzed over night in buffer A and concentrated to a final protein concentration of 1 mg/ml using a 50 ml Amicon ultra filtration cell and regenerated cellulose ultra filtration membrane NMWL 10,000 (Millipore Corporation): weak binders (3.3 mg protein, fractions 7-11), medium binders (10.8 mg protein, fraction 12-20) and tight binders (7.8 mg protein, fractions 21-29).

**UV cross-linking with [<sup>33</sup>P]c-di-GMP, DGC and PDE activity assays.** Procedures for enzymatic production of [<sup>33</sup>P]c-di-GMP and UV cross-linking with [<sup>33</sup>P]c-di-GMP, as well as for diguanylate cyclase and phosphodiesterase reactions were published earlier (46, 47). Nucleotides were analyzed by PEI-Cellulose chromatography as described in (46, 47). The cellular concentration of c-di-GMP was determined by anionic exchange chromatography as described in (47).

**Adenylosuccinate synthetase enzyme assay.** The enzyme activity was determined at 25 °C by measuring the increase in absorbance at 280 nm which results from the conversion of IMP to adenylosuccinate ( $\epsilon_{280}=1.17 \times 10^4 \text{ M}^{-1} \text{ cm}^{-1}$ ) (39). The standard assay solution used to monitor enzyme activity contained 10 mM  $\text{MgCl}_2$ , 2.5 mM aspartate, 200  $\mu\text{M}$  IMP, and 150  $\mu\text{M}$  GTP in 20 mM Hepes, pH 7.7, in a total volume of 1 mL. Purified recombinant PurA enzyme was used at a final concentration of 0.04 mg/ml.

### 3.5.2 The substrate specificity of diguanylate cyclases

**Mechanism of c-di-GMP synthesis.** Like guanylate and adenylate cyclases (GC, AC) and DNA polymerases, diguanylate cyclases (DGCs) catalyze the nucleophilic attack of the 3' hydroxyl group on the  $\alpha$ -phosphate of a nucleoside triphosphate. Despite the lack of obvious sequence similarities, the PleD X-ray structure confirmed that DGCs possess a similar Palm-domain architecture like AC and GC (24, 47, 68) (Figure 8). Based on mutational analysis (24, 25, 46) and on structural comparisons between DGC, AC, GC and DNA polymerases (69), a model for DGC catalysis can be proposed.

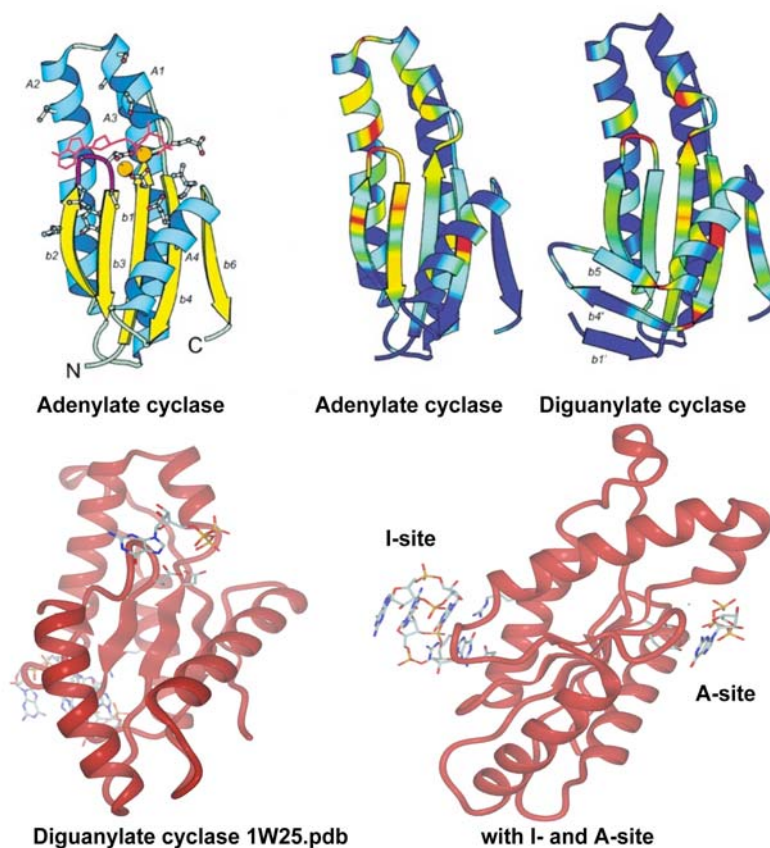


Figure 8: Comparison between adenylate cyclase and diguanylate cyclase

Upper lane: homology model between AC and DGC according to (68). Lower lane: X-ray structure of PleD (24) with modeled GTP bound to the active site (A-site) and a dimer of c-di-GMP bound at the allosteric inhibition site (I-site).



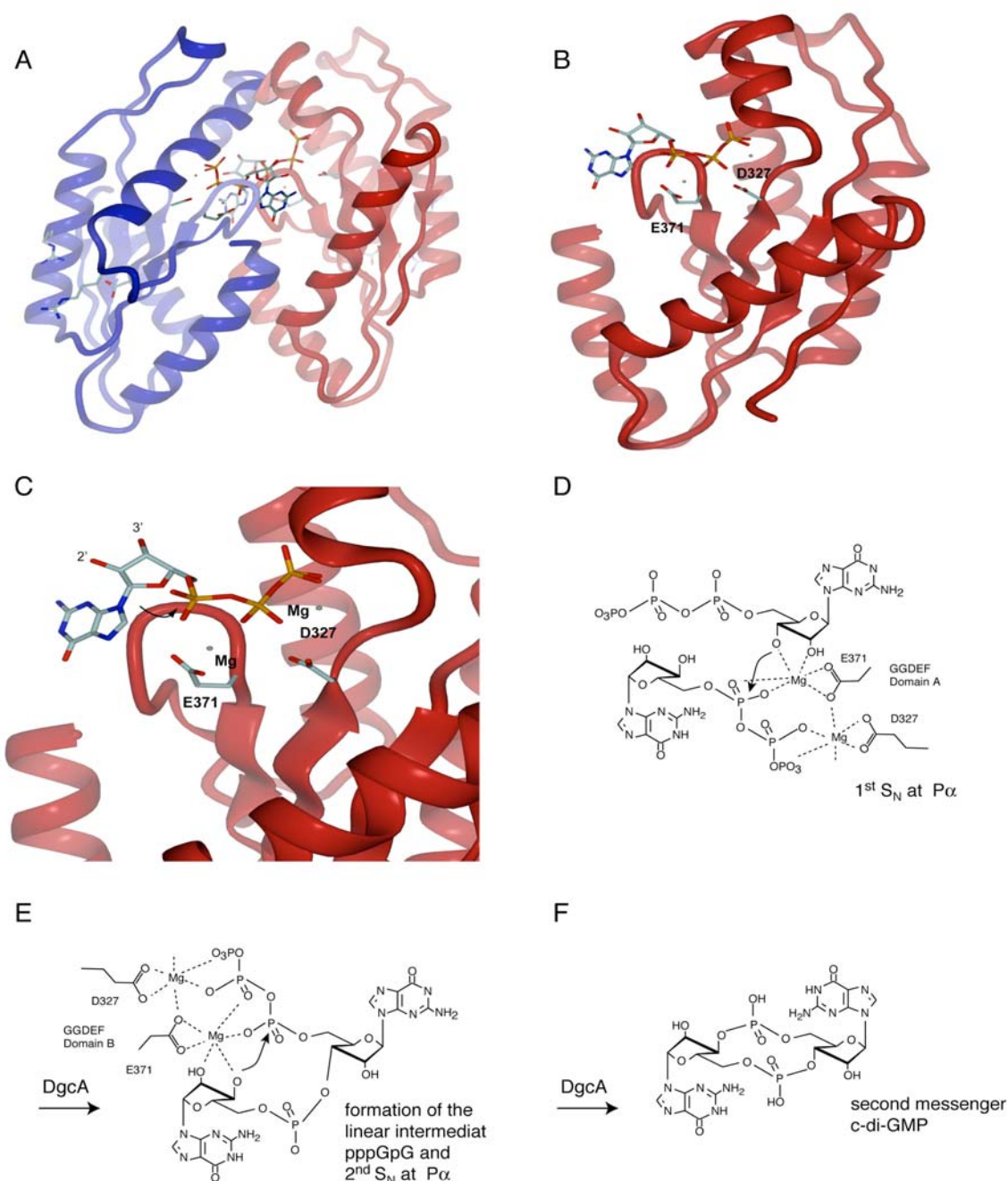


Figure 9: Model for the catalytic mechanism of c-di-GMP formation.

**A)** Model of the GGDEF domain arrangement of an enzymatically active DGC dimer with a GTP molecule bound at each active site. **B)** Monomeric GGDEF domain with bound GTP in the A-site. **C)** Zoom into the substrate-binding site of the GGDEF domain with one GTP molecule bound at the active site homology modeled according to the X-ray structure of the activated adenylate cyclase. Negatively charged amino acids, which are proposed to coordinate metal ions, are indicated. **D-F)** Schematic of the reaction mechanism for c-di-GMP synthesis through the linear intermediate pppGpG. We assume that the intermolecular nucleophilic attack of the 3'-hydroxyl group occurs under inversion of the stereochemistry at the  $\alpha$ -phosphate as it was shown for many DNA and RNA polymerases.

In contrast to the heterodimeric ACs and GCs, DGCs form homodimers, with a GTP molecule bound within the catalytic core of each DGC monomer (Figure 9A) (24). Two  $Mg^{2+}$  ions are coordinated by the highly conserved glutamic acid residue E371<sup>1</sup>, which is part of the GGDEF motif, and possibly by D327 on the opposing  $\beta$ -sheet (Figure 9B,C). Both residues are strictly required for DGC activity of WspR. The divalent  $Mg^{2+}$  carboxyl complex coordinates the triphosphate moiety of GTP and activates the 3' hydroxyl group for an intermolecular nucleophilic attack (1<sup>st</sup>  $S_N2$  at  $P\alpha$ ) of the  $\alpha$ -phosphate of the neighboring GTP substrate (Figure 9C,D). In the transition state the entering hydroxyl oxygen and the leaving pyrophosphate oxygen are in line (Figure 9D). In the transition state, the negative charge of the pentagonal-bipyramidal hybridized  $\alpha$ -phosphate is stabilized via the positively charged  $Mg^{2+}$  complex and presumably by a hydrogen bond between E370. After electron transfer and protonation pyrophosphate is released and the intermediate linear dinucleotide pppGpG is formed (Figure 9E). By a sequential similar reaction performed at the opposing active site of the second DGC subunit the 3' hydroxyl moiety of the linear intermediate pppGpG undergoes an intramolecular nucleophilic substitution of the 5'  $\alpha$ -phosphate (2<sup>nd</sup>  $S_N2$  at  $P\alpha$ ) resulting in the release of pyrophosphate and the formation of the second messenger c-di-GMP (Figure 9E,F).

By using a combination of structural, genetic, biochemical and modeling techniques it has been shown, that a distinct allosteric binding site for c-di-GMP (I-site) is responsible for non-competitive product inhibition of DGCs (47) (Figure 10). The I-site was mapped in both multi- and single domain DGC proteins and is fully contained within the GGDEF domain itself (47). *In vivo* selection experiments and kinetic analysis of the evolved I-site mutants led to the definition of an RXXD motif as the core c-di-GMP binding site. Based on these results and based on the observation that the I-site is conserved in a majority of known and potential DGC proteins, we have been proposed that product inhibition of DGCs is of fundamental importance for c-di-GMP signaling and cellular homeostasis. According to the proposed active site model, two alternative allosteric product inhibition mechanisms can be envisaged. In a first scenario, binding of c-di-GMP to the I-site would change the orientation of R366 and would thereby disturb the guanine-binding pocket resulting in an increased  $K_m$  for GTP. Alternatively, c-di-GMP binding to the I-site could rearrange the  $Mg^{2+}$  carboxyl complex and thus destabilize the active state.

---

<sup>1</sup> For the nomenclature of DGC key residues, we refer to the amino acid sequence of the diguanylate cyclase PleD from *caulobacter crescentus* for which an X-ray structure has been published (PDB entry 1w25.pdb).

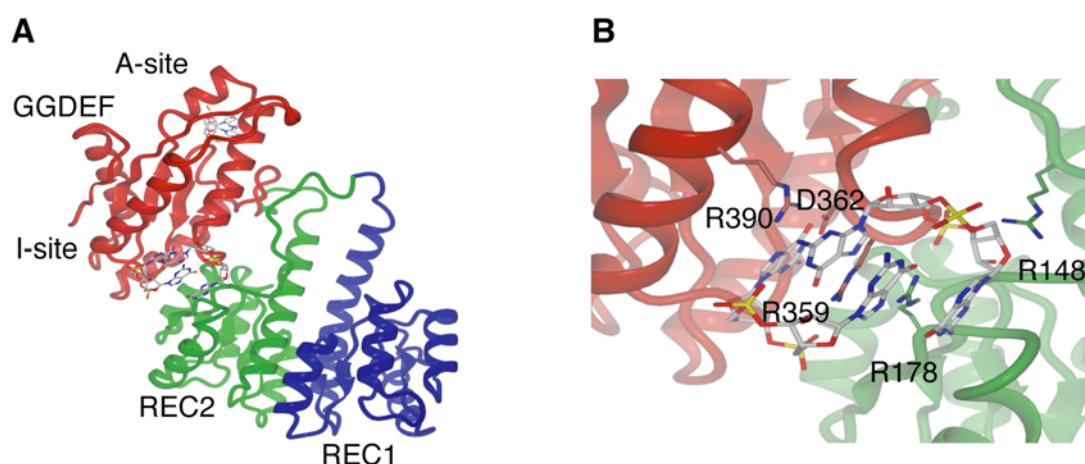


Figure 10: Crystal structure of the diguanylate cyclase PleD

**A)** 1W25.pdb according to (24, 47). **B)** Zoom into the allosteric product inhibition site of PleD.

### 3.5.3 Diguanylate cyclase Inhibition studies

Both I- and A-site of DGC represent potential interaction sites for targeted drug design. The I-site has been examined by extensive biochemical studies on different diguanylate cyclases. It has been proposed that the I-site binding pocket provides an entry point into unraveling the molecular mechanisms of ligand-protein interactions involved in c-di-GMP signaling. I-site mediated feedback inhibition makes DGCs a valuable target for drug design to develop new strategies against biofilm-related diseases (47). But DGC inhibition by I-site ligands might also harbor some disadvantages. Since c-di-GMP is binding to this allosteric inhibition site, potential I-site DGC inhibitors might exhibit similar chemical properties as the second messenger itself. Therefore unwanted cross reactivity with components of the c-di-GMP signaling pathways like activation of downstream c-di-GMP receptors or inactivation of c-di-GMP specific phosphodiesterases have to be considered.

DGC inhibition using A-site inhibitors represents an alternative, so far not investigated approach. Therefore, we decided to examine the substrate-binding site of DgcA, a single GGDEF domain model DGC with A and I-site from *Caulobacter crescentus*, and to define crucial residues (so called chemophores) required for substrate binding affinity as well as enzymatic catalysis. Previous diguanylate cyclase activity assays revealed that DgcA is specific for the substrate GTP and has very low affinities for ATP, UTP, CTP or the guanosine mono- and diphosphates (M. Christen, unpublished data), indicating that the base and the triphosphate moiety are crucial for ligand binding.

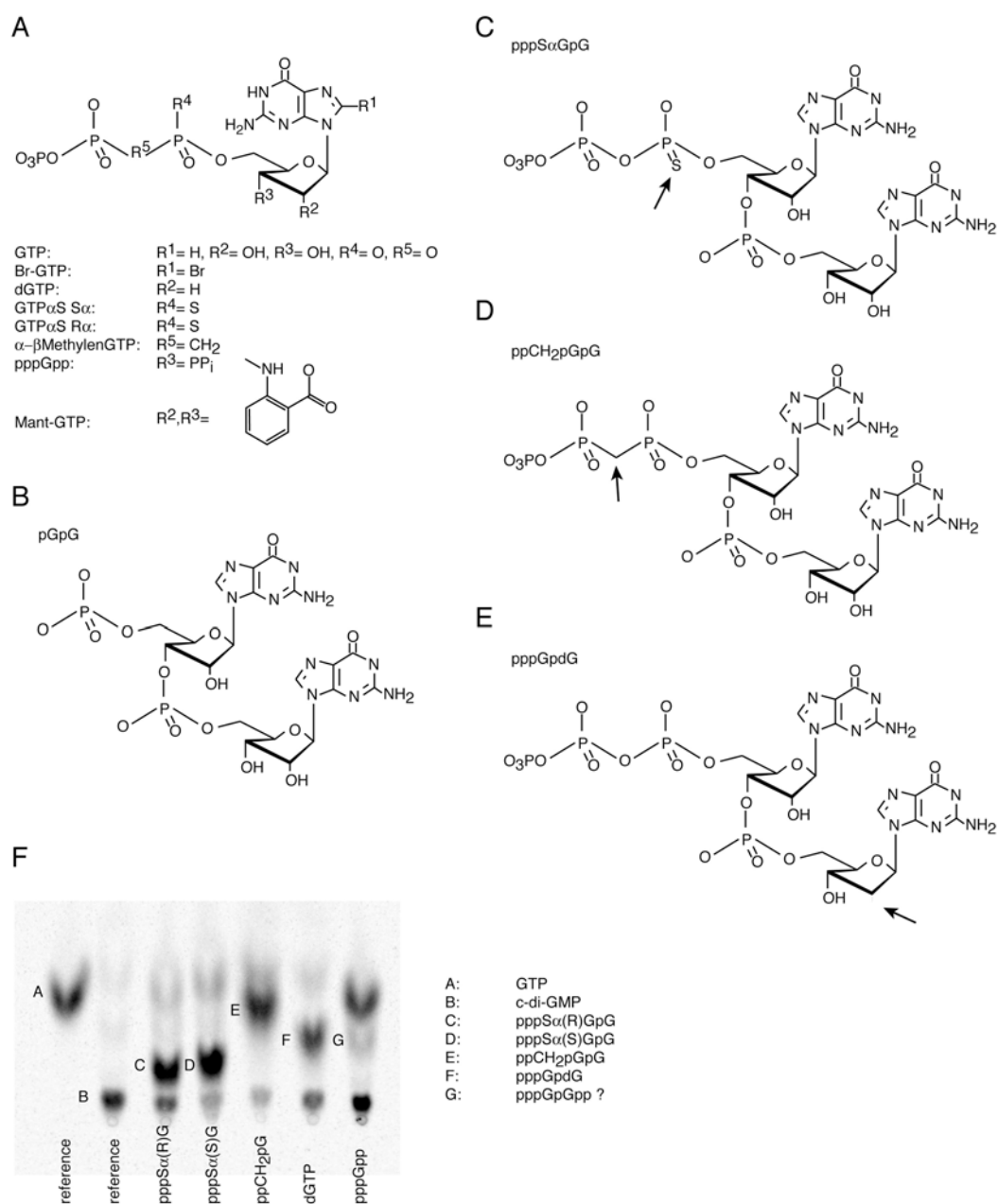


Figure 11: Analogs of substrate and reaction intermediates and their inhibition activity on DgcA.

**A)** Overview of the substrate modifications used to examine the substrate specificity of DgcA. **B)** Structure of the linear dinucleotide pGpG, the enzymatic product of c-di-GMP specific phosphodiesterases. **C-D)** Structures of reaction intermediate analogs. **F)** PEI-cellulose thin layer chromatogram of the reaction products obtained after incorporation of DgcA with a mixture of GTP and different substrate analogs as substrate.

**Table 1: Diguanylate cyclase inhibition constants of different guanosine nucleotide derivatives**

Inhibitor	$K_i^a$ in $\mu\text{M}$	$\Delta K_i^a$	$K_i^b$ in $\mu\text{M}$	$\Delta K_i^b$	Intermediate <sup>c</sup>
dGTP	231.2	$\pm 28.2$	19	$\pm 12$	pppGp(dG)
ppCH <sub>2</sub> pG	30	$\pm 16$	2.5	$\pm 5.6$	ppCH <sub>2</sub> pGpG
GTP <sub><math>\alpha</math></sub> S S <sub>a</sub>	108	$\pm 11$	3.7	$\pm 4.1$	pppS <sub><math>\alpha</math></sub> (S)GpG
GTP <sub><math>\alpha</math></sub> S R <sub>a</sub>	41.6	$\pm 23$	19	$\pm 1.4$	pppS <sub><math>\alpha</math></sub> (R)GpG
pGpG	124	$\pm 12.5$	123	$\pm 12.7$	no intermediate
pppGpp	52.9	$\pm 3.5$	40	$\pm 2.7$	no intermediate
Br-GTP	28.0	$\pm 3.3$	28.2	$\pm 3.5$	no intermediate
Mant-GTP	20.6	$\pm 2.5$	20.6	$\pm 2.2$	no intermediate
di-bu-cGMP	-	-	-	-	no intermediate

a: Inhibition constant with respect to GTP consumption

b: Inhibition constant with respect to c-di-GMP production

c: observed intermediate of the diguanylate cyclase reaction

A total of seven substrate analogs (Br-GTP, Mant-GTP, GTP $\alpha$ S,  $\alpha$ - $\beta$ CH<sub>2</sub>GTP, dGTP, pppGpp, Figure 11A) have been used to characterize chemophores required for ligand binding and substrate conversion. In addition analogs of the reaction intermediate pppGpG were produced (pGpG, Figure 11A A and B) enzymatically in a DGC-PDE tandem reaction and were purified as TEAC salt by PEI and RP18-HPLC (M. Christen, unpublished) and tested with respect to their inhibition potential.

All GTP derivatives were tested with respect to their ability to interfere with the DGC reaction. The assay was performed in the presence of 100  $\mu$ M inhibitor, 0.5  $\mu$ M DgcA and 25  $\mu$ M <sup>33</sup>P labeled GTP. Reaction samples were taken at regular time intervals and reactions were stopped by adding equal volumes of 0.5 M EDTA. The nucleotide composition was analyzed by PEI cellulose thin layer chromatography. After exposure on a phosphoimager screen and scanning, the intensity of the nucleotide species was quantified with the software ImageJ1.3. GTP consumption, intermediate formation and c-di-GMP production was compared for each individual inhibitor (Figure 11). The respective K<sub>i</sub> was determined with the software ProFit 4.6 by calculating the initial velocity V<sub>0</sub> of each reaction and determine the relative decrease in GTP consumption and c-di-GMP formation, respectively. For a more detailed description see Materials and Methods in (47).

The measured inhibitors could be divided in two classes: compounds that form a reaction intermediate with GTP and compounds that don't accumulate an intermediate inhibitor (Table 1A). GTP $\alpha$ S,  $\alpha$ - $\beta$ CH<sub>2</sub>GTP and dGTP were enzymatically condensed with a substrate GTP and formed non reactive linear heteromeric dinucleotide intermediates (Figure 11C-F). Adding these compounds to the reaction resulted in inhibition constants between 2.5 and 19 $\mu$ M for c-di-GMP production (Table 1). Due to the fact that the heterodimeric intermediate analogs were synthesized *in situ* from the corresponding non hydrolysable GTP derivatives, the K<sub>i</sub> values only represent a tendency of the DGC inhibition. To determine the exact inhibition constant the formed heterodimeric intermediates have to be purified by HPLC and have to be added to a DGC assay as such. Additional experiments in the presence of increasing substrate concentration have to be done to distinguish, whether the inhibition is competitive or uncompetitive.

Mant-GTP, Br-GTP, pppGpp and pGpG did not form an intermediate with a substrate GTP and blocked the GTP consumption with K<sub>i</sub> values of 20 to 124  $\mu$ M. Based on these results we suggest a different inhibition strategies for Mant-GTP, Br-GTP, pppGpp and pGpG: these GTP analogs occupy the A-site of the diguanylate cyclase, block the binding of GTP and in this way inhibit c-di-GMP formation with inhibition constants from 20.6 $\mu$ M to 123 $\mu$ M.



### 3.5.4 The enzymatic synthesis of c-di-GMP

#### Introduction

Ross et al reported the first chemical synthesis of the second messenger c-di-GMP and its derivatives. In their study, a series of 13 analogs of c-di-GMP was synthesized, employing a modified hydroxybenzotriazol phosphotriester approach (4, 48, 70). Hayakawa and coworkers (71) published a synthesis, which includes two strategies different from those reported by Ross et al (48). They use the phosphoramidite method for the preparation of a linear guanylyl(3'-->5')guanylic acid intermediate and allyl protection for guanine bases and internucleotide linkages. Although these distinctive strategies resulted in a 51 % yield of c-di-GMP, the chemical synthesis of the second messenger is, due to the complex synthesis of the two required building blocks, of no significant commercial value. Moreover, biochemically useful modifications like the generation of  $^{33}\text{P}$  and  $^{32}\text{P}$  radiolabeled c-di-GMP, or  $^{13}\text{C}$  and  $^{15}\text{N}$  labeled c-di-GMP for NMR studies are not easily accessible by a conventional chemical synthesis. For these applications, the enzymatic production of c-di-GMP using an appropriate diguanylate cyclase and GTP as the reaction substrate represents a convincing strategy. However, allosteric product inhibition of diguanylate cyclases (47) and the fact, that only the activated dimeric DGC performs the cyclisation reaction, have to be considered.



## Results and Discussion

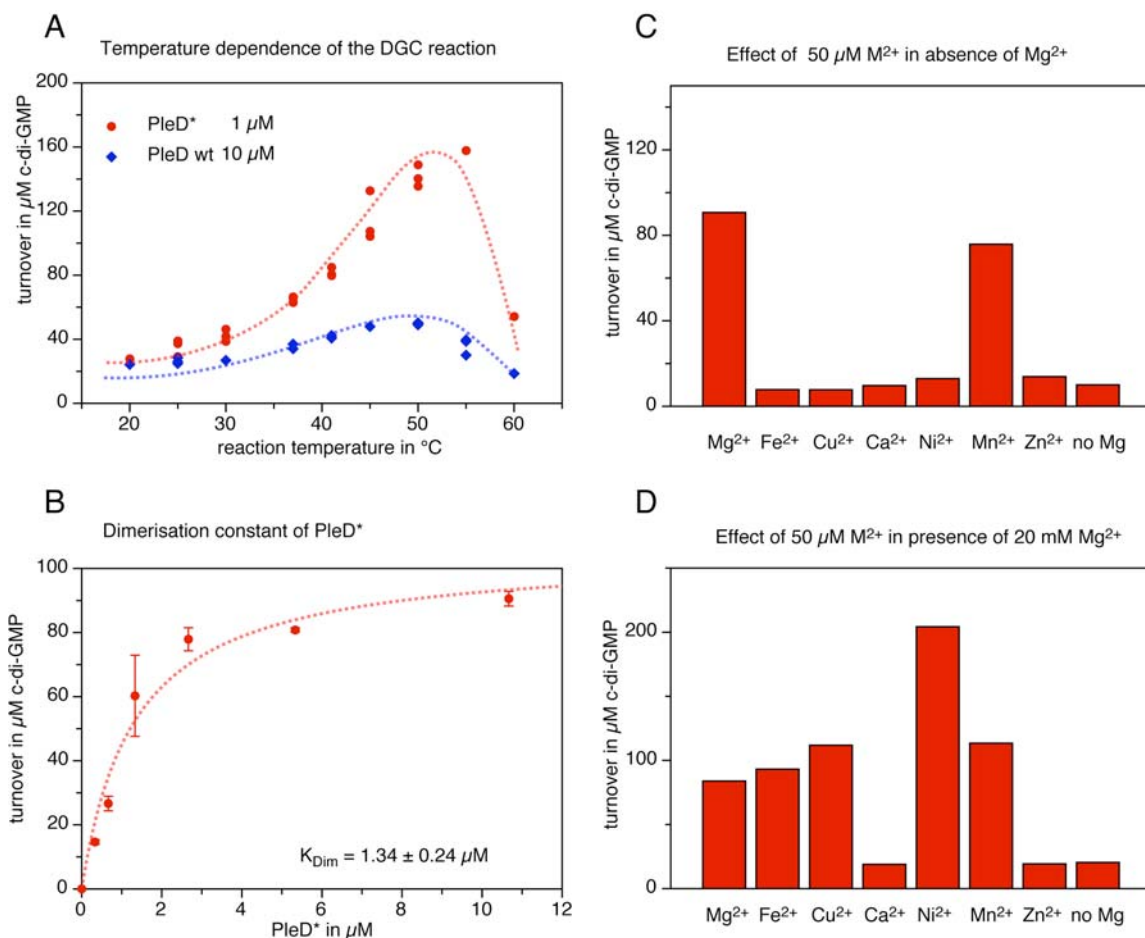


Figure 12 Optimization of the reaction conditions for various DGCs

**A)** Comparison of the temperature dependence of the diguanylate cyclase reaction of PleDwt (10  $\mu\text{M}$ ) and PleD\* (1  $\mu\text{M}$ ). Substrate concentration was 0.5 mM and the reaction time 1h. **B)** Dimerisation constant of PleD\*. The Substrate concentration was 0.5 mM GTP, the reaction time 1h and the reaction temperature 30 $^{\circ}\text{C}$ . **C, D)** Effect of 50  $\mu\text{M}$  of various  $\text{M}^{2+}$  metals on the diguanylate cyclase activity in absence of 20 mM  $\text{Mg}^{2+}$  (C) and in presence of 20 mM  $\text{Mg}^{2+}$  (D). Reaction time was 1h, 30 $^{\circ}\text{C}$ , protein concentration 5  $\mu\text{M}$  PleD\*.

**Optimization of the diguanylate cyclase reaction.** The second messenger c-di-GMP is formed by the condensation of two GTP molecules (4, 24, 72) upon the action of the dimeric diguanylate cyclase enzymes. A starting point for the optimization of the enzymatic synthesis was given by the diguanylate cyclase reaction condition reported by Ross et al. (48). His tag fusions of the *C. crescentus* diguanylate cyclases PleD and the constitutive active allele PleD\* were used to determine the optimal reaction conditions (24, 25, 47).

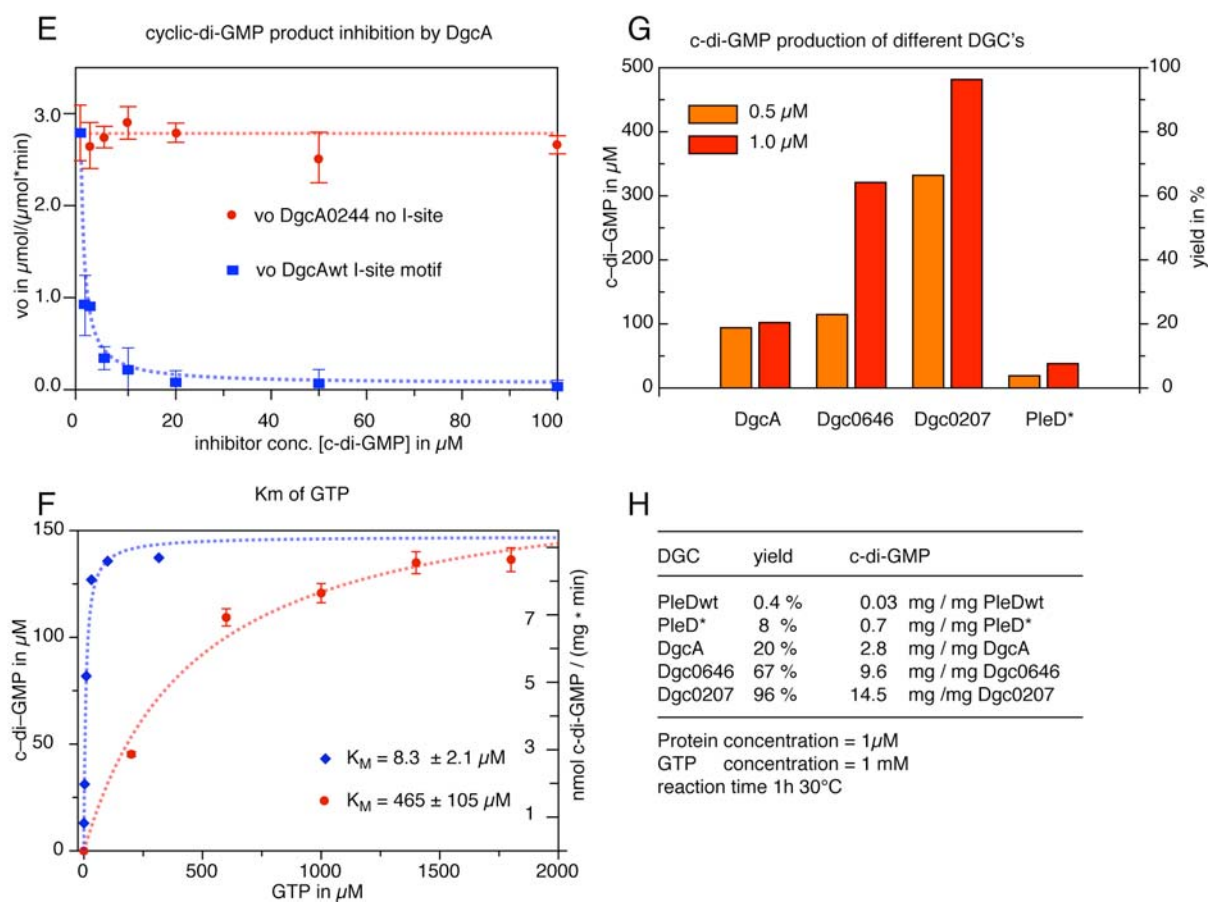


Figure 13 Effect of c-di-GMP binding on the enzymatic DGC activity

**E)** c-di-GMP product inhibition of DgcA. Initial velocities of the wild type diguanylate cyclase DgcA (blue graph) and the non-feedback inhibited I-site mutant DgcA0244 (red graph) in presence of increasing concentrations of c-di-GMP. **F)** Km for GTP of PleD\* in absence of c-di-GMP (blue line) and increasing Km for GTP upon addition of 10  $\mu$ M c-di-GMP (red graph). Kinetics were measured at 30°C in presence of 5  $\mu$ M PleD\*. Initial velocities were measured for the non-inhibited reaction in nmol c-di-GMP / (mg protein \* min) and for the inhibited reaction, due to the lower activity, in  $\mu$ M c-di-GMP /  $\mu$ M Protein\*h. **G)** comparison of the reaction yield of various diguanylate cyclases mutants. Reaction time was 1h, 30°C, protein concentration 5  $\mu$ M PleD\*. **H)** Overview of reaction yield and c-di-GMP production per mg protein.

In a first approach, the constitutive active allele PleD\* has been investigated in order to optimize the reaction conditions for semi-preparative synthesis of c-di-GMP. The temperature dependence of the PleD DGC reaction revealed an optimal enzymatic turnover for both wild type and PleD\* at 47 °C (Figure 12A). However, at this temperature, the half live of the enzymatic activity dramatically decreases to 10 min for PleDwt and 24 min for PleD\* compared to 36 min for PleDwt and 140 min for PleD\* at 37°C. For reasons of protein stability, a reaction temperature of 30 °C is recommended. In addition, the experimentally determined dimerization constant of 1.34  $\mu\text{M}$  for PleD\*, demands for a minimal enzyme concentration of 1-2  $\mu\text{M}$  (Figure 12B). The diguanylate cyclase reaction requires  $\text{Mg}^{2+}$  or  $\text{Mn}^{2+}$  as cofactor and is inhibited by  $\text{Ca}^{2+}$  and  $\text{Zn}^{2+}$ , the addition of 50  $\mu\text{M}$   $\text{Ni}^{2+}$  seems to stimulate the DGC activity, presumably upon dimerisation of the C-terminal His-tag fusions (Figure 12C,D).

PleD, like other diguanylate cyclases, is subjected to allosteric product inhibition with an experimental  $K_i$  of 1  $\mu\text{M}$  (47) (Figure 12E). Allosteric product inhibition is the reason, why enzymatic c-di-GMP synthesis using PleD\*, does not exceed a maximal yield of more than 20%. The observed product inhibition operates mainly by increasing the  $K_m$  for GTP (from 8.3  $\mu\text{M}$  in absence of c-di-GMP to 465  $\mu\text{M}$  in presence of 10  $\mu\text{M}$  c-di-GMP), (Figure 12F). To overcome this product inhibition, a genetic screen has been performed with the constitutive active diguanylate cyclase DgcA from *C. crescentus* (CC3285), a single GGDEF domain protein with no obvious signal input domain (47).

Out of this screen, a set of mutants have been isolated, which had lost product inhibition: Dgc0207 and Dgc0646 in which the RESD I-site motive 5 AA upstream of the highly conserved GGDEF active site motive is replaced by GMGG and GRDC, respectively, exhibited massive increased DGC activity: 1  $\mu\text{M}$  Dgr0207 synthesizes in 1 h at 30°C in presence of 1 mM GTP 480  $\mu\text{M}$  c-di-GMP with an overall yield of 96%. Per mg purified Dgr0207, 14.5 mg second messenger can be synthesized compared to 0.7 mg for PleD\* (Table G). In the following part a detailed description of the enzymatic production of c-di-GMP by Dgc0207 is given:

**Synthesis and Purification of [<sup>33</sup>P]c-di-GMP.** [<sup>33</sup>P] labeled c-di-GMP was produced enzymatically using  $\alpha$ -labeled [<sup>33</sup>P] GTP (3000 Ci/mmol Amersham Bioscience) and purified hexahistidine-tagged Dgc0207 a non feedback inhibited, constitutive active form of the DgrA diguanylate cyclase (25). To a mixture of 87.5  $\mu\text{l}$  reaction buffer (250 mM NaCl, 25 mM Tris-HCl, pH 8.0, 10 mM  $\text{MgCl}_2$ , 5 mM  $\beta$ -mercaptoethanol and 1  $\mu\text{M}$  Dgc0207-H6), 12.5  $\mu\text{l}$   $\alpha$ -labeled [<sup>33</sup>P] GTP (125  $\mu\text{Ci}$ , 41.66 pmol, 3000 Ci/mmol) were added. After 5 min at 30°C, the reaction was stopped by adding an

equal volume of 0.5 M EDTA, pH 8.0. The protein was precipitated by heating for 5 min at 95°C followed by centrifugation for 2 min at 10,000xg. The supernatant was loaded on a batch RP-18 column, salt was removed by washing 5 times with 200  $\mu$ l 25 mM TEAC buffer (triethylenammonium carbonat) pH 7.0 containing 1% (vol/vol) MeOH. c-di-GMP was eluted with two times 200  $\mu$ l TEAC containing 5% (vol/vol) MeOH. The buffer was subsequently removed in the speed-vac and the purity of the compound was tested by separation on PEI-cellulose plates (1:1.5 vol/vol saturated  $\text{NH}_4\text{SO}_4$  and 1.5 M  $\text{KH}_2\text{PO}_4$ , pH 3.6).

**Synthesis and Purification of  $^{13}\text{C}$ ,  $^{15}\text{N}$  labeled c-di-GMP for NMR studies.**  $^{13}\text{C}$ ,  $^{15}\text{N}$  labeled c-di-GMP was produced enzymatically using  $^{13}\text{C}$ ,  $^{15}\text{N}$  labeled GTP (>98%  $^{13}\text{C}$ ,  $^{15}\text{N}$ , >95% GTP, Division of spectra Gases, Columbia, USA) and purified hexahistidine-tagged Dgc0207 a non feedback inhibited, constitutive active form of the diguanylate cyclase DgrA (47). To a mixture of 2 ml reaction buffer (100 mM triethylammonium carbonate pH 7.0, 20 mM  $\text{MgCl}_2$ , and 1 mM  $^{13}\text{C}$ ,  $^{15}\text{N}$  labeled GTP). Dgr0207 was added to a final concentration of 1 mM. After 1 h at 30°C, the enzymatic reaction was stopped and protein was precipitated by heating for 5 min at 95°C followed by centrifugation for 2 min at 10,000xg. The supernatant was filtered through a 0.45  $\mu\text{M}$  pore size syringe filter (Milipore) and lyophilized. The resulting powder was resuspended in 1 ml  $\text{H}_2\text{O}$  containing 6 mM formic acid, loaded on a VP 250/10 NUCLEOSIL 4000-7 PEI column (Macherey-Nagel) and separated with the following methode: Buffer A; 6 mM  $\text{KH}_2\text{PO}_4$  pH 3.6, Buffer B; 1 M  $\text{Na}_2\text{SO}_4$ , 0.5M  $\text{KH}_2\text{PO}_4$  pH 5.5, program; wavelength 254 nm, flow 1 ml/min, 0 min 0% B, 2.5 min 17% B, 3.5 min 33% B, 13 min 100 % B, 31 min 0% B, 50 min 0% B end method. The time of migration for the solvent was 16 min and c-di-GMP was eluted after 24.7 min. Fraction 24-26 were collected and loaded on a 250/10 NUCLEOSIL 100-7 C18 column (Macherey-Nagel). Buffer A; 250 mM triethylammonium carbonate pH7.0, Buffer B; MeOH, program; wavelength 254 nm, flow 1 ml/min, 0 min 0% B, 2.5 min 1% B, 5 min 5% B, 10 min 30 % B, 20 min 0% B, 40 min 0% B end method. Fractions containing the c-di-GMP TEAC salt were collected and the triethylammonium carbonat buffer was removed by lyophilizing over night. The remaining white powder was collected, resolved in  $\text{H}_2\text{O}$  and c-di-GMP concentration was determined by measuring UV absorbance at 254 nm.

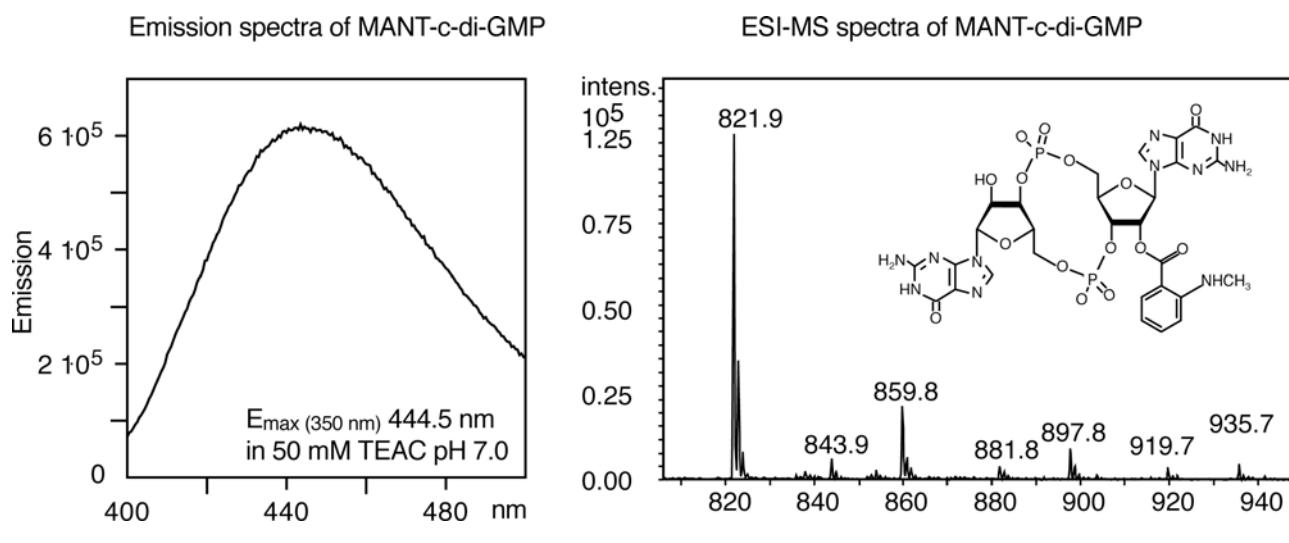


Figure 14 Synthesis of MANT c-di-GMP

left panel fluorescence emission spectra of MANT-c-di-GMP, right panel ESI-MS spectra of MANT-c-di-GMP

**Synthesis of mono-2'-MANT c-di-GMP - a fluorescent c-di-GMP derivative.** In a PCR tube, 2.18 mg of enzymatically synthesized c-di-GMP-TEAC salt solved in 100  $\mu$ l H<sub>2</sub>O (2.34 nmol 1 eq.) were added to 4.5 mg MANT anhydride (3.51 nmol, 15 eq.). The pH was adjusted to 9.6 by adding 15  $\mu$ l 1M NaOH and the reaction was performed at 38°C for 4h in a PCR heating block. The reaction product was separated on a 12/3 NUCLEOSIL 100-7 C18 RP18 column; flow 0.3 ml/min, wavelengths 254 and 350 nm, 250 mM triethylammonium carbonate, 7.5 % MeOH 0-30 min, followed by a linear gradient to 100% MeOH within 20 min,  $t_R$  c-di-GMP = 10 min,  $t_R$  MANT-c-di-GMP = 14 min  $t_R$  MANT-anhydride = 19 min. TLC analysis on RP18 TLC plates; Solvent 20% MeOH, 250 mM TEAC in H<sub>2</sub>O pH 7.0,  $R_f$  MANT c-di-GMP 0.15 blue fluorescent compound. MS analysis M/Z 821.9 H<sup>+</sup> adduct of MANT-c-di-GMP, 859.8 Na<sup>+</sup> adduct and 898 K<sup>+</sup> adduct. Fluorescence spectrum; absorption at 260, 280 and 350 nm Emission (350nm) at 444.5 nm.

### 3.5.5 Analysis of in vivo c-di-GMP levels

#### Introduction

It has been suggested that pole development in *C. crescentus* is regulated by a novel bacterial signal transduction mechanism, which relies on the controlled synthesis and breakdown of the second messenger cyclic di-guanosine monophosphate (c-di-GMP)(23, 25). These and other studies have proposed that c-di-GMP is a general modulator of the transition from a motile, single cell state to a sessile, multi cellular form of growth, which is often associated with biofilm formation and persistence in pathogenic bacteria. Whereas biochemical *in vitro* studies with purified DGCs and PDEs are suitable for investigating catalytic, structural and regulatory aspects of the synthesis and degradation of c-di-GMP, an appropriate *in vivo* assay for investigate intracellular c-di-GMP levels was still missing.

Such an *in vivo* assay would allow to correlate altered levels of the second messenger c-di-GMP with a particular observed phenotype, such as congo red straining, motility, attachment or biofilm formation and allows to exclude that changes in other nucleotide pools, e.g. a decrease in GTP concentration or an increased of the pGpG level, are responsible for these cellular effects. In addition, investigating c-di-GMP pools in different bacterial species, different phenotypes, under various growth conditions, during the cell cycle or biofilm formation, or in mutants lacking specific DGC and PDEs enzymes will become accessible with an *in vivo* assay.

**Nucleotide extraction and analysis.** In order to address these questions, the intracellular concentrations of nucleotides, including c-di-GMP level, were assayed by high-performance liquid chromatography on a polyethylenimine column after extraction with 0.5 M formic acid. To normalize the amounts of nucleotides found in different cultures, the amounts were expressed relative to the dry cell weight measured at the time of harvesting, i.e., picomoles per milligram (dry weight) of cells. The following procedure was applied to cell cultures of *C. crescentus*, *E. coli*, *P. aeruginosa*, *Salmonella Thyphimurium*, *Yersinia enterocolitica*, *Streptomyces coelicolor*, and *Synechocystis PCC6803*. The HPLC method is based on nucleotide separation on a PEI column, using a linear gradient of high-ionic-strength buffer (0.5 M  $\text{KH}_2\text{PO}_4$  plus 0.5 M  $\text{Na}_2\text{SO}_4$ ). In order to enhance the signal of the second messenger c-di-GMP and to increase the separation between ADP ( $t_R$  7.21

min) and c-di-GMP ( $t_R$  7.82 min), the UV detector wavelength was changed from 254 nm to 280 nm.

**Procedure.** 2.0 ml of *C. crescentus* cell cultures (OD<sub>600</sub> 0.4) were harvested by centrifugation for 30 s at 16'000 rpm and the supernatant was discarded. The cell pellet was dissolved in 200  $\mu$ l 0.5 M formic acid and nucleotides were extracted for 10 min at 4°C. Insoluble cellular components were then pelleted and the supernatant was directly analyzed by chromatography. Nucleotides were extracted and separated according to (73) on a 125/4 Nucleosil 4000-1 PEI column (Macherey-Nagel) using a SMART-System (Pharmacia). The nucleotide peak corresponding to c-di-GMP was verified by co-elution with chemically synthesized c-di-GMP standard and by incubating the nucleotide extract for 20 min with the c-di-GMP specific phosphodiesterase PdeA (CC3396) from *C. crescentus* (46) (data not shown).

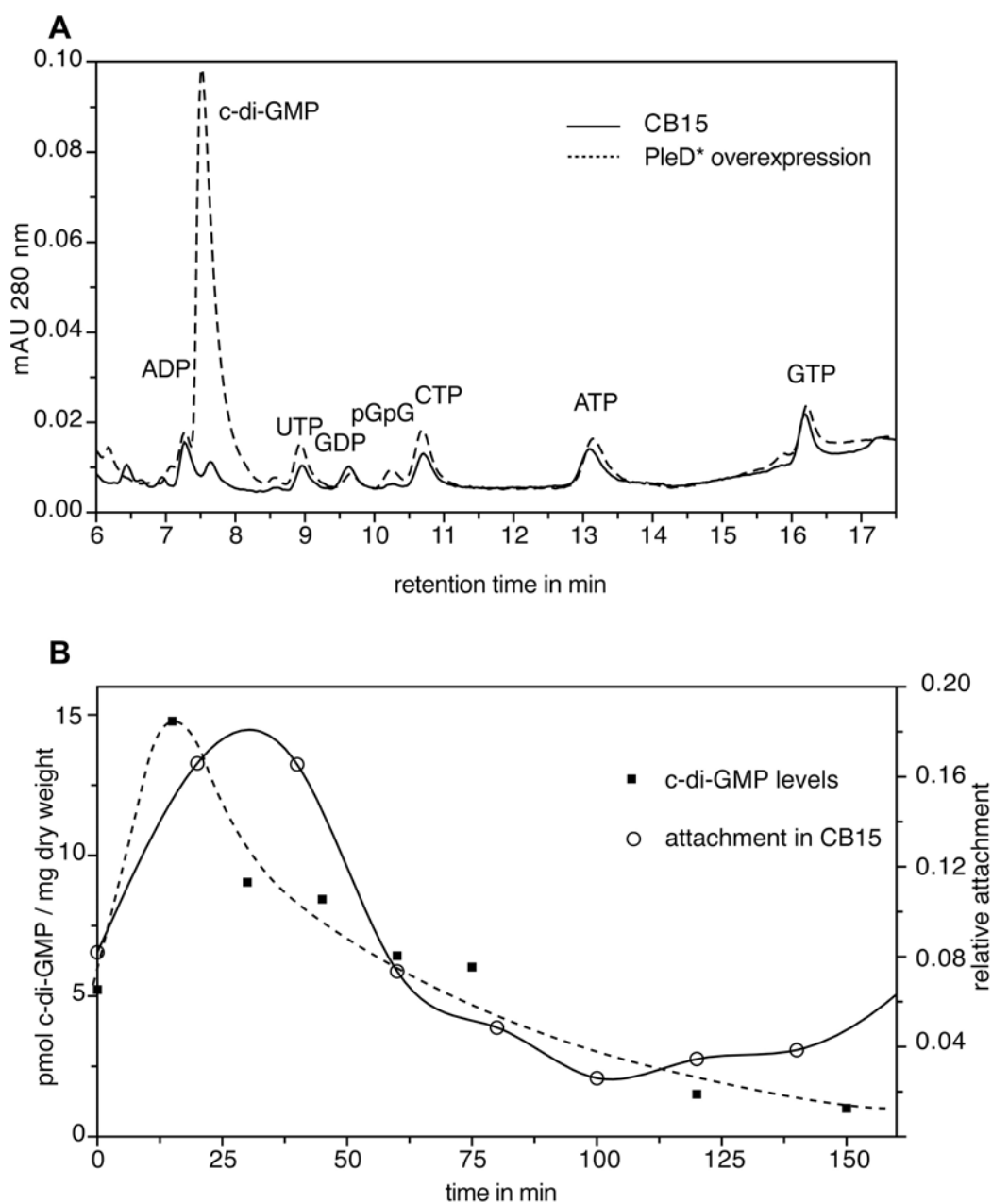


Figure 15 Intracellular c-di-GMP levels in *C. crescentus*.

**A)** HPLC chromatogramm of total cell nucleotide extraction in wild type and PleD\* overexpression strain indicating a massif burst of c-di-GMP but unaffected GTP and ATP pools. **B)** Fluctuation of the c-di-GMP level over *C. crescentus* cellcycle as measured by nucleotide extraction of synchronized cells. The data concerning the relative attachment over cell cycle was kindly provided by A. Levi.



**Results and discussion.** The analysis of the nucleotide pool of different mutants in *C. crescentus*, *E. coli* and *S. Typhimurium* for the first time allowed to demonstrate that the observed phenotype caused by overexpression of diguanylate cyclase enzymes correlates with a massive increased intracellular level of the second messenger c-di-GMP and is not correlated to a change in other nucleotides, such as a drop in GTP pool or accumulation of pGpG. Overexpression of the constitutive active diguanylate cyclase PleD\* in *C. crescentus* only affected, the level of c-di-GMP but not the level of GTP (Figure 15A).

In *C. crescentus*, obligate asymmetric cell division at each replicative cycle generates two genetically identical but morphologically different daughter cells, which undergo different developmental programs: The progeny sessile stalked cell equipped with an adhesive stalk initiates a new replication cycle immediately after cell division has completed whereas the motile, polar flagellated swarmer cell undergoes an obligate, planktonic life phase, during which cell division programs and DNA replication are inhibited (19, 20). In order to become replication competent and progress cell cycle, the swarmer cell has to differentiate and undergoes subsequent remodeling of its polar organelles, which involves ejection of the flagellum, retraction of the pili, and generation of a stalk and adhesive holdfast at the pole previously occupied by the flagellum. Precise timing of assembly and loss of polar organelles is critical for optimal surface colonization. Both acquisition of flagellar motility in the predivisional cell and its replacement by an adhesive holdfast later in development are dependent on the polar localized diguanylate cyclase PleD (21-26). The *in vivo* measurement of the c-di-GMP level during the *C. crescentus* cell cycle revealed that a peak of c-di-GMP correlates with PleD dependent pole morphogenesis (Figure 15B). These findings link the second messenger c-di-GMP to the developmental process of the swarmer-to-stalk cell transition and suggest a general role for the second messenger c-di-GMP in coordinating developmental processes in bacteria.

## 4 Discussion

The pioneering work of the late Moshe Benziman and his collaborators has not only identified cyclic diguanosine monophosphate as a signaling molecule involved in bacterial metabolism but has also led to the recognition of proteins containing GGDEF and EAL domains as being involved in the synthesis and breakdown of c-di-GMP (reviewed in (74)). Building on this foundation, an increasing number of genetic studies have in recent years highlighted a global role for c-di-GMP as signaling molecule in bacteria. Most of these studies have reported mutant and/or overexpression phenotypes of proteins containing GGDEF or EAL domains (16, 23, 30, 31, 75-83). The common finding appearing from these studies is that changes associated with an increase of the cellular concentration of c-di-GMP negatively modulate cell motility and induce biofilm formation, while modifications that led to a presumable decrease of c-di-GMP in the cell had the opposite effect. However, limited information was available on the downstream activities and possible targets of c-di-GMP and on the specific biochemical properties of enzymes involved in c-di-GMP turnover. The present study contributes to the emerging understanding of the c-di-GMP regulatory network in bacteria and provides new insights on the specific biochemical and regulatory properties of enzymes involved in synthesis and hydrolysis of c-di-GMP. Furthermore, by using biochemical, genetic and molecular biological approaches, we identified novel components of the c-di-GMP signaling circuitry, report the biochemical purification of c-di-GMP receptor proteins from *C. crescentus* crude extract and describe their physiological role in c-di-GMP dependent repression of cell motility.

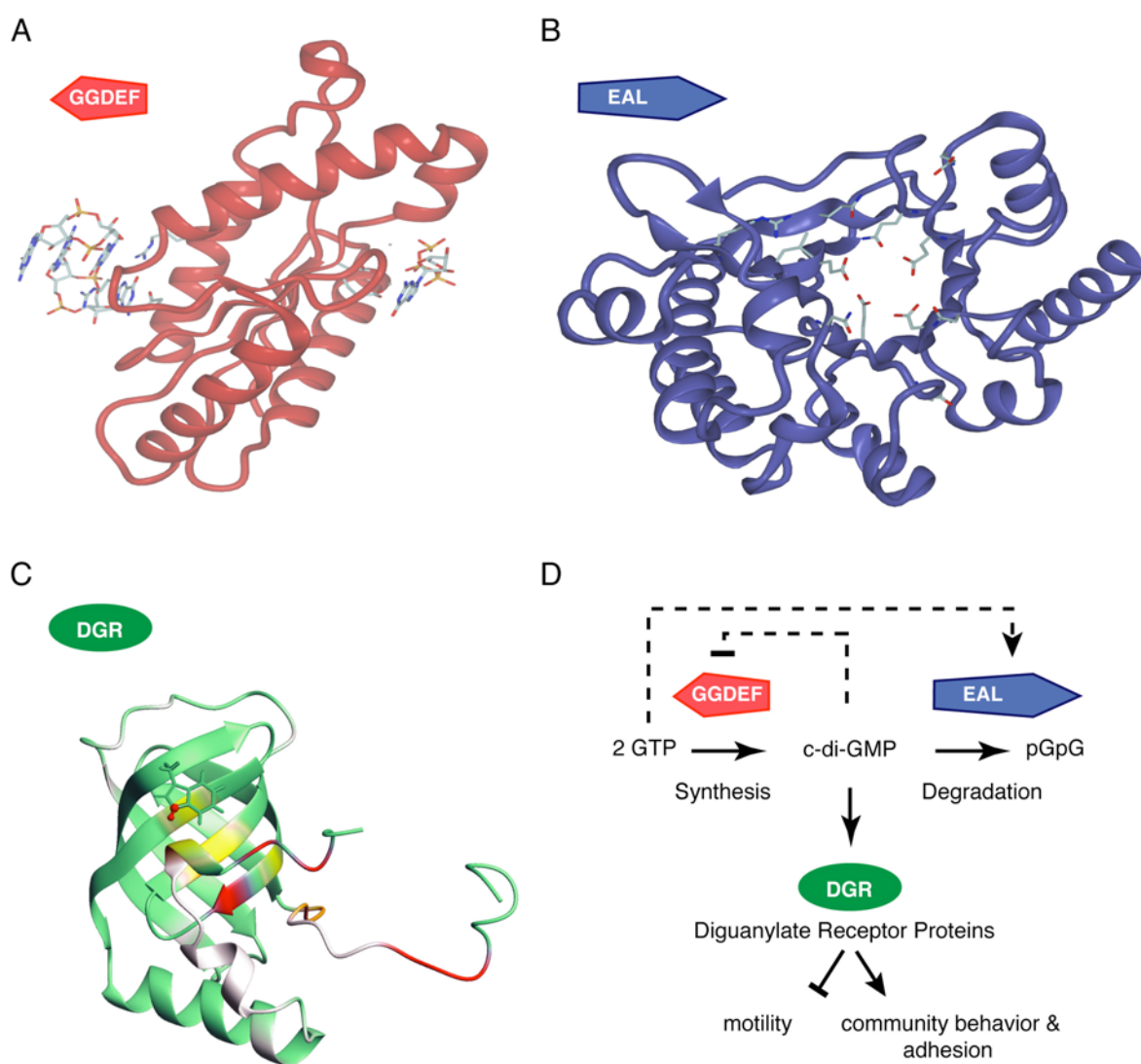


Figure 16 Components of the c-di-GMP signaling network

**A)** Homology model of the DgcA GGDEF domain according to 1W25.pdb harboring, in its dimerized state, diguanylate cyclase activity. The substrate GTP is bound to the active site (A-site) located 5 AA upstream of the identified allosteric product inhibition site (I-site) (47). **B)** Homology model of the EAL domain from PdeA (CC3396) harboring c-di-GMP specific phosphodiesterase activity (46) (based on X-ray structure of the *B. subtilis* EAL protein Yku1 1bas.pdb) The EAL domain exhibits an eight-stranded  $\alpha/\beta$  barrel (TIM barrel) fold. Highly conserved charged key residues required for the Mg dependent hydrolysis of c-di-GMP are located in the center of the TIM barrel structure. **C)** Domain structure of the isolated diguanylate receptor protein. The c-di-GMP binding site, which has been mapped by genetic, biochemical and NMR studies, is located on the surface of a split-barrel. Colors indicate the Combined amide  $^1\text{H}$  and  $^{15}\text{N}$  shift differences ( $\Delta\delta$ ) upon addition of c-di-GMP to PA4608 from *P. aeruginosa*. **D)** Schematic of c-di-GMP signaling involving synthesis, hydrolysis and effector mechanism of c-di-GMP. The GGDEF domain harboring the diguanylate cyclase activity (red), the EAL domain responsible for degradation of the second messenger into the linear dinucleotide pGpG (blue) and the newly identified diguanylate receptor DGR (green) are indicated. Dashed lines symbolize product inhibition of diguanylate cyclases by c-di-GMP (47) and allosteric activation of c-di-GMP specific Phosphodiesterases by GTP (46).

**Feedback inhibition is a general control mechanism of diguanylate cyclases**

The data presented here propose a general mechanism to regulate the activity of diguanylate cyclases (DGCs), key enzymes of c-di-GMP based signal transduction in bacteria. High affinity binding of c-di-GMP to a site distant from the catalytic pocket (I-site) efficiently blocks enzymatic activity in a non-competitive manner with an apparent  $K_i$  of  $1\mu\text{M}$ . Mutational analysis of multi- and single-domain DGC proteins has provided convincing evidence for the role of several charged amino acids in c-di-GMP binding and allosteric regulation. An *in vivo* selection experiment using a random tetrapeptide library, and designed to re-engineer the I-site has led to the definition of a highly conserved RXXD core motif of the c-di-GMP binding pocket. The RXXD motif forms a turn at the end of a short five amino acid  $\beta$ -sheet that directly connects the I-site with the conserved catalytic A-site motif, GG[D/E]EF (Figure 16A). This raised the question how I-site ligand binding modulates DGC enzyme activity. In the multidomain protein PleD, c-di-GMP bound to the I-site physically connects the GGDEF domain with the REC1-REC2 dimerization stem. It was speculated that product inhibition occurs by domain immobilization, which would prevent the encounter of the two DGC substrate-binding sites (24). Several observations argue in favor of a more direct communication between I- and A-sites. First, with a large variety of domains found to be associated with GGDEF domains it seems unlikely that functional I-sites are generally formed by the interface of a GGDEF with its neighboring domain (84). In agreement with this, residues of the PleD REC2 domain are not required for c-di-GMP binding and feedback inhibition. Second, the single domain DGC protein, DgcA, shows I-site dependent allosteric control with a  $K_i$  of  $1\mu\text{M}$ . Third, atomistic simulations of ligated and unligated PleD predicted a marked drop in flexibility of  $\text{C}\alpha$ -atoms both in the I- and A-site upon ligand binding. Simultaneous with motion quenching,  $\beta 2$  and its flanking I- and A-loops undergo a balance-like movement that repositions A-site residues in the catalytic active site (Figure 16A). This is consistent with the idea that structural changes within the GGDEF domain upon binding of c-di-GMP at the I-site lead to repositioning of active site residues and possibly altered kinetic parameters. Thus, we propose that c-di-GMP binding and allosteric control represents an intrinsic regulatory property of DGCs that contain an RXXD motif. Based on the enzymatic mechanism of the diguanylate cyclase reaction, two alternative inhibition mechanisms can be envisaged. In a first scenario, binding of c-di-GMP to the I-site would change the orientation of R366 and would thereby disturb the guanine binding site, resulting in an increased  $K_m$  for GTP. In addition, inhibitor binding could rearrange the  $\text{Mg}^{2+}$  carboxyl complex and thus destabilize the active state. Our observations with the diguanylate cyclases PleD suggest, that the observed product inhibition operates mainly by increasing the  $K_m$  for GTP (from  $8.3\mu\text{M}$  in

absence of c-di-GMP to 465  $\mu\text{M}$  in presence of 10  $\mu\text{M}$  c-di-GMP), (Figure 12F). However this observation does not exclude a decrease in  $v_{\text{max}}$  upon c-di-GMP binding.

### **In silico analysis of the GGDEF protein family indicates that product inhibition is a general regulatory mechanism**

DGC activity of GGDEF domain proteins seems to strictly depend on conserved GGDEF or GGEEF motifs in the active site (25, 30, 72, 82, 85, 86). Consistent with this, about 90% of the GGDEF and 62% of the GGDEF/EAL composite proteins show a conserved GG[D/E]EF A-site motif. Of the GGDEF proteins with a highly conserved A-site motif, more than 60% have conserved RXXD I-site residues and a conserved spacer length between I- and A-site, arguing that the three-dimensional arrangement of catalytic and allosteric pocket is likely to be similar in all DGCs. From a total of 19 GGDEF proteins, for which convincing evidence for a DGC activity exists, 14 have a conserved I-site. Ryjenkov and coworkers reported severe toxicity problems when expressing diguanylate cyclases lacking I-site residues in *E. coli* BL21 (72). This is consistent with the growth defect observed upon expression of *dgcA* feedback inhibition mutants in *E. coli* BL21, and argues that these proteins are not feedback controlled. The molecular basis of growth interference under these conditions is unclear. It is possible that depletion of the GTP pool, or adverse effects of unphysiologically high levels of c-di-GMP are responsible for this effect.

### **Regulatory significance of DGC feedback control**

GGDEF domains are often associated with sensory domains in one- or two-component signaling systems (32, 87). Thus it is reasonable to assume that in most cases DGC activity is controlled by direct signal input through these domains. But why then would a substantial portion of these enzymes also be subject to feedback inhibition? There are several possibilities, which among them are not mutually exclusive. Given the anticipated regulatory complexity of the c-di-GMP signaling network (32, 84) and the potentially dramatic changes in cellular physiology and behavior caused by fluctuating levels of c-di-GMP, it is in the cell's best interest to rigorously control the production of the second messenger. Product inhibition of DGCs allows the establishment of precise threshold concentrations of the second messenger, or, in combination with counteracting PDEs, could produce short spikes, or even generate oscillations of c-di-GMP. In addition, negative feedback loops have been implicated in neutralizing noise and providing robustness in genetic networks by limiting the range over which the concentrations of the network components fluctuate (88, 89). Similarly, product inhibition of DGCs could contribute to the reduction of stochastic perturbations

and increase the stability of the c-di-GMP circuitry by keeping c-di-GMP levels in defined concentration windows. Alternatively, DGC autoregulation may influence the kinetics of c-di-GMP signaling. Mathematical modeling and experimental evidence suggested that negative autoregulation in combination with strong promoters substantially shortens the rise-time of transcription responses (90-92). In analogy, a desired steady-state concentration of c-di-GMP can in principle be achieved by two regulatory designs: A) a low-activity DGC with no product inhibition, and B) a high-activity DGC with built-in negative autoregulation. In cases where circuits have been optimized for fast up-kinetics, design B will be superior. It is plausible that DGCs with or without I-site motifs can be divided into these two kinetically different classes.

### **The c-di-GMP specific Phosphodiesterase activity resides in the EAL domain**

Recent biochemical and structural studies have proposed a catalytic and regulatory mechanism for the synthesis of c-di-GMP by the GGDEF protein PleD (24, 25). Here we show that CC3396, a GGDEF-EAL protein of *C. crescentus* harbors c-di-GMP-specific PDE activity but lacks DGC activity. Analysis of the catalytic activities of the individual domains strongly suggested that the PDE activity of CC3396 is confined to the C-terminal EAL domain, and does not depend on the physical presence of the N-terminal GGDEF domain. To our knowledge, this is the first report that directly links an isolated EAL domain with the ability to catalyze the hydrolysis of c-di-GMP in vitro. Our data further propose a regulatory role for the N-terminal GGDEF domain of CC3396. The in vitro PDE activity of CC3396 is increased about 40-fold upon addition of GTP. Activation of the PDE activity seems to occur via the reduction of the  $K_M$  for c-di-GMP from above 100  $\mu\text{M}$  in the absence of GTP to 420 nM when GTP was present. Several lines of evidence suggest that GGDEF mediates this allosteric control through an interaction with the associated EAL domain. i) While the basal level PDE activity of full-length CC3396 and the isolated EAL domain are comparable, GTP activation could only be detected if the GGDEF domain was present. ii) Compared to the bona fide DGC PleD (25), the GGDEF domain of CC3396 has a slightly altered consensus sequence A-site motif (GEDEF). Consistent with this, CC3396 does not seem to possess diguanylate cyclase activity in vitro (the activity measured is about corresponds to. iii) GTP specifically binds to the GGDEF but not to the associated catalytic EAL domain. iv) A defined mutation in the A-site motif of the GGDEF domain (GQNEF) abolished allosteric activation and resulted in a constitutive activity of the associated EAL domain. This last observation implies that the GGDEF domain of CC3396 is a GGDEF-like domain, which is still able to bind GTP in the A-site cavity with a relatively high affinity ( $K_D$  4  $\mu\text{M}$ ) but does not catalyze the formation of c-di-GMP. If so, an original GGDEF domain might have been recruited as sensory domain for GTP through the loss of its catalytic function and the evolution of a regulatory interaction with EAL. If such a regulatory role of a

GGDEF domain has indeed evolved from an enzymatically active GGDEF domain, two scenarios are possible. Either the GGDEF domain has lost DGC activity because key catalytic residues are missing, or because, in the context of the GGDEF-EAL composite protein, it is no longer able to form a dimeric structure required to condense two GTP molecules into c-di-GMP.

Thus, we propose that GGDEF domains, depending on their sequence conservation or on their oligomeric status, can have two alternative biological activities and can play different roles in the controlled formation and hydrolysis of c-di-GMP. It is conceivable that at least a subgroup of the large family of bacterial GGDEF-EAL composite proteins represents PDEs with an associated regulatory GGDEF domain that can act as GTP sensor. This hypothesis has recently been confirmed by the c-di-GMP specific PDE FimX from *P. aeruginosa*, which is also activated by GTP (66). At the same time GGDEF-EAL proteins may exist that combine both a GGDEF-born DGC and an EAL-associated PDE activity. As a direct consequence of our findings, each GGDEF or EAL domain will first have to be carefully analyzed biochemically before a catalytic or regulatory role can be assigned.

#### **Why would phosphodiesterase activity be coupled to the cellular concentration of GTP?**

Römling and colleagues have reported that upon expression of the DGC protein AdrA in *Salmonella typhimurium* the cellular GTP to c-di-GMP ratio reverses from about 100:1 to 1:10 (30). Thus, it is possible that when c-di-GMP synthesis is fully induced, uncontrolled hydrolysis of c-di-GMP to pGpG and GMP would deplete the cellular GTP pool. A massive reduction of the cellular GTP concentration has been reported as a consequence of the increased production of the 'alarmone' pppGpp upon amino acid starvation in *Bacillus subtilis* (93). Similarly, the GTP concentration decreases considerably upon nitrogen starvation in *C. crescentus* (94). It is possible that in order to prevent drainage of the cellular GTP pool, specific PDEs are quickly turned off when the GTP concentration drops under a threshold level. Considering that the KD for GTP of CC3396 is about 4  $\mu$ M, one would expect such a threshold GTP concentration to be in the low micromolar range. Together with the observation that DGCs can be subject to tight allosteric feedback inhibition by their own product, this could be interpreted as a simple means for flux-controlled sensitivity, which would allow breaching the threshold for signal transduction by either increased production or decreased degradation of the second messenger. Alternatively, the prevailing GTP level of the cell itself could be used as a physiological signal to control the internal concentration of c-di-GMP through the controlled activity of PDEs. A drastic drop of the GTP concentration to the low micromolar range could lead to a rapid and substantial increase of the

cellular c-di-GMP concentration through the inhibition of one or several key PDEs, which respond to GTP in a similar manner as observed for CC3396. While such a regulatory role for GTP remains speculative, cellular GTP pools are known to affect developmental transitions in bacteria. A decrease in the cellular GTP concentration, but not of other purine or pyrimidine nucleotides, correlates with the initiation of morphological differentiation during nutrient starvation of *B. subtilis* and *Streptomyces griseus* (95-97). The signal responsible for the induction of sporulation is the reduced GTP pool, rather than pppGpp, which is formed under the same starvation conditions (96). The cellular GTP concentration is sensed by CodY, a transcriptional repressor of several sporulation and motility genes, whose repression activity depends on binding of GTP with a  $K_D$  in the physiologically relevant millimolar range (98, 99). It remains to be shown if the GTP concentration plays a similar regulatory role in cellular c-di-GMP signaling.

### **How are increased levels of c-di-GMP sensed and how is this information transmitted to the flagellar motor?**

The data presented here suggest that two members of a novel family of c-di-GMP binding proteins, DgrA and DgrB, mediate motor control in response to fluctuating concentrations of the second messenger. We show that DgrA, DgrB, and its homologs in *S. typhimurium* (YcgR) and *P. aeruginosa* (PA4608) bind c-di-GMP specifically and with high affinity ( $K_D$  in the nM range). Mutants that lack DgrA, DgrB, or both were motile in the presence of a plasmid-encoded copy of the soluble diguanylate cyclase DgcA. These mutants no longer respond to c-di-GMP, implying that DgrA and DgrB are part of the c-di-GMP-dependent pathway that controls flagellar rotation. The observation that single *dgrA* or *dgrB* deletion mutants partially restored motility, whereas motility was fully restored in a *dgrAdgrB* double mutant, suggested that both proteins contribute to c-di-GMP mediated motility control. Consistent with this, overexpression of both *dgrA* and *dgrB* produced an exact phenocopy of the motility block caused by DgcA; components of the flagellum are expressed and assembled normally, but the resulting structure is not functional. Together this suggested that DgrA and DgrB are high affinity receptors for c-di-GMP that, in a ligand-bound form, interfere with the flagellar motor either directly or indirectly.

### **How does DgrA interfere with the function of the flagellum?**

Motor control by DgrA-like proteins is not unique to *Caulobacter*. *E. coli* H-NS mutants lack flagella because the expression of the flagellar master control operon *flhCD* is reduced. Ectopic expression of *flhCD* restores flagellation but leaves the motors partially paralyzed (100). Under these conditions flagellar function can be restored either by a mutation in *ycgR*, coding for the *E. coli*



DgrA homolog, or by providing multiple copies of *yhjH*, which encodes a presumable c-di-GMP specific phosphodiesterase (100). Together with our data demonstrating that the *Salmonella* YcgR protein specifically binds c-di-GMP, this suggests that flagellar motor function might be controlled by c-di-GMP in *C. crescentus* and in enteric bacteria via similar mechanisms. But how would DgrA or YcgR interfere with the function of the flagellum? Several observations suggested the FliL protein as a candidate for such a function. FliL was the only flagellar protein that showed significantly reduced levels in non-motile cells overexpressing *dgrA*. In *C. crescentus* the FliL protein is not part of the flagellar structure but is required for flagellar rotation (101). Intriguingly, *fliL* mutant strains exhibit an identical motility phenotype like cells that have high levels of c-di-GMP or overexpress *dgrA* (101). Because the expression of *fliM*, the gene located immediately downstream of *fliL* in the same operon (102), was not affected by DgrA, FliL changes must be the result of altered translation or protein stability. An intergenic suppressor mutation that restored motility under these conditions also re-established normal FliL concentrations, indicating that the two phenotypes are linked. The simplest model that is in agreement with these results predicts that DgrA, upon binding of c-di-GMP, represses FliL by a so far unknown mechanism and through this blocks motor function. We are currently investigating how DgrA and its ligand c-di-GMP modulate FliL levels. Recently, FliL was reported to be involved in surface sensing and virulence gene expression in the urinary tract pathogen *Proteus mirabilis* (103). Thus, it is possible that FliL has a more general role in controlling the switch between a planktonic and a surface-associated lifestyle.

#### **Which key residues define the c-di-GMP binding pocket of the diguanylate receptor?**

A bioinformatics study recently proposed that the PilZ domain is a specific c-di-GMP binding module (104). Here we presented genetic, biochemical, and structural evidence that validate this hypothesis. Based on our data we propose a model for ligand binding and activation of proteins containing a PilZ domain. NMR studies with the DgrA homolog PA4608 showed that a dimer of c-di-GMP binds to a well-defined binding site on the surface of the  $\beta$ -barrel (Figure 16C). Large chemical shift differences between free and ligand-bound PA4608, which indicate changes in the local environment, were also observed in both termini of the protein, with the largest differences observed for residues R30-R32, V142, and A144. These regions are structurally ill defined in the absence of ligand (PDB 1YWU) and are probably flexible. The observed chemical shift differences indicate that these regions come in direct contact with the ligand after complex formation. The N-terminal part of PA4608 contains three consecutive Arg residues, which are conserved in most PilZ domains (104). One of these highly conserved Arg residue, R35, could not be observed in the NMR spectra of PA4608 but might well be of equal importance. Arg side chains are likely involved in hydrogen bonds or in electrostatic or  $\pi$  stacking interactions with c-di-GMP, as has been shown

for the allosteric binding site of the PleD diguanylate cyclase (24, 47). Furthermore, it is conceivable that the positively charged head groups of Arg are sufficient for transient binding to phosphate groups of c-di-GMP and that their position on the flexible N-terminus increases the ligand capture radius of the protein, as in the “fly-casting mechanism” proposed in (105). Alternatively, the observed folding of previously flexible parts of the protein may be responsible for communication of the c-di-GMP signal to downstream elements, either by forming new interaction surfaces or, in proteins like YcgR, where other domains connect to the N-terminus of a PilZ domain, by determining the relative position of neighboring domains. Similarly, the chemical shift differences of the C-terminal part of PA4608 could be explained by a specific role in ligand binding. However, the fact that residues V142 and A144, which showed the largest chemical shift differences are not conserved, argues against this possibility. Several of the motile *dgrA* loss of function suppressors that were isolated had frameshift mutations in the very C-terminus of DgrA, suggesting that this part of the protein is critical for its *in vivo* function. One possibility is that the C-terminus contributes to the specific readout mechanism of this protein family. Upon c-di-GMP binding to the  $\beta$ -barrel surface, the C-terminus could be untied to interact with downstream components. In accordance with such a view, the very C-terminus of the *P. aeruginosa* PilZ protein has recently been proposed to interact with the PilF protein required for type 4-pilus assembly (106). To complement our picture of the c-di-GMP circuitry, future studies will have to focus on interaction partners of DgrA and related PilZ domain proteins. It is intriguing that genetic and biochemical studies of the *C. crescentus* DgrA protein and structural analysis of the PA4608 from *P. aeruginosa* identified the same set of key amino acid residues involved in c-di-GMP binding. This finding is a strong indication that these proteins bind c-di-GMP in a similarly way and argues that they may share a common signaling mechanism. Based on these results we postulate that most or all PilZ domain proteins function as c-di-GMP receptors.

Although the molecular components regulating the c-di-GMP signaling cascade have been identified and general regulatory principles for the synthesis and degradation of the second messenger have been defined, it is evident that there are more questions than answers regarding the c-di-GMP signaling system in bacteria. However, since the molecular key players involved in c-di-GMP signaling have now been characterized, the current emphasis for the next generation of PhD students on the c-di-GMP signaling research field, lies on the investigation of further downstream regulatory mechanisms, and processes controlled by c-di-GMP with the long-term goal of approaching a detailed systems-level understanding of c-di-GMP signaling.

## 5 Outlooks

Further effort has to focus on the investigation of downstream regulatory mechanisms, and processes controlled by c-di-GMP with the long-term goal of approaching a detailed systems-level understanding of c-di-GMP signaling. In particular the c-di-GMP dependent regulation of developmental processes, virulence traits, exopolysaccharide synthesis and biofilm formation have to be clarified. The presence of many orthologous GGDEF and EAL protein in one bacterial species (*C. crescentus* 14, *E.coli* 37, *P. aeruginosa* 40, *V. vulnificus* 59) raises the question of their interconnection and their spatial and temporal distribution within the bacterial cell. And subsequent, what is the molecular mode of action and what are regulatory mechanisms controlling individuals PDE and DGC activities inside the cell? What kind of external stimuli are activating the individual DGC and PDE's? What are the interaction partner of the diguanylate receptor proteins DgrA and DgrB and upon which mechanism they mediate c-di-GMP dependent output functions? Are there, beside the large family of diguanylate receptor proteins, additional, so far uncharacterized c-di-GMP receptor proteins present? The application of the presented biochemical tools on model organisms for c-di-GMP signaling, which are easily accessible to genetics, cell biology, and systems approaches, may develop into powerful explanatory tools to facilitate a more complete understanding of the molecular and cellular mechanisms of second-messenger control.

## **Appendix**

## References

1. Harman, J. G. (2001) *Biochimica Et Biophysica Acta-Protein Structure and Molecular Enzymology* **1547**, 1-17.
2. Reiness, G., Yang, H. L., Zubay, G. & Cashel, M. (1975) *Proceedings of the National Academy of Sciences of the United States of America* **72**, 2881-2885.
3. Paul, B. J., Berkmen, M. B. & Gourse, R. L. (2005) *Proceedings of the National Academy of Sciences of the United States of America* **102**, 7823-7828.
4. Ross, P., Weinhouse, H., Aloni, Y., Michaeli, D., Weinberger-Ohana, P., Mayer, R., Braun, S., de Wroom, E., van der Marel, G. A., van Boom, J. H. & Benziman, M. (1987) *Nature* **325**, 279-281.
5. Tal, R., Wong, H. C., Calhoon, R., Gelfand, D., Fear, A. L., Volman, G., Mayer, R., Ross, P., Amikam, D., Weinhouse, H., Cohen, A., Sapir, S., Ohana, P. & Benziman, M. (1998) *J Bacteriol* **180**, 4416-25.
6. Schultz, J., Milpetz, F., Bork, P. & Ponting, C. P. (1998) *Proc Natl Acad Sci U S A* **95**, 5857-64.
7. Cook, K. E. & Colvin, J. R. (1980) *Current Microbiology* **3**, 203-205.
8. Sowden, L. C. & Colvin, J. R. (1978) *Canadian Journal of Microbiology* **24**, 772-779.
9. D'Argenio, D. A., Calfee, M. W., Rainey, P. B. & Pesci, E. C. (2002) *J Bacteriol* **184**, 6481-9.
10. Anriany, Y. A., Weiner, R. M., Johnson, J. A., De Rezende, C. E. & Joseph, S. W. (2001) *Applied and Environmental Microbiology* **67**, 4048-4056.
11. AllenVercoe, E., DibbFuller, M., Thorns, C. J. & Woodward, M. J. (1997) *Fems Microbiology Letters* **153**, 33-42.
12. Zogaj, X., Nimtz, M., Rohde, M., Bokranz, W. & Romling, U. (2001) *Mol Microbiol* **39**, 1452-63.
13. Zogaj, X., Bokranz, W., Nimtz, M. & Romling, U. (2003) *Infect Immun* **71**, 4151-8.
14. Romling, U., Rohde, M., Olsen, A., Normark, S. & Reinkoster, J. (2000) *Mol Microbiol* **36**, 10-23.
15. Jones, H. A., Lillard, J. W., Jr. & Perry, R. D. (1999) *Microbiology* **145 ( Pt 8)**, 2117-28.
16. Bomchil, N., Watnick, P. & Kolter, R. (2003) *J Bacteriol* **185**, 1384-90.
17. Lobedanz, S. & Sogaard-Andersen, L. (2003) *Genes Dev* **17**, 2151-61.
18. Sogaard-Andersen, L., Overgaard, M., Lobedanz, S., Ellehauge, E., Jelsbak, L. & Rasmussen, A. A. (2003) *Mol Microbiol* **48**, 1-8.
19. Skerker, J. M. & Laub, M. T. (2004) *Nat Rev Microbiol* **2**, 325-37.
20. McAdams, H. H. & Shapiro, L. (2003) *Science* **301**, 1874-7.
21. Bodenmiller, D., Toh, E. & Brun, Y. V. (2004) *J Bacteriol* **186**, 1438-47.
22. Hecht, G. B. & Newton, A. (1995) *J Bacteriol* **177**, 6223-9.
23. Aldridge, P., Paul, R., Goymer, P., Rainey, P. & Jenal, U. (2003) *Mol Microbiol* **47**, 1695-708.
24. Chan, C., Paul, R., Samoray, D., Amiot, N. C., Giese, B., Jenal, U. & Schirmer, T. (2004) *Proc Natl Acad Sci U S A* **101**, 17084-9.
25. Paul, R., Weiser, S., Amiot, N. C., Chan, C., Schirmer, T., Giese, B. & Jenal, U. (2004) *Genes Dev* **18**, 715-727.
26. Levi, A. & Jenal, U. (2006) *J Bacteriol* **188**, 5315-8.
27. Aldridge, P. & Jenal, U. (1999) *Mol Microbiol* **32**, 379-91.
28. Jacobs-Wagner, C. (2004) *Mol Microbiol* **51**, 7-13.
29. Chang, A. L., Tuckerman, J. R., Gonzalez, G., Mayer, R., Weinhouse, H., Volman, G., Amikam, D., Benziman, M. & Gilles-Gonzalez, M. A. (2001) *Biochemistry* **40**, 3420-6.
30. Simm, R., Morr, M., Kader, A., Nimtz, M. & Romling, U. (2004) *Mol Microbiol* **53**, 1123-34.
31. Tischler, A. D. & Camilli, A. (2004) *Mol Microbiol* **53**, 857-69.

32. Galperin, M. Y., Nikolskaya, A. N. & Koonin, E. V. (2001) *FEMS Microbiol Lett* **203**, 11-21.
33. Galperin, M. Y., Natale, D. A., Aravind, L. & Koonin, E. V. (1999) *J Mol Microbiol Biotechnol* **1**, 303-5.
34. Iancu, C. V., Borza, T., Fromm, H. J. & Honzatko, R. B. (2002) *Journal of Biological Chemistry* **277**, 40536-40543.
35. Spector, T. & Miller, R. L. (1976) *Biochimica Et Biophysica Acta* **445**, 509-517.
36. Kang, C. H. & Fromm, H. J. (1995) *Journal of Biological Chemistry* **270**, 15539-15544.
37. Stayton, M. M. & Fromm, H. J. (1979) *Journal of Biological Chemistry* **254**, 2579-2581.
38. Atkinson, M. R., Murray, A. W. & Morton, R. K. (1964) *Biochemical Journal* **92**, 398-&.
39. Rudolph, F. B. & Fromm, H. J. (1969) *Journal of Biological Chemistry* **244**, 3832-&.
40. Borza, T., Iancu, C. V., Pike, E., Honzatko, R. B. & Fromm, H. J. (2003) *Journal of Biological Chemistry* **278**, 6673-6679.
41. Markham, G. D. & Reed, G. H. (1977) *Archives of Biochemistry and Biophysics* **184**, 24-35.
42. Clark, S. W. & Rudolph, F. B. (1976) *Biochimica Et Biophysica Acta* **437**, 87-93.
43. Wyngaarden, J. B. & Greenland, R. A. (1963) *Journal of Biological Chemistry* **238**, 1054-&.
44. Honzatko, R. B. & Fromm, H. J. (1999) *Archives of Biochemistry and Biophysics* **370**, 1-8.
45. Lee, P., Gorrell, A., Fromm, H. J. & Colman, R. F. (1999) *Biochemistry* **38**, 5754-5763.
46. Christen, M., Christen, B., Folcher, M., Schauerte, A. & Jenal, U. (2005) *J Biol Chem* **280**, 30829-37.
47. Christen, B., Christen, M., Paul, R., Schmid, F., Folcher, M., Jenoe, P., Meuwly, M. & Jenal, U. (2006) *Journal of Biological Chemistry* **281**, 32015-32024.
48. Ross, P., Mayer, R., Weinhouse, H., Amikam, D., Huggirat, Y., Benziman, M., de Vroom, E., Fidler, A., de Paus, P., Sliedregt, L. A. & et al. (1990) *J Biol Chem* **265**, 18933-43.
49. Weinhouse, H., Sapir, S., Amikam, D., Shilo, Y., Volman, G., Ohana, P. & Benziman, M. (1997) *FEBS Lett* **416**, 207-11.
50. Qian, J. C., Cai, X. P., Chu, J., Zhuang, Y. P. & Zhang, S. L. (2006) *Biotechnology Letters* **28**, 937-941.
51. Iancu, C. V., Zhou, Y., Borza, T., Fromm, H. J. & Honzatko, R. B. (2006) *Biochemistry* **45**, 11703-11711.
52. Raman, J., Mehrotra, S., Anand, R. P. & Balaram, H. (2004) *Molecular and Biochemical Parasitology* **138**, 1-8.
53. Eaazhisai, K., Jayalakshmi, R., Gayathri, P., Anand, R. P., Sumathy, K., Balaram, H. & Murthy, M. R. N. (2004) *Journal of Molecular Biology* **335**, 1251-1264.
54. Jayalakshmi, R., Sumathy, K. & Balaram, H. (2002) *Protein Expression and Purification* **25**, 65-72.
55. Iancu, C. V., Borza, T., Fromm, H. J. & Honzatko, R. B. (2002) *Journal of Biological Chemistry* **277**, 26779-26787.
56. Hou, Z. L., Wang, W. Y., Fromm, H. J. & Honzatko, R. B. (2002) *Journal of Biological Chemistry* **277**, 5970-5976.
57. Gorrell, A., Wang, W. Y., Underbakke, E., Hou, Z. L., Honzatko, R. B. & Fromm, H. J. (2002) *Journal of Biological Chemistry* **277**, 8817-8821.
58. Cooper, B. F., Fromm, H. J. & Rudolph, F. B. (1986) *Biochemistry* **25**, 7323-7327.
59. Bass, M. B., Fromm, H. J. & Rudolph, F. B. (1984) *Journal of Biological Chemistry* **259**, 2330-2333.
60. Lieberman, I. (1956) *Journal of the American Chemical Society* **78**, 251-251.
61. Poland, B. W., Fromm, H. J. & Honzatko, R. B. (1996) *Journal of Molecular Biology* **264**, 1013-1027.
62. Poland, B. W., Lee, S. F., Subramanian, M. V., Siehl, D. L., Anderson, R. J., Fromm, H. J. & Honzatko, R. B. (1996) *Biochemistry* **35**, 15753-15759.
63. Moe, O. A., Baker-Malcolm, J. F., Wang, W. Y., Kang, C. H., Fromm, H. J. & Colman, R. F. (1996) *Biochemistry* **35**, 9024-9033.

64. Saxild, H. H. & Nygaard, P. (1991) *Journal of General Microbiology* **137**, 2387-2394.
65. Hou, Z. L., Cashel, M., Fromm, H. J. & Honzatko, R. B. (1999) *Journal of Biological Chemistry* **274**, 17505-17510.
66. Kazmierczak, B. I., Lebron, M. B. & Murray, T. S. (2006) *Mol Microbiol* **60**, 1026-43.
67. Ely, B. (1991) *Meth. Enzymol.* **204**, 372-384.
68. Pei, J. & Grishin, N. V. (2001) *Proteins* **42**, 210-6.
69. Tesmer, J. J., Sunahara, R. K., Johnson, R. A., Gosselin, G., Gilman, A. G. & Sprang, S. R. (1999) *Science* **285**, 756-60.
70. Ross, P., Aloni, Y., Weinhouse, H., Michaeli, D., Weinberger-Ohana, P., Mayer, R. & Benziman, M. (1986) *Carbohydrate Research* **149**, 101-117.
71. Hyodo, M. & Hayakawa, Y. (2004) *Bulletin of the Chemical Society of Japan* **77**, 2089-2093.
72. Ryjenkov, D. A., Tarutina, M., Moskvina, O. V. & Gomelsky, M. (2005) *J Bacteriol* **187**, 1792-8.
73. Ochi, Y., Hosoda, S., Hachiya, T., Yoshimura, M., Miyazaki, T. & Kajita, Y. (1981) *Acta Endocrinol (Copenh)* **98**, 62-7.
74. Jenal, U. (2004) *Curr Opin Microbiol* **7**, 185-91.
75. Spiers, A. J., Kahn, S. G., Bohannon, J., Travisano, M. & Rainey, P. B. (2002) *Genetics* **161**, 33-46.
76. Drenkard, E. & Ausubel, F. M. (2002) *Nature* **416**, 740-3.
77. Huang, B., Whitchurch, C. B. & Mattick, J. S. (2003) *J Bacteriol* **185**, 7068-76.
78. Guvener, Z. T. & McCarter, L. L. (2003) *J Bacteriol* **185**, 5431-41.
79. Thomas, C., Andersson, C. R., Canales, S. R. & Golden, S. S. (2004) *Microbiology* **150**, 1031-40.
80. Garcia, B., Latasa, C., Solano, C., Garcia-del Portillo, F., Gamazo, C. & Lasa, I. (2004) *Mol Microbiol* **54**, 264-77.
81. Choy, W. K., Zhou, L., Syn, C. K., Zhang, L. H. & Swarup, S. (2004) *J Bacteriol* **186**, 7221-8.
82. Kirillina, O., Fetherston, J. D., Bobrov, A. G., Abney, J. & Perry, R. D. (2004) *Mol Microbiol* **54**, 75-88.
83. Johnson, M. R., Montero, C. I., Connors, S. B., Shockley, K. R., Bridger, S. L. & Kelly, R. M. (2005) *Mol Microbiol* **55**, 664-674.
84. Romling, U., Gomelsky, M. & Galperin, M. Y. (2005) *Mol Microbiol* **57**, 629-39.
85. Hickman, J. W., Tifrea, D. F. & Harwood, C. S. (2005) *Proc Natl Acad Sci U S A* **102**, 14422-7.
86. Mendez-Ortiz, M. M., Hyodo, M., Hayakawa, Y. & Membrillo-Hernandez, J. (2006) *J Biol Chem*.
87. Ulrich, L. E., Koonin, E. V. & Zhulin, I. B. (2005) *Trends Microbiol* **13**, 52-6.
88. Becskei, A. & Serrano, L. (2000) *Nature* **405**, 590-3.
89. Gardner, T. S., Cantor, C. R. & Collins, J. J. (2000) *Nature* **403**, 339-42.
90. McAdams, H. H. & Arkin, A. (1997) *Proc Natl Acad Sci U S A* **94**, 814-9.
91. Rosenfeld, N., Elowitz, M. B. & Alon, U. (2002) *J Mol Biol* **323**, 785-93.
92. Savageau, M. A. (1974) *Nature* **252**, 546-9.
93. Ochi, K., Kandala, J. & Freese, E. (1982) *J Bacteriol* **151**, 1062-5.
94. Chiaverotti, T. A., Parker, G., Gallant, J. & Agabian, N. (1981) *J Bacteriol* **145**, 1463-5.
95. Freese, E., Heinze, J. E. & Galliers, E. M. (1979) *J Gen Microbiol* **115**, 193-205.
96. Lopez, J. M., Marks, C. L. & Freese, E. (1979) *Biochim Biophys Acta* **587**, 238-52.
97. Ochi, K. (1987) *J Bacteriol* **169**, 3608-16.
98. Ratnayake-Lecamwasam, M., Serron, P., Wong, K. W. & Sonenshein, A. L. (2001) *Genes Dev* **15**, 1093-103.
99. Bergara, F., Ibarra, C., Iwamasa, J., Patarroyo, J. C., Aguilera, R. & Marquez-Magana, L. M. (2003) *J Bacteriol* **185**, 3118-26.

100. Ko, M. & Park, C. (2000) *J Mol Biol* **303**, 371-82.
101. Jenal, U., White, J. & Shapiro, L. (1994) *J Mol Biol* **243**, 227-44.
102. Yu, J. & Shapiro, L. (1992) *J Bacteriol* **174**, 3327-38.
103. Belas, R. & Suvanasuthi, R. (2005) *J Bacteriol* **187**, 6789-803.
104. Amikam, D. & Galperin, M. Y. (2006) *Bioinformatics* **22**, 3-6.
105. Shoemaker, B. A., Portman, J. J. & Wolynes, P. G. (2000) *Proceedings of the National Academy of Sciences of the United States of America* **97**, 8868-+.
106. Kim, K., Oh, J., Han, D., Kim, E. E., Lee, B. & Kim, Y. (2006) *Biochemical and Biophysical Research Communications* **340**, 1028-1038.



## Biochemical characterized GGDEF and EAL proteins from *C. crescentus*














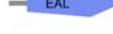
Domain organization	ORF	gene name	DGC activity	I-site	PDE activity	DGC activity	References
	CC3285	dgcA	yes	+	no	yes	Christen 2006
	CC1842	pdpA	no	-	no	no	Jenal 2006, Thesis A. Dürig
	CC1850	dgcB	yes	-	no	yes	Jenal 2006, Thesis A. Dürig
	CC2462	pleD	yes	-	no	yes	Aldridge 2003, Paul 2004 Chan 2004, Christen 2006
	CC3396	pdeA	no	-	yes GTP activated	no	Christen 2005
	CC0091	pdeB	no	-	yes not GTP activated	no	Thesis A. Levi, D. Meyer
	CC0896		n.d.	-	n.d.	n.d.	
	CC0655		n.d.	-	n.d.	n.d.	
	CC0740		n.d.	+	n.d.	n.d.	
	CC3094		n.d.	-	n.d.	n.d.	
	CC0857		n.d.	+	n.d.	n.d.	
	CC0710	tipF	no	-	no	no	Huitema 2006
	CC1086		n.d.	-	n.d.	n.d.	
	CC3148		no	-	no	no	

Figure 17 Overview of the GGDEF and EAL proteins from *Caulobacter crescentus*.

DGC activity has been shown for PleD (25, 47), DgcA (47) and DgcB. PDE activity has been demonstrated for PdeA (CC3396) (46) and PdeB (CC0091). No enzymatic activity has been detected for PdpA, TipF and CC3148. The Strain ID for all overexpression strains can be found in the strain list on the following page.

## List of constructs

Strain	Genotype	Reference
BC425	<i>S.typhimurium</i> LT2 <i>trp::T7RNAP</i>	Christen unpublished
BC428	<i>E.coli</i> S17-1/ pAS22:: <i>pdeA</i>	Christen et al 2005, JBC
BC430	<i>E.coli</i> S17-1/ pNPTS138:: <i>KOdgcA</i>	Christen et al 2006, JBC
BC431	<i>E.coli</i> S17-1/ pNPTS138:: <i>KOpdeA</i>	Christen et al 2005, JBC
BC432	<i>E.coli</i> S17-1/ pUJ142:: <i>dgcA</i>	Christen et al 2006, JBC
BC433	<i>E.coli</i> S17-1/ pAS22:: <i>dgcA</i>	Christen et al 2006, JBC
BC434	<i>E.coli</i> S17-1/ pUJ142:: <i>pdeA</i>	Christen et al 2006, JBC
BC478	<i>S.typhimurium</i> LT2 <i>araBAD::dgcA</i>	Christen et al 2006, JBC
BC480	<i>S.typhimurium</i> LT2/ pET42b:: <i>dgcA5002-his6</i>	Christen unpublished
BC482	<i>S.typhimurium</i> LT2 <i>trp::T7RNAP</i> / pET42b:: <i>dgcA5002-his6</i>	Christen unpublished
BC498	<i>S.typhimurium</i> LT2 <i>araBAD::dgcA bcsA::Tn10Tc</i>	Christen unpublished
BC500	<i>S.typhimurium</i> LT2 <i>araBAD::dgcA bcsA::Tn10Tc</i>	Christen unpublished
BC506	<i>E.coli</i> BL21(DE3)/ pET42b:: <i>ycgR</i>	Christen et al 2007, PNAS
BC512	<i>E.coli</i> BL21(DE3)/ pET42b:: <i>dgrAD38A</i>	Christen et al 2007, PNAS
BC514	<i>E.coli</i> BL21(DE3)/ pET42b:: <i>dgrARR11AA</i>	Christen et al 2007, PNAS
BC516	<i>E.coli</i> S17-1/ pBBR:: <i>dgrA-his6</i>	Christen et al 2007, PNAS
BC517	<i>E.coli</i> S17-1/ pBBR:: <i>dgrB-his6</i>	Christen et al 2007, PNAS
BC535	<i>C.crescentus</i> CB15ATCC/ pBBR:: <i>dgrA-his6</i>	Christen et al 2007, PNAS
BC538	<i>C.crescentus</i> CB15ATCC/ pBBR:: <i>dgrB-his6</i>	Christen et al 2007, PNAS
BC541	<i>C.crescentus</i> CB15ATCC/ pBBR	Christen et al 2007, PNAS
BC546	<i>E.coli</i> S17-1/ pNPTS138:: <i>KOdgrA</i>	Christen et al 2007, PNAS

Strain	Genotype	Reference
BC547	<i>E. coli</i> S17-1/ pNPTS138::KodgrB	Christen et al 2007, PNAS
BC548	<i>E. coli</i> DH10B/ pBBR::dgrA-his6	Christen et al 2007, PNAS
BC558	<i>E. coli</i> S17-1/ pBBR::dgrA-his6	Christen et al 2007, PNAS
BC559	<i>E. coli</i> S17-1/ pBBR::dgrB-his6	Christen et al 2007, PNAS
BC562	<i>C. crescentus</i> CB15ATCC $\Delta$ dgrB	Christen et al 2007, PNAS
BC568	<i>C. crescentus</i> CB15ATCC $\Delta$ dgrA	Christen et al 2007, PNAS
BC680	<i>C. crescentus</i> CB15ATCC $\Delta$ dgrA $\Delta$ dgrB	Christen et al 2007, PNAS
BC695	<i>S. typhimurium</i> LT2 <i>trp</i> ::T7RNAP/ pET42b	Christen et al 2006, JBC
BC719	<i>C. crescentus</i> CB15ATCC/ pBBR::dgrAV74A-his6	Christen et al 2007, PNAS
BC777	<i>C. crescentus</i> CB15ATCC/ pUJ142	Christen et al 2007, PNAS
BC779	<i>C. crescentus</i> CB15ATCC/ pAS22::dgrA	Christen et al 2007, PNAS
BC827	<i>E. coli</i> BL21(DE3)/ pET42b::dgrAW75A	Christen et al 2007, PNAS
BC831	<i>E. coli</i> S17-1/ pBBR::dgrAW75A-his6	Christen et al 2007, PNAS
BC834	<i>E. coli</i> S17-1/ pBBR::dgrA-his6	Christen et al 2007, PNAS
BC862	<i>E. coli</i> S17-1/ pBBR::dgrARR11AA-his6	Christen et al 2007, PNAS
BC864	<i>E. coli</i> S17-1/ pBBR::dgrAD41A-his6	Christen et al 2007, PNAS
BC867	<i>E. coli</i> S17-1/ pBBR::dgrAW75A-his6	Christen et al 2007, PNAS
BC871	<i>C. crescentus</i> CB15ATCC/ pUJ142::dgcA	Christen et al 2007, PNAS
BC877	<i>C. crescentus</i> CB15ATCC $\Delta$ dgrA/ pUJ142::dgcA	Christen et al 2007, PNAS
BC880	<i>C. crescentus</i> CB15ATCC $\Delta$ dgrA/ pAS22::dgcA	Christen et al 2007, PNAS
BC883	<i>C. crescentus</i> CB15ATCC $\Delta$ dgrB/ pUJ142::dgcA	Christen et al 2007, PNAS
BC886	<i>C. crescentus</i> CB15ATCC $\Delta$ dgrB/ pAS22::dgcA	Christen et al 2007, PNAS

Strain	Genotype	Reference
BC889	<i>C. crescentus</i> CB15ATCC $\Delta dgrA \Delta dgrB$ pUJ142:: <i>dgcA</i>	Christen et al 2007, PNAS
BC892	<i>C. crescentus</i> CB15ATCC $\Delta dgrA \Delta dgrB$ pAS22:: <i>dgcA</i>	Christen et al 2007, PNAS
BC913	<i>E. coli</i> S17-1/ pBBR:: <i>dgrARR11AA-his6</i>	Christen et al 2007, PNAS
BC915	<i>C. crescentus</i> CB15ATCC/ pBBR:: <i>dgrARR11AAV74A-his6</i>	Christen et al 2007, PNAS
BC918	<i>C. crescentus</i> CB15ATCC/ pBBR:: <i>dgrAD38A-his6</i>	Christen et al 2007, PNAS
BC921	<i>C. crescentus</i> CB15ATCC/ pBBR:: <i>dgrAW75A-his6</i>	Christen et al 2007, PNAS
BC939	<i>C. crescentus</i> NA1000 $\Delta recA$ pBBR:: <i>dgrA-his6</i>	Christen et al 2007, PNAS
BC940	<i>C. crescentus</i> NA1000 $\Delta recA$ pBBR:: <i>dgrA-his6</i>	Christen et al 2007, PNAS
BC941	<i>C. crescentus</i> NA1000 $\Delta recA$ pBBR:: <i>dgrA-his6</i>	Christen et al 2007, PNAS
BC942	<i>C. crescentus</i> NA1000 $\Delta recA$ pBBR:: <i>dgrA-his6</i>	Christen et al 2007, PNAS
BC943	<i>C. crescentus</i> NA1000 $\Delta recA$ pBBR:: <i>dgrA-his6</i>	Christen et al 2007, PNAS
BC944	<i>C. crescentus</i> NA1000 $\Delta recA$ pBBR:: <i>dgrA-his6</i>	Christen et al 2007, PNAS
BC945	<i>C. crescentus</i> NA1000 $\Delta recA$ pBBR:: <i>dgrA-his6</i>	Christen et al 2007, PNAS
BC946	<i>C. crescentus</i> NA1000 $\Delta recA$ pBBR:: <i>dgrA-his6</i>	Christen et al 2007, PNAS
BC947	<i>C. crescentus</i> NA1000 $\Delta recA$ pBBR:: <i>dgrA-his6</i>	Christen et al 2007, PNAS
BC948	<i>C. crescentus</i> NA1000 $\Delta recA$ pBBR:: <i>dgrA-his6</i>	Christen et al 2007, PNAS
BC949	<i>C. crescentus</i> NA1000 $\Delta recA$ pBBR:: <i>dgrA-his6</i>	Christen et al 2007, PNAS
BC950	<i>C. crescentus</i> NA1000 $\Delta recA$ pBBR:: <i>dgrA-his6</i>	Christen et al 2007, PNAS
BC951	<i>C. crescentus</i> NA1000 $\Delta recA$ pBBR:: <i>dgrA-his6</i>	Christen et al 2007, PNAS
BC952	<i>C. crescentus</i> NA1000 $\Delta recA$ pBBR:: <i>dgrA-his6</i>	Christen et al 2007, PNAS
BC953	<i>C. crescentus</i> NA1000 $\Delta recA$ pBBR:: <i>dgrA-his6</i>	Christen et al 2007, PNAS
BC954	<i>C. crescentus</i> NA1000 $\Delta recA$ pBBR:: <i>dgrA-his6</i>	Christen et al 2007, PNAS

Strain	Genotype	Reference
BC955	<i>C. crescentus</i> NA1000 $\Delta$ <i>recA</i> / pBBR:: <i>dgrA-his6</i>	Christen et al 2007, PNAS
BC956	<i>C. crescentus</i> NA1000 $\Delta$ <i>recA</i> / pBBR:: <i>dgrA-his6</i>	Christen et al 2007, PNAS
BC961	<i>C. crescentus</i> CB15ATCC/ pBBR:: <i>dgrAR11AA-his6</i>	Christen et al 2007, PNAS
BC965	<i>E. coli</i> S17-1/ pMR10::CC2058-CC2069	Christen unpublished
BC966	<i>E. coli</i> S17-1/ pMR10::fliLM	Christen unpublished
BC972	<i>C. crescentus</i> NA1000 :: <i>Tn5Tc rpsAH323R</i> / pBBR:: <i>dgrA-his6</i>	Christen et al 2007, PNAS
BC973	<i>C. crescentus</i> NA1000 :: <i>Tn5Tc rpsAH323R</i> / pBBR:: <i>dgrA-his6</i>	Christen et al 2007, PNAS
BC974	<i>C. crescentus</i> NA1000 :: <i>Tn5Tc rpsAH323R</i> / pBBR:: <i>dgrA-his6</i>	Christen et al 2007, PNAS
BC975	<i>C. crescentus</i> NA1000 :: <i>Tn5Tc rpsAH323R</i> / pBBR:: <i>dgrA-his6</i>	Christen et al 2007, PNAS
BC976	<i>C. crescentus</i> NA1000 :: <i>Tn5Tc rpsAH323R</i> / pBBR:: <i>dgrA-his6</i>	Christen et al 2007, PNAS
BC977	<i>C. crescentus</i> NA1000 :: <i>Tn5Tc</i>	Christen et al 2007, PNAS
BC978	<i>C. crescentus</i> NA1000 :: <i>Tn5Tc</i>	Christen et al 2007, PNAS
BC979	<i>C. crescentus</i> NA1000 :: <i>Tn5Tc</i>	Christen et al 2007, PNAS
BC980	<i>C. crescentus</i> NA1000 :: <i>Tn5Tc</i>	Christen et al 2007, PNAS
BC981	<i>C. crescentus</i> NA1000 :: <i>Tn5Tc</i>	Christen et al 2007, PNAS
BC995	<i>E. coli</i> BL21(DE3)/ pET21c:: <i>dgcA</i>	Christen et al 2006, JBC
BC997	<i>E. coli</i> BL21(DE3)/ pET21c:: <i>pdeA</i>	Christen et al 2005, JBC
BC999	<i>E. coli</i> BL21(DE3)/ pET21c:: <i>dgcB</i>	Christen unpublished
BC1000	<i>E. coli</i> BL21(DE3)/ pET21c:: <i>pdpA</i>	Christen unpublished
BC1001	<i>E. coli</i> BL21(DE3)/ pET21c::CC3148	Christen unpublished
BC1002	<i>E. coli</i> BL21(DE3)/ pET15:: <i>pleD<math>\Delta</math>1-290</i>	Christen et al 2006, JBC
BC1003	<i>E. coli</i> BL21(DE3)/ pET21:: <i>pleD<math>\Delta</math>1-290</i>	Christen et al 2006, JBC

Strain	Genotype	Reference
BC1004	<i>E. coli</i> BL21(DE3)/ pET21b	Christen et al 2005, JBC
BC1005	<i>E. coli</i> BL21(DE3)/ pET21c	Christen et al 2005, JBC
BC1007	<i>E. coli</i> BL21(DE3)	Christen unpublished
BC1008	<i>E. coli</i> BL21(DE3)/ pET42b:: <i>pdeAE323Q</i>	Christen et al 2005, JBC
BC1009	<i>E. coli</i> BL21(DE3)/ pET21c:: <i>pdeAED213QN</i>	Christen et al 2005, JBC
BC1010	<i>E. coli</i> BL21(DE3)/ pET21c:: <i>pdeAthrB</i>	Christen et al 2005, JBC
BC1011	<i>E. coli</i> BL21(DE3)/ pET21c:: <i>pdeAΔ1-112</i>	Christen et al 2005, JBC
BC1012	<i>E. coli</i> BL21(DE3)/ pET21c:: <i>pdeAhybrid</i>	Christen unpublished
BC1013	<i>E. coli</i> BL21(DE3)/ pET21c:: <i>dgrA</i>	Christen et al 2007, PNAS
BC1014	<i>E. coli</i> BL21(DE3)/ pET21c:: <i>dgrB</i>	Christen et al 2007, PNAS
BC1015	<i>E. coli</i> BL21(DE3)/ pET15::PA4608	Christen unpublished
BC1016	<i>E. coli</i> BL21(DE3)/ pET21::CC0095short	Christen unpublished
BC1017	<i>E. coli</i> BL21(DE3)/ pET21c:: <i>flmA</i> short	Christen unpublished
BC1018	<i>E. coli</i> BL21(DE3)/ pET21c:: <i>ppx</i>	Christen unpublished
BC1019	<i>E. coli</i> BL21(DE3)/ pET42b:: <i>cheYII</i>	Christen unpublished
BC1020	<i>E. coli</i> BL21(DE3)/ pET42b:: <i>flmA</i>	Christen unpublished
BC1021	<i>E. coli</i> BL21(DE3)/ pET42b:: <i>pdeB</i>	Christen unpublished
BC1022	<i>E. coli</i> BL21(DE3)/ pET42b:: <i>dgcA0207</i>	Christen et al 2006, JBC
BC1023	<i>E. coli</i> BL21(DE3)/ pET42b:: <i>dgcA0230</i>	Christen et al 2006, JBC
BC1024	<i>E. coli</i> BL21(DE3)/ pET42b:: <i>dgcA0244</i>	Christen et al 2006, JBC
BC1025	<i>E. coli</i> BL21(DE3)/ pET42b:: <i>dgcA0306</i>	Christen et al 2006, JBC
BC1026	<i>E. coli</i> BL21(DE3)/ pET42b:: <i>dgcA0347</i>	Christen et al 2006, JBC

---

<b>Strain</b>	<b>Genotype</b>	<b>Reference</b>
BC1027	<i>E. coli</i> BL21(DE3)/ pET42b:: <i>dgcA0427</i>	Christen et al 2006, JBC
BC1028	<i>E. coli</i> BL21(DE3)/ pET42b:: <i>dgcA0613</i>	Christen et al 2006, JBC
BC1029	<i>E. coli</i> BL21(DE3)/ pET42b:: <i>dgcA0617</i>	Christen et al 2006, JBC
BC1030	<i>E. coli</i> BL21(DE3)/ pET42b:: <i>dgcA0642</i>	Christen et al 2006, JBC
BC1031	<i>E. coli</i> BL21(DE3)/ pET42b:: <i>dgcA0646</i>	Christen et al 2006, JBC
BC1032	<i>E. coli</i> BL21(DE3)/ pET42b:: <i>dgcA0913</i>	Christen et al 2006, JBC
BC1033	<i>E. coli</i> BL21(DE3)/ pET42b:: <i>dgcA1007</i>	Christen et al 2006, JBC
BC1034	<i>E. coli</i> BL21(DE3)/ pET42b:: <i>dgcA1040</i>	Christen et al 2006, JBC
BC1035	<i>E. coli</i> BL21(DE3)/ pET42b:: <i>dgcA1229</i>	Christen et al 2006, JBC
BC1036	<i>E. coli</i> BL21(DE3)/ pET42b:: <i>dgcA1230</i>	Christen et al 2006, JBC
BC1037	<i>E. coli</i> BL21(DE3)/ pET42b:: <i>dgcA1231</i>	Christen et al 2006, JBC
BC1038	<i>E. coli</i> BL21(DE3)/ pET42b:: <i>dgcA1300</i>	Christen et al 2006, JBC
BC1039	<i>E. coli</i> BL21(DE3)/ pET42b:: <i>dgcA1301</i>	Christen et al 2006, JBC
BC1040	<i>E. coli</i> BL21(DE3)/ pET42b:: <i>dgcA1307</i>	Christen et al 2006, JBC
BC1041	<i>E. coli</i> BL21(DE3)/ pET42b:: <i>dgcA1311</i>	Christen et al 2006, JBC
BC1043	<i>E. coli</i> BL21(DE3)/ pET42b:: <i>dgcA1406</i>	Christen et al 2006, JBC
BC1044	<i>E. coli</i> BL21(DE3)/ pET42b:: <i>dgcA1524</i>	Christen et al 2006, JBC
BC1045	<i>E. coli</i> BL21(DE3)/ pET42b:: <i>dgcA1529</i>	Christen et al 2006, JBC
BC1046	<i>E. coli</i> BL21(DE3)/ pET42b:: <i>dgcA1724</i>	Christen et al 2006, JBC
BC1047	<i>E. coli</i> BL21(DE3)/ pET42b:: <i>dgcA1733</i>	Christen et al 2006, JBC
BC1048	<i>E. coli</i> BL21(DE3)/ pET42b:: <i>dgcA1840</i>	Christen et al 2006, JBC
BC1049	<i>E. coli</i> BL21(DE3)/ pET42b:: <i>dgcA3011</i>	Christen et al 2006, JBC

Strain	Genotype	Reference
BC1050	<i>E. coli</i> BL21 (DE3)/ pET42b:: <i>dgcA3016</i>	Christen et al 2006, JBC
BC1051	<i>E. coli</i> BL21 (DE3)/ pET42b:: <i>dgcA3018</i>	Christen et al 2006, JBC
BC1052	<i>E. coli</i> BL21 (DE3)/ pET42b:: <i>dgcA3123</i>	Christen et al 2006, JBC
BC1053	<i>E. coli</i> BL21 (DE3)/ pET42b:: <i>dgcA3200</i>	Christen et al 2006, JBC
BC1054	<i>E. coli</i> BL21 (DE3)/ pET42b:: <i>dgcA3203</i>	Christen et al 2006, JBC
BC1055	<i>E. coli</i> BL21 (DE3)/ pET42b:: <i>dgcA0751</i>	Christen et al 2006, JBC
BC1056	<i>E. coli</i> BL21 (DE3)/ pET42b:: <i>dgcA1250</i>	Christen et al 2006, JBC
BC1057	<i>E. coli</i> BL21 (DE3)/ pET42b:: <i>dgcA2006</i>	Christen et al 2006, JBC
BC1058	<i>E. coli</i> BL21 (DE3)/ pET42b:: <i>dgcAwt</i>	Christen et al 2006, JBC
BC1059	<i>E. coli</i> BL21 (DE3)/ pET42b:: <i>dgcAΔRES</i>	Christen et al 2006, JBC
BC1060	<i>E. coli</i> S17-1/ pPHU281:: <i>fliLM</i>	Christen unpublished
BC1110	<i>C. crescentus</i> CB15ATCC <i>dgrAW75A</i>	Christen et al 2007, PNAS
BC1113	<i>C. crescentus</i> CB15ATCC <i>dgrAW75A</i> / pUJ142:: <i>dgcA</i>	Christen et al 2007, PNAS
BC1116	<i>C. crescentus</i> CB15ATCC <i>dgrAW75A</i> / pAS22:: <i>dgcA</i>	Christen et al 2007, PNAS
UJ2505	<i>C. crescentus</i> NA1000 <i>clpX::Ω xylX::pUJ175 xylR0012::Tn5</i>	Christen unpublished
UJ2506	<i>C. crescentus</i> NA1000 <i>clpX::Ω xylX::pUJ175 xylR0042::Tn5</i>	Christen unpublished
UJ2507	<i>C. crescentus</i> NA1000 <i>clpX::Ω xylX::pUJ175 xylR0046::Tn5</i>	Christen unpublished
UJ2510	<i>C. crescentus</i> NA1000 <i>clpX::Ω xylX::pUJ175 xylO0304</i>	Christen unpublished
UJ2511	<i>C. crescentus</i> NA1000 <i>clpX::Ω xylX::pUJ175 xylO0305</i>	Christen unpublished
UJ2512	<i>C. crescentus</i> NA1000 <i>clpX::Ω xylX::pUJ175 xylO0512</i>	Christen unpublished
UJ2513	<i>C. crescentus</i> NA1000 <i>clpX::Ω xylX::pUJ175 xylO0601</i>	Christen unpublished
UJ2514	<i>C. crescentus</i> NA1000 <i>clpX::Ω xylX::pUJ175 xylO0607</i>	Christen unpublished



---

<b>Strain</b>	<b>Genotype</b>	<b>Reference</b>
UJ2515	<i>C.crescentus</i> NA1000 <i>clpX::Ω xylX::pUJ175 xylO0612</i>	Christen unpublished
UJ3000	<i>C.crescentus</i> NA1000 / <i>pCS225</i>	Christen unpublished
UJ3002	<i>C.crescentus</i> NA1000 <i>xylR0012::Tn5 / pCS225</i>	Christen unpublished
UJ3003	<i>C.crescentus</i> NA1000 <i>xylR0042::Tn5 / pCS225</i>	Christen unpublished
UJ3004	<i>C.crescentus</i> NA1000 <i>xylR0046::Tn5 / pCS225</i>	Christen unpublished

**List of figures**

Figure 1 Ubiquitous ribonucleotide second messengers.....	2
Figure 2 The cell cycle of <i>Caulobacter crescentus</i> and polar localization of PleD .....	5
Figure 3 Isolation of c-di-GMP binding proteins from <i>C. crescentus</i> .....	118
Figure 4 Lineweaver-Burk plots of inhibited adenylosuccinate synthetase.....	120
Figure 5 UV cross linking of PurA with [ <sup>33</sup> P]c-di-GMP in presence of GTP, IMP or AMP.....	121
Figure 6 The de novo AMP synthesis from IMP by PurA (EC 6.3.4.4) and PurB (EC 4.3.2.2).....	122
Figure 7 Reaction mechanism of the adenylosuccinate sythetase PurA .....	124
Figure 8: Comparison between adenylate cyclase and diguanylate cyclase .....	127
Figure 9: Model for the catalytic mechanism of c-di-GMP formation. ....	128
Figure 10: Crystal structure of the diguanylate cyclase PleD .....	130
Figure 11: Analogs of substrate and reaction intermediates and their inhibition activity on DgcA.	131
Figure 12 Optimization of the reaction conditions for various DGCs .....	136
Figure 13 Effect of c-di-GMP binding on the enzymatic DGC activity.....	137
Figure 14 Synthesis of MANT c-di-GMP .....	140
Figure 15 Intracellular c-di-GMP levels in <i>C. crescentus</i> .....	143
Figure 16 Identified components of the c-di-GMP signaling network.....	146
Figure 17 Overview of the GGDEF and EAL proteins from <i>Caulobacter crescentus</i> . ....	160

## Acknowledgments

I would like to thank the following people, without whom this thesis would never have been written:

My parents for introducing my brothers and me into the fascinating world of science and for their support in founding the Elyssia-laboratories in 1994.

Yvonne for her helps and advises in scientific and non-scientific situations.

My brother Beat for his efforts in teaching genetics, his reliance during scientific collaborations and for the wonderful three years in the same laboratory.

Marc Folcher for introducing me into the world of biochemistry and, his prospective scientific project validation and supervision, and for the excellent teamwork we had.

Prof. Dr. Helma Wennemers for inspiration of combinatorial approaches, Prof. Dr. Tilman Schirmer for scientific discussions, Prof. Dr. Markus Meuwly for introducing into the computational chemistry, Dr. Paul Jenö for the wonderful MS-MS data and Prof. Dr. Wolf-D Woggon for his helpful discussions and his support during the past 5 years,

Further, I would like to thank

Martin Allan, Sören Abel, Arnaud Basle, Carmen Chan, Wanda Dischert, Anna Dürig, Martha Gerber, Fabienne Hamburger, Assaf Levi, Jacob Malone, Flora Mauch, Suzette Moes, Dietrich Samoray, Salvo San Paolo and Franziska Schmid

## Curriculum vitae

### Personal Information

Surname / First name CHRISTEN Matthias  
Date and place of birth 20.03 1978, Basel, Switzerland  
Adress Benkenstrasse 51, 4104 Oberwil  
Telephone 061 / 401 07 11  
E-mail matthias.christen@unibas.ch

### Education

Nov. 2003 to Feb. 2007 PhD  
Principal subjects Molecular Microbiology/ Signal Transduction  
Departement of Microbiology, Biozentrum, University of Basel,  
Klingelbergstr. 50/70, 4056 Basel, Switzerland  
Supervisor Prof. Dr. Urs Jenal  
Subject Mechanisms of c-di-GMP signaling

April 1998 – March 2003 Studies in Chemistry at University of Basel  
02.04.2003 Diploma for Chemistry, mark 5.5  
1994 – 1997 Certificate of Matura type C

### Awards

März 1998 Basler Maturandenpreis der Novartis  
März 2007 Swiss Society of Microbiology Encouragement Award 2007

### Publications

- [1] M. Christen, B. Christen, M. Allan, M. Folcher, S. Moes, P. Jenö, S. Grzesiek, U. Jenal (2006): DgrA is a member of a new family of cyclic di-GMP receptors and controls flagellar motor function in *Caulobacter crescentus* PNAS *manuscript accepted October 25, 2006*
- [2] B. Christen, M. Christen, R. Paul, F. Schmid, M. Folcher, P. Jenö, M. Meuwly, U. Jenal (2006): Allosteric Control of Cyclic di-GMP Signaling *J Biol Chem.* October 20, 2006; 281 (42):32015-24. Epub August 21. 2006
- [3] M. Christen, B. Christen, M. Folcher, A. Schauerte, U. Jenal (2005): Identification and Characterization of a c-di-GMP Specific Phosphodiesterase and its Allosteric Control by GTP *J. Biol. Chem.* September 2, 2005; 280 (35):30829-37. Epub July 1, 2005
- [4] J.G. Malone, R. Williams, M. Christen, U. Jenal, A.J. Spiers, and P.B. Rainey (2006): The structure-function relationship of WspR; a *Pseudomonas fluorescens* response

regulator with a GGDEF output domain *Microbiology manuscript accepted November 25, 2006*

[5]

**Talks and Presentations on international Meetings and conferences**

2006

- [6] M. Christen, B. Christen (2006): Mechanisms of c-di-GMP Signaling *Seminar at Developmental Biology Department, Stanford University School of Medicine, May 26, Stanford, CA USA*
- [7] M. Christen, B. Christen, M. Folcher, S. Möes, P. Jenö, U. Jenal (2006): Isolation and Characterization of Diguanylate Receptor Proteins (DGRs) from *Caulobacter crescentus* *106<sup>st</sup> General ASM Conference, May 21-25, 2006 - Orlando, FL USA*
- [8] M. Christen, B. Christen, M. Allan, M. Folcher, S. Moes, P. Jenö, S. Grzesiek, U. Jenal (2006): The c-di-GMP receptor DgrA controls flagellar motor function in *Caulobacter crescentus* *Biozentrum Symposium, October 20, 2006 - Basel, Switzerland*
- [9] B. Christen, M. Christen, R. Paul, M. Folcher, U. Jenal (2006): An Allosteric Control Mechanism Coordinates c-di-GMP Signaling *106<sup>st</sup> General ASM Conference, May 21-25, 2006 - Orlando, FL USA*
- [10] M. Folcher, M. Christen, B. Christen, I. Wiederkehr, S. Moes, P. Jenö, U. Jenal (2006): C-di-GMP regulate key enzyme in nucleotide biosynthesis pathway *Biozentrum Symposium, October 20, 2006 - Basel, Switzerland*
- [11] M. Allan, M. Christen, B. Christen, M. Folcher, S. Moes, P. Jenö, U. Jenal, S. Grzesiek (2006): Structural characterization of a cyclic di-GMP receptor protein. *Symposium core program structural biology and biophysics, June 16, 2006 - Basel, Switzerland*
- [12] A. Dürig, M. Christen and U. Jenal (2006): A C-di-GMP Binding Protein Localizes to the Cell Pole and Controls Cell Motility during *C. crescentus* Development *106<sup>th</sup> General ASM Conference, May 21-25, 2006 - Orlando, FL, USA*
- [13] A. Dürig, M. Christen, A. Schauerte and U. Jenal (2006): A C-di-GMP Binding Protein Localizes to the Cell Pole and Controls Cell Motility during *C. crescentus* Development *SSM SGM annual Congress, March 7-8, 2006 -Lausanne, Switzerland*

2005

- [14] M. Christen, B. Christen, M. Folcher, A. Schauerte, U. Jenal (2005): Identification and Characterization of a c-di-GMP Specific Phosphodiesterase and its Allosteric Control by GTP 2<sup>nd</sup> *Caulobacter meeting, July 11 - 13, 2005 - Vancouver Canada*
- [15] M. Christen, B. Christen, R. Paul, T. Schirmer, P. Jenö, U. Jenal (2005): A Novel Regulatory Mechanism Controls the Production of c-di-GMP by Diguanylate Cyclases *SSM SGM annual Congress, 31.3.-1.4, 2005 - Geneva, Switzerland*
- [16] M. Christen, B. Christen, U. Jenal (2005): The Make and Break of c-di-GMP *Biozentrum Symposium, October 21. 2005 - Basel, Switzerland*
- [17] M. Christen, B. Christen, M. Folcher, A. Schauerte, T. Schirmer, T. Augst, U. Jenal (2005): Identification of a c-di-GMP specific Phosphodiesterase and its allosteric control by GTP *SWIMM Meeting, 15-17 March 2005 - ETH Zürich Switzerland*
- [18] B. Christen, M. Christen, M. Folcher, U. Jenal (2005): Biochemical and Genetic Identification of a c-di-GMP Binding Motif 2<sup>nd</sup> *ASM Conference on Prokaryotic Development, July 13 - 16, 2005 - Vancouver, Canada*
- [19] B. Christen, M. Christen, R. Paul, A. Schauerte, T. Schirmer, P. Jenö, U. Jenal (2005): A Novel Regulatory Mechanism Controls the Production of c-di-GMP *SWIMM Meeting, 15-17 March 2005 - ETH Zürich Switzerland*
- [20] A. Dürig, M. Christen, Alexandra Schauerte & Urs Jenal (2005): Cell Cycle dependent Dynamic Localization of a Diguanylate Cyclase-like Protein in *Caulobacter crescentus* Development *Biozentrum Symposium, October 19, 2005 – Basel, Switzerland*
- [21] A. Dürig, M. Christen & U. Jenal (2006): Dynamic Localization of a GGDEF Domain Protein involved in *Caulobacter crescentus* Development and Cell Cycle Control *Biozentrum Symposium, October 19, 2006 – Basel, Switzerland*
- [22] R. Paul, M. Christen, B. Christen, A. Schauerte, P. Jenö, U. Jenal (2005): The PleD Diguanylate Cyclase is Activated Through Dimerization and is Subject to Tight Allosteric Feedback Control 2<sup>nd</sup> *ASM Conference on Prokaryotic Development, July 13 - 16, 2005 - Vancouver Canada*
- [23] A. Levi, D. Meyer, M. Christen & Urs Jenal (2005): Developmental Control of Microbial Surface Colonization by the Timed Synthesis and Destruction of c-di-GMP *Biozentrum Symposium, October 19, 2005 - Basel, Switzerland*

2003-2004

- [24] M. Christen, R. Paul. B. Christen, A. Schauerte, P. Jenö, U. Jenal (2004): Characterization of the c-di-GMP binding site of the diguanylate cyclase (DGC) *PleD* *Biozentrum Symposium, October 14, 2004 - Basel Switzerland*
- [25] B. Christen, M. Christen, U. Jenal (2004): Interaction Map of two-Component Signal Transduction Proteins in *Caulobacter crescentus* *EuroConference on Inter- and Intracellular Signalling and Global Regulation in Bacteria, May 8-13, 2003 – Barcelona, Spain*

### Teaching experience

#### Supervision of Masterthesis

M. Gerber (2006): Designing Diguanylate Cyclase Inhibitors. *Masterthesis of M. Gerber supervised by M & B. Christen, Laboratory of Prof. Dr. Urs Jenal, Oktober 2005-November 2006 - Biozentrum University of Basel*

F. Mauch (2006): Genetic Identification of Diguanylate Receptor Proteins Regulating Biofilm Formation in *Salmonella enterica* Serovar Typhimurium. *Masterthesis of F. Mauch supervised by B & M. Christen, Laboratory of Prof. Dr. Urs Jenal, Oktober 2005-Oktober 2006 - Biozentrum University of Basel*

#### Teaching assistantship

Microbiology block course 2004-2006 (2 weeks per year) - Teaching assistantship in practical courses at the Biozentrum University of Basel

### Practices and diploma thesis

- |                        |  |
|------------------------|--|
| Nov. 2002 – March 2003 | Diploma thesis Prof. Dr. W.D. Woggon and Prof. Dr. Urs Jenal<br>Institut für organische Chemie und Biozentrum der Universität Basel<br>Title: Overexpression of TocA - A Tocopherol Cyase from <i>Anabaena</i> sp. |
| March 2002 - May 2002  | Praktica by Prof. Dr. Helma Wennemers, Institut für Organische Chemie der Universität Basel<br>Topic: Peptide chemistry, Synthesis of oligopeptides using combinatorial solid phase chemistry                      |
| Nov. 2001 – Feb. 2002  | Praktica by Prof. Dr. Wolf D. Woggon, Institut für Organische Chemie der Universität Basel<br>Topic: Synthesis of deazaflavine derivatives   |